



HAL
open science

Heterogeneous Fenton-like process based on copper oxide and peroxydisulfate for urban wastewater treatment

Chan Li

► **To cite this version:**

Chan Li. Heterogeneous Fenton-like process based on copper oxide and peroxydisulfate for urban wastewater treatment. Other. Université Montpellier, 2021. English. NNT: 2021MONTG059 . tel-03572403

HAL Id: tel-03572403

<https://theses.hal.science/tel-03572403>

Submitted on 14 Feb 2022

HAL is a multi-disciplinary open access archive for the deposit and dissemination of scientific research documents, whether they are published or not. The documents may come from teaching and research institutions in France or abroad, or from public or private research centers.

L'archive ouverte pluridisciplinaire **HAL**, est destinée au dépôt et à la diffusion de documents scientifiques de niveau recherche, publiés ou non, émanant des établissements d'enseignement et de recherche français ou étrangers, des laboratoires publics ou privés.

THÈSE POUR OBTENIR LE GRADE DE DOCTEUR DE L'UNIVERSITÉ DE MONTPELLIER

En Sciences de l'Eau

École doctorale GAIA – Biodiversité, Agriculture, Alimentation, Environnement, Terre, Eau

Unité de recherche HydroSciences Montpellier

Heterogeneous Fenton-like process based on copper oxide and peroxydisulfate for urban wastewater treatment

Présentée par Chan LI

Le 15 decembre 2021

Sous la direction de Serge CHIRON
et Vincent GOETZ

Devant le jury composé de

Jean Marc CHOVELON, Professeur, Université Claude Bernard Lyon 1

Maria Concetta TOMEI, Directeur de recherche, Water Research Institute C.N.R.

Gianluigi BUTTIGLIERI, Chercheur, Catalan Institute for Water Research

André SAUVETRE, Maître-assistant, Ecole des Mines d'Alès

Serge CHIRON, Directeur de recherche, Institut de Recherche pour le Développement

Vincent GOETZ, Directeur de recherche, Centre National de la Recherche Scientifique

Président / Examineur

Rapporteur

Rapporteur

Examineur

Directeur de thèse

Co-directeur de thèse



UNIVERSITÉ
DE MONTPELLIER

Abstract

Advanced oxidation processes (AOPs) have been proven to be effective to simultaneously degrade contaminants of emerging concerns (CECs, e.g., pharmaceuticals, pesticides, and personal care products) and inactivate pathogens (i.e., bacteria, viruses, protozoan) and resistant microorganisms (e.g., antibiotic-resistant bacteria and antibiotic resistance genes (ARB&Gs)) in wastewater, which make them one of the best available technologies for tertiary urban wastewater treatment. Among the AOPs, heterogeneous Fenton-like oxidation processes (HFOPs) are particularly promising for application because of their relatively low-cost to suitable with biological decentralized wastewater treatment plants (e.g., constructed wetland) in rural areas, and because they might be easily implemented at field-scale through filtration units. To preserve the nutrients and carbon in urban wastewater, a HFOP relying on highly selective non-radical reactive species is strongly recommended. In this thesis, a HFOP based on the copper oxide (CuO) catalyzed peroxydisulfate (PDS) system was investigated because both radical and non-radical species have been reported to form.

In this context, the mechanism of the micro-size CuO (10 g/L) / PDS (1 mM) system in batch mode was first explored. Phenol was selected as the targeted compound and was effectively degraded. Cupryl (Cu(III)) species was suggested to be the predominant reactive species and led to a polymerization reaction of phenol. This system was suggested to be a non-radical involved system and was not significantly affected by dissolved organic matter and ions (e.g., sulfate, and bicarbonate ions) in wastewater. Effective oxidation of several waterborne antibiotics by Cu(III) demonstrated its selectivity and practical applicability.

The inactivation performance evaluation of this system for pathogens and resistant microorganisms in urban wastewater was carried out in batch mode. Complete inactivation of *Escherichia coli*, *Enterococcus*, *F-specific RNA bacteriophages* from

secondary treated urban wastewater was achieved after a short time (15-30 min) treatment, but *spores of sulfite-reducing bacteria* took 120 min. A significant reduction of sulfamethoxazole-resistant *E. coli*, selected genes including ARGs (i.e., blaTEM, qnrS, emrB, and sul1), and genes related to the dissemination of antibiotic resistance (i.e., intI1 and IS613) was achieved after treatment.

From the perspective of applying this system at pilot-scale, CuO particles can be implemented in a packed fixed column to provide the necessary contact time between a liquid to be treated and CuO particles. Millimeter-sized CuO pellets were employed instead of micro-sized CuO particles. The experiments carried out corresponded to the first tests provided on peroxydisulfate activation by using millimetric CuO pellets as a heterogeneous catalyst in a packed fixed-bed column (FBC-CuO). FBC-CuO showed high stability once it was put into operation and a high sensitivity to operating conditions. FBC-CuO/PDS system demonstrated a high removal efficiency for target antibiotics and pathogens in secondary treated urban wastewater, except for *spores of sulfite-reducing bacteria*.

Key words: urban wastewater, copper oxide, peroxydisulfate, antibiotics, disinfection, fixed-bed column.

Résumé

Les procédés d'oxydation avancée (AOPs) sont efficaces pour dégrader simultanément les contaminants émergents préoccupants (CECs, par exemple, les produits pharmaceutiques, les pesticides et les produits de soins personnels), pour inactiver les pathogènes (par exemple, les bactéries, les virus, les protozoaires) et les micro-organismes résistants (par exemple, les bactéries résistantes aux antibiotiques et les gènes de résistance aux antibiotiques (ARB&G)) dans les eaux usées, ce qui en fait l'une des meilleures technologies disponibles pour le traitement tertiaire des eaux usées urbaines. Parmi les AOPs, les procédés d'oxydation hétérogènes de type Fenton (HFOP) sont particulièrement prometteurs en raison de leur coût relativement faible adapté au fonctionnement des stations d'épuration biologique décentralisées (par exemple, une zone humide artificielle) dans les territoires ruraux, et parce qu'ils pourraient être facilement mis en œuvre comme unités de filtration. Pour préserver les nutriments et le carbone dans les eaux usées urbaines traitées, un HFOP reposant sur des espèces réactives non radicalaires hautement sélectives est fortement recommandé. Dans cette thèse, un HFOP basé sur l'activation de peroxydisulfate (PDS) par l'oxyde de cuivre (CuO) a été étudié, car il a été démontré que des espèces radicalaires et non radicalaires se formaient.

Dans ce contexte, le mécanisme de fonctionnement du système CuO (10 g/L de taille micrométrique) / PDS (1 mM) en mode batch a d'abord été exploré. Le phénol a été sélectionné comme composé sonde et a été efficacement dégradé. L'ion cupryl (Cu(III)) a été proposé comme étant l'espèce réactive prédominante dans le système conduisant à une réaction de polymérisation du phénol. Ce système est un système fonctionnement majoritairement sans espèces radicalaires et n'est pas significativement affecté par la matière organique dissoute et les ions (par exemple, les ions sulfate et bicarbonate) dans les eaux usées. L'oxydation de plusieurs antibiotiques par Cu(III) a démontré sa sélectivité et son applicabilité.

L'évaluation des performances d'inactivation d'agents pathogènes et de microorganismes résistants dans les eaux usées urbaines a été réalisée en mode batch. L'inactivation complète des *E. coli*, *Enterococcus*, *bactériophages ARN F spécifiques* des eaux usées urbaines après un traitement biologique secondaire a été obtenue après un temps de traitement court (15-30 min), une durée plus longue de 120 min s'est avérée nécessaire pour l'élimination des *spores de micro-organismes anaérobies sulfito-réducteurs*. Une réduction significative des *E. coli* résistants au sulfaméthoxazole, des ARGs ciblés (*blaTEM*, *qnrS*, *emrB* et *sul1*) et de gènes liés à la dissémination de la résistance aux antibiotiques (*intI1* et *IS613*) a été également obtenu après le traitement.

Afin d'évaluer l'applicabilité, les particules de CuO ont été mises en place dans une colonne à lit fixe pour assurer un temps de contact suffisant entre le liquide à traiter et les particules de CuO. Des granulés de CuO de taille millimétrique ont été utilisés à la place de particules de CuO de taille micrométrique. Les expériences réalisées correspondent aux premiers tests effectués sur l'activation du peroxydisulfate en utilisant des granulés de CuO millimétriques comme catalyseur hétérogène dans une colonne à lit fixe garnie (FBC-CuO). Le FBC-CuO a montré une grande stabilité et avec des performances extrêmement sensibles aux conditions de fonctionnement. Le système FBC-CuO/PDS a démontré une efficacité d'élimination élevée pour les antibiotiques et les agents pathogènes ciblés dans les eaux usées urbaines ayant été traitées au préalable par boues activées, à l'exception des *spores de micro-organismes anaérobies sulfito-réducteurs*.

Mots clés: eaux usées urbaines, oxyde de cuivre, peroxydisulfate, antibiotiques, désinfection, colonne à lit fixe.

Acknowledgement

The work presented in this thesis was carried out at HydroScience Montpellier, France. The time I spend in HSM was a wonderful and memorable experience as I have met a lot of great people who have helped me a lot with my thesis and personal development.

First of all, I would like to express my sincere gratitude to my supervisor Serge Chiron, for giving me the opportunity to join his research team. Thanks also for Vincent Goetz. I am really lucky to be their student during the past three years. Thanks for their precious time, patience, advice, encouragement, knowledge, and continuous support in the experimental work, writing of manuscripts, and preparation of this thesis.

I sincerely thank all my excellent and intelligent colleagues. Monica, Nayara, Rayana, Cedric, Thibaut, Andres, Juan, Dorde, and every student I have met here, thanks for your professional suggestions and help. I would also like to thanks the laboratory stuff, Mireille, David, and Abdel for the administrative and technical help.

A special thank you to my roommate, Meng, thanks for your three years of accompany. Also, thanks to my old friends for more than ten years, especially, Lu, Bingbing, Fang, and Ju, thank you for your continuous encouragement and help.

I would like to express my very profound gratitude to all my beloved family members, dad, mom, and my brother for providing me continuous support, encouragement, and love throughout my life. Thank you.

I am very grateful for the Occitanie Region for my PhD grant. This research was financially supported in part by the Water Joint Programming Initiative (JPI) through the research project IDOUM (Innovative Decentralized and low cost treatment systems for Optimal Urban wastewater Management) and in part by the MITI CNRS/IRD program through the research project FREE (AC/CuO Filter Regenerated by solar Energy for water rEuse).

Table of Contents

List of Figures	9
List of Tables	9
List of Abbreviations	10
General Introduction	11
Chapter 1. Introduction and context	14
1. Water scarcity	15
2. Wastewater reuse in irrigation	15
2.1. Guidelines and regulations	15
2.2. Urban wastewater treatment technologies	17
3. Advanced oxidation processes	19
3.1. Homogeneous AOPs	19
3.1.1. Ozone-based AOPs	19
3.1.2. UV/H ₂ O ₂ and UV/PS.....	22
3.1.3. Photo Fenton and Fenton-like AOPs.....	23
3.2. Heterogeneous Fenton-like oxidation processes	25
3.2.1. Radical-based systems.....	25
3.2.2. Non-radical-based systems.....	27
4. Fixed-bed column	30
5. Aims	30
Chapter 2. Peroxydisulfate activation process on copper oxide: Cu(III) as the predominant selective intermediate oxidant for phenol and waterborne antibiotics removal	48
Abstract	49
1. Introduction	50
2. Material and Methods	50
2.1. Chemicals.....	50
2.2. Characterization of CuO	50
2.3. Experimental procedures	50
2.4. Analytical methods	50
3. Results and discussion	51
3.1. Characterization of CuO.....	51
3.2. PDS activation by CuO-batch experiments.....	51

3.3. Identification of reactive species	52
3.4. Phenol transformation pathways and mechanisms.....	53
3.5. Influence of operating parameters	54
3.6. Applicability of CuO/PDS system.....	56
4. Conclusions	57
Supporting information	59
Chapter 3. Copper oxide / peroxydisulfate system for urban wastewater disinfection: Performances, reactive species, and antibiotic resistance genes removal	76
Abstract	77
1. Introduction	77
2. Material and Methods	78
2.1. Chemicals	78
2.2. Pathogens inactivation	78
2.3. Identification of reactive species	79
2.4. Antibiotic-resistant-bacteria and antibiotic resistance genes	79
3. Results and discussion	80
3.1. Inactivation performances of pathogens	80
3.2. Identification of reactive species.....	81
3.3. Antibiotic-resistant-bacteria and antibiotic resistance genes removal	84
4. Conclusions	85
Supporting information	87
Chapter 4. Peroxydisulfate activation by CuO pellet in a fixed-bed column for antibiotics degradation and urban wastewater disinfection	102
Abstract	103
1. Introduction	104
2. Experimental section	106
2.1. Chemicals.....	106
2.2. Characterization of CuO pellet	106
2.3. Fixed-bed column set up.....	106
2.4. Experimental procedures	107
2.5. Analytical methods	110
3. Results and discussion	111

3.1. Working mode of CuO fixed-bed column.....	111
3.2. Degradation of antibiotics	116
3.3. Pathogens inactivation	119
3.4. Stability of FBC-CuO	121
4. Conclusions	123
Supporting information	129
Chapter 5. Conclusions and perspectives	141
Appendix.....	148

List of Figures

Figure 1. Water stress by country.	17
Figure 2. Sectoral water withdraws comparison in the different regions	17
Figure 3. The activation pathways initiated by the (a) magnetite activated H ₂ O ₂ and (b) hematite activated PMS processes	28
Figure 4. (a) Surface activated complexes and (b) singlet oxygen-based processes ...	30
Figure 5. The formation of ferryl ion in (a) Fe(II)/PDS, (c) Fe(III) doped g-C ₃ N ₄ /PMS, and cupryl ion in (b) Cu(II)/PMS, (d) CuO-Fe ₃ O ₄ /PDS systems	31

List of Tables

Table 1. Performance target for reclaimed water use in agricultural irrigation in EU 2020/741	18
Table 2. Categorization of CEC according to their abatement during ozonation of biologically treated wastewater (0.4–0.6 g O ₃ /g DOC) and their reactivity with ozone	22

List of Abbreviations

AMX	: Amoxicillin
AOPs	: Advanced Oxidation Processes
ARB	: Antibiotic-Resistant Bacteria
ARGs	: Antibiotic Resistance Genes
ARB&Gs	: Antibiotic Resistant Bacteria and Resistance Genes
BDOC	: BioDegradable Organic Carbons
BOD	: Biochemical Oxygen Demand
CECs	: Contaminants of Emerging Concerns
CFX	: Cefalexin
CIP	: Ciprofloxacin
CLA	: Clarithromycin
CuO	: Copper Oxide
DBPs	: Disinfection By-Products
DOM	: Dissolved Organic Matters
E. coli	: Escherichia coli
EDDS	: ethylenediamine-N, N'-disuccinic acid
EPA	: Environmental Protection Agency
EU	: European Union
FBC-CuO	: Fixed-Bed Column packed with Copper Oxide
HFOP	: Heterogeneous Fenton-like Oxidation Process
LC-HRMS	: Liquid Chromatography-High Resolution-Mass Spectrometry
LED	: Light Emitting Diodes
NDMA	: N-nitrosodimethylamine
OFL	: Ofloxacin
PAA	: Peracetic Acid
PDS	: Peroxydisulfate
PMS	: Peroxymonosulfate
PS	: Persulfate
ROS	: Reactive Oxygen Species
SEM	: Scanning Electron Microscopy
SMX	: Sulfamethoxazole
TPs	: Transformation Products
TSS	: Total Suspended Solids
USAID	: United States Agency for International Development
UV	: Ultraviolet
UWTPs	: Urban Wastewater Treatment Plants
WHO	: World Health Organization
XRD	: X-ray diffraction

General Introduction

Reclaimed urban wastewater reuse in agricultural irrigation is a global practice to meet the increasing water demand and to use the nutrients and organic matters as fertilizers. Regulations and guidelines for the safe reuse of wastewater in irrigation are enacted to protect the environment and human health, which underlined the microbial risk caused by pathogenic microorganisms (i.e., bacteria, viruses, protozoan). Moreover, contaminants of emerging concerns (CECs, e.g., pharmaceuticals, pesticides, and personal care products) and resistant microorganisms (e.g., antibiotic-resistant bacteria (ARB) and antibiotic resistance genes (ARGs)) have also raised safety concerns, especially in some high-income level countries. However, conventional urban wastewater treatment plants (UWTPs) are poorly effective to degrade CECs, inactivate pathogens and limit the spread of antibiotic resistance. Additional treatment technologies for simultaneous degradation of micropollutants and inactivation of pathogens and resistant microorganisms from urban wastewater are highly recommended. Advanced oxidation processes (AOPs) are among the promising alternatives capable of meeting these requirements. Among the AOPs, heterogeneous Fenton-like oxidation processes (HFOPs) relying on non-radical based mechanisms have attracted increasing attention for tertiary urban wastewater treatment and reuse in irrigation because of the ability to preserve maximum nutrients and carbon, and because of their powerful, low-cost, and easy-to-manage characteristics.

In this context, a HFOP based on the copper oxide (CuO) catalyzed peroxydisulfate (PDS) system was investigated because diverse radical and non-radical mechanisms have been proposed for this system. Therefore, the deep mechanism investigation was first carried out. Then, the performances of this system in the degradation of micropollutants, inactivation of pathogens, and reduction of antibiotic resistance in urban wastewater were evaluated in batch mode, respectively. Finally, from the point

of view of the pilot-scale application of this system, CuO particles can be implemented in a packed fixed bed to provide the necessary contact time between a liquid to be treated and CuO particles. Millimeter-sized CuO pellets were employed instead of micro-sized CuO particles to avoid the catalyst release, to comply with the requirement of limiting the pressure drop inside the column, and to prevent potential clogging problems. Thus, the performances of decontamination and disinfection of secondary treated urban wastewater were evaluated by persulfate oxidation activated by millimetric CuO pellets in a packed fixed-bed column.

Given what has been said, this work has been structured in the following form:

Chapter 1 first briefly introduces the water scarcity and related regulations and available technologies for wastewater reuse in irrigation, then mainly describes the literature knowledge of AOPs that have been widely used including ozonation and ultraviolet irradiation based AOPs, and have received the most attention including photo-Fenton and heterogeneous Fenton-like oxidation processes.

Chapter 2 is written as a scientific article “Peroxydisulfate activation process on copper oxide: Cu(III) as the predominant selective intermediate oxidant for phenol and waterborne antibiotics removal”. It describes the degradation kinetics and transformation mechanisms of phenol and targeted antibiotics in the CuO/PDS system. The article also reported the stability and reusability of this system in batch mode

Chapter 3 is written as a scientific article “Copper oxide / peroxydisulfate system for urban wastewater disinfection: Performances, reactive species, and antibiotic resistance genes removal”. It describes the raw and secondary treated urban wastewater disinfection performance and bacterial regrowth during storage, the role of reactive species in pathogens inactivation, and removal efficiency of resistant microorganisms in secondary treated urban wastewater.

Chapter 4 is written as a scientific article “Peroxydisulfate activation by CuO pellet in a fixed-bed column for antibiotics degradation and urban wastewater disinfection”. It describes the working mode of a packed fixed-bed column filled with CuO pellet under various operating conditions, such as varying flow rates, initial persulfate and phenol concentrations. Then, it also reported the removal efficiency of antibiotics and pathogens by this system. Finally, the stability of the packed CuO fixed-bed column was discussed.

Chapter 5 describes the conclusions and perspectives of this thesis.

Chapter 1. Introduction and context

1. Water scarcity

Water scarcity is recognized worldwide as one of the most pressing environmental issues of this century, and the water stress by country is shown in Figure 1 [1]. About 70% of global freshwater is supplied for agricultural irrigation (Figure 2) [2]. Wastewater reuse for agricultural irrigation is a growing practice to alleviate the demand pressure on freshwater sources, moderate water pollution, and reduce the use of additional fertilizers resulting in savings for the environment, wastewater treatment, and farmers [3,4].

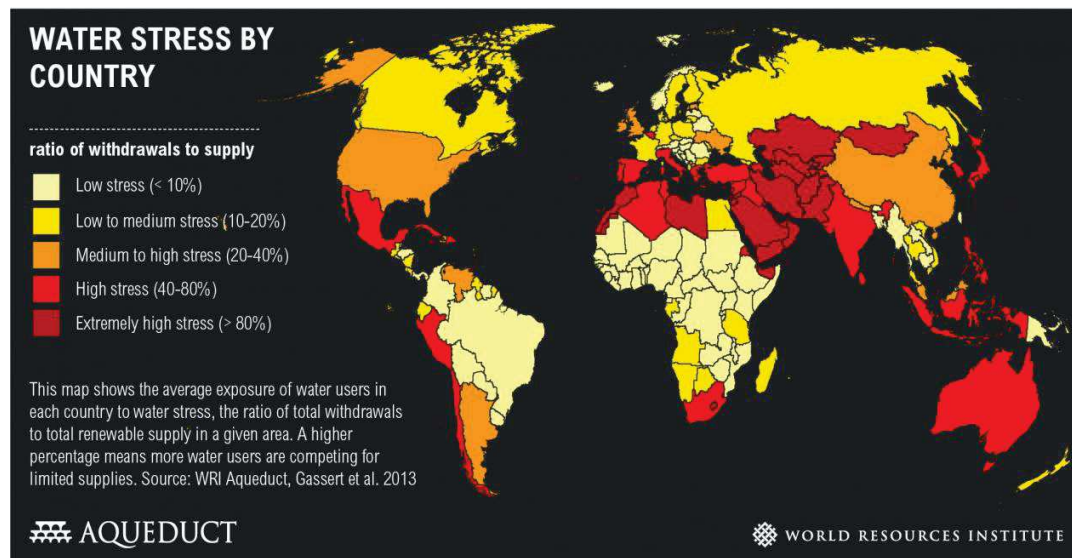


Figure 1. Water stress by country [1].

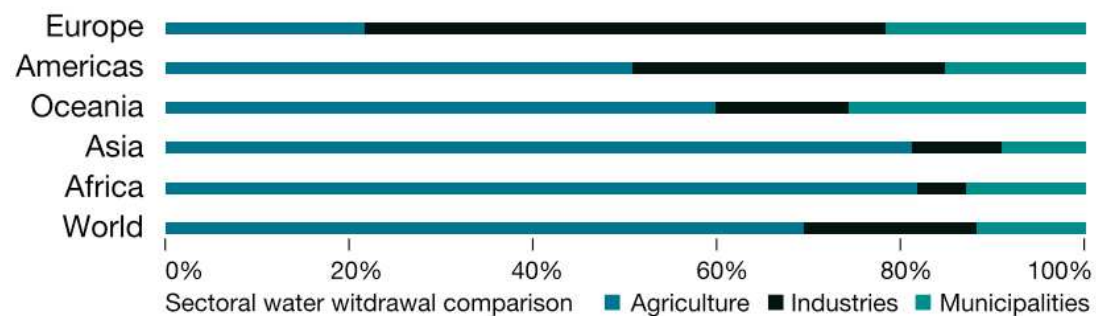


Figure 2. Sectoral water withdraws comparison in the different regions [2].

2. Wastewater reuse in irrigation

2.1. Guidelines and regulations

Wastewater reuse can pose risks to public health if treatment, storage and piping are not adequate [3,5]. The main risk, in particular in some poor and developing countries, is related to the consumption of foods contaminated with pathogenic microorganisms from the reuse of untreated or inadequately treated wastewater for agricultural irrigation [5,6]. To protect public health, regulations and guidelines about the reuse of treated wastewater for irrigation are enacted, such as World Health Organization (WHO) Guidelines for Safe Use of Wastewater, Excreta and Greywater [7], Environmental Protection Agency (EPA) and the United States Agency for International Development (USAID) Guidelines for Wastewater Reuse [8], and the European Union (EU) Regulation 2020/741[9]. Most guidelines put heavy emphasis on microbial standards, the performance target for the treatment chain is expressed in terms of log₁₀ pathogens reduction from raw wastewater to reclaimed wastewater. Specifically, the health-based target in WHO's 2006 guideline [7], for unrestricted and localized irrigation (i.e., lettuce and onion), can be achieved by 6-7 log unit reduction of rotavirus. While, to comply with EU Regulation 2020/741[9], the performance target of the treatment chain is for the most stringent reclaimed water quality class (Class A: all food crops consumed raw where the edible part is in direct contact with reclaimed water and root crops consumed raw), by monitoring the indicator microorganisms associated with each group of pathogens (i.e., bacteria, viruses, and protozoa) as shown in Table 1, which is also the regulatory basis of this work.

Table 1. Performance target for reclaimed water use in agricultural irrigation in EU 2020/741 [9].

Indicator microorganisms (*)	Performance targets for the treatment chain (log ₁₀ reduction)
E. coli	≥ 5.0
Total coliphages/F-specific coliphages/somatic coliphages/coliphages (**)	≥ 6.0
Clostridium perfringens spores/spore-forming sulfate-reducing bacteria (***)	≥ 4.0 (in case of Clostridium perfringens spores)

≥ 5.0 (in case of spore-forming sulfate-reducing bacteria)

(*) The reference pathogens *Campylobacter*, Rotavirus and *Cryptosporidium* may also be used for validation monitoring purposes instead of the proposed indicator microorganisms. The following log₁₀ reduction performance targets shall then apply: *Campylobacter* (≥ 5,0), Rotavirus (≥ 6,0) and *Cryptosporidium* (≥ 5,0).

(**) Total coliphages is selected as the most appropriate viral indicator. However, if analysis of total coliphages is not feasible, at least one of them (F-specific or somatic coliphages) shall be analyzed.

(***) *Clostridium perfringens* spores is selected as the most appropriate protozoa indicator. However, spore-forming sulfate-reducing bacteria are an alternative if the concentration of *Clostridium perfringens* spores does not make it possible to validate the requested log₁₀ removal.

Since effective disinfection processes are typically included in the treatment train in some developed countries, the concerns tend to shift from microbial risk to contaminants of emerging concerns (CECs), such as pesticides, pharmaceuticals, hormones, personal care products, and resistant microorganisms, such as antibiotic-resistant bacteria and antibiotic resistance genes (ARB&Gs) [5,10]. CECs could exert toxic effects on human and aquatic life even at low concentrations. Particularly, some CECs, such as antibiotics, can cause selection pressure. Some antibiotics-sensitive microorganisms are eliminated, but some resistant cells can overcome the adverse effects of antibiotics and obtain antibiotic resistance [11]. Antibiotic resistance leads to higher medical costs, prolonged hospital stays, and increased mortality when humans are infected [12]. Therefore, ARB&Gs have been recognized by WHO as one of the major challenges for human health in 2015 even though they are not currently included in any international regulation [12].

2.2. Urban wastewater treatment technologies

Conventional urban wastewater treatment plants (UWTPs) that consist of primary and secondary treatment processes can effectively address typical parameters set in wastewater reuse regulation and guidelines, such as biochemical oxygen demand

($BOD_5 \leq 10$ mg/L), total suspended solids ($TSS \leq 10$ mg/L), turbidity (≤ 5 NTU) [5,13]. However, UWTs are poorly effective to comprehensively inactivate a broad range of pathogenic microorganisms, remove chemical emerging contaminants, and limit the spread of antibiotics resistance (ARB&Gs) [5,10,14]. To achieve the safe reuse of wastewater in agricultural irrigation, additional effective wastewater treatment technologies are highly recommended.

Traditional disinfection methods such as chlorination, ultraviolet (UV) irradiation treatment, and peracetic acid (PAA) have been widely applied as tertiary treatment for water disinfection, however, their limitations are still remaining. For example, chlorination is not efficient for cryptosporidium removal together with the well-known problem of unhealthy disinfection by-products (DBPs) generation, such as trihalomethanes and haloacetic acids, due to chlorine reacts readily with a wide range of organics [15,16]. PAA has shown poor effectiveness in removing enteric viruses, and potential microbial regrowth [17,18]. More importantly, neither the disinfectants (chlorination, PAA) nor UV-C is effective for the removal of emerging contaminants [5,19]. On contrary, adsorption on activated carbons as one additional treatment coupling with UWTs presented excellent removal performance of CECs due to its high surface area [5,20–22]. But it is clearly established in the literature that it is poorly effective for the removal of pathogens as well as ARB&Gs [23,24]. In terms of simultaneous degradation of micropollutants, inactivation of pathogens, and reduction of resistant microorganisms (i.e., ARB&Gs) from wastewater, membrane filtration [5,25,26] and advanced oxidation processes (AOPs) [27–31] are possible options. CECs can be efficiently removed by nanofiltration and reverse osmosis, however, poor removal performance by ultrafiltration and microfiltration, in addition, membrane fouling and possible permeate flux decreasing is a major issue, which may need expensive cleaning and regeneration schemes [5,25,26]. Thereupon, AOPs are considered as promising technologies for urban wastewater treatment to meet the minimum quality requirements for wastewater safely reuse in agricultural irrigation.

3. Advanced oxidation processes

AOPs were first proposed in the 1980s for potable water treatment and later were widely applied for the treatment of different wastewaters [32,33]. AOPs mainly rely on the highly reactive oxygen species (ROS) generated from photocatalysis, electrochemistry, or peroxides, which can initiate the oxidation reaction in water to degrade micropollutants and damage microorganisms [34]. For chemical oxidation based-AOPs, ozone (O₃), hydrogen peroxide (H₂O₂), and persulfate (PS) are the most commonly used oxidant precursors [27,33]. Various oxidants activation methods, such as heat, ultraviolet, alkaline, transition metals, and carbonaceous materials, have been applied to generate ROS more efficiently [33,35,36]. A possible classification of AOPs includes two groups: homogeneous AOPs and heterogeneous AOPs.

3.1. Homogeneous AOPs

Here, the homogeneous AOPs employ O₃, H₂O₂, and persulfate, including peroxydisulfate (PDS, S₂O₈²⁻) and peroxymonosulfate (PMS, HSO₅⁻) are mainly discussed.

3.1.1. Ozone-based AOPs

Ozone is a strong oxidant with a high redox potential ($E^0 = 2.1 \text{ V}$) and can oxidize inorganic and organic substances, inactivate pathogens and ARB&Gs from water [22,29,37–39]. Ozonation of contaminants are processed via two ways: direct reaction by O₃ molecule, which preferentially reacts with the ionized and dissociated form of organic compounds, and indirect oxidation by hydroxy radical ([•]OH), which was generated from O₃ (Eq. (1)) to initiate the indiscriminate oxidation [33,38].



Ozone act as a disinfectant and as an oxidant has been applied at full-scale as tertiary treatment of urban wastewater to remove micropollutants and microorganisms in many

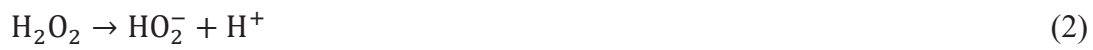
industrialized countries before discharge into the environment [38]. Switzerland is among the first to implement ozonation in full-scale and plans to upgrade about 100 out of 700 wastewater treatment plants [40]. Generally, an ozonation system is implemented after the activated sludge treatment where dissolved organic carbon (DOC) is lowest to minimize the ozone consumption, and followed by at least a biological filtration step (e.g., sand, biological activated carbon filtration) to remove biodegradable organic carbons (BDOC) generated as a consequence of the reaction of ozone and dissolved organic matters (DOM) and to prevent the regrowth of pathogenic bacteria after ozonation [38].

Micropollutant abatement is one important objective of ozone in wastewater treatment. Rizzo et al. recently reviewed the abatement kinetics of CECs at commonly applied specific ozone doses (0.4–0.6 g O₃/g DOC) and classified them into three categories, as shown in Table 2 [41]. CECs of group A, including azithromycin, bisphenol-A, carbamazepine, ciprofloxacin, clarithromycin, diclofenac, erythromycin, metoprolol, sulfamethoxazole, and the hormones 17-alpha-ethinylestradiol and 17-beta-estradiol, that predominantly react with ozone because their electron-rich moieties highly react with ozone [41]. The selectivity of the ozone reactivity is still decisive for the abatement of CECs of group B, including benzotriazole, bezafibrate, mecoprop and methylenbenzotriazole [41]. CECs of group C (i.e., acesulfame, iopromide and primidone) react too slowly with ozone to be eliminated and are considered as ozone-resistant, their reactivity was suggested to be influenced by their reaction of $\cdot\text{OH}$ [38,41,42].

Table 2. Categorization of CEC according to their abatement during ozonation of biologically treated wastewater (0.4–0.6 g O₃/g DOC) and their reactivity with ozone [41].

Group	Abatement	Reactivity with ozone	Reaction rate k_{O_3} ($M^{-1} s^{-1}$)
A	>80	High	$>10^3$
B	50–80%	Intermediate	10^2-10^3
C	<50%	Low	$<10^2$

To increase the utilization efficiency of ozone and to enhance the efficiency of organic pollutants mineralization, catalytic ozonation processes have been applied, peroxone process (O_3/H_2O_2 , Eq. (2)- (3)) and photolysis of ozone with UV light (UV/ O_3 , Eq. (4)- (5)) are the best-known ozone-based AOPs [38,43].



However, ozonation may result in the oxidation by-products deriving from the wastewater matrix, such as N-nitrosodimethylamine (NDMA) and bromate, and the formation of transformation products (TPs) resulting from the oxidation of CECs, and these TPs maybe not susceptible to ozone and can be even more toxic than the initial compounds [29,41]. The subsequent biological filter treatment step can be used to reduce the effluent toxicity.

Overall, the ozonation combined with a biological filter can be a good option for large UWTPs to simultaneously effectively degrade a wide range of CECs as well as limit the toxicity of its TPs and remove the abundance of pathogens as well as the ARB&Gs. For example, for a large UWTP (10,000 to 500,000 person equivalents) and DOC contents (6 to 20 g DOC m^{-3}), considering the capital investment and annual operation cost including post-filtration step, the total costs of ozonation were estimated to range between 0.05 and 0.15 € m^{-3} , depending on plant size and secondary effluent quality [38]. However, ozonation is generally only used at medium to large-sized plants after at least secondary treatment and is not economical for wastewater with high levels of organic carbon [27,44]. However, it should be noted that for wastewater reuse in

irrigation, in order to save transportation costs, the decentralized and small-sized UWTs near farmland in the suburbs or rural areas are the priority, thus ozonation is not considered in this study.

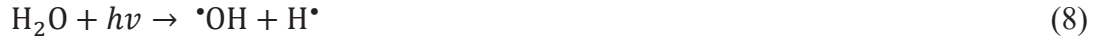
H₂O₂, PMS, and PDS-based homogeneous AOPs have been studied for water and wastewater treatment over past decades and exhibited effective degradation of a broad range of micropollutants, inactivation of pathogens, and reduction of ARB&Gs from urban wastewater [5,19,27,45–51]. Reactive species, such as free •OH, sulfate (SO₄^{•-}), and superoxide ion radicals (•O₂⁻) are usually believed as the primary ROSs and can be produced by different activation methods, such as UV, transition metal ions, complexing agents.

3.1.2. UV/ H₂O₂ and UV/PS

Conventional UV lamps use of mercury have widely applied for urban wastewater disinfection, which can effectively inhibit cell replication by damaging their DNA [17]. The application of light emitting diodes (LED) make UV-C LED very promising for water disinfection since they are much cheaper, smaller, lighter, and less fragile than traditional mercury vapor lamps [5,52]. Single UV can effectively degrade some organic contaminants but at high dose (> 10, 000 mJ/cm²), such as high abatement efficiency (>85%) of sulfonamides, quinolones, NDMA, herbicides and pesticides from water [5,53,54], however, it exhibited low removal capacity for most CECs [54,55].

In combination with peroxides (e.g., H₂O₂, PS), UV-based AOPs leading to the formation of •OH and SO₄^{•-} through the fission of O-O bond by energy input of UV as presented in Eq. (5) - (7), or through photolysis of water (Eq. (8)) at a UV less than 242 nm [33,55], can significantly enhance the micropollutants degradation and pathogens inactivation efficiency in water [56–58].

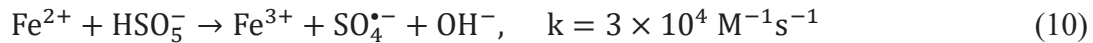
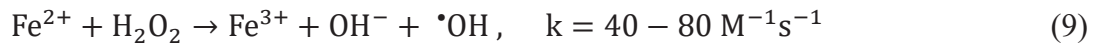




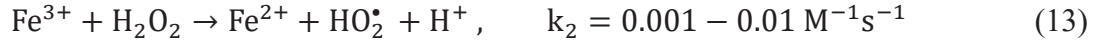
However, for wastewater application, since turbidity and TSS can drastically decrease UV efficiency, UV irradiation requires extensive secondary treatment and conventional depth filtration (e.g., sand filtration) to reach a recommended water transmittance value over 50% and probably it is not adapted to open treatment systems (e.g., lagoons or constructed wetlands) where green colored microscopic algae can grow [5,15]. More importantly, the efficiency of those technologies is decreased in wastewater since the radicals are easily scavenged by DOM, and the toxic and sensory-unpleasant TPs are commonly generated during UV-AOPs of organic micropollutants and DOM [59,60]. These are all potential barriers to their practical applications.

3.1.3. Photo Fenton and Fenton-like AOPs

Compared with energy input activation methods (e.g., UV), transition metal ions, such as ferrous ions (Fe^{2+}), exhibited the advantages of low energy consumption and strong activity. The classical Fenton reaction describes the activation H_2O_2 of by dissolving Fe^{2+} in solution to generate $\bullet\text{OH}$ (Eq. (9)) [61]. Fe^{2+} is also efficient for PMS and PDS activation (Eq. (10)-(12)) [62].



The formed ferric ion (Fe^{3+}) is a major limitation of homogeneous Fe-based AOPs because it starts to precipitate in the form of ferric hydroxides when pH is higher than 3 [62]. Even though the regeneration of Fe^{2+} occurred in the system, noted as Eq. (13), but its reaction rate is much slower than the oxidation of Fe^{2+} , and the steady accumulation of Fe^{3+} can cause heavy iron sludge production.



Therefore, homogeneous Fe-based AOPs are limited for practical application because of the strict low pH operation condition and heavy iron sludge production [51,61]. To overcome the disadvantages of the conventional Fenton process, apart from using the appropriate ratio of iron ions to oxidants, adding Fe solution sequentially, photo-Fenton processes were widely studied, which can enhance the reduction of Fe^{3+} to Fe^{2+} and improve the generation of generate $\bullet\text{OH}$, as presented in Eq. (5), (9), and (14) [33,62–65].



With the addition of irradiation, less H_2O_2 and Fe^{2+} consumption leading less iron sludge production compared with the conventional Fenton process [63]. Besides, photo-Fenton can use sunlight instead of UV light to save energy costs and to make the process sustainable [30,63]. Nevertheless, the strict acidic working pH problem of photo-Fenton processes still exists. Under these circumstances, to take advantage of the good performance of the photo-Fenton process, one possible way to improve this process to work at wider pH is to introduce chelating agents (L), such as oxalate, ethylenediamine-N, N'-disuccinic acid (EDDS), to the solar photo-Fenton system to solubilize Fe^{3+} to form Fe(III) complex, as noted in Eq. (15), which can absorb UV–vis light and undergo photochemical reductions leading to Fe^{2+} ions to realize the Fe redox cycle, as presented in Eq. (16) [64].



For example, Maniakova et al., recently reported efficient simultaneous removal CECs and pathogens from urban wastewater by solar driven photo-Fenton with the addition of EDDS [30]. However, the cost of the chelator, the biodegradability and ecotoxicity

of the complex formed, and the strong weather variation effects of solar photo-Fenton processes should be considered. In addition, one limitation is the low volume able to be treated by this photo-Fenton even when using raceway open reactors [30,65].

Another method to overcome the processing and economic constraints associated with homogeneous Fenton and Fenton-like oxidation processes, such as recycling difficulty, acidic working pH, and iron sludge production, is to make use of recyclable solid catalysts instead of iron metal ions [63], which defined as heterogeneous Fenton and Fenton-like oxidation processes (HFOPs).

3.2. Heterogeneous Fenton-like oxidation processes

HFOPs using transition metal oxides, such as iron oxides, copper oxides (CuO), and manganese (MnO₂), as catalysts have drawn increasing attention recently to degrade organic contaminants and inactivate pathogens effectively due to their low cost, relatively low toxicity levels, high catalytic activity and easy methods for recovery and scale-up [27,66–69]. However, there has been a long-term debate on the peroxide's activation pathways and the produced intermediate oxidants (e.g., radicals, singlet oxygen, catalysts - peroxide complexes, high valent metal ions) in HFOPs [66,70,71].

3.2.1. Radical-based systems

$\cdot\text{OH}$ (E^0 ($\cdot\text{OH}$) = 1.9–2.7 V) and $\text{SO}_4^{\cdot-}$ (E^0 ($\text{SO}_4^{\cdot-}$) = 2.5–3.1 V) with high redox potential are long recognized as the responsible reactive species in HFOPs to degrade organic pollutants and inactivate pathogens [27,66,67,72]. Using iron oxides as examples, the possible surface bound radicals-based activation pathways (Figure 3) in HFOPs are similar to homogeneous peroxide activation (Eq. (9)-(11)) [73–75].

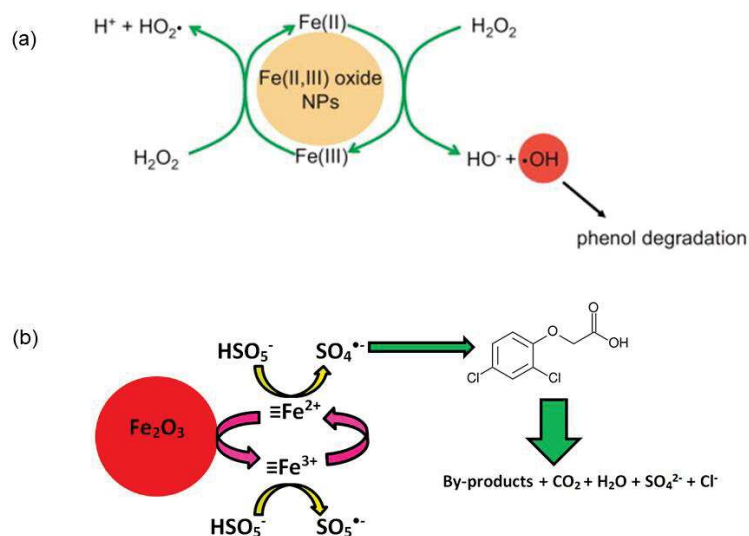


Figure 3. The activation pathways initiated by the (a) magnetite activated H_2O_2 [73] and (b) hematite activated PMS processes [74].

$\bullet\text{OH}$ is known as non-selective species that can degrade a wide range of organic contaminants, while $\text{SO}_4^{\bullet-}$ has a higher redox potential of key radical species ($E^0(\text{SO}_4^{\bullet-}) = 2.5\text{--}3.1\text{ V} > E^0(\bullet\text{OH}) = 1.9\text{--}2.7\text{ V}$), a longer half time ($3\text{--}4 \times 10^{-5}\text{ s} > 2 \times 10^{-8}\text{ s}$), a wider working pH range ($\text{pH} = 2.0\text{--}8.0$), and higher selectivity to the electron-rich compounds via a single electron transfer pathway [36,76]. However, both radicals can be quenched by organic matter, moreover, the oxidation by $\text{SO}_4^{\bullet-}$ favors the direct electron abstraction and can transform some anions (e.g., Cl^- and NO_2^-) into their corresponding radicals potentially leading to troublesome chlorinated and nitrated TPs [48,77]. It should be noted that the HFOPs with the purpose to remove micropollutants, pathogens, and antibiotic resistance are widely applied as the last barrier in the wastewater reclamation train after carbon and nutrients removals. However, in irrigation application, what is needed is a technology that can work in presence of high contents of dissolved organic matter and nutrients because both are valuable agronomic parameters to be preserved [4]. Thus, HFOPs relying on radical-based mechanisms undergo efficiency losses in organic-rich wastewater such as urban wastewater due to the competing organic/inorganic constituents of water [48] and due to the difficulty in

the regeneration of active sites on the surface of the catalyst due to the energetically unfavorable metal ion redox cycle [69].

In contrast to radical-based processes, the non-radical oxidative pathway is much more selective than radicals, accounting for the only removal of electron-rich organic contaminants (e.g., phenols and anilines) [78,79]. In addition, the mild non-radical based processes consume less amount of oxidant and are less influenced by the competing organic/inorganic constituent in urban wastewater, thereby limiting the formation of hazardous TPs.

3.2.2. Non-radical-based systems

The non-radical pathway including (1) oxidant surface metastable complexes over the catalyst, (2) singlet oxygen ($^1\text{O}_2$), and (3) the high valent metal-oxo oxidant species have been proposed for HFOPs [36,69,70,80].

(1) Surface activated complexes

Surface activated complexes result from the interaction between catalyst and oxidant through an outer-sphere surface complexation [78,79]. Surface activated complexes have not been reported on single iron oxides yet but on FeMn composite oxide and layered CuFe oxide [81,82]. As shown in Figure 4a, the activated PDS acted as a two-electrons transfer oxidant that directly accepts electrons from organic pollutants through an electron shuttle material leading to sulfate anions (SO_4^{2-}) release [78,79]. To the best of our knowledge, the investigation of surface activated complexes has only been reported in the field of organic contaminants degradation.

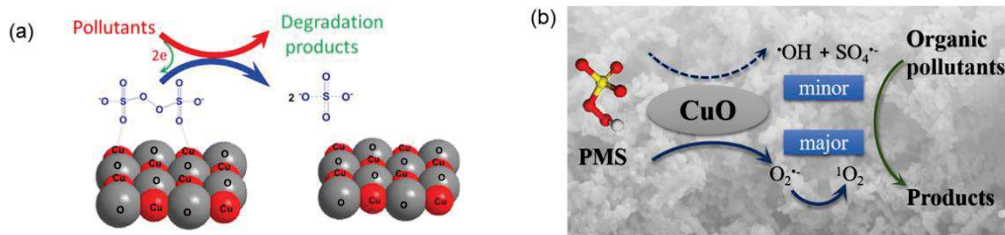


Figure 4. (a) Surface activated complexes and (b) singlet oxygen-based processes [78,83].

(2) Single oxygen

Certain recent studies have reported the occurrence of $^1\text{O}_2$ as another type of non-radical process as previously reported in the HFOPs [83–86]. $\text{O}_2^{\bullet-}$ might function as a precursor for the generation of $^1\text{O}_2$ through $\text{O}_2^{\bullet-}$ oxidation or disproportionation reactions, as shown in Eq. (17) and Figure 4b.



The $^1\text{O}_2$ -based systems are very known for their resistance to background substances in the water matrix and for inactivating a wide range of bacteria and viruses as a potential disinfectant due to its oxidation capacity of proteins and DNA [87–89]. However, $^1\text{O}_2$ based systems have been regarded to be poorly efficient because $^1\text{O}_2$ is rapidly quenched by water [90,91].

(3) High valent metal ions

High valent metal ions, such as ferryl ions (Fe(IV)) and cupryl ions (Cu(III)) have been also recently suggested and proved to be the working oxidant in homogeneous (Figure 5a and b) and heterogeneous (Figure 5c and d) Fenton and Fenton-like processes [92–96].

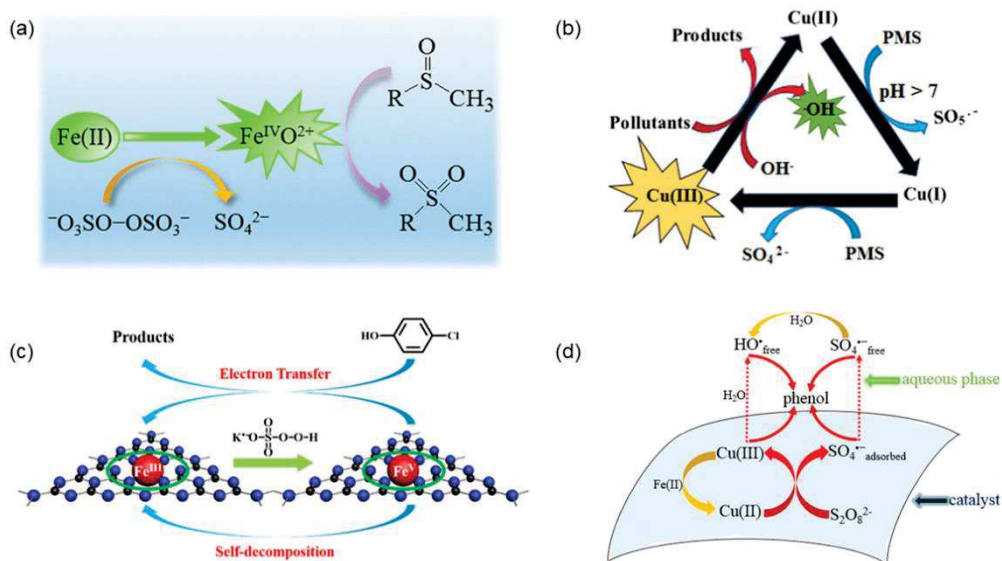


Figure 5. The formation of ferryl ion in (a) Fe(II)/PDS, (c) Fe(III) doped $g\text{-C}_3\text{N}_4$ /PMS, and cupryl ion in (b) Cu(II)/PMS, (d) CuO-Fe₃O₄/PDS systems [94,96–98].

As shown in Figure 5a, the generated ferryl oxo ($\text{Fe}^{\text{IV}}\text{O}^{2+}$) is a powerful oxidant that can react with inorganic ions and organic compounds (e.g., aromatic substrates and aliphatic alcohols) through electron or atom (hydride, hydrogen, or oxygen) transfer, it can also oxidize sulfoxide to sulfone, which is the specific reaction associated to Fe(IV) and Cu(III) [96]. The generation of Cu(III) in a highly electron deficient state offers the highest redox potential for PMS activation ($E^0\text{Cu(III)/Cu(II)} = 2.3 \text{ V}$) that can oxidize electron-rich organic contaminants [94,99] or decompose into $\cdot\text{OH}$, depending on the water pH value [100]. Fe(IV) and Cu(III) have also been identified as the working species in HFOPs during PS activation by using Fe(III) doped $g\text{-C}_3\text{N}_4$ and CuO-Fe₃O₄ [97,98]. However, it has not been reported yet on single iron oxide or copper oxide. In addition to the electron-rich compounds degradation capacity, Cu(III) also exhibited excellent antimicrobial activity, especially against viruses [101,102].

Therefore, this study aimed to contemplate the possibility to implement a HFOP relying on more selective reactive species than sulfate and hydroxyl radicals, which might work in organic-rich wastewater for urban wastewater treatment in terms of micro-pollutant

degradation, pathogen inactivation, and reduction of antibiotic resistance. CuO was selected as the heterogeneous catalyst because it has a similar redox behavior to iron oxide, but has been less studied and has more diverse activation pathways [69]. In addition, CuO in form of nanoparticles exhibits effective antimicrobial activity [103–106]. PDS was selected as the working oxidant taking into consideration its lower costs of storage and transportation due to the availability and stability of peroxydisulfate salts (0.74 \$/kg of PDS vs. 1.5 \$/kg of H₂O₂ vs. 2.2 \$/kg of PMS) [48].

4. Fixed-bed column

The evaluation of the performances of HFOPs presented in the literature and cited throughout this introduction is carried out in its vast majority by working on very small quantities of solid materials of nano or micrometric characteristic dimension, suspended in the solution to be treated and placed in closed reactors operating in batch mode [75,78,79,84,107]. These conditions are ideal and perfectly adapted to mechanistic and kinetic studies at the laboratory scale. In such systems that can be considered as perfectly stirred, the concentrations are uniform, the adopted particle sizes are by definition favorable to obtain high reaction rates due to a large effluent/catalyst contact surface. Nevertheless, a complete evaluation of the feasibility of a process whose aim is to be applied in a water treatment plant requires to be evaluated according to the continuous flow operating mode. In the case of solid/liquid two-phases systems, a common design for this type of operation in process engineering is the packed fixed bed. It is the standard in filtration processes [108], it is commonly used in adsorption separation processes [109] and reaction catalysts [110], but it has been scarcely studied in advanced oxidation [111–116]. To our knowledge, in this configuration, only one study has been done on the copper oxides in the case of a column of small size filled with nanoparticles deposited on alumina beds [117].

5. Aims

Therefore, the main aim of this thesis is to investigate the heterogeneous Fenton-like system based on copper oxide and peroxydisulfate for urban wastewater treatment in terms of simultaneous decontamination and disinfection as well as limit the spreading of antibiotic resistance to meet the minimum safety irrigation quality requirements.

The specific aims of this study were to:

- 1) Explore the mechanisms of the CuO/PDS system, and evaluate the selectivity and applicability of this system to CECs in batch mode. Phenol was first selected as the probe pollutant. Kinetic studies, identification of reactive species by using scavengers, identification of TPs by liquid chromatography-high resolution-mass spectrometry (LC-HRMS) and the elucidation of transformation pathways were carried out to unveil the mechanisms. Then, the effects of operating parameters such as reusability in wastewater were investigated. Finally, antibiotics (i.e., cephalexin (CFX), ciprofloxacin (CIP), clarithromycin (CLA), and sulfamethoxazole (SMX)) as representatives of CECs were applied to this system (Chapter 2).
- 2) Evaluate the performances of the CuO/PDS system in terms of inactivating a broad range of pathogenic microorganisms, antibiotic-resistant bacteria, and antibiotic-resistance genes in urban wastewater in batch mode. To achieve this purpose, the disinfection performance of this system was firstly evaluated and compared with chlorination as a reference of conventional disinfectant and thermally activated PDS as a reference of sulfate radical-based disinfection process by using *Escherichia coli* (*E. coli*), *Enterococcus*, *F-specific RNA coliphages*, and *spores of sulfite-reducing bacteria* as pathogenic indicators. In addition to secondary treated urban wastewater (STWW), raw wastewater was also collected and disinfected to contemplate the possibility of applying this system in the areas that lack well-equipped UWTPs. Then, the predominant reactive species were identified to better understand the system. Last but equally importantly, the abundance reduction of selected ARB&Gs was evaluated (Chapter 3).

3) Demonstrate the feasibility of continuous treatment of emerging contaminants and pathogens contained in urban wastewater treatment. In order to do this, we firstly performed a comprehensive experimental study using the simplest solution to be treated that consisted of phenol in distilled water to determine the effect of operational parameters, such as the inflow PDS concentration, flow rate, and to better understand the working mode of this new process. The decontamination and disinfection performances of STWW were investigated by using a mixture of antibiotics (i.e., CFX, CLA, SMX, amoxicillin (AMX), and ofloxacin (OFL)) and the same pathogenic indicator as to the batch mode. Cu(II) leaching analysis and the characterization of CuO pellet before and after treatment by scanning electron microscopy (SEM) and X-ray diffraction (XRD) were conducted at the end for catalyst stability evaluation (Chapter 4).

To end, the global objective will be to achieve enough data and certainty to be able to estimate according to quantitative and qualitative facts the possibility to develop, at mid-term, a robust and low-cost HFOP based on CuO and PDS is adapted for advanced wastewater treatment system. Such a process has, ideally, to be able to perform simultaneously micropollutants degradation, pathogens inactivation, as well as antibiotic resistance reduction, while preserving the maximum amount of carbon and nutrients.

References

- [1] World Resources Institute, Water stress by country, (2013). <https://www.wri.org/insights/17-countries-home-one-quarter-worlds-population-face-extremely-high-water-stress>
- [2] AQUASTAT - FAO's global water information system, Water factsheets, AQUASTAT, FAO's Glob. Water Inf. Syst. (2014) 6. https://doi.org/http://www.fao.org/nr/water/aquastat/infographics/Infographics_all_eng.pdf.
- [3] S. Ofori, A. Puškáčová, I. Růžičková, J. Wanner, Treated wastewater reuse for irrigation: Pros and cons, *Sci. Total Environ.* 760 (2021). <https://doi.org/10.1016/j.scitotenv.2020.144026>.
- [4] M.F. Jaramillo, I. Restrepo, Wastewater reuse in agriculture: A review about its limitations and benefits, *Sustain.* 9 (2017). <https://doi.org/10.3390/su9101734>.
- [5] L. Rizzo, W. Gernjak, P. Krzeminski, S. Malato, C.S. McArdell, J.A.S. Perez, H. Schaar, D. Fatta-Kassinos, Best available technologies and treatment trains to address current challenges in urban wastewater reuse for irrigation of crops in EU countries, *Sci. Total Environ.* 710 (2020) 136312. <https://doi.org/10.1016/j.scitotenv.2019.136312>.
- [6] H. Aslani, R. Nabizadeh, M. Alimohammadi, A. Mesdaghinia, K. Nadafi, R. Nemati, M. Ghani, Disinfection of raw wastewater and activated sludge effluent using Fenton like reagent, *J. Environ. Heal. Sci. Eng.* 12 (2014) 1–7. <https://doi.org/10.1186/s40201-014-0149-8>.
- [7] World Health Organization, Guidelines for the safe use of wastewater, excreta and greywater, 2006.
- [8] EPA/625/R-04/108, Guidelines for Water Reuse, Development. (2004).
- [9] EU, Official Journal of the European Union, *Off. J. Eur. Union.* 63 (2020).
- [10] P.Y. Hong, N. Al-Jassim, M.I. Ansari, R.I. Mackie, Environmental and public health implications of water reuse: Antibiotics, antibiotic resistant bacteria, and

- antibiotic resistance genes, *Antibiotics*. 2 (2013) 367–399. <https://doi.org/10.3390/antibiotics2030367>.
- [11] M. Pazda, J. Kumirska, P. Stepnowski, E. Mulkiewicz, Antibiotic resistance genes identified in wastewater treatment plant systems – A review, *Sci. Total Environ.* 697 (2019) 134023. <https://doi.org/10.1016/j.scitotenv.2019.134023>.
- [12] World Health Organization, Global antimicrobial resistance surveillance system, 2015.
- [13] M. Salgot, M. Folch, Wastewater treatment and water reuse, *Curr. Opin. Environ. Sci. Heal.* 2 (2018) 64–74. <https://doi.org/10.1016/j.coesh.2018.03.005>.
- [14] J. Wang, L. Chu, L. Wojnárovits, E. Takács, Occurrence and fate of antibiotics, antibiotic resistant genes (ARGs) and antibiotic resistant bacteria (ARB) in municipal wastewater treatment plant: An overview, *Sci. Total Environ.* 744 (2020) 140997. <https://doi.org/10.1016/j.scitotenv.2020.140997>.
- [15] H. Hashemi, A. Bovini, Y. Hung, M. Amin, A review on wastewater disinfection, *Int. J. Environ. Health Eng.* 2 (2013) 22. <https://doi.org/10.4103/2277-9183.113209>.
- [16] X. Yang, C. Shang, J.C. Huang, DBP formation in breakpoint chlorination of wastewater, *Water Res.* 39 (2005) 4755–4767. <https://doi.org/10.1016/j.watres.2005.08.033>.
- [17] R. Gehr, M. Wagner, P. Veerasubramanian, P. Payment, Disinfection efficiency of peracetic acid, UV and ozone after enhanced primary treatment of municipal wastewater, *Water Res.* 37 (2003) 4573–4586. [https://doi.org/10.1016/S0043-1354\(03\)00394-4](https://doi.org/10.1016/S0043-1354(03)00394-4).
- [18] M. Kitis, Disinfection of wastewater with peracetic acid: A review, *Environ. Int.* 30 (2004) 47–55. [https://doi.org/10.1016/S0160-4120\(03\)00147-8](https://doi.org/10.1016/S0160-4120(03)00147-8).
- [19] V.K. Sharma, N. Johnson, L. Cizmas, T.J. McDonald, H. Kim, A review of the influence of treatment strategies on antibiotic resistant bacteria and antibiotic resistance genes, *Chemosphere.* 150 (2016) 702–714.

- <https://doi.org/10.1016/j.chemosphere.2015.12.084>.
- [20] V. Kårelid, G. Larsson, B. Björleinius, Pilot-scale removal of pharmaceuticals in municipal wastewater: Comparison of granular and powdered activated carbon treatment at three wastewater treatment plants, *J. Environ. Manage.* 193 (2017) 491–502. <https://doi.org/10.1016/j.jenvman.2017.02.042>.
- [21] C. Sophia A., E.C. Lima, C.S. A., E.C. Lima, Removal of emerging contaminants from the environment by adsorption, *Ecotoxicol. Environ. Saf.* 150 (2018) 1–17. <https://doi.org/10.1016/j.ecoenv.2017.12.026>.
- [22] J. Margot, C. Kienle, A. Magnet, M. Weil, L. Rossi, L.F. de Alencastro, C. Abegglen, D. Thonney, N. Chèvre, M. Schärer, D.A. Barry, Treatment of micropollutants in municipal wastewater: Ozone or powdered activated carbon?, *Sci. Total Environ.* 461–462 (2013) 480–498. <https://doi.org/10.1016/j.scitotenv.2013.05.034>.
- [23] M.J. Ahmed, B.H. Hameed, Removal of emerging pharmaceutical contaminants by adsorption in a fixed-bed column: A review, *Ecotoxicol. Environ. Saf.* 149 (2018) 257–266. <https://doi.org/10.1016/j.ecoenv.2017.12.012>.
- [24] M. Brienza, S. Nir, G. Plantard, V. Goetz, S. Chiron, Combining micelle-clay sorption to solar photo-Fenton processes for domestic wastewater treatment, *Environ. Sci. Pollut. Res.* 26 (2019) 18971–18978. <https://doi.org/10.1007/s11356-018-2491-3>.
- [25] M. Bodzek, K. Konieczny, M. Rajca, Membranes in water and wastewater disinfection – review, *Arch. Environ. Prot.* 45 (2019) 3–18. <https://doi.org/10.24425/aep.2019.126419>.
- [26] S. Hube, M. Eskafi, K.F. Hrafnkelsdóttir, B. Bjarnadóttir, M.Á. Bjarnadóttir, S. Axelsdóttir, B. Wu, Direct membrane filtration for wastewater treatment and resource recovery: A review, *Sci. Total Environ.* 710 (2020). <https://doi.org/10.1016/j.scitotenv.2019.136375>.
- [27] Y. di Chen, X. Duan, X. Zhou, R. Wang, S. Wang, N. qi Ren, S.H. Ho, Advanced

- oxidation processes for water disinfection: Features, mechanisms and prospects, *Chem. Eng. J.* 409 (2021) 128207. <https://doi.org/10.1016/j.cej.2020.128207>.
- [28] D. Ghernaout, Advanced oxidation processes for wastewater treatment: facts and future trends, *OALib.* 07 (2020) 1–15. <https://doi.org/10.4236/oalib.1106139>.
- [29] I.C. Iakovides, I. Michael-Kordatou, N.F.F. Moreira, A.R. Ribeiro, T. Fernandes, M.F.R. Pereira, O.C. Nunes, C.M. Manaia, A.M.T. Silva, D. Fatta-Kassinos, Continuous ozonation of urban wastewater: Removal of antibiotics, antibiotic-resistant *Escherichia coli* and antibiotic resistance genes and phytotoxicity, *Water Res.* 159 (2019) 333–347. <https://doi.org/10.1016/j.watres.2019.05.025>.
- [30] G. Maniakova, I. Salmerón, M.I. Polo-López, I. Oller, L. Rizzo, S. Malato, Simultaneous removal of contaminants of emerging concern and pathogens from urban wastewater by homogeneous solar driven advanced oxidation processes, *Sci. Total Environ.* 766 (2021) 144320. <https://doi.org/10.1016/j.scitotenv.2020.144320>.
- [31] Y. Luo, W. Guo, H.H. Ngo, L.D. Nghiem, F.I. Hai, J. Zhang, S. Liang, X.C. Wang, A review on the occurrence of micropollutants in the aquatic environment and their fate and removal during wastewater treatment, *Sci. Total Environ.* 473–474 (2014) 619–641. <https://doi.org/10.1016/j.scitotenv.2013.12.065>.
- [32] W.H. Glaze, J.W. Kang, D.H. Chapin, The chemistry of water treatment processes involving ozone, hydrogen peroxide and ultraviolet radiation, *Ozone Sci. Eng.* 9 (1987) 335–352. <https://doi.org/10.1080/01919518708552148>.
- [33] Y. Deng, R. Zhao, Advanced oxidation processes (AOPs) in wastewater treatment, *Curr. Pollut. Reports.* 1 (2015) 167–176. <https://doi.org/10.1007/s40726-015-0015-z>.
- [34] X. Duan, H. Sun, Z. Shao, S. Wang, Nonradical reactions in environmental remediation processes: Uncertainty and challenges, *Appl. Catal. B Environ.* 224 (2018) 973–982. <https://doi.org/10.1016/j.apcatb.2017.11.051>.
- [35] A. Vogelpohl, S.M. Kim, Advanced oxidation processes (AOPs) in wastewater

- treatment, *J. Ind. Eng. Chem.* 10 (2004) 33–40.
- [36] J. Lee, U. Von Gunten, J.H. Kim, Persulfate-based advanced oxidation: Critical assessment of opportunities and roadblocks, *Environ. Sci. Technol.* 54 (2020) 3064–3081. <https://doi.org/10.1021/acs.est.9b07082>.
- [37] L. Chen, Z. Zhou, C. Shen, Y. Xu, Inactivation of antibiotic-resistant bacteria and antibiotic resistance genes by electrochemical oxidation/electroFenton process, *Water Sci. Technol.* 81 (2020) 2221–2231. <https://doi.org/10.2166/wst.2020.282>.
- [38] C. von Sonntag, U. von Gunten, Chemistry of ozone in water and wastewater treatment: From basic principles to applications, 2015. <https://doi.org/10.2166/9781780400839>.
- [39] U. Von Gunten, Ozonation of drinking water: Part II. Disinfection and by-product formation in presence of bromide, iodide or chlorine, *Water Res.* 37 (2003) 1469–1487. [https://doi.org/10.1016/S0043-1354\(02\)00458-X](https://doi.org/10.1016/S0043-1354(02)00458-X).
- [40] N. Czekalski, S. Imminger, E. Salhi, M. Veljkovic, K. Kleffel, D. Drissner, F. Hammes, H. Bürgmann, U. Von Gunten, Inactivation of antibiotic resistant bacteria and resistance genes by ozone: From laboratory experiments to full-scale wastewater treatment, *Environ. Sci. Technol.* 50 (2016) 11862–11871. <https://doi.org/10.1021/acs.est.6b02640>.
- [41] L. Rizzo, S. Malato, D. Antakyali, V.G. Beretsou, M.B. Đolić, W. Gernjak, E. Heath, I. Ivancev-Tumbas, P. Karaolia, A.R. Lado Ribeiro, G. Mascolo, C.S. McArdell, H. Schaar, A.M.T. Silva, D. Fatta-Kassinos, Consolidated vs new advanced treatment methods for the removal of contaminants of emerging concern from urban wastewater, *Sci. Total Environ.* 655 (2019) 986–1008. <https://doi.org/10.1016/j.scitotenv.2018.11.265>.
- [42] U. Von Gunten, Ozonation of drinking water: Part I. Oxidation kinetics and product formation, *Water Res.* 37 (2003) 1443–1467. <http://www.sciencedirect.com/science/article/pii/S0043135402004578>.

- [43] J. Wang, H. Chen, Catalytic ozonation for water and wastewater treatment: Recent advances and perspective, *Sci. Total Environ.* 704 (2020) 135249. <https://doi.org/10.1016/j.scitotenv.2019.135249>.
- [44] US EPA, Wastewater technology fact sheet ozone disinfection, 1999.
- [45] L.L.S. Silva, C.G. Moreira, B.A. Curzio, F. V. da Fonseca, Micropollutant removal from water by membrane and advanced oxidation processes—A review, *J. Water Resour. Prot.* 09 (2017) 411–431. <https://doi.org/10.4236/jwarp.2017.95027>.
- [46] D. Kiejza, U. Kotowska, W. Polińska, J. Karpińska, Peracids - New oxidants in advanced oxidation processes: The use of peracetic acid, peroxymonosulfate, and persulfate salts in the removal of organic micropollutants of emerging concern – A review, *Sci. Total Environ.* 790 (2021). <https://doi.org/10.1016/j.scitotenv.2021.148195>.
- [47] M. Brienza, I.A. Katsoyiannis, Sulfate radical technologies as tertiary treatment for the removal of emerging contaminants from wastewater, *Sustain.* 9 (2017) 1–18. <https://doi.org/10.3390/su9091604>.
- [48] S. Waclawek, H. V Lutz, K. Gröbel, V.V.T. Padil, M. Černík, D.D. Dionysiou, Chemistry of persulfates in water and wastewater treatment: A review, *Chem. Eng. J.* 330 (2017) 44–62. <https://doi.org/10.1016/j.cej.2017.07.132>.
- [49] C. shuang Zhou, J. wen Wu, L. li Dong, B. feng Liu, D. feng Xing, S. shan Yang, X. kun Wu, Q. Wang, J. ning Fan, L. ping Feng, G. li Cao, Removal of antibiotic resistant bacteria and antibiotic resistance genes in wastewater effluent by UV-activated persulfate, *J. Hazard. Mater.* 388 (2020) 122070. <https://doi.org/10.1016/j.jhazmat.2020.122070>.
- [50] Q. Qiu, G. Li, Y. Dai, Y. Xu, P. Bao, Removal of antibiotic resistant microbes by Fe(II)-activated persulfate oxidation, *J. Hazard. Mater.* 396 (2020) 122733. <https://doi.org/10.1016/j.jhazmat.2020.122733>.
- [51] B. Jain, A.K. Singh, H. Kim, E. Lichtfouse, B. Jain, A.K. Singh, H. Kim, E.

- Lichtfouse, V.S. Treatment of organic pollutants by homogeneous and heterogeneous Fenton reaction processes, *Environ. Chem. Lett.* 16 (2019) 947–967.
- [52] S.E. Beck, H. Ryu, L.A. Boczek, J.L. Cashdollar, K.M. Jeanis, J.S. Rosenblum, O.R. Lawal, K.G. Linden, Evaluating UV-C LED disinfection performance and investigating potential dual-wavelength synergy, *Water Res.* 109 (2017) 207–216. <https://doi.org/10.1016/j.watres.2016.11.024>.
- [53] S. Sarathy, M. Mohseni, An overview of UV-based advanced oxidation processes for drinking water treatment, *IUVA News.* 7 (2006) 1–12. http://www.iuva.org/sites/default/files/member/news/IUVA_news/Vol08/Issue2/MohseniArticle.pdf.
- [54] Y. Lee, D. Gerrity, M. Lee, S. Gamage, A. Pisarenko, R.A. Trenholm, S. Canonica, S.A. Snyder, U. Von Gunten, Organic contaminant abatement in reclaimed water by UV/H₂O₂ and a combined process consisting of O₃/H₂O₂ followed by UV/H₂O₂: Prediction of abatement efficiency, energy consumption, and byproduct formation, *Environ. Sci. Technol.* 50 (2016) 3809–3819. <https://doi.org/10.1021/acs.est.5b04904>.
- [55] J. Wang, S. Wang, Activation of persulfate (PS) and peroxymonosulfate (PMS) and application for the degradation of emerging contaminants, *Chem. Eng. J.* 334 (2018) 1502–1517. <https://doi.org/10.1016/j.cej.2017.11.059>.
- [56] S. Bounty, R. Rodriguez, K.G. Linden, Inactivation of adenovirus using low-dose UV/H₂O₂ advanced oxidation, *Water Res.* (2012). <https://doi.org/10.1016/j.watres.2012.08.036>.
- [57] P. Sun, C. Tyree, C.H. Huang, Inactivation of *Escherichia coli*, bacteriophage MS2, and *Bacillus* Spores under UV/H₂O₂ and UV/peroxydisulfate advanced disinfection conditions, *Environ. Sci. Technol.* 50 (2016) 4448–4458. <https://doi.org/10.1021/acs.est.5b06097>.
- [58] M. Li, W. Li, D. Wen, J.R. Bolton, E.R. Blatchley, Z. Qiang, Micropollutant

- degradation by the UV/H₂O₂ process: kinetic comparison among various radiation sources, *Environ. Sci. Technol.* 53 (2019) 5241–5248. <https://doi.org/10.1021/acs.est.8b06557>.
- [59] W.L. Wang, Q.Y. Wu, N. Huang, Z. Bin Xu, M.Y. Lee, H.Y. Hu, Potential risks from UV/H₂O₂ oxidation and UV photocatalysis: A review of toxic, assimilable, and sensory-unpleasant transformation products, *Water Res.* 141 (2018) 109–125. <https://doi.org/10.1016/j.watres.2018.05.005>.
- [60] W. Zhang, S. Zhou, J. Sun, X. Meng, J. Luo, D. Zhou, J. Crittenden, Impact of chloride ions on UV/H₂O₂ and UV/persulfate advanced oxidation processes, *Environ. Sci. Technol.* 52 (2018) 7380–7389. <https://doi.org/10.1021/acs.est.8b01662>.
- [61] H.J.H. Fenton, Oxidation of tartaric acid in presence of iron, *J. Chem. Soc. Trans.* 65 (1984) 899–910.
- [62] S. Xiao, M. Cheng, H. Zhong, Z. Liu, Y. Liu, X. Yang, Q. Liang, Iron-mediated activation of persulfate and peroxymonosulfate in both homogeneous and heterogeneous ways: A review, *Chem. Eng. J.* 384 (2020) 123265. <https://doi.org/10.1016/j.cej.2019.123265>.
- [63] A. De Luca, Fenton and Photo-Fenton like at neutral pH for the removal of emerging contaminants in water and wastewater effluents, 2016.
- [64] L. Clarizia, D. Russo, I. Di Somma, R. Marotta, R. Andreozzi, Homogeneous photo-Fenton processes at near neutral pH: A review, *Appl. Catal. B Environ.* 209 (2017) 358–371. <https://doi.org/10.1016/j.apcatb.2017.03.011>.
- [65] I. de la Obra Jiménez, S. Giannakis, D. Grandjean, F. Breider, G. Grunauer, J.L. Casas López, J.A. Sánchez Pérez, C. Pulgarin, Unfolding the action mode of light and homogeneous vs. heterogeneous photo-Fenton in bacteria disinfection and concurrent elimination of micropollutants in urban wastewater, mediated by iron oxides in Raceway Pond Reactors, *Appl. Catal. B Environ.* 263 (2020) 118158. <https://doi.org/10.1016/j.apcatb.2019.118158>.

- [66] H. Luo, Y. Zeng, D. He, X. Pan, Application of iron-based materials in heterogeneous advanced oxidation processes for wastewater treatment: A review, *Chem. Eng. J.* 407 (2021) 127191. <https://doi.org/10.1016/j.cej.2020.127191>.
- [67] A. V. Karim, Y. Jiao, M. Zhou, P. V. Nidheesh, Iron-based persulfate activation process for environmental decontamination in water and soil, *Chemosphere*. 265 (2021) 129057. <https://doi.org/10.1016/j.chemosphere.2020.129057>.
- [68] A.D. Bokare, W. Choi, Review of iron-free Fenton-like systems for activating H₂O₂ in advanced oxidation processes, *J. Hazard. Mater.* 275 (2014) 121–135. <https://doi.org/10.1016/j.jhazmat.2014.04.054>.
- [69] Y. Ding, L. Fu, X. Peng, M. Lei, C. Wang, J. Jiang, Copper catalysts for radical and nonradical persulfate based advanced oxidation processes: Certainties and uncertainties, *Chem. Eng. J.* 427 (2022) 131776. <https://doi.org/10.1016/j.cej.2021.131776>.
- [70] X. Duan, H. Sun, Z. Shao, S. Wang, Nonradical reactions in environmental remediation processes: Uncertainty and challenges, *Appl. Catal. B Environ.* 224 (2018) 973–982. <https://doi.org/10.1016/j.apcatb.2017.11.051>.
- [71] J. Huang, H. Zhang, Mn-based catalysts for sulfate radical-based advanced oxidation processes: A review, *Environ. Int.* 133 (2019) 105141. <https://doi.org/10.1016/j.envint.2019.105141>.
- [72] E. Safety, Rate constants of sulfate radical anion reactions with organic molecules: A review of Wojnárovits, Erzsébet, *Chemosphere*. 220 (2019) 1014–1032. <https://doi.org/10.1016/j.chemosphere.2018.12.156>.
- [73] K. Rusevova, F.D. Kopinke, A. Georgi, Nano-sized magnetic iron oxides as catalysts for heterogeneous Fenton-like reactions-Influence of Fe(II)/Fe(III) ratio on catalytic performance, *J. Hazard. Mater.* 241–242 (2012) 433–440. <https://doi.org/10.1016/j.jhazmat.2012.09.068>.
- [74] N. Jaafarzadeh, F. Ghanbari, M. Ahmadi, Catalytic degradation of 2,4-dichlorophenoxyacetic acid (2,4-D) by nano-Fe₂O₃ activated peroxymonosulfate:

- Influential factors and mechanism determination, *Chemosphere*. 169 (2017) 568–576. <https://doi.org/10.1016/j.chemosphere.2016.11.038>.
- [75] Y.C. Cho, R.Y. Lin, Y.P. Lin, Degradation of 2,4-dichlorophenol by CuO-activated peroxydisulfate: Importance of surface-bound radicals and reaction kinetics, *Sci. Total Environ.* 699 (2020) 134379. <https://doi.org/10.1016/j.scitotenv.2019.134379>.
- [76] W. Huang, S. Xiao, H. Zhong, M. Yan, X. Yang, Activation of persulfates by carbonaceous materials: A review, *Chem. Eng. J.* 418 (2021) 129297. <https://doi.org/10.1016/j.cej.2021.129297>.
- [77] L.R. Bennedsen, J. Muff, E.G. Søgaard, Influence of chloride and carbonates on the reactivity of activated persulfate, *Chemosphere*. 86 (2012) 1092–1097. <https://doi.org/10.1016/j.chemosphere.2011.12.011>.
- [78] T. Zhang, Y. Chen, Y. Wang, J. Le Roux, Y. Yang, J.P. Croué, Efficient peroxydisulfate activation process not relying on sulfate radical generation for water pollutant degradation, *Environ. Sci. Technol.* 48 (2014) 5868–5875. <https://doi.org/10.1021/es501218f>.
- [79] X. Du, Y. Zhang, I. Hussain, S. Huang, W. Huang, Insight into reactive oxygen species in persulfate activation with copper oxide: Activated persulfate and trace radicals, *Chem. Eng. J.* 313 (2017) 1023–1032. <https://doi.org/10.1016/j.cej.2016.10.138>.
- [80] S. Zhu, X. Li, J. Kang, X. Duan, S. Wang, Persulfate activation on crystallographic manganese oxides: Mechanism of singlet oxygen evolution for nonradical selective degradation of aqueous contaminants Shishu, *Environ. Sci. Technol.* 53 (2018) 307–315. <https://doi.org/10.1021/acs.est.8b04669>.
- [81] L. Yu, G. Zhang, C. Liu, H. Lan, H. Liu, J. Qu, Interface stabilization of undercoordinated iron centers on manganese oxides for nature-inspired peroxide activation, *ACS Catal.* 8 (2018) 1090–1096. <https://doi.org/10.1021/acscatal.7b03338>.

- [82] J. Liu, P. Wu, S.S. Yang, S. Rehman, Z. Ahmed, N. Zhu, Z. Dang, Z. Liu, A photo-switch for peroxydisulfate non-radical/radical activation over layered CuFe oxide: Rational degradation pathway choice for pollutants, *Appl. Catal. B Environ.* 261 (2020) 118232. <https://doi.org/10.1016/j.apcatb.2019.118232>.
- [83] S. Wang, S. Gao, J. Tian, Q. Wang, T. Wang, X. Hao, F. Cui, A stable and easily prepared copper oxide catalyst for degradation of organic pollutants by peroxymonosulfate activation, *J. Hazard. Mater.* 387 (2020) 121995. <https://doi.org/10.1016/j.jhazmat.2019.121995>.
- [84] S. Xing, W. Li, B. Liu, Y. Wu, Y. Gao, Removal of ciprofloxacin by persulfate activation with CuO: A pH-dependent mechanism, *Chem. Eng. J.* 382 (2020) 122837. <https://doi.org/10.1016/j.cej.2019.122837>.
- [85] S. Wang, J. Tian, Q. Wang, F. Xiao, S. Gao, W. Shi, F. Cui, Development of CuO coated ceramic hollow fiber membrane for peroxymonosulfate activation: a highly efficient singlet oxygen-dominated oxidation process for bisphenol a degradation, *Appl. Catal. B Environ.* 256 (2019) 117783. <https://doi.org/10.1016/j.apcatb.2019.117783>.
- [86] A. Jawad, K. Zhan, H. Wang, A. Shahzad, Z. Zeng, J. Wang, X. Zhou, H. Ullah, Z.Z.Z.Z.Z. Chen, Z.Z.Z.Z.Z. Chen, Tuning of Persulfate Activation from a Free Radical to a Nonradical Pathway through the Incorporation of Non-Redox Magnesium Oxide, *Environ. Sci. Technol.* 54 (2020) 2476–2488. <https://doi.org/10.1021/acs.est.9b04696>.
- [87] D. García-Fresnadillo, Singlet oxygen photosensitizing materials for point-of-use water disinfection with solar reactors, *ChemPhotoChem.* 2 (2018) 512–534. <https://doi.org/10.1002/cptc.201800062>.
- [88] F. Manjón, M. Santana-Magaña, D. García-Fresnadillo, G. Orellana, Singlet oxygen sensitizing materials based on porous silicone: Photochemical characterization, effect of dye reloading and application to water disinfection with solar reactors, *Photochem. Photobiol. Sci.* 9 (2010) 838–845.

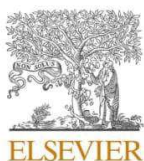
- <https://doi.org/10.1039/c0pp00026d>.
- [89] P. Di Mascio, G.R. Martinez, S. Miyamoto, G.E. Ronsein, M.H.G. Medeiros, J. Cadet, Singlet molecular oxygen reactions with nucleic acids, lipids, and proteins, *Chem. Rev.* 119 (2019) 2043–2086. <https://doi.org/10.1021/acs.chemrev.8b00554>.
- [90] Y. Yang, G. Banerjee, G.W. Brudvig, J.H. Kim, J.J. Pignatello, Oxidation of organic compounds in water by unactivated peroxymonosulfate, *Environ. Sci. Technol.* 52 (2018) 5911–5919. <https://doi.org/10.1021/acs.est.8b00735>.
- [91] J. Scully, F.E., Jr.; Hoigne, Rate constants for reactions of singlet oxygen with phenols and other compounds in water, *Chemosphere.* 16 (1987) 681–694.
- [92] J. Chen, X. Zhou, P. Sun, Y. Zhang, C.H. Huang, Complexation enhances Cu(II)-activated peroxydisulfate: A novel activation mechanism and Cu(III) contribution, *Environ. Sci. Technol.* 53 (2019) 11774–11782. <https://doi.org/10.1021/acs.est.9b03873>.
- [93] Y.N. Ogibin, E.I. Troyanskii, E.K. Starostin, S.I. Moryasheva, G.I. Nikishin, Participation of Cu(III) in copper sulfate-catalyzed oxidation of 3-carboxypropyl radicals with $S_2O_8^{2-}$ ions, *Bull. Acad. Sci. USSR, Div. Chem. Sci.* 26 (1977) 859–862.
- [94] L. Wang, H. Xu, N. Jiang, Z. Wang, J. Jiang, T. Zhang, Trace cupric species triggered decomposition of peroxymonosulfate and degradation of organic pollutants: Cu(III) being the primary and selective intermediate oxidant, *Environ. Sci. Technol.* 54 (2020) 4686–4694. <https://doi.org/10.1021/acs.est.0c00284>.
- [95] P. Salgado, V. Melin, D. Contreras, Y. Moreno, H.D. Mansilla, Fenton reaction driven by iron ligands, *J. Chil. Chem. Soc.* 58 (2013) 2096–2101. <https://doi.org/10.4067/S0717-97072013000400043>.
- [96] Z. Wang, J. Jiang, S. Pang, Y. Zhou, C. Guan, Y. Gao, J. Li, Y. Yang, W. Qiu, C. Jiang, Is sulfate radical really generated from peroxydisulfate activated by iron(II) for environmental decontamination?, *Environ. Sci. Technol.* 52 (2018)

- 11276–11284. <https://doi.org/10.1021/acs.est.8b02266>.
- [97] H. Li, C. Shan, B. Pan, Fe(III)-Doped g-C₃N₄ Mediated peroxymonosulfate activation for selective degradation of phenolic compounds via high-valent iron-oxo species, *Environ. Sci. Technol.* 52 (2018) 2197–2205. <https://doi.org/10.1021/acs.est.7b05563>.
- [98] Y. Lei, C.S. Chen, Y.J. Tu, Y.H. Huang, H. Zhang, Heterogeneous degradation of organic pollutants by persulfate activated by CuO-Fe₃O₄: Mechanism, stability, and effects of pH and bicarbonate ions, *Environ. Sci. Technol.* 49 (2015) 6838–6845. <https://doi.org/10.1021/acs.est.5b00623>.
- [99] Y. Feng, W. Qing, L. Kong, H. Li, D. Wu, Y. Fan, P.H. Lee, K. Shih, Factors and mechanisms that influence the reactivity of trivalent copper: A novel oxidant for selective degradation of antibiotics, *Water Res.* 149 (2019) 1–8. <https://doi.org/10.1016/j.watres.2018.10.090>.
- [100] D. Meyerstein, Trivalent copper. I. A pulse radiolytic study of the chemical properties of the aquo complex, *Inorg. Chem.* 10 (1971) 638–641. <https://doi.org/10.1021/ic50097a040>.
- [101] H.E. Kim, T.T.M.M. Nguyen, H. Lee, C. Lee, Enhanced inactivation of *Escherichia coli* and MS2 coliphage by cupric ion in the presence of hydroxylamine: dual microbicidal effects, *Environ. Sci. Technol.* 49 (2015) 14416–14423. <https://doi.org/10.1021/acs.est.5b04310>.
- [102] T.T.M. Nguyen, H.J. Park, J.Y. Kim, H.E. Kim, H. Lee, J. Yoon, C. Lee, Microbial inactivation by cupric ion in combination with H₂O₂: Role of reactive oxidants, *Environ. Sci. Technol.* 47 (2013) 13661–13667. <https://doi.org/10.1021/es403155a>.
- [103] H.S. Ebrahim-Saraie, H. Heidari, V. Rezaei, S.M.J. Mortazavi, M. Motamedifar, Promising antibacterial effect of copper oxide nanoparticles against several multidrug resistant uropathogens, *Pharm. Sci.* 24 (2018) 213–218. <https://doi.org/10.15171/PS.2018.31>.

- [104] M.J. Al-Jassani, H.Q. Raheem, Anti-bacterial activity of CuO nanoparticles against some pathogenic bacteria, *Int. J. ChemTech Res.* 10 (2017) 818–822.
- [105] M. Hans, A. Erbe, S. Mathews, Y. Chen, M. Solioz, F. Mücklich, Role of copper oxides in contact killing of bacteria, *Langmuir.* 29 (2013) 16160–16166. <https://doi.org/10.1021/la404091z>.
- [106] A. Azam, A.S. Ahmed, M. Oves, M.S. Khan, S.S. Habib, A. Memic, Antimicrobial activity of metal oxide nanoparticles against Gram-positive and Gram-negative bacteria: A comparative study, *Int. J. Nanomedicine.* 7 (2012) 6003–6009. <https://doi.org/10.2147/IJN.S35347>.
- [107] Y. Zhang, C. Zhang, Z. Zhou, Y. Wu, S. Xing, Degradation of ciprofloxacin by persulfate activation with CuO supported on Mg Al layered double hydroxide, *J. Environ. Chem. Eng.* 9 (2021) 106178. <https://doi.org/10.1016/j.jece.2021.106178>.
- [108] K.J.H. and G.T. John C. Crittenden, R. Rhodes Trussell, David W. Hand, *MHW's water treatment principles and design*, 2012.
- [109] H. Patel, Fixed-bed column adsorption study: a comprehensive review, *Appl. Water Sci.* 9 (2019) 1–17. <https://doi.org/10.1007/s13201-019-0927-7>.
- [110] O. Levenspiel, *Chemical reaction engineering*, 1999. <https://doi.org/10.1201/9781420087567-13>.
- [111] G. Vilaridi, J.M. Ochando-Pulido, M. Stoller, N. Verdone, L. Di Palma, Fenton oxidation and chromium recovery from tannery wastewater by means of iron-based coated biomass as heterogeneous catalyst in fixed-bed columns, *Chem. Eng. J.* 351 (2018) 1–11. <https://doi.org/10.1016/j.cej.2018.06.095>.
- [112] C. di Luca, P. Massa, J.M. Grau, S.G. Marchetti, R. Fenoglio, P. Haure, Highly dispersed Fe³⁺-Al₂O₃ for the Fenton-like oxidation of phenol in a continuous up-flow fixed bed reactor. Enhancing catalyst stability through operating conditions, *Appl. Catal. B Environ.* 237 (2018) 1110–1123. <https://doi.org/10.1016/j.apcatb.2018.05.032>.

- [113] X. Zhang, B. Bai, G. Li Puma, H. Wang, Y. Suo, Novel sea buckthorn biocarbon SBC@ β -FeOOH composites: Efficient removal of doxycycline in aqueous solution in a fixed-bed through synergistic adsorption and heterogeneous Fenton-like reaction, *Chem. Eng. J.* 284 (2016) 698–707. <https://doi.org/10.1016/j.cej.2015.09.012>.
- [114] C. Kantar, O. Oral, O. Urken, N.A. Oz, Role of complexing agents on oxidative degradation of chlorophenolic compounds by pyrite-Fenton process: Batch and column experiments, *J. Hazard. Mater.* 373 (2019) 160–167. <https://doi.org/10.1016/j.jhazmat.2019.03.065>.
- [115] S. Mohammadi, G. Moussavi, S. Shekoohiyan, M.L. Marín, F. Boscá, S. Giannakis, A continuous-flow catalytic process with natural hematite-alginate beads for effective water decontamination and disinfection: Peroxymonosulfate activation leading to dominant sulfate radical and minor non-radical pathways, *Chem. Eng. J.* 411 (2021). <https://doi.org/10.1016/j.cej.2020.127738>.
- [116] P. Khamdahsag, D.Y.S. Yan, P. Poompang, N. Supannafai, V. Tanboonchuy, Continuous fixed-bed column studies of arsenite removal via oxidation and adsorption coprocesses, *J. Water Process Eng.* 42 (2021). <https://doi.org/10.1016/j.jwpe.2021.102176>.
- [117] J.M. Mazurkow, N.S. Yüzbası, K.W. Domagala, S. Pfeiffer, D. Kata, T. Graule, Nano-Sized copper (oxide) on alumina granules for water filtration: Effect of copper oxidation state on virus removal performance, *Environ. Sci. Technol.* 54 (2020) 1214–1222. <https://doi.org/10.1021/acs.est.9b05211>.

**Chapter 2. Peroxydisulfate activation process on copper oxide: Cu(III)
as the predominant selective intermediate oxidant for phenol and
waterborne antibiotics removal**



Contents lists available at ScienceDirect

Journal of Environmental Chemical Engineering

journal homepage: www.elsevier.com/locate/jece

Peroxydisulfate activation process on copper oxide: Cu(III) as the predominant selective intermediate oxidant for phenol and waterborne antibiotics removal

Chan Li^a, Vincent Goetz^b, Serge Chiron^{a,*}^a UMR HydroSciences Montpellier, Montpellier University, IRD, 15 Ave Charles Flahault, 34093 Montpellier cedex 5, France^b PROMES-CNRS UPR 8521, PROcess Material and Solar Energy, Rambla de la Thermodynamique, 66100 Perpignan, France

ARTICLE INFO

Editor: Dr. G. Palmisano

Keywords:

Copper oxide
Peroxydisulfate
Cupryl ion
Non-radical mechanism
Transformation pathways
Antibiotics

ABSTRACT

In this study, activated peroxydisulfate (PDS) by micrometer copper oxide (CuO) particles effectively degraded phenol and several antibiotics in water. Cupryl ion (Cu(III)) was proposed for the first time to be the predominant reactive species accounting for contaminants degradation in the CuO/PDS oxidation system. Singlet oxygen was also heavily produced from the superoxide radical anion ($^{\bullet}\text{O}_2^-$) decomposition was found to be but slightly involved in the degradation since it was rapidly quenched by water. Transformation pathways of phenol and several antibiotics were elucidated. The proposed mechanism mainly involved the generation of $^{\bullet}\text{O}_2$ resulting from an outer-sphere surface PDS complexation which prompted the reduction of Cu(II) to Cu(I). Cu(I) was oxidized in Cu(III) by PDS or H_2O_2 and was reduced to Cu(II) by a one-electron oxidation of contaminants so that the catalytic effect involved alternate oxidation and reduction of copper. As the degradation process did not rely on sulfate or hydroxyl radical, chloride and bicarbonate ions showed no effect on phenol degradation, while sulfate ions and humic acid slightly hindered phenol degradation probably due to their sorption on CuO. Interestingly, the copper leaching from CuO was significantly limited to $< 500 \mu\text{g/L}$ in wastewater. These findings indicated the potential applicability of CuO/PDS system for electron-rich compounds degradation including antibiotics due to good catalyst stability against time.

1. Introduction

The success of many advanced oxidation processes (AOPs) based on persulfate (PS) including peroxydisulfate (PDS) and peroxymonosulfate (PMS) for water treatment relies on the strong oxidizing power of the generated free radical species (hydroxyl ($^{\bullet}\text{OH}$) E^0 1.9–2.7 V and sulfate ($\text{SO}_4^{\bullet-}$) E^0 2.5–3.1 V) towards a broad spectrum of recalcitrant organic contaminants and towards pathogens [1,2]. However, radical-based PS activation requires the input of energy mainly in the form of light, ultrasound and heat which elevates the operational costs of treatments [3,4]. Consequently, among the different strategies to activate PS, transition metals (Fe^{2+} , Cu^{2+} , Mn^{2+}), their oxides (Fe_3O_4 , CuO , MnO_2), and bimetallic composites (CuFe_2O_4 , $\text{CuO-Fe}_3\text{O}_4$, $\text{Mn}_{1.8}\text{Fe}_{1.2}\text{O}_4$, etc.) and supported metal oxides ($\text{CuOMgO-Fe}_3\text{O}_4$, $\text{CuO-Al}_2\text{O}_3$) have been recognized as the most cost-efficient approaches [4–6]. Iron oxides received particular attention to heterogeneously activate PS, because they are not consumed during the activation, can work at neutral pH,

and no additional energy is required [7,8]. However, the low efficiency of present heterogeneous activation processes in terms of long contact time (usually in days) and high PS dose requested (over 100 times higher than the pollutant concentration) is still a major limitation for its industrial application [9]. Consequently, copper, mainly in the forms of pure copper oxides (e.g., CuO or Cu_2O) [10,11], bimetallic oxides (e.g., CuFe_2O_4 , CuFeO_2) [12,13] and different materials supported copper oxides (e.g., CuO supported on alumina, or CuO coated on ceramic hollow fiber membrane) [6,14] has obtained increasing attention because of their higher efficiency than iron oxides to activate PS with still relatively low toxicity of Cu^{2+} ion in case of leaching. Indeed, an upper Cu^{2+} concentration limit of 2.0 mg/L is admitted in drinking water and Cu^{2+} is not regarded as a potential carcinogen [15].

Processes relying on radical-based mechanisms undergo efficiency losses in organic-rich wastewater such as domestic wastewater due to the competing organic/inorganic constituents of water [4] and due to the difficulty in the regeneration of active sites on the surface of the catalyst

* Corresponding author.

E-mail address: serge.chiron@umontpellier.fr (S. Chiron).<https://doi.org/10.1016/j.jece.2021.105145>

Received 21 December 2020; Received in revised form 26 January 2021; Accepted 27 January 2021

Available online 29 January 2021

2213-3437/© 2021 Elsevier Ltd. All rights reserved.

due to the energetically unfavorable Cu redox cycle. In particular, the oxidation by $\text{SO}_4^{\cdot-}$ favors the direct electron abstraction and can transform some anions (e.g., Cl^- and NO_2^-) into their corresponding radicals potentially leading to troublesome chlorinated and nitrated transformation products (TPs) [4,16]. More recently, mild non-radical PS activation mechanisms have been also suggested to limit the formation of these hazardous TPs. In contrast to radical-based processes, the non-radical oxidative pathway is much more selective, accounting for the only removal of electron-rich organic contaminants (e.g., phenols and anilines) [11,17,18]. In addition, the non-radical pathway requires a small amount of oxidant and is less influenced by the competing organic/inorganic constituent of the water. Three major mechanisms have been proposed for the non-radical pathway including the involvement of 1) oxidant surface metastable complexes on CuO particles, 2) superoxide radical anion ($^{\cdot}\text{O}_2^-$) and singlet oxygen ($^1\text{O}_2$) and 3) the high valent cupryl ion oxidant symbolized by Cu^{3+} in solution and Cu(III) in its solid form. Surface activated complexes result from the interaction between CuO and PS through an outer-sphere surface complexation [11,17]. PS is thought to function as a two-electrons transfer oxidant that directly accepts electrons from an organic contaminant through an electron shuttle material leading to sulfate anions ($\text{SO}_4^{\cdot-}$) release. Certain recent studies have reported the occurrence $^1\text{O}_2$ as another type of non-radical process as previously reported in the CuOs/PS system [18,19]. $^{\cdot}\text{O}_2^-$ might function as a precursor for the generation of $^1\text{O}_2$ through $^{\cdot}\text{O}_2^-$ oxidation or disproportionation reactions. The $^1\text{O}_2$ based systems are well-known for their resistance to background substances in the water matrix but have been regarded to be poorly efficient because $^1\text{O}_2$ is rapidly quenched by water [20]. Cu(III) has been also suggested to be the working oxidant in the copper involved activated PS processes [21–23]. The generation of Cu in a highly electron deficient state offers the highest redox potential for PS activation (Cupric ion symbolized by Cu^{2+} in solution and Cu(II) in its solid form, $E^0\text{Cu(III)/Cu(II)} = 2.3 \text{ V}$), but Cu(III), as an unstable species and an one-electron oxidant, might also directly oxidize electron-rich organic contaminants [24] or decompose into $^{\cdot}\text{OH}$, depending on the water pH value [25].

Consequently, using CuO, there is still a great deal of uncertainty concerning the identification of reactive species since all the different above mentioned pathways have been reported in the literature from the radical pathway, the surface bound complex, the $^1\text{O}_2$ pathway and the high-valent metal-induced Cu(III) oxidation pathway during PS activation. The mechanisms behind the identification of reactive species and transformation of organics still need further exploration. This is the main contribution of this work by taking PDS as the working oxidant because PDS is a more promising oxidant than PMS for potential applications due to a better chemical stability during transport and storage, a lower cost and a longer half-life [26]. Specific objectives of this work include: (i) kinetic studies, (ii) identification of reactive species by using scavengers, (iii) identification of TPs by liquid chromatography-high resolution-mass spectrometry (LC-HRMS) and elucidation of transformation pathways, (iv) investigating the effect of operating parameters, and (v) investigating the practical applicability on the removal of several antibiotics. Phenol was selected as one probe organic contaminant because of its well-known reactions with common radical and non-radical species and the applicability of the CuO/PDS system was investigated by using several antibiotics (i.e. cephalexin (CFX), ciprofloxacin (CIP), clarithromycin (CLA) and sulfamethoxazole (SMX)) of environmental relevance.

2. Material and methods

2.1. Chemicals

Micrometer copper oxide particles ($\text{CuO}_{\mu\text{m}}$, 44 μm , 97%) were purchased from Alfa Aesar (Kandel, Germany). Nanometer copper oxide (CuO_{nm} , < 50 nm), iron (II, III) oxide (Fe_3O_4), cuprospinel (CuFe_2O_4), ammonium molybdate ($(\text{NH}_4)_6\text{Mo}_7\text{O}_{24}\cdot 4\text{H}_2\text{O}$), anisole (> 99%), benzoic

acid (> 99%), benzotriazole (> 98%), catechol (> 99%), CFX (> 99%), CIP (> 98%), CLA (> 99.5), furfuryl alcohol (FFA, > 99%), humic acids sodium salt (technical grade), hydrochloric acid (HCl, 37%), hydroxyquinone (HQ, > 99%), nitrobenzene (NB, > 98%), Oxone ($\text{KHSO}_5\cdot 0.5\text{KHSO}_4\cdot 0.5\text{K}_2\text{SO}_4$), *p*-benzoquinone (BQ, > 98%), phenol (> 99%), salicylic acid (> 99%), sodium azide (NaN_3 , > 99.5%), SMX (> 99%), sulfuric acid (H_2SO_4 , 98%), sodium bicarbonate (NaHCO_3), sodium hydroxide (NaOH), starch solution, 4-hydroxybenzoic acid (> 99%) and 4-phenoxyphenol (> 99%) were purchased from Sigma-Aldrich (Saint Quentin Fallavier, France). CuO supported on alumina ($\text{CuO@Al}_2\text{O}_3$), potassium iodide (KI), and potassium periodate (KIO_4) were purchased from Honeywell (Germany). Copper sulfate pentahydrate ($\text{CuSO}_4\cdot 5\text{H}_2\text{O}$), potassium persulfate ($\text{K}_2\text{S}_2\text{O}_8$) and tris(hydroxymethyl)aminomethane (Tris) were purchased from Merck KGaA (Germany). Acetonitrile (HPLC grade), methanol (MeOH, HPLC grade) and sodium chloride (NaCl) were purchased from Carlo Erba reagents (France). All solutions were prepared with ultrapure water obtained from a Milli-Q Plus system (Millipore, Bedford, MA). Stock solutions of phenol (1000 ppm) and PDS (100 mM) were prepared in ultrapure water.

2.2. Characterization of CuO

$\text{CuO}_{\mu\text{m}}$, CuO_{nm} , Fe_3O_4 , CuFe_2O_4 , $\text{CuO@Al}_2\text{O}_3$ were used as received without any further purification. Only $\text{CuO}_{\mu\text{m}}$ underwent further characterization as it was selected for deeper investigation. The surface morphology and chemical composition of $\text{CuO}_{\mu\text{m}}$ were analyzed using a scanning electron microscope (SEM). To identify its crystal structure, X-ray diffraction (XRD) analyses were performed at room temperature using a PANalytical XPert Pro diffractometer (CuK α radiation, $\lambda = 0.15418 \text{ nm}$). XRD measurements of θ - θ symmetrical scans were made over an angular range of 10 – 80° . BET surface area and average pore size were analyzed by the N_2 adsorption method.

2.3. Experimental procedures

Batch experiments were conducted in 100 mL glass serum bottles under continuous shaking by roller mixer (STUART® SRT9D, UK) at 60 rpm and using 200 mM Tris buffer adjusted at pH 7 with HCl or NaOH. The use of phosphate and borate buffers were discarded to set the pH at 7 or slightly basic pH because phosphate is a strong coordinate for transition metals and particularly Cu^{2+} while PS activation by borate has been reported [27]. In contrast, Tris buffer did not react with PDS and was selected for further experiments. Typically, compound, metal oxides, and PDS were sequentially added into the bottles to reach initial concentrations of 20 mg/L (0.213 mM), 10 g/L and 1 mM, respectively. Sample aliquots (5 mL) were taken at predetermined times and filtered through 0.45 μm membrane filters, and then stored in 6 mL glass tubes at 4°C before analysis. Control experiments without the addition of metal oxide or oxidant were also performed under the same experimental conditions. High concentration of scavengers (usually more than 100 times of phenol concentration), like MeOH, anisole, NB, BQ, FFA, NaN_3 , neocuproine and hydroxylamine were added in the CuO /PDS system, respectively to probe the generated reactive oxidant species. Results are presented as an average of two experiments.

2.4. Analytical methods

Phenol, BQ, and HQ were quantified by LC with a diode-array detector at $\lambda = 280, 244$ and 254 nm , respectively using an Agilent ZORBAX Eclipse XDB C $_8$ column ($150 \times 3 \text{ mm i.d.}$, $3.5 \mu\text{m}$ particle size) for kinetic studies. The separation was performed using an isocratic mode of elution with a mobile phase composed of 0.1% formic acid in Milli-Q water and acetonitrile at a volume ratio of 50/50 for phenol and 90/10 for BQ and HQ. The flow rate was set at 0.5 mL/min. TPs were detected by LC-HRMS composed of a Dionex Ultimate 3000 liquid chromatograph equipped with an electrospray source and a Exactive Orbitrap mass spectrometer

(Thermo Fisher Scientific, Les Ulis, France) operated in full scan MS (mass range m/z 50–900) and using an Agilent ZORBAX Eclipse XDB C₁₈ plus column (150 × 2.1 mm i.d., 3.5 μm particle size). Phenol TPs detected in negative ionization mode and the LC gradient of Milli-Q water (solvent A) and acetonitrile (solvent B) was as follow: 0–1.5 min, 98% A; 11.25 min, 55% A; 12.75 min, 30% A; 13.0–20 min, 98% A. The flow rate was 0.3 mL/min. The energy collisional dissociation was set to 20 eV and a drying gas temperature of 275 °C was used. Quantification of phenoxyphenol dimers were carried out by external calibration using 4-phenoxyphenol as available analytical standard. Antibiotic TPs detected in positive ionization mode and the LC gradient of Milli-Q water with 1% acetonitrile and 0.1% formic acid (solvent A) and acetonitrile with 1% Milli-Q water and 0.1% formic acid (solvent B) was as follow: 0–5 min, 95% A; 15–20 min, 5% A; 21–30 min, 95% A. The flow rate was 0.15 mL/min. The energy collisional dissociation was set to 20 eV and a drying gas temperature of 300 °C was used.

Analysis of PDS. PDS was determined by using a UV-Vis spectrophotometer (Shimadzu, Japan) following the protocol developed by Liang et al. [28]. Briefly, the method consisted in analyzing adsorption spectra of mixed solutions of 1 mL sample, 1 mL 60 mM NaHCO₃, and 1 mL 600 mM KI in a quartz cuvette at $\lambda = 352$ nm.

Analysis of hydrogen peroxide-H₂O₂ was determined by using UV-Vis spectrophotometry following the protocol developed by Graf and Penniston [29]. Briefly, the method consisted in analyzing adsorption spectra of mixed solutions of 2 mL 50 mM HCl, 0.2 mL 1 M KI, 0.2 mL 1 mM ammonium molybdate in 0.5 M H₂SO₄, 0.2 mL 50 g/L starch solution and 0.2 mL sample in a quartz cuvette at $\lambda = 570$ nm.

Analysis of Cu(III). The Cu(III) periodate complex was analyzed by UV-Vis spectrophotometry following the protocol of Wang et al., [23]. Briefly, KIO₄ (4 g/L) was added in the basic solution (pH = 13) consisted of CuO (10 g/L) and PDS (1 mM) and NaOH. Samples (3 mL) were filtered through 0.45 μm membrane filters after 5 min reaction and the 300–600 nm UV/Vis absorption spectra of the filtered solution were recorded.

3. Results and discussion

3.1. Characterization of CuO

Representative SEM image and XRD diffraction pattern of the investigated micrometer CuO are shown in Fig. 1. The SEM image shows that CuO particles were irregularly shaped crystals with mean diameters

of about 44 μm. The XRD pattern of CuO matched well with the standard XRD pattern of copper oxide (ICDD 01-089-5897) and indicated that CuO was a monoclinic system with 100% crystallinity. The specific surface area was found to be 0 m²g⁻¹ and there was no porosity.

3.2. PDS activation by CuO – batch experiments

First, the degradation of PDS and phenol (see Fig. S1 in Supporting Material) with three different catalysts (i.e., CuO, Fe₃O₄ and CuFe₂O₄) has been compared to demonstrate the higher reactivity originated from CuO for the degradation of phenol and the oxidant consumption. Then, the same comparison was conducted among different types of CuO (i.e., CuOnm, CuOμm, CuO supported on alumina) (see Fig. S2). CuOμm was selected in this work because of its high reactivity for phenol degradation, and because micro-sized particles allow for easy catalyst separation and recovery, which is of great importance in practical applications.

At neutral pH (7.0 ± 0.3), PDS alone could not degrade phenol and CuO alone could not adsorb phenol. Interestingly, the phenol degradation reached 100% in 15 min in presence of CuO and PDS (Fig. 2a). Phenol degradation fitted a first-order kinetic model with an apparent degradation kinetic rate constant (k_{obs}) of 0.32 min⁻¹. The corresponding PDS decomposition is shown in Fig. 2b. The presence of catalysts without an organic component decomposed PDS to a significant extent. The lack of decrease or increase in the decomposition of PDS after phenol addition ruled out the mediator role of the catalysts through the direct transfer of electrons between phenol and PDS. As previously reported [11,17], the interaction between CuO and PDS likely occurred through an outer-sphere surface complexation. Due to the positively charged CuO and the negatively charged PDS at neutral pH, strong electrostatic interactions and adsorption of PDS on the CuO surface were anticipated. However, this adsorption process could not be quantified due to the simultaneous PDS reactivity on the CuO particle surface. Besides, since Cu²⁺ ions neither catalyzed PDS activation nor degraded phenol (Fig. 2a and b), the effects of Cu²⁺ leaching could be ruled out and the predominant role of heterogeneous PDS activation could be stated. Cu²⁺ was previously reported to donate one electron to PDS, thus inducing PDS decomposition into sulfate anion and sulfate radical. However, this process is very slow, making effective degradation of water pollutants nearly impossible except for specific compounds, which can directly complex with Cu²⁺ [21,30]. The stoichiometric efficiency (η), defined as the number of moles of phenol oxidized for every mole of PDS activated ($\eta = \Delta[\text{phenol}]/\Delta[\text{S}_2\text{O}_8^{2-}] \times 100\%$) was also calculated.

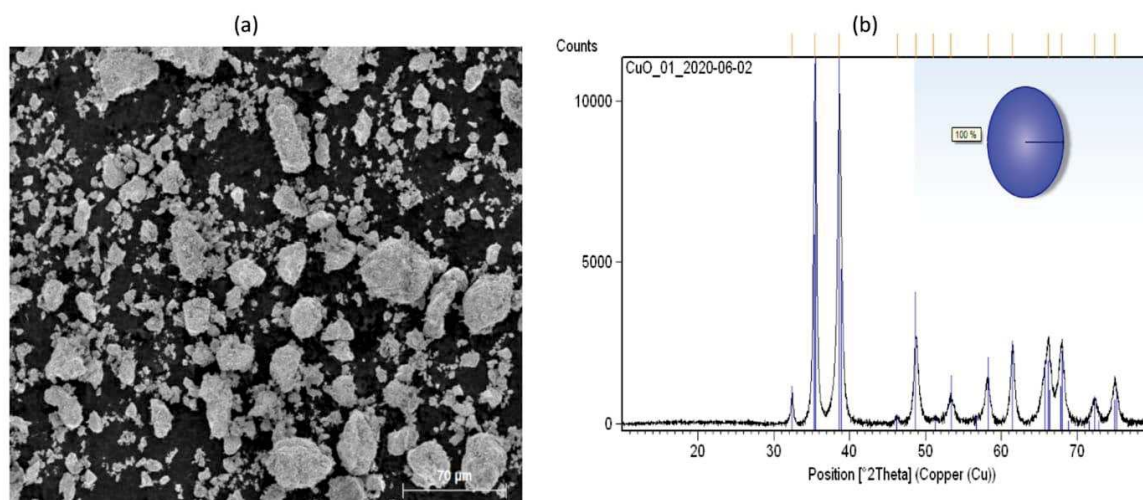


Fig. 1. (a) SEM image and (b) XRD pattern of the investigated micro-sized copper oxide.

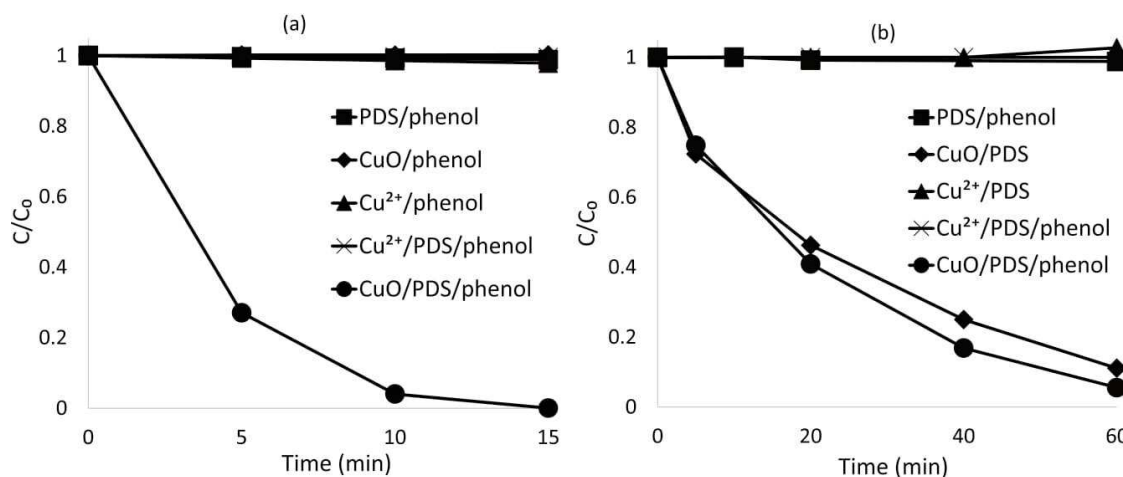


Fig. 2. (a) Phenol degradation and (b) PDS decomposition in PDS alone, CuO alone, Cu²⁺ solution, Cu²⁺/PDS and CuO/PDS systems. [CuO] = [CuSO₄.5H₂O] = 10 g/L; [PDS] = 1 mM; [phenol] = 20 mg/L; pH = 7 with Tris buffer.

45–50% was found to be the maximum value that could be obtained. This meant that two moles of PDS was needed to degrade one mole of phenol on average.

3.3. Identification of reactive species

A central question was the identification of the active oxidant species in the chemical transformation of the probe compound at neutral pH. It has been suggested that $\cdot\text{OH}$, $\text{SO}_4^{\cdot-}$, $\cdot\text{O}_2^-$, $^1\text{O}_2$ and probably Cu(III) are formed in CuO catalyzed PDS processes [17,19,31,32]. MeOH was first used to investigate a possible formation of radical species. MeOH reacts with $\cdot\text{OH}$ and $\text{SO}_4^{\cdot-}$ with nearly the same rate ($k_2(\text{MeOH}, \text{SO}_4^{\cdot-}) = 1 \times 10^7 \text{ M}^{-1}\text{s}^{-1}$, [33]), ($k_2(\text{MeOH}, \cdot\text{OH}) = 5 \times 10^8 \text{ M}^{-1}\text{s}^{-1}$, [25]) and can theoretically be used to trap these radicals. The inhibitory effect of MeOH was limited as k_{obs} only change from 0.32 min^{-1} to 0.18 min^{-1} after applying an excess amount of MeOH (see Table 1 and Fig. S3a). This result confirmed earlier findings that the CuO/PDS system did not predominantly rely on radical mechanisms. The lack of ability for MeOH to scavenge surface bound radicals might also account for the observed small inhibition in phenol degradation [13]. To scavenge the surface bound radicals, inhibitors that can interact onto the CuO surface and can lead to the subsequent occupation of activated sites are needed [34]. For this purpose, the addition of anisole which can complex with Cu(II) [35] and react with $\cdot\text{OH}$ and $\text{SO}_4^{\cdot-}$ ($k_2(\text{anisole}, \text{SO}_4^{\cdot-}) = 7.8 \times 10^9 \text{ M}^{-1}\text{s}^{-1}$, [36]; $k_2(\text{anisole}, \cdot\text{OH}) = 4.9 \times 10^9 \text{ M}^{-1}\text{s}^{-1}$, [37]) was tested. Similarly, anisole had a very limited inhibitory effect ($k_{\text{obs}} = 0.24 \text{ min}^{-1}$, Table 1 and Fig. S3a), confirming the limited implication of radicals in solution

Table 1
Apparent first-order degradation kinetic rate constants (K_{obs}) of phenol in presence of different scavengers.

Reactive species	Scavenger	Concentration (mM)	$K_{\text{obs}}(\text{min}^{-1})$	R^2
	none		0.32	0.99
$\cdot\text{OH}$ and $\text{SO}_4^{\cdot-}$	methanol	4900	0.18	0.99
$\cdot\text{OH}$ and $\text{SO}_4^{\cdot-}$	anisole	18.5	0.24	0.98
$\cdot\text{OH}$	nitrobenzene	19.4	0.32	0.96
$\cdot\text{O}_2^-$	<i>p</i> -benzoquinone	18.5	0	–
$^1\text{O}_2$	furfuryl alcohol	100	0.04	0.94
$^1\text{O}_2$	azide	100	0.02	0.98
Cu(I)	neocuproine	0.19	0.05	0.94
Cu(I)	hydroxylamine	0.06	0.40	0.96

and/or adsorbed on CuO surface in the phenol degradation process.

To discriminate against the different radicals (i.e., $\cdot\text{OH}$ and $\text{SO}_4^{\cdot-}$), NB as a specific $\cdot\text{OH}$ quencher ($k_2(\text{NB}, \cdot\text{OH}) = 3.2 \times 10^9 \text{ M}^{-1}\text{s}^{-1}$, [38]; $k_2(\text{NB}, \text{SO}_4^{\cdot-}) < 10^6 \text{ M}^{-1}\text{s}^{-1}$, [39]) was applied. As shown in Table 1 and Fig. S3a, the no NB effect on the phenol degradation kinetic ($k_{\text{obs}} = 0.32 \text{ min}^{-1}$) excluded the involvement of $\cdot\text{OH}$ in the system. This result validated the selection of Tris buffer to set the pH at 7 because it is known that Tris quickly reacts with $\cdot\text{OH}$ to generate formaldehyde with a second-order rate constant of $1.1 \times 10^9 \text{ M}^{-1}\text{s}^{-1}$ [40]. The observed difference between k_{obs} in presence of anisole or NB could only be ascribed to some generated $\text{SO}_4^{\cdot-}$ radicals. BQ as a known scavenger for $\cdot\text{O}_2^-$ ($k_2(\text{BQ}, \cdot\text{O}_2^-) = 8 \times 10^9 \text{ M}^{-1}\text{s}^{-1}$, [41]) was also applied. The degradation of phenol was totally inhibited, which demonstrated the predominant role of $\cdot\text{O}_2^-$ in CuO/PDS system. Besides, $\cdot\text{O}_2^-$ reacts relatively rapidly with Cu²⁺ and H₂O ($k_2(\text{Cu}^{2+}, \cdot\text{O}_2^-) = 8 \times 10^9 \text{ M}^{-1}\text{s}^{-1}$; $k_2(\text{H}_2\text{O}, \cdot\text{O}_2^-) = 1.0 \times 10^5 \text{ M}^{-1}\text{s}^{-1}$, [42]) compared with phenol ($k_2(\text{phenol}, \cdot\text{O}_2^-) = 5.8 \times 10^2 \text{ M}^{-1}\text{s}^{-1}$, [43]). Consequently, the major role of $\cdot\text{O}_2^-$ was not to degrade phenol but might function as precursors to reduce Cu²⁺ to Cu⁺ and to generate $^1\text{O}_2$ along with H₂O₂ generation through bimolecular dismutation.

To confirm this point, the formation of Cu⁺, $^1\text{O}_2$, and H₂O₂ was examined individually. To verify Cu⁺ formation, neocuproine as a specific Cu⁺ chelating agent and trace hydroxylamine as a reductant to promote Cu²⁺ conversion to Cu⁺ were selected to apply in the CuO/PDS system [23,44]. Neocuproine was prepared in presence of methanol (4.9 M) due to its poor water solubility. Neocuproine hindered the degradation of phenol with $k_{\text{obs}} = 0.05 \text{ min}^{-1}$ and trace hydroxylamine slightly promoted the degradation of phenol with $k_{\text{obs}} = 0.40 \text{ min}^{-1}$ (Table 1 and Fig. S3b). Both results indicated that Cu⁺ most likely played an important role in the copper redox cycle in the presence of PDS to generate reactive species.

$^1\text{O}_2$ exhibits highly selective oxidant properties and reacts exclusively towards unsaturated organics via electrophilic or electron abstraction [3]. FFA ($k_2(\text{FFA}, ^1\text{O}_2) = 1.2 \times 10^9 \text{ M}^{-1}\text{s}^{-1}$) and NaN₃ ($k_2(\text{NaN}_3, ^1\text{O}_2) = 1 \times 10^9 \text{ M}^{-1}\text{s}^{-1}$) were therefore selected rather than the saturated compounds (e.g., MeOH) [5,18] to quench $^1\text{O}_2$ since PDS could not be directly decomposed by FFA and azide (Fig. S4a). The degradation kinetics of phenol was significantly reduced in presence of excess FFA ($k_{\text{obs}} = 0.04 \text{ min}^{-1}$) and NaN₃ ($k_{\text{obs}} = 0.02 \text{ min}^{-1}$) (Table 1). Besides, NaN₃ was further used as the chemical probe for $^1\text{O}_2$ generation, which manifested a higher second order rate of $1 \times 10^9 \text{ M}^{-1}\text{s}^{-1}$ than the targeted phenolic compound ($2.0\text{--}3.0 \times 10^6 \text{ M}^{-1}\text{s}^{-1}$), but

excess NaN_3 could only delay the removal of phenol (Fig. S4b), which suggested the involvement of $^1\text{O}_2$ in PDS/CuO system but excluded $^1\text{O}_2$ as a predominant reactive oxygen species for phenol degradation. The rapid physical quenching with water with a rate constant of $k_1 = 2.5 \times 10^5 \text{ s}^{-1}$ further explained this point [45]. To detect the occurrence of H_2O_2 due to further transformation of $\text{O}_2^{\cdot-}$, molybdate salt was used because this latter rapidly reacts with H_2O_2 to produce a peroxymolybdate complex, which can be easily detected by UV/Vis spectrophotometry at $\lambda = 570 \text{ nm}$. As shown in Fig. S5, the adsorption for the peroxymolybdate complex was detected in CuO alone, which indirectly proved that a minor amount of $^{\cdot}\text{O}_2$ was produced by oxygen reduction, while the majority of $^{\cdot}\text{O}_2$ was generated in the CuO/PDS system which was highlighted by a higher absorbance. These results thus confirmed the intermediate role of $^{\cdot}\text{O}_2$ during the generation of $^1\text{O}_2$. However, in the CuO/PDS system, $^{\cdot}\text{O}_2$ reaction with Cu^{2+} ($k_2 = 8 \times 10^9 \text{ M}^{-1}\text{s}^{-1}$) was likely a more important sink of $^{\cdot}\text{O}_2$ than $^{\cdot}\text{O}_2$ bimolecular dismutation leading to Cu^+ generation. This result also discarded $^1\text{O}_2$ as the leading reactive oxygen species for phenol degradation.

Consequently, Cu(III) was assumed to be the working oxidant in the CuO/PDS process. To verify this hypothesis, periodate was added to the reactive medium as it was reported to be able to stabilize the labile Cu(III) species by forming a Cu(III)-periodate complex. This complex has a characteristic light absorbance at 415 nm [23]. Interestingly, significant absorbance at this wavelength was observed when periodate was added into CuO/PDS, while no absorbance was found for CuO and PDS alone (Fig. 3a). This result supported our hypothesis of the presence of Cu(III) in the CuO/PDS process but without knowing if Cu(III) was surface-bound or in solution.

To collect additional evidence for the involvement of Cu(III) in phenol transformation, different compounds were tested because Cu(III) is highly selective towards electron-rich compounds (e.g., benzotriazole) but not reactive to electron-deficient compounds (e.g., benzoic acid) [24]. As shown in Fig. 3b, benzotriazole were readily transformed with $k_{\text{obs}} = 0.57 \text{ min}^{-1}$ and benzoic acid was not degraded at all while salicylic acid and 4-hydroxybenzoic acid showed an intermediate behavior with $k_{\text{obs}} = 0.09 \text{ min}^{-1}$ and $k_{\text{obs}} = 0.21 \text{ min}^{-1}$, respectively.

3.4. Phenol transformation pathways and mechanisms

Phenol transformation pathways were investigated by identifying phenol TPs following a suspect screening workflow in LC-HRMS. For this purpose, a database was made up of a list of possible TPs with their molecular formula, exact mass and structure (Table S2). This list was

established from a literature search of TPs of phenol formed during AOPs experiments. In a first step, TPs with intensities lower than 1×10^4 cps, signal to noise ratios lower than 10, isotopic ratios higher than 10%, and mass accuracy errors higher than 5 ppm were eliminated. Following this approach, only TPs resulting from phenol polymerization were detected. The structure of the first one with a retention time (RT) = 11.6 min and a pseudo-molecular $[\text{M-H}]^-$ ion at $m/z = 185.0597$ was assigned to 4-phenoxyphenol (dimer) after deconvolution of the TIC of samples (Fig. 4) and injection of an analytical standard. This compound did not accumulate with time. The structure of the following TPs with a RT = 13.8 min and 14.5 min and a $[\text{M-H}]^-$ ion at $m/z = 277.0859$ (and a related fragment ion at $m/z 185.0597$) and 369.1127, respectively were assigned to a trimer and a tetramer of phenol, respectively (Fig. 4).

Catechol, HQ and BQ were reported as common TPs of phenol in radical and non-radical based PDS activation systems [46]. Available catechol analytical standard was injected in LC-HRMS but was never detected during degradation experiments. Since BQ and HQ could not be analyzed in MS due to a very poor response in electrospray mode of ionization, standard addition of BQ and HQ were performed in LC/UV analysis, with limits of detection below 0.1 mg/L. Figs. S6 and S7 show the lack of formation BQ and HQ during the degradation experiments. Consequently, the polymerization reaction was found to be the only main phenol transformation pathway probably through an one-electron oxidation process of phenol under Cu(III) reactivity. The peak area variations of detected TPs are shown in Fig. S8. The dimer only accounted for 3% of the initial phenol concentration and the amount of trimer and tetramer could not be quantified as no standard was commercially available. A mass balance was also not reached because compounds corresponding to a high degree of polymerization of phenol probably precipitated in the reactive medium.

On the basis of the elucidated phenol transformation pathway and on the knowledge of the different involved reactive species (see Section 3.2), a mechanism was suggested as depicted in Fig. 5. Similar to what was suggested for the MnO_2/PDS system [47], a metastable copper complex was most likely formed at the surface of the hydrous CuO micro-particles. This was a reasonable assumption since at neutral pH, the CuO surface is positively charged (pHpzc of 8–9 have been reported for CuO, [48]) and PDS is an anion calling for strong electrostatic interactions. As a result, the S–O bond of PDS weakened and broke (Eq. (1)) and the adsorption of PDS on the surface of CuO facilitated the generation of metastable $[\equiv\text{Cu(III)}-\text{O}-\text{O}-\text{SO}_3]$ intermediate. The latter resulting complex underwent hydrolysis along with the generation of $^{\cdot}\text{O}_2$ (see Eq. (2)). Afterward, the recombination of two $^{\cdot}\text{O}_2$ could evolve

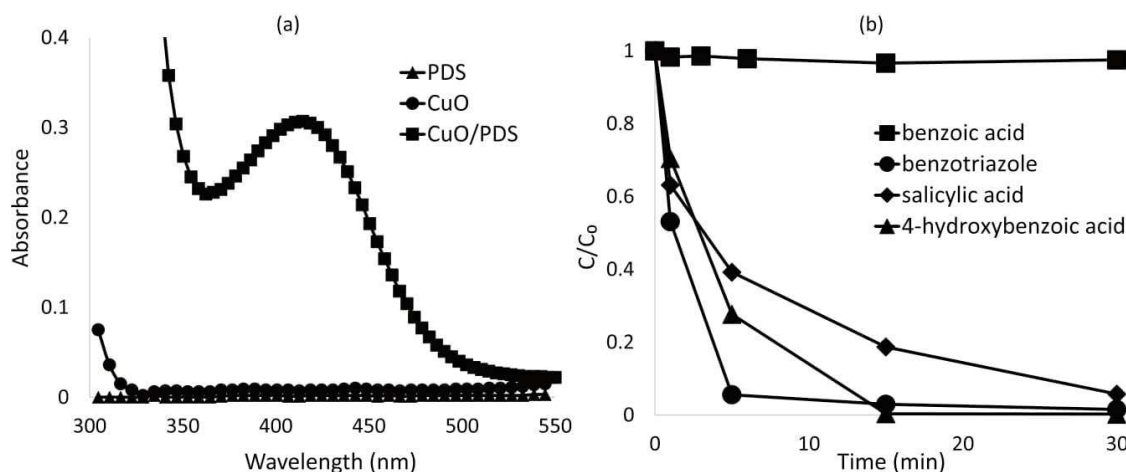


Fig. 3. (a) UV–Vis absorbance spectra of CuO/PDS after the addition of periodate for Cu(III) detection at pH 13, (b) degradation of selected compounds in CuO/PDS systems. $[\text{CuO}] = 10 \text{ g/L}$; $[\text{PDS}] = 1 \text{ mM}$; $[\text{KIO}_4] = 4 \text{ g/L}$; $[\text{benzoic acid}] = [\text{benzotriazole}] = [\text{salicylic acid}] = [4\text{-hydroxybenzoic acid}] = 20 \text{ mg/L}$.

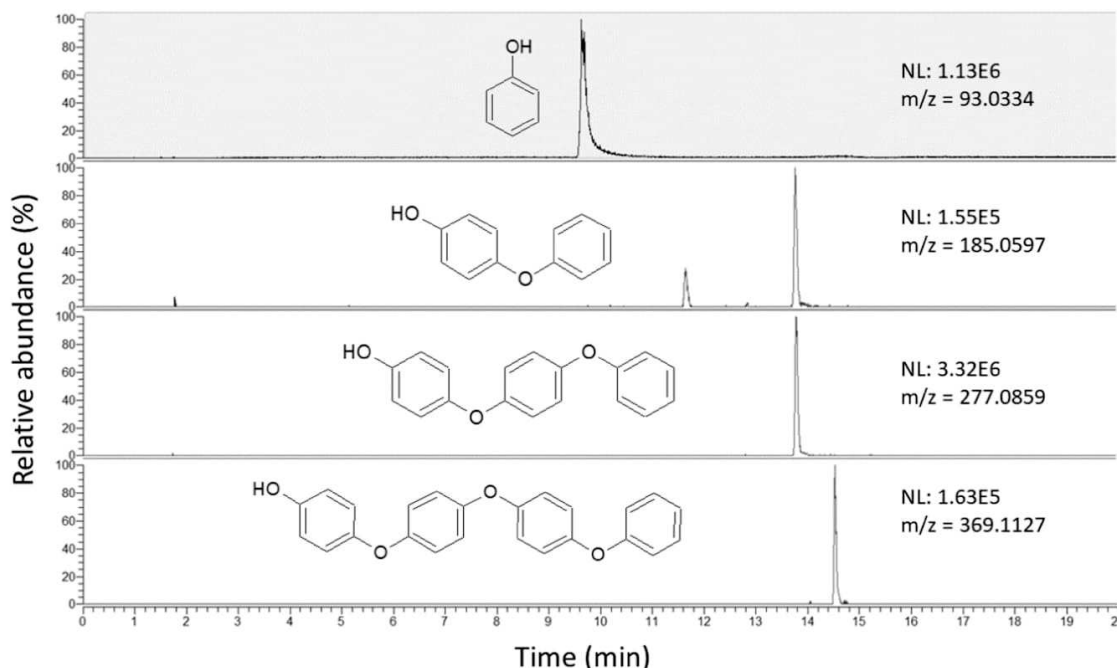


Fig. 4. Extracted Ion Chromatograms (EIC) of detected phenol transformation products.

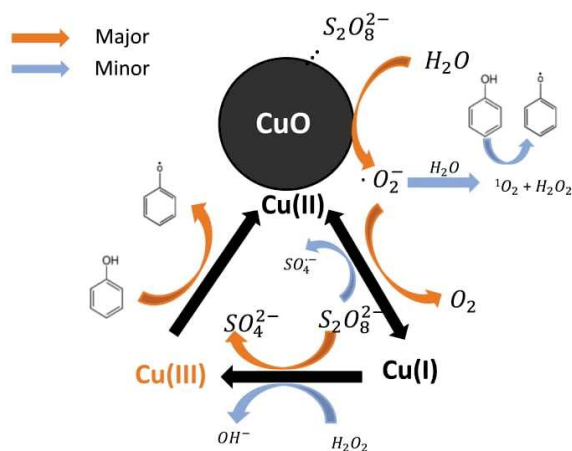
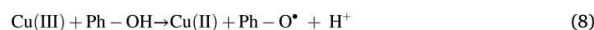
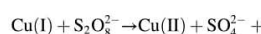
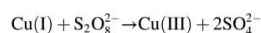
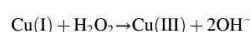
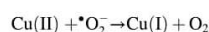
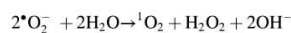
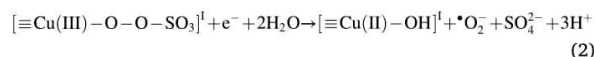
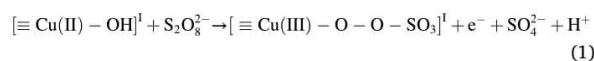


Fig. 5. Scheme of phenol transformation mechanisms in CuO/PDS system.

into $^1\text{O}_2$ with the concomitant release of H_2O_2 (Eq. (3)). However, most probably $^{\bullet}\text{O}_2^-$ reacted with Cu(II) to generate Cu(I) (Eq. (4)) which could be spontaneously oxidized by PDS or H_2O_2 to give Cu(III) or Cu(II) (Eqs. (5)–(7)). In turn, Cu(III) could selectively oxidize the electron-rich phenol to the corresponding phenoxyl radical leading to phenol polymerization, while it was reduced in Cu(II) (Eq. (8)) so that the catalytic effect involved alternate oxidation and reduction of copper. Phenol could be also oxidized by $^1\text{O}_2$ ($k_2 = 10^6 \text{ M}^{-1}\text{s}^{-1}$, Eq. (9)) but this reaction was probably not significant due to $^1\text{O}_2$ physical quenching with water. In neutral solutions, $^{\bullet}\text{OH}$ is not an intermediate in the decomposition reaction of Cu(III), except when Cu(III) is not efficiently consumed by organic compounds [25]. In our experiments, the Cu(III) ions seemed to oxidize phenol without a need for a complexation step of Cu(II) with the organic contaminant to enhance PDS activation as was

observed in case of the antibiotic cephalixin [21].



$^{\bullet}\text{OH}$ and $\text{SO}_4^{\bullet -}$ radicals [19,31,32], CuO surface metastable complexes [11,17,19] and $^1\text{O}_2$ [19] have been reported as the responsible reactive species for the degradation of organic compounds in the CuO/PDS system. Differently, Cu(III) was proposed as the primary oxidant species in this study.

3.5. Influence of operating parameters

3.5.1. Solution pH

The solution pH can affect the surface charge property of CuO, the PDS activation and the dissociation and the degradation efficiency of phenol. The pH effect was firstly investigated at three different pH values (i.e., 4, 7 and 9). Neutral and alkaline conditions were obtained

using Tris buffer, while acidic conditions were reached in distilled water through PDS decomposition. pH values were kept constant ($\text{pH}_0 \pm 0.2$) during the degradation experiments. The k_{obs} at different pH are reported in Fig. 6a, showing that degradation was faster at acidic and basic pH than at neutral pH.

Recent empirical evidence suggested that base-activated PDS must be conducted at $\text{pH} > 10$ to be effective [49] and this process did not therefore account for faster phenol degradation at pH 9. More plausibly, with a pKa of 10, a very small percentage of phenol appeared as phenolate ion which was much easily oxidized than the neutral phenol ($k_{\text{obs}} = 0.53 \text{ min}^{-1}$ vs $k_{\text{obs}} = 0.32 \text{ min}^{-1}$). At acidic pH, Cu(III) readily decomposed into $^{\bullet}\text{OH}$ which might explain a higher apparent kinetic rate constant ($k_{\text{obs}} = 0.44 \text{ min}^{-1}$). To confirm this point, NB was applied in the CuO/PDS/phenol system. As shown in Fig. S9, NB had a stronger inhibitory effect on the phenol degradation under acidic condition than under neutral condition. This result also indirectly confirmed the generation of Cu(III) in CuO/PDS system since Cu(III) decomposed in $^{\bullet}\text{OH}$ at acidic pH.

3.5.2. Water constituents

The influence of natural anions and dissolved organic matter (DOM) on phenol degradation was investigated separately. Cl^- and HCO_3^- are common background electrolytes in real water and they usually negatively influence the efficiency of radical-based AOPs as they are radical quenchers. In the CuO/PDS system, Cl^- (0.2 g/L) and HCO_3^- (0.5 g/L) anions had no significant influence on the phenol degradation (Table 2). These results confirmed earlier findings that Cu(III) was not very reactive towards Cl^- avoiding the formation of the chloride radicals (e.g., $\text{Cl}_2^{\bullet-}$) which are common to radical-based processes. The lack of Cl^- reactivity was confirmed by the lack of detection of 2-chlorophenol, 4-chlorophenol, and 2,4-dichlorophenol in LC-HRMS after injecting their analytical standards (Fig. S10). In homogeneous Cu^{2+} /PMS system, the negative role of HCO_3^- was ascribed to their coordination with Cu^{2+} [50]. This was not observed in CuO/PDS system most likely because most of the reactive Cu^{2+} ions were surface bound. Humic acids were also used as a surrogate for DOM at a concentration level of 2 mg/L, a value representative of DOM level in groundwater. In these conditions, the phenol degradation was only slightly inhibited ($k_{\text{obs}} = 0.27 \text{ min}^{-1}$ instead of $k_{\text{obs}} = 0.32 \text{ min}^{-1}$ in distilled water, Table 2) even though a competition of humic acids and phenol for the oxidant was expected. This small decrease in degradation was most likely due to adsorption of humic acid on the surface of the catalyst which could minimize the complexation of PDS on the catalyst surface.

Table 2

Water matrix effect on phenol degradation.

Water constituent	k_{obs} (min^{-1})	R^2
Pure water	0.32	0.99
Cl^-	0.32	0.97
HCO_3^-	0.28	0.99
HA	0.27	0.96
SO_4^{2-}	0.07	0.99
Wastewater	0.11	0.96

[phenol] = 20 mg/L; [CuO] = 10 g/L; [PDS] = 1 mM; $[\text{Cl}^-] = 200 \text{ mg/L}$; $[\text{HCO}_3^-] = 500 \text{ mg/L}$; $[\text{SO}_4^{2-}] = 500 \text{ mg/L}$; [Humic acids (HA)] = 2 mg/L; pH = 7 with Tris buffer.

More surprisingly, the CuO/PDS system was strongly blocked when sulfate anion concentrations were increased. This result meant that sulfate anions probably interacted with positively charged CuO blocking reactive sites for PDS activation. To confirm this specific point, different SO_4^{2-} concentrations were generated in the CuO/PDS system by varying the PDS concentrations used. Assuming that each mole of PDS led to two moles of SO_4^{2-} , 192, 96 and 38.4 mg/L of SO_4^{2-} were generated when adding 1, 0.5 and 0.2 mM of PDS, respectively. The results for phenol and PDS degradation are shown in Fig. 7a and 7b, respectively. Half-lives of PDS decreased from 15 min to 8 min in presence of 1 mM or 0.2 mM PDS, supporting the SO_4^{2-} sorption on catalyst surfaces as an inhibitory process for PDS decomposition. However, phenol degradation was much higher at 1 mM PDS ($k_{\text{obs}} = 0.32 \text{ min}^{-1}$) than at 0.2 mM ($k_{\text{obs}} = 0.02 \text{ min}^{-1}$), supporting that PDS decomposition was likely not the limiting step in phenol degradation kinetics.

3.5.3. Real wastewater

The investigated oxidation process was also applied for the treatment of a domestic wastewater treatment plant effluent spiked with 20 mg/L of phenol. The major physico-chemical properties of the wastewater are reported in Table S2. The phenol degradation was still effective with only a three-fold decrease in phenol half-lives when switching from distilled water to wastewater ($k_{\text{obs}} = 0.11 \text{ min}^{-1}$, Table 2). The slower degradation was likely due to the competition of DOM (TOC = 12.65 mg/L) for oxidant.

3.5.4. Cu leaching from CuO

The stability of the catalyst was assessed against the leached concentration of Cu measured in solution by ICP-AES after a filtration step on 0.45 μm cellulose filters. The Cu leaching from CuO in presence of PDS and phenol was investigated in different waters including distilled

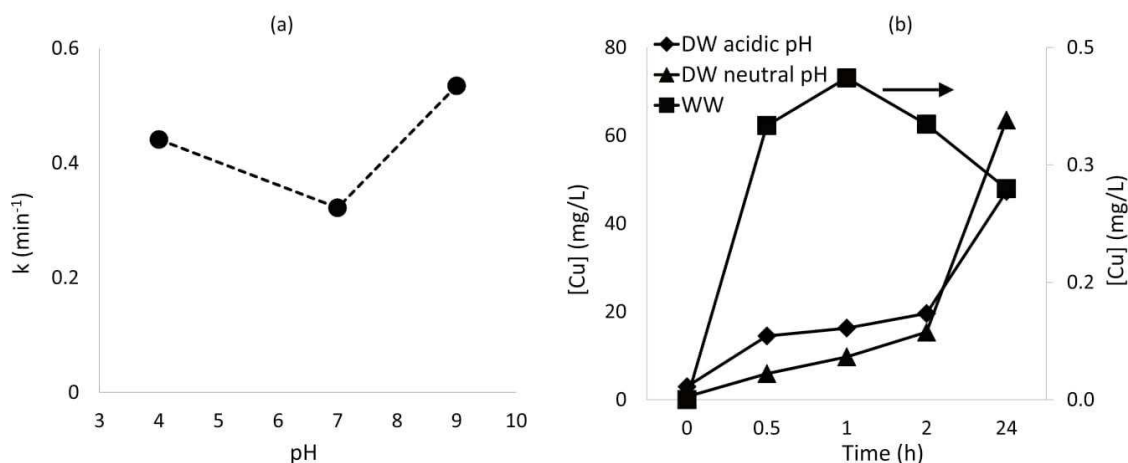


Fig. 6. (a) Degradation kinetic rate constants of phenol at different solution pH and (b) the effect of water matrix on copper ion leaching. The WW was filtered (0.45 μm) before adding CuO, PDS and phenol. [CuO] = 10 g/L; [PDS] = 1 mM; [phenol] = 20 mg/L.

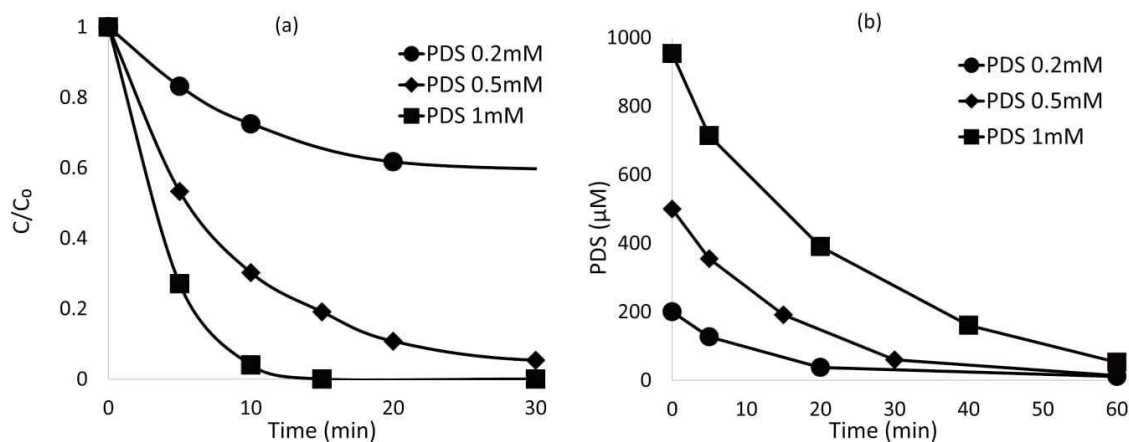


Fig. 7. Effect of PDS concentration on degradation kinetics of (a) phenol and (b) PDS in CuO/PDS system at pH = 7 using TRIS buffer. $[\text{CuO}] = 10 \text{ g/L}$; $[\text{PDS}] = 0.2, 0.5 \text{ and } 1 \text{ mM}$; $[\text{phenol}] = 20 \text{ mg/L}$.

water (DW) at acidic (pH = 3.5) and neutral pH and in secondary treated domestic wastewater (WW, pH = 7.8). The results are shown in Fig. 6b. Surprisingly, the Cu leaching dramatically decreased when moving from distilled water at neutral pH (63.5 mg/L after 24 h reaction time) to wastewater (0.27 \pm mg/L at the end of the 24 h reaction time). An unexpected result was a lower Cu leaching (47.3 mg/L after 24 h reaction time) at acidic pH in distilled water without a clear explanation for this experimental result. Moreover, the Cu release was not linearly correlated with the oxidant concentration since a Cu concentration value of 0.21 mg/L was reached at a PDS concentration of 0.1 mM which was close to the concentration obtained at 1 mM PDS (Table S3). The low Cu leaching in wastewater treatment might be ascribed to HCO_3^- and its complexing ability to Cu^{2+} . Indeed, in presence of 1–10 mM of HCO_3^- , Cu^{2+} may predominantly exist as surface insoluble CuCO_3 [50]. The Cu leaching was far less than that of 1 mg/L which is required by environmental quality standards for surface water and by drinking water regulations, making the CuO/PDS oxidation system promising in application. In addition, the CuO/PDS was still efficient in phenol removal with only a three-fold decrease in phenol half-lives when switching from distilled water to wastewater.

3.5.5. Stability and reusability

For a sustainable operation with high performance, the CuO particles need to maintain high catalytic activity and stable structure for prolonged operation time. Therefore, sequential experiments were carried out to investigate the reusability of CuO. After four cycles of CuO use, no significant deterioration in the catalytic activity was observed and the phenol degradation rates remained higher than 82% (Fig. 8a). Interestingly, compared with distilled water, the PDS decomposition was significantly limited in wastewater (Fig. 8b) and steadily decreased across the successive experiments (Fig. 8b), likely due to increased sorption of SO_4^{2-} anions and/or DOM on CuO active sites. A lower PDS activation led to catalyst preservation and calls for avoiding the PDS usage in excess.

3.6. Applicability of CuO/PDS system

To evaluate the practical applicability of CuO/PDS system, we investigated the removal of several antibiotics namely SMX, CLA, CIP and CFX, belonging to several different families of environmental relevance (i.e., sulfonamide, macrolide, fluoroquinolone and cephalosporin, respectively) in distilled water. SMX, CLA, CIP and CFX were all

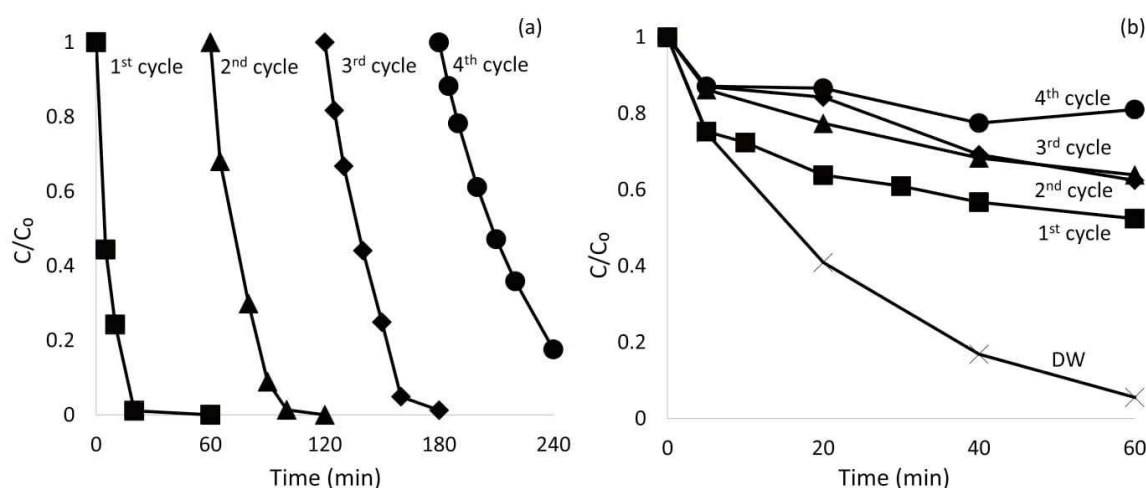


Fig. 8. (a) Phenol degradation and (b) PDS decomposition kinetics across four sequential experiments. $[\text{CuO}] = 10 \text{ g/L}$; $[\text{PDS}] = 1 \text{ mM}$; $[\text{phenol}] = 20 \text{ mg/L}$. Every treatment cycle lasted 60 min.

degraded and degradation kinetics fitted to a first order kinetic model with $k_{obs} = 0.24 \pm 0.02, 0.12 \pm 0.01, 0.31 \pm 0.03, 3.10 \pm 0.22 \text{ min}^{-1}$, respectively. Their transformation pathways were elucidated by identifying their TPs following a suspect screening workflow in LC-HRMS (see Fig. 9). The databases were made up of a list of possible antibiotic TPs with their molecular formula and exact mass (Tables S4–S7). All detected TPs of target antibiotics with a mass error < 5 ppm are shown in Figs. S11–S14 and were previously identified under different oxidative processes. Consequently, detailed interpretation of MS data is not presented. As shown in Fig. 9a, the CIP degradation could be due to the stepwise decomposition of the piperazine ring by Cu(III) through electron transfer at the secondary amine leading to ring opening and the generation of N-desethyleno-CIP (CIP 2) by losses of a formaldehyde group from CIP 1. CIP 2 was further oxidized to CIP 3 through N-dealkylation reaction. This piperazine ring cleavage pathway has been previously reported under $\text{SO}_4^{\cdot-}$ oxidation. However, in contrast to $\text{SO}_4^{\cdot-}$, which is another well-known one-electron oxidant [51], the hydroxylation pathway with hydroxyl radical firstly attacking on the quinolone ring and the substitution of the fluorine atom by a hydroxyl group were not observed. As shown in Fig. 9b, two oxidation pathways were operating simultaneously for SMX degradation: (1) oxidation of the amine group through a one electron oxidation process to form a N-central radical, yielding to the generation of a dimer (SMX 1, m/z 503) and (2) cleavage of the sulfonamide bond leading to SMX 2 (m/z 174) and SMX 3 (m/z 99). In contrast to SMX degradation under $\text{SO}_4^{\cdot-}$ oxidation, hydroxylation of the benzene and isoxazole rings was not observed, neither was observed the formation of the nitro-SMX derivative which involved $\cdot\text{OH}$ [52]. Three main TPs of CFX were detected: CFX 1 (m/z 364), CFX 2 (m/z 336) and CFX 3 (m/z 151). Under thermal activated persulfate, the formation of six isomers at m/z 364 was reported resulting from either oxygen transfer or hydroxylation processes [53]. Only one TP at m/z 364 was detected in CuO/PDS system. The formation of the sulfoxide derivative was the most reasonable pathway because this transformation was observed in presence of PDS alone. It was also shown that the complex of Cu^{2+} with CFX could efficiently activate PDS to induce rapid

degradation of CFX [21] with CFX 2 generation, as the predominant TP. This transformation reaction most likely took place in CuO/PDS due to Cu^{2+} leaching and was ascribed to cupryl ion reactivity. CFX 2 resulted from a decarboxylation reaction of CFX 1. CFX 3 was likely to be evolved from a dealkylation reaction following single electron transfer at the N of the amide group. As shown in Fig. 9d, CLA underwent two transformation reactions including N-demethylation leading to CLA 1 (m/z 734) and O-dealkylation leading to cladinose and desosamine sugar losses, while the lactone ring was preserved. These N- and O-dealkylation reactions were most likely initiated by a one-electron oxidation of the heteroatom. Hydroxylation reactions, which were reported for the degradation of erythromycin under UV-C/PDS irradiation were not observed [54]. Collectively, the results of this work confirmed that Cu(III) is a strong one-electron oxidant due to its high reduction potential in solid ($\text{Cu(III)/Cu(II)} = 2.3 \text{ V}$) and presented high reactivity against N and O containing electron rich moieties leading to the degradation of different classes of antibiotics. Higher Cu(III) selectivity than $\text{SO}_4^{\cdot-}$ was also observed, since hydroxylation reactions were avoided. $\text{SO}_4^{\cdot-}$ oxidation and $\cdot\text{OH}$ oxidation (resulting from $\text{SO}_4^{\cdot-}$ decomposition) lead to the formation of 6-hydroxy-6-defluoro-CIP, 14-hydroxy-CLA and 4-nitro-SMX. All these TPs preserve biological activity. Consequently, Cu(III) oxidant appeared to restrict the number of generated TPs of toxicological concern.

4. Conclusions

In this study, the CuO catalyzed PDS activation system was deeply investigated and presented high efficiency for phenol degradation in different waters including wastewater at neutral pH. Identification of reactive species and phenol TPs identification demonstrated that Cu(III) most likely acted as the predominant reactive species for phenol degradation. $^1\text{O}_2$, even though highly formed in the CuO/PDS system, was a minor contributor during the phenol degradation process due to physical quenching with water. Therefore, the CuO catalyzed PDS system showed great advantages for water treatment application as the

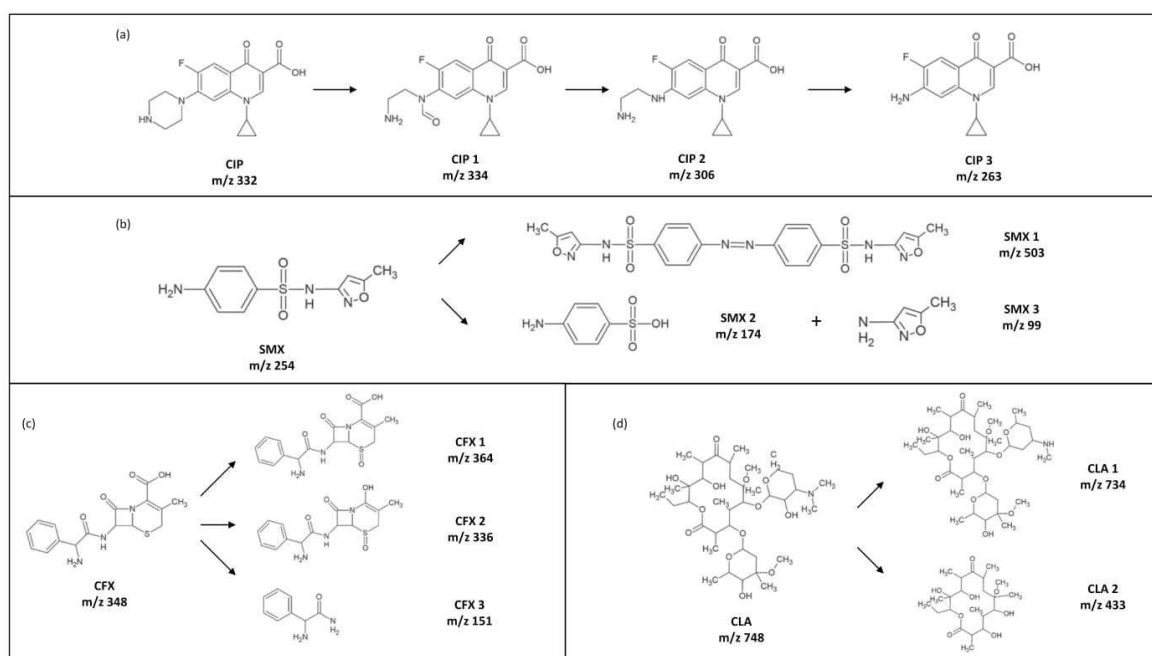


Fig. 9. Proposed transformation pathways of (a) ciprofloxacin (CIP), (b) sulfamethoxazole (SMX), (c) cephalexin (CFX) and (d) clarithromycin (CLA) in the CuO/PDS system.

high resistance to the background Cl^- anions without the formation of chlorinated by-products, with limited Cu^{2+} leaching (below 0.5 mg/L) and limited oxidant consumption in wastewater due to poor reactivity of Cu(III) with DOM. Cu(III) being an one-electron transfer oxidant, the system presented a preference to react with electron-rich compounds such as phenols leading to polymerization reactions. The efficient degradation of selected antibiotics by CuO/PDS system also demonstrated the practical applicability of this system for emerging contaminants removal. However, besides Cu(III), $^1\text{O}_2$ and Cu(I) were generated in the CuO/PDS. All these species are known to be good biocides which opens a possibility to use the CuO/PDS system for water disinfection.

CRedit authorship contribution statement

Chan Li: Formal analysis, Writing - original draft, Writing - review & editing. **Vincent Goetz:** Experimental data interpretation. **Serge Chiron:** Conceptualization, Writing - review & editing.

Declaration of Competing Interest

The authors declare that they have no known competing financial interests or personal relationships that could have appeared to influence the work reported in this paper.

Acknowledgements

This research was financially supported by the Water Joint Programming Initiative (JPI) through the research project IDOUM - Innovative Decentralized and low cost treatment systems for Optimal Urban wastewater Management. Chan Li thanks the Occitanie Region for her Ph.D. grant.

Appendix A. Supporting information

Supplementary data associated with this article can be found in the online version at [doi:10.1016/j.jece.2021.105145](https://doi.org/10.1016/j.jece.2021.105145).

References

- [1] E.J. Behrman, Peroxydisulfate chemistry in the environmental literature: a brief critique, *J. Hazard. Mater.* 35 (2018) 0–1, <https://doi.org/10.1016/j.jhazmat.2018.11.018>.
- [2] J. Wang, S. Wang, Activation of persulfate (PS) and peroxymonosulfate (PMS) and application for the degradation of emerging contaminants, *Chem. Eng. J.* 334 (2018) 1502–1517, <https://doi.org/10.1016/j.cej.2017.11.059>.
- [3] J. Lee, U. Von Gunten, J.H. Kim, Persulfate-based advanced oxidation: critical assessment of opportunities and roadblocks, *Environ. Sci. Technol.* 54 (2020) 3064–3081, <https://doi.org/10.1021/acs.est.9b07082>.
- [4] S. Wacławek, H.V. Lütze, K. Grübel, V.V.T. Padil, M. Černík, D.D. Dionysiou, Chemistry of persulfates in water and wastewater treatment: a review, *Chem. Eng. J.* 330 (2017) 44–62, <https://doi.org/10.1016/j.cej.2017.07.132>.
- [5] A. Jawad, K. Zhan, H. Wang, A. Shahzad, Z. Zeng, J. Wang, X. Zhou, H. Ullah, Z. Chen, Z. Chen, Tuning of persulfate activation from a free radical to a nonradical pathway through the incorporation of non-redox magnesium oxide, *Environ. Sci. Technol.* 54 (2020) 2476–2488, <https://doi.org/10.1021/acs.est.9b04696>.
- [6] J. Yan, J. Li, J. Peng, H. Zhang, Y. Zhang, B. Lai, Efficient degradation of sulfamethoxazole by the $\text{CuO}/\text{Al}_2\text{O}_3$ (EPC) coupled PMS system: optimization, degradation pathways and toxicity evaluation, *Chem. Eng. J.* 359 (2019) 1097–1110, <https://doi.org/10.1016/j.cej.2018.11.074>.
- [7] Y. Leng, W. Guo, X. Shi, Y. Li, A. Wang, F. Hao, L. Xing, Degradation of Rhodamine B by persulfate activated with Fe_3O_4 : effect of polyhydroquinone serving as an electron shuttle, *Chem. Eng. J.* 240 (2014) 338–343, <https://doi.org/10.1016/j.cej.2013.11.090>.
- [8] R. Li, X. Jin, M. Megharaj, R. Naidu, Z. Chen, Heterogeneous Fenton oxidation of 2,4-dichlorophenol using iron-based nanoparticles and persulfate system, *Chem. Eng. J.* 264 (2015) 587–594, <https://doi.org/10.1016/j.cej.2014.11.128>.
- [9] A. Jawad, J. Lang, Z. Liao, A. Khan, J. Iftikhar, Z. Lv, S. Long, Z. Chen, Z. Chen, Activation of persulfate by $\text{CuOx}/\text{Co-LDH}$: a novel heterogeneous system for contaminant degradation with broad pH window and controlled leaching, *Chem. Eng. J.* 335 (2018) 548–559, <https://doi.org/10.1016/j.cej.2017.10.097>.
- [10] F. Ji, C. Li, L. Deng, Performance of CuO/Oxone system: heterogeneous catalytic oxidation of phenol at ambient conditions, *Chem. Eng. J.* 178 (2011) 239–243, <https://doi.org/10.1016/j.cej.2011.10.059>.
- [11] T. Zhang, Y. Chen, Y. Wang, J. Le Roux, Y. Yang, J.P. Croué, Efficient peroxydisulfate activation process not relying on sulfate radical generation for water pollutant degradation, *Environ. Sci. Technol.* 48 (2014) 5868–5875, <https://doi.org/10.1021/es501218f>.
- [12] Y. Ding, H. Tang, S. Zhang, S. Wang, H. Tang, Efficient degradation of carbamazepine by easily recyclable microscaled CuFe_2O_4 mediated heterogeneous activation of peroxymonosulfate, *J. Hazard. Mater.* 317 (2016) 686–694, <https://doi.org/10.1016/j.jhazmat.2016.06.004>.
- [13] Y. Xu, J. Ai, H. Zhang, The mechanism of degradation of bisphenol A using the magnetically separable CuFe_2O_4 /peroxymonosulfate heterogeneous oxidation process, *J. Hazard. Mater.* 309 (2016) 87–96, <https://doi.org/10.1016/j.jhazmat.2016.01.023>.
- [14] S. Wang, J. Tian, Q. Wang, F. Xiao, S. Gao, W. Shi, F. Cui, Development of CuO coated ceramic hollow fiber membrane for peroxymonosulfate activation: a highly efficient singlet oxygen-dominated oxidation process for bisphenol A degradation, *Appl. Catal. B Environ.* 256 (2019), 117783, <https://doi.org/10.1016/j.apcatb.2019.117783>.
- [15] WHO, Copper in drinking water, Background document for development of WHO guidelines for drinking-water quality, (2004). (https://www.who.int/water_sanitation_health/dwq/chemicals/copper.pdf).
- [16] L.R. Bennedsen, J. Muff, E.G. Søgaard, Influence of chloride and carbonates on the reactivity of activated persulfate, *Chemosphere* 86 (2012) 1092–1097, <https://doi.org/10.1016/j.chemosphere.2011.12.011>.
- [17] X. Du, Y. Zhang, I. Hussain, S. Huang, W. Huang, Insight into reactive oxygen species in persulfate activation with copper oxide: activated persulfate and trace radicals, *Chem. Eng. J.* 313 (2017) 1023–1032, <https://doi.org/10.1016/j.cej.2016.10.138>.
- [18] S. Wang, S. Gao, J. Tian, Q. Wang, T. Wang, X. Hao, F. Cui, A stable and easily prepared copper oxide catalyst for degradation of organic pollutants by peroxymonosulfate activation, *J. Hazard. Mater.* 387 (2020), 121995, <https://doi.org/10.1016/j.jhazmat.2019.121995>.
- [19] S. Xing, W. Li, B. Liu, Y. Wu, Y. Gao, Removal of ciprofloxacin by persulfate activation with CuO: a pH-dependent mechanism, *Chem. Eng. J.* 382 (2020), 122837, <https://doi.org/10.1016/j.cej.2019.122837>.
- [20] Y. Yang, G. Banerjee, G.W. Brudvig, J.H. Kim, J.J. Pignatello, Oxidation of organic compounds in water by unactivated peroxymonosulfate, *Environ. Sci. Technol.* 52 (2018) 5911–5919, <https://doi.org/10.1021/acs.est.8b00735>.
- [21] J. Chen, X. Zhou, P. Sun, Y. Zhang, C. Huang, Complexation enhances Cu(II)-activated peroxydisulfate: a novel activation mechanism and Cu(III) contribution, *Environ. Sci. Technol.* 53 (2019) 11774–11782, <https://doi.org/10.1021/acs.est.9b03873>.
- [22] Y.N. Ogibin, I. Troyanskii, E.K. Starostin, S.I. Moryasheva, G.I. Nikishin, Participation of Cu(III) in copper sulfate-catalyzed oxidation of 3-carboxypropyl radicals with $\text{S}_2\text{O}_8^{2-}$ ions, *Bull. Acad. Sci. USSR Div. Chem. Sci.* 26 (1977) 859–862, <https://doi.org/10.1007/bf01108221>.
- [23] L. Wang, H. Xu, N. Jiang, Z. Wang, J. Jiang, T. Zhang, Trace cupric species triggered decomposition of peroxymonosulfate and degradation of organic pollutants: Cu(III) being the primary and selective intermediate oxidant, *Environ. Sci. Technol.* 54 (2020) 4686–4694, <https://doi.org/10.1021/acs.est.0c00284>.
- [24] Y. Feng, W. Qing, L. Kong, H. Li, D. Wu, Y. Fan, Factors and mechanisms that influence the reactivity of trivalent copper: a novel oxidant for selective degradation of antibiotics, *Water Res.* 149 (2019) 1–8, <https://doi.org/10.1016/j.watres.2018.10.090>.
- [25] D. Meyerstein, Trivalent copper. I. A pulse radiolytic study of the chemical properties of the aquo complex, *Inorg. Chem.* 10 (1971) 638–641, <https://doi.org/10.1021/ic50097a040>.
- [26] L.W. Matzek, K.E. Carter, Activated persulfate for organic chemical degradation: a review, *Chemosphere* 151 (2016) 178–188, <https://doi.org/10.1016/j.chemosphere.2016.02.055>.
- [27] Z. Chen, Q. Wan, G. Wen, X. Luo, X. Xu, J. Wang, K. Li, T. Huang, J. Ma, Effect of borate buffer on organics degradation with unactivated peroxymonosulfate: influencing factors and mechanisms, *Sep. Purif. Technol.* 256 (2021), 117841, <https://doi.org/10.1016/j.seppur.2020.117841>.
- [28] C. Liang, C.F. Huang, N. Mohanty, R.M. Kurakalva, A rapid spectrophotometric determination of persulfate anion in ISCO, *Chemosphere* 73 (2008) 1540–1543, <https://doi.org/10.1016/j.chemosphere.2008.08.043>.
- [29] E. Graf, J.T. Penniston, Method for determination of hydrogen peroxide, with its application illustrated by glucose assay, *Clin. Chem.* 26 (1980) 658–660, <https://doi.org/10.1093/clinchem/26.5.658>.
- [30] S.V. Lapsin, V.G. Alekseev, Copper(II) complexation with ampicillin, amoxicillin, and cephalaxin, *Russ. J. Inorg. Chem.* 54 (2009) 1066–1069, <https://doi.org/10.1134/S0036023609070122>.
- [31] H. Liang, Y. Zhang, S. Huang, I. Hussain, Oxidative degradation of p-chloroaniline by copper oxidate activated persulfate, *Chem. Eng. J.* 218 (2013) 384–391, <https://doi.org/10.1016/j.cej.2012.11.093>.
- [32] Y. Cho, R. Lin, Y. Lin, Degradation of 2,4-dichlorophenol by CuO-activated peroxydisulfate: Importance of surface-bound radicals and reaction kinetics, *Sci. Total Environ.* 699 (2020), 134379, <https://doi.org/10.1016/j.scitotenv.2019.134379>.
- [33] C.L. Clifton, R.E. Huie, Rate constants for hydrogen abstraction reactions of the sulfate radical, SO_4^- alcohols, *Int. J. Chem. Kinet.* 21 (1989) 677–687, <https://doi.org/10.1002/kin.550210807>.
- [34] J. Hu, H. Dong, J. Qu, Z. Qiang, Enhanced degradation of iopamidol by peroxymonosulfate catalyzed by two pipe corrosion products (CuO and $\Delta\text{-MnO}_2$), *Water Res.* 112 (2017) 1–8, <https://doi.org/10.1016/j.watres.2017.01.025>.

Supporting Material

Peroxydisulfate activation process on copper oxide: Cu(III) as the predominant selective intermediate oxidant for waterborne antibiotics removal

Chan Li¹, Vincent Goetz² and Serge Chiron^{1*}

¹UMR HydroSciences Montpellier, Montpellier University, IRD, 15 Ave Charles Flahault 34093 Montpellier cedex 5, France

²PROMES-CNRS UPR 8521, PROcess Material and Solar Energy, Rambla de la Thermodynamique, 66100 Perpignan, France

Table S1. List of previously identified transformation products of phenol under sulfate and hydroxyl radical-based advanced oxidation [1], under superoxide radical [2] and singlet oxygen reactivity [3].

Compound	Formula	Monoisotopic mass	[M - H] ⁻
Phenol	C ₆ H ₆ O	94.0419	93.0341
Phenoxyphenol	C ₁₂ H ₁₀ O ₂	186.0681	185.0603
Benzaldehyde	C ₇ H ₆ O	106.0419	105.0341
<i>p</i> -Benzoquinone	C ₆ H ₄ O ₂	108.0211	107.0133
Hydroquinone	C ₆ H ₆ O ₂	110.0368	109.0290
Catechol	C ₆ H ₆ O ₂	110.0368	109.0290
Resorcinol	C ₆ H ₆ O ₂	110.0368	109.0290
3-Hydroxybenzaldehyde	C ₇ H ₆ O ₂	122.0368	121.0290
<i>p</i> -Hydroxybenzoic acid	C ₇ H ₆ O ₃	138.0317	137.0239
3,4-Dimethyl-benzoic acid	C ₉ H ₁₀ O ₂	150.0681	149.0603
Resorcinol monoacetate	C ₈ H ₈ O ₃	152.0473	151.0395
2-Isopropylphenol	C ₉ H ₁₂ O ₂	152.0837	151.0759
Phenol, 5-methyl-2-(1-methylethyl)-acetate	C ₁₂ H ₁₆ O ₂	192.1150	191.1072
2-Chlorophenol	C ₆ H ₆ ClO	128.0029	126.9951
2,4-Dichlorophenol	C ₆ H ₄ Cl ₂ O	161.9639	160.9561
2,2-Dimethyl-3-hexanone	C ₈ H ₁₆ O	128.1201	127.1123
2-Ethyl-4-methyl-benzoic acid	C ₈ H ₁₈ O	130.1358	129.1280

Table S2. Major physico-chemical properties of the investigated secondary treated domestic wastewater after filtration on 0.45 μm cellulose filter.

Parameter	pH	HCO ₃ ⁻	Cl ⁻	NO ₃ ⁻	SO ₄ ²⁻	TOC	Cu
Value	7.8	514.3	195.3	12.9	58.9	12.65	3.75

	mg/L	mg/L	mg/L	mg/L	mg/L	μg/L
--	------	------	------	------	------	------

Table S3. Cu leaching from CuO in wastewater (WW) during phenol degradation in CuO/PDS system. [CuO] = 10 g/L; [PDS] = 1 mM; [phenol] = 20 mg/L.

Time (h)	[Cu] (mg/L)	
	1 mM PDS	0.1 mM PDS
0	0	0
0.5	0.35	0.11
1	0.41	0.10
2	0.35	0.10
24	0.27	0.21

Table S4. List of previously identified transformation products of cephalexin (CFX) under different oxidative systems [4–9].

Compound	Formula	Monoisotopic mass	[M + H] ⁺
CFX	C ₁₆ H ₁₇ N ₃ O ₄ S	347.0940	348.1018
TP336	C ₁₅ H ₁₇ N ₃ O ₄ S	335.0940	336.1018
TP364	C ₁₆ H ₁₇ N ₃ O ₅ S	363.0889	364.0967
TP207	C ₁₁ H ₁₄ N ₂ O ₂	206.1055	207.1133
TP386	C ₁₅ H ₁₉ N ₃ O ₇ S	385.0944	386.1022
TP370	C ₁₅ H ₁₉ N ₃ O ₆ S	369.0995	370.1073
TP327	C ₁₄ H ₁₈ N ₂ O ₅ S	326.0936	327.1014
TP194	C ₆ H ₁₁ NO ₄ S	193.0409	194.0487
TP176	C ₆ H ₈ NO ₃ S	175.0303	176.0381
TP159	C ₆ H ₈ NO ₂ S	158.0276	159.0354
TP140	C ₇ H ₇ O ₃	139.0395	140.0473
TP151	C ₈ H ₁₀ N ₂ O	150.0793	151.0871
TP137	C ₈ H ₈ N ₂ O	136.0524	137.0602
TP105	C ₃ H ₄ O ₃	104.0110	105.0188
TP103	C ₅ H ₁₀ O ₂	102.0681	103.0759
TP101	C ₅ H ₈ O ₂	100.0524	101.0602
TP104	C ₃ H ₅ NOS	103.0092	104.0170
TP86	C ₃ H ₃ NO ₂	85.0164	86.0242
TP75	C ₂ H ₆ N ₂ O	74.0480	75.0558

TP61	C ₂ H ₄ O ₂	60.0211	61.0289
TP200	C ₈ H ₉ NO ₃ S	199.0303	200.0381
TP136	C ₈ H ₉ NO	135.0684	136.0762
TP101	C ₅ H ₈ O ₂	100.0524	101.0602
TP74	C ₃ H ₇ NO	73.0528	74.0606
TP71	C ₄ H ₆ O	70.0419	71.0497
TP186	C ₈ H ₁₁ NO ₂ S	185.0510	186.0588
TP188	C ₈ H ₁₃ NO ₂ S	187.0667	188.0745
TP144	C ₇ H ₁₃ NS	143.0769	144.0847
TP146	C ₇ H ₁₅ NS	145.0925	146.1003
TP86	C ₅ H ₁₁ N	85.0891	86.0969
TP63	C ₂ H ₆ S	62.0190	63.0268
TP121	C ₈ H ₈ O	120.0575	121.0653
TP107	C ₈ H ₁₀	106.0783	107.0861
TP109	C ₈ H ₁₂	108.0939	109.1017
TP318	C ₁₅ H ₁₅ N ₃ O ₃ S	317.0834	318.0912
TP265	C ₁₄ H ₂₀ N ₂ OS	264.1296	265.1374
TP334	C ₁₅ H ₁₅ N ₃ O ₄ S	333.0783	334.0861
TP362	C ₁₆ H ₁₅ N ₃ O ₅ S	361.0732	362.0810
TP378	C ₁₆ H ₁₅ N ₃ O ₆ S	377.0682	378.0760
TP394	C ₁₆ H ₁₅ N ₃ O ₇ S	393.0631	394.0709
TP412	C ₁₆ H ₁₇ N ₃ O ₈ S	411.0736	412.0814
TP396	C ₁₆ H ₁₇ N ₃ O ₇ S	395.0787	396.0865
TP346	C ₁₆ H ₁₅ N ₃ O ₄ S	345.0783	346.0861

Table S5. List of previously identified transformation products of ciprofloxacin (CIP) under different oxidative systems [10-14].

Compound	Formula	Monoisotopic mass	[M + H] ⁺
CIP	C ₁₇ H ₁₈ FN ₃ O ₃	331.1332	332.1410
TP306	C ₁₅ H ₁₆ FN ₃ O ₃	305.1176	306.1254
TP263	C ₁₃ H ₁₁ FN ₂ O ₃	262.0753	263.0832
TP348	C ₁₇ H ₁₈ FN ₃ O ₄	347.1281	348.1359
TP315	C ₁₇ H ₁₇ FN ₃ O ₂	314.1305	315.1383
TP374	C ₁₇ H ₁₅ N ₃ O ₇	373.0910	374.0988
TP389	C ₁₇ H ₁₄ N ₃ O ₈	388.0781	389.0859

TP321	C ₁₅ H ₁₅ FN ₃ O ₄	320.1047	321.1125
TP250	C ₁₂ H ₁₂ FN ₃ O ₂	249.0914	250.0992
TP345	C ₁₇ H ₁₈ N ₃ O ₅	344.1246	345.1324
TP360	C ₁₇ H ₁₇ N ₃ O ₆	359.1117	360.1195
TP332	C ₁₆ H ₁₇ N ₃ O ₅	331.1168	332.1246
TP348	C ₁₆ H ₁₇ N ₃ O ₆	347.1117	348.1195
TP378	C ₁₇ H ₁₉ N ₃ O ₇	377.1223	378.1301
TP344	C ₁₇ H ₁₇ N ₃ O ₅	343.1168	344.1246
TP316	C ₁₆ H ₁₇ N ₃ O ₄	315.1219	316.1297
TP288	C ₁₅ H ₁₇ N ₃ O ₃	287.1270	288.1348
TP245	C ₁₃ H ₁₂ N ₂ O ₃	244.0848	245.0926
TP330	C ₁₇ H ₁₆ FN ₃ O ₃	329.1176	330.1254
TP365	C ₁₇ H ₁₉ FN ₃ O ₅	364.1309	365.1387
TP346	C ₁₇ H ₁₆ FN ₃ O ₄	345.1125	346.1203
TP362	C ₁₇ H ₁₆ FN ₃ O ₅	361.1074	362.1152
TP334	C ₁₆ H ₁₆ FN ₃ O ₄	333.1125	334.1203
TP330	C ₁₇ H ₁₉ N ₃ O ₄	329.1376	330.1454
TP346	C ₁₇ H ₁₉ N ₃ O ₅	345.1325	346.1403
TP291	C ₁₄ H ₁₁ FN ₂ O ₄	290.0703	291.0781

Table S6. List of previously identified transformation products of clarithromycin (CLA) under different oxidative systems [15-18].

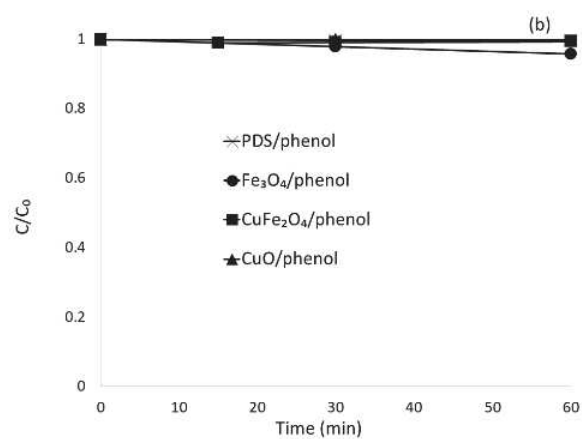
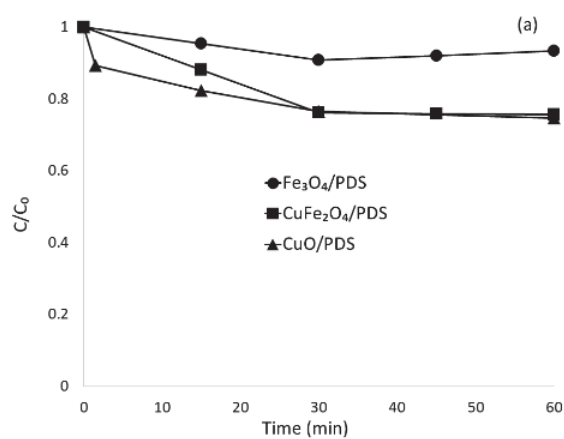
Compound	Formula	Monoisotopic mass	[M + H] ⁺
CLA	C ₃₈ H ₆₉ NO ₁₃	747.4769	748.4847
TP764	C ₃₈ H ₆₉ NO ₁₄	763.4718	764.4796
TP762a	C ₃₈ H ₆₇ NO ₁₄	761.4562	762.4640
TP762b	C ₃₉ H ₇₁ NO ₁₃	761.4925	762.5003

TP734	C ₃₇ H ₆₇ NO ₁₃	733.4612	734.4690
TP590	C ₃₀ H ₅₅ NO ₁₀	589.3826	590.3904
TP606	C ₃₀ H ₅₅ NO ₁₁	605.3775	606.3853
TP576	C ₂₉ H ₅₃ NO ₁₀	575.3669	576.3747
TP604	C ₃₁ H ₅₇ NO ₁₀	603.3982	604.4060
TP780	C ₃₈ H ₆₉ NO ₁₅	779.4662	780.4740
TP796	C ₃₈ H ₆₉ NO ₁₆	795.4611	796.4689
TP812	C ₃₈ H ₆₉ NO ₁₇	811.4560	812.4638
TP746	C ₃₈ H ₆₇ NO ₁₃	745.4607	746.4685
TP622	C ₃₀ H ₅₅ NO ₁₂	621.3719	622.3797
TP704	C ₃₆ H ₆₅ NO ₁₂	703.4501	704.4579
TP705	C ₃₆ H ₆₄ O ₁₃	704.4341	705.4419
TP732	C ₃₈ H ₆₉ NO ₁₂	731.4814	732.4892
TP716	C ₃₇ H ₆₅ NO ₁₂	715.4501	716.4579
TP764	C ₃₈ H ₆₉ NO ₁₄	763.4713	764.4791
TP762	C ₃₈ H ₆₇ NO ₁₄	761.4556	762.4634
TP591	C ₃₀ H ₅₄ O ₁₁	590.3661	591.3739
TP433	C ₂₂ H ₄₀ O ₈	432.2718	433.2796
TP431	C ₂₂ H ₃₈ O ₈	430.2561	431.2639
TP403	C ₂₁ H ₃₈ O ₇	402.2612	403.2690
TP387	C ₂₁ H ₃₈ O ₆	386.2663	387.2741
TP359	C ₁₉ H ₃₄ O ₆	358.2350	359.2428
TP329	C ₁₈ H ₃₂ O ₅	328.2244	329.2322
TP327	C ₁₈ H ₃₀ O ₅	326.2088	327.2166
TP325	C ₁₈ H ₂₈ O ₅	324.1931	325.2009

Table S7. List of previously identified transformation products of sulfamethoxazole (SMX)

under different oxidative systems [19-23].

Compound	Formula	Monoisotopic mass	[M + H] ⁺
SMX	C ₁₀ H ₁₁ N ₃ O ₃ S	253.0516	254.0594
TP256	C ₉ H ₉ N ₃ O ₄ S	255.0308	256.0386
TP270	C ₁₀ H ₁₁ N ₃ O ₄ S	269.0465	270.0543
TP284	C ₁₀ H ₉ N ₃ O ₅ S	283.0257	284.0335
TP503	C ₂₀ H ₁₈ N ₆ O ₆ S ₂	502.0724	503.0802
TP519	C ₂₀ H ₁₈ N ₆ O ₇ S ₂	518.0673	519.0751
TP99	C ₄ H ₆ N ₂ O	98.0475	99.0553
TP174	C ₆ H ₇ NO ₃ S	173.0141	174.0219
TP215	C ₈ H ₁₀ N ₂ O ₃ S	214.0407	215.0485
TP296	C ₁₂ H ₁₃ N ₃ O ₄ S	295.0621	296.0699
TP312	C ₁₂ H ₁₃ N ₃ O ₅ S	311.0570	312.0648
TP268	C ₁₀ H ₉ N ₃ O ₄ S	267.0308	268.0386
TP255	C ₁₀ H ₁₀ N ₂ O ₄ S	254.0356	255.0434
TP239	C ₁₀ H ₁₀ N ₂ O ₃ S	238.0407	239.0485
TP221	C ₁₀ H ₈ N ₂ O ₂ S	220.0301	221.0379
TP179	C ₈ H ₆ N ₂ OS	178.0195	179.0273
TP176	C ₄ H ₄ N ₂ O ₄ S	175.9886	176.9964
TP149	C ₂ HN ₂ O ₄ S	148.9652	149.9730



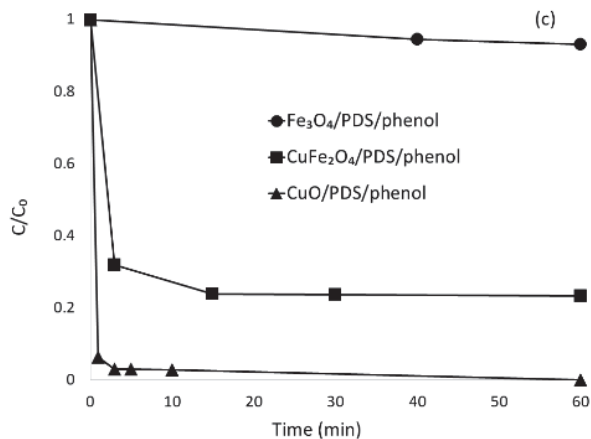


Fig. S1. (a) Decomposition of PDS, (b) the degradation of phenol in presence of PDS, CuO, Fe₃O₄ and CuFe₂O₄ alone and (c) combined system in distilled water. [CuO μm] = [Fe₃O₄ μm] = [CuFe₂O₄ nm] = 10 g/L; [PDS] = 1 mM; [phenol] = 20 mg/L.

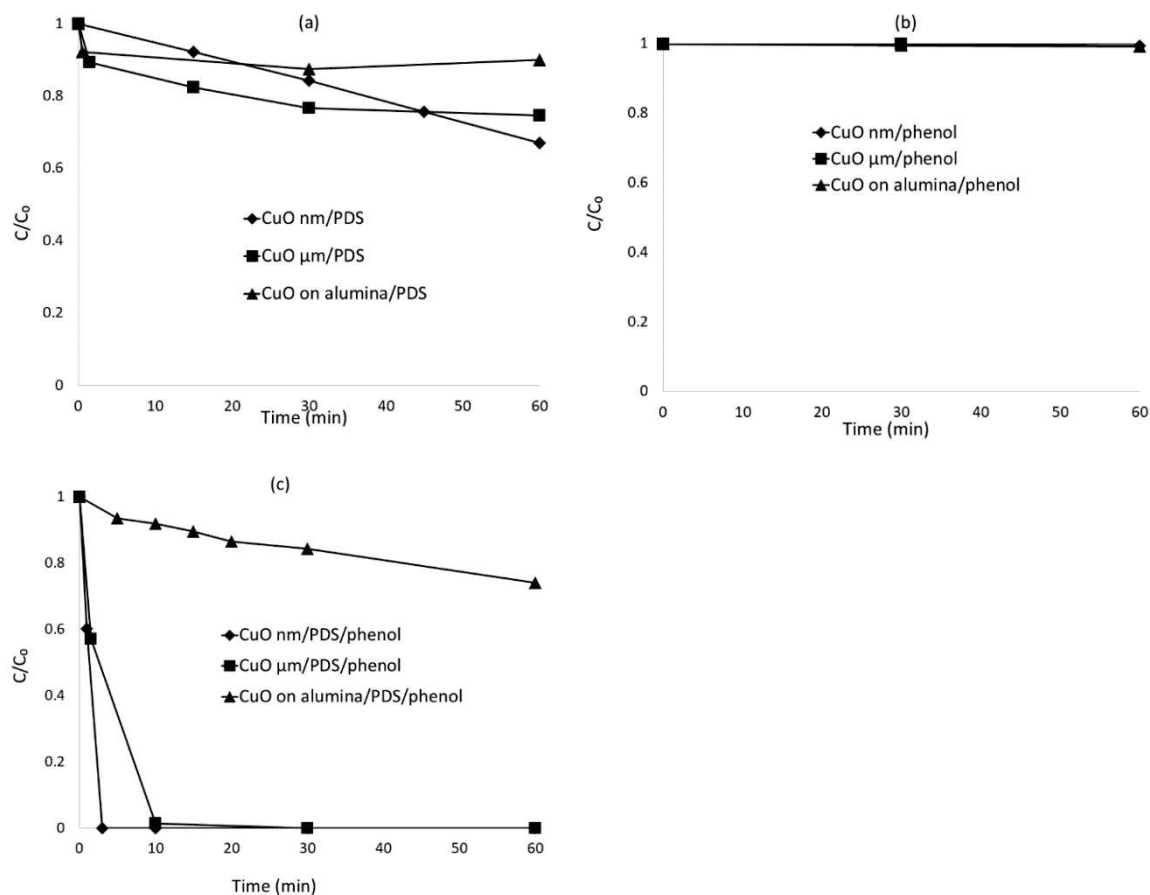


Fig. S2. (a) Decomposition of PDS, (b) the adsorption of phenol on different types of copper oxides: CuO nm, CuO μm and CuO supported on alumina and (c) the degradation of phenol in different CuOs/PDS systems in distilled water. [CuOs] = 10 g/L; [PDS] = 1 mM; [phenol] = 20 mg/L.

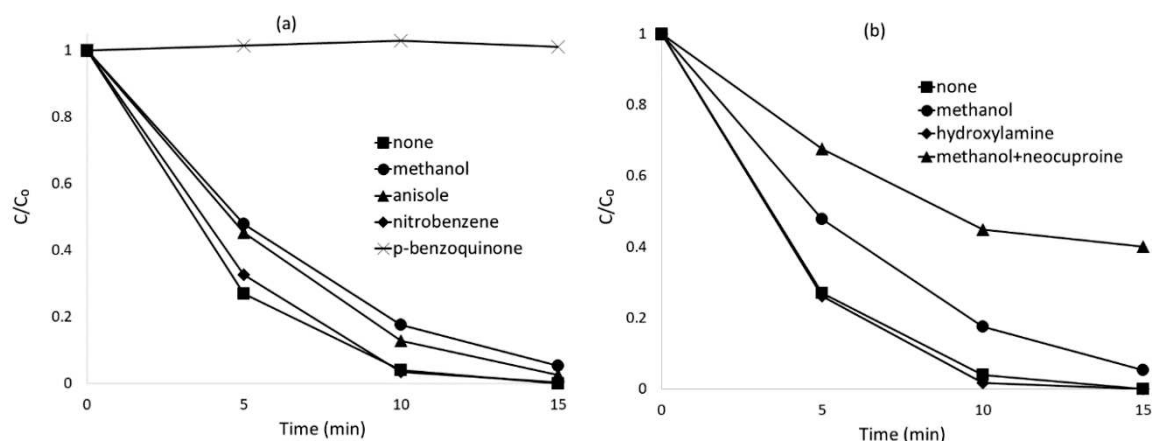


Fig. S3. (a) Degradation kinetics of phenol in CuO/PDS system in presence of different scavengers including methanol, anisole, nitrobenzene and p-benzoquinone and (b) in presence of neocuproine and hydroxylamine at neutral pH using a Tris buffer. $[CuO] = 10 \text{ g/L}$; $[PDS] = 1 \text{ mM}$; $[phenol] = 20 \text{ mg/L}$; $[methanol] = 4.9 \text{ M}$; $[anisole] = 18.5 \text{ mM}$; $[nitrobenzene] = 19.4 \text{ mM}$; $[p\text{-benzoquinone}] = 18.5 \text{ mM}$; $[hydroxylamine] = 0.19 \text{ mM}$; $[neocuproine] = 0.06 \text{ mM}$.

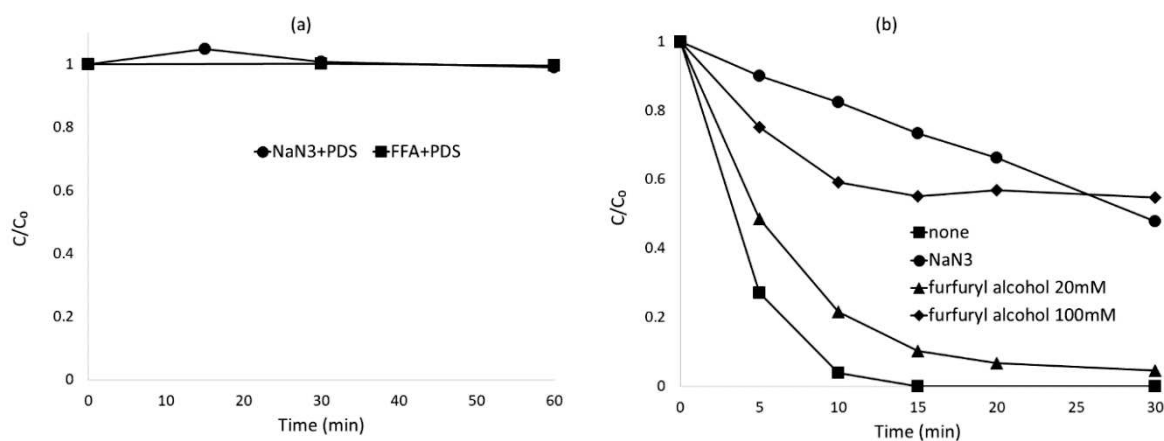


Fig. S4. Degradation kinetics of (a) PDS in presence of sodium azide (NaN_3) and furfuryl alcohol (FFA) and (b) phenol in CuO/PDS system in presence of different scavengers including furfuryl alcohol and sodium azide (NaN_3) at neutral pH using a Tris buffer. $[CuO] = 10 \text{ g/L}$; $[PDS] = 1 \text{ mM}$; $[phenol] = 20 \text{ mg/L}$; $[NaN_3] = 100 \text{ mM}$; $[furfuryl \text{ alcohol}] = 20 \text{ and } 100 \text{ mM}$.

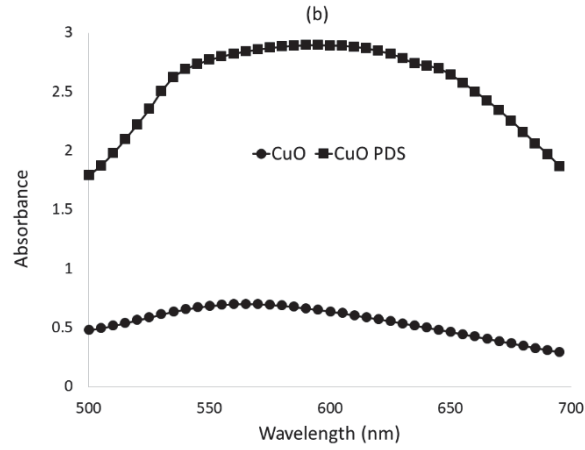


Fig. S5. UV-vis absorbance spectra of CuO/PDS after the addition of molybdate salt for H_2O_2 detection at pH 7. $[CuO] = 10 \text{ g/L}$; $[PDS] = 1 \text{ mM}$; $[phenol] = 20 \text{ mg/L}$.

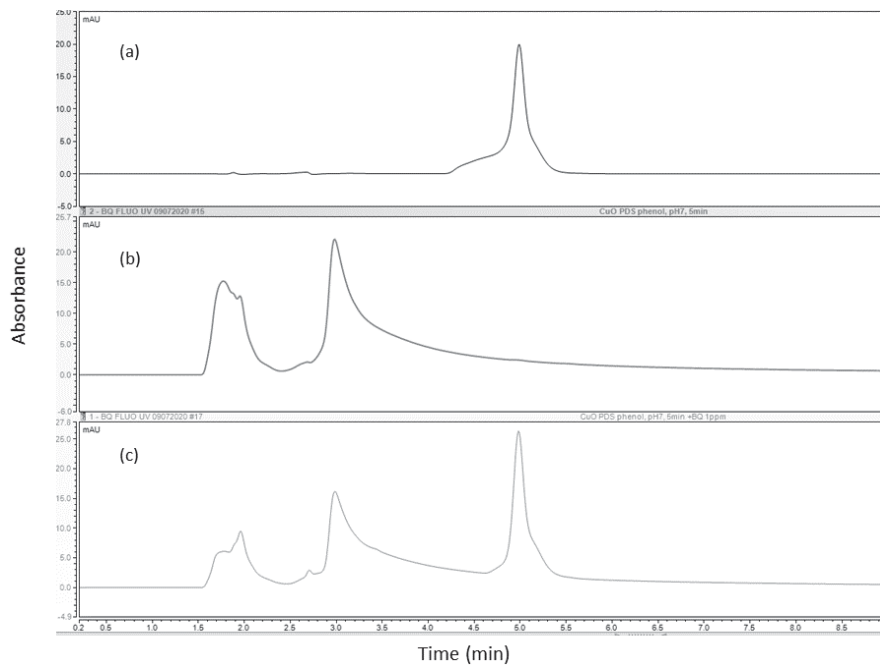


Fig. S6. HPLC-UV chromatograms at $\lambda = 244 \text{ nm}$ corresponding to the analysis of (a) analytical standard of *p*-benzoquinone (1 mg/L), (b) sample of phenol degradation in CuO/PDS system after 5 min treatment and (c) after standard addition of 1 mg/L *p*-benzoquinone. $[CuO] = 10 \text{ g/L}$; $[PDS] = 1 \text{ mM}$; $[phenol] = 20 \text{ ppm}$.

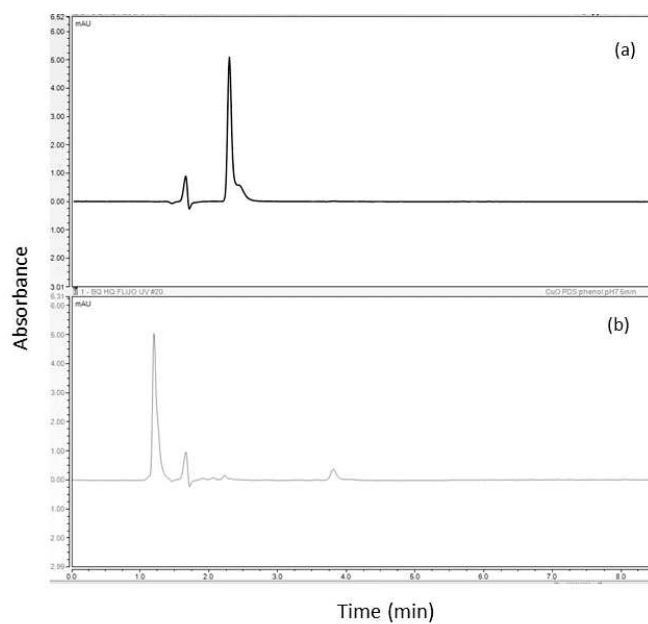


Fig. S7. HPLC-UV chromatograms at $\lambda=254$ nm corresponding to the analysis of (a) analytical standard of hydroquinone (1 mg/L) and (b) sample of phenol degradation in CuO/PDS system after 5 min treatment. [CuO] = 10 g/L; [PDS] = 1mM; [phenol] = 20 ppm.

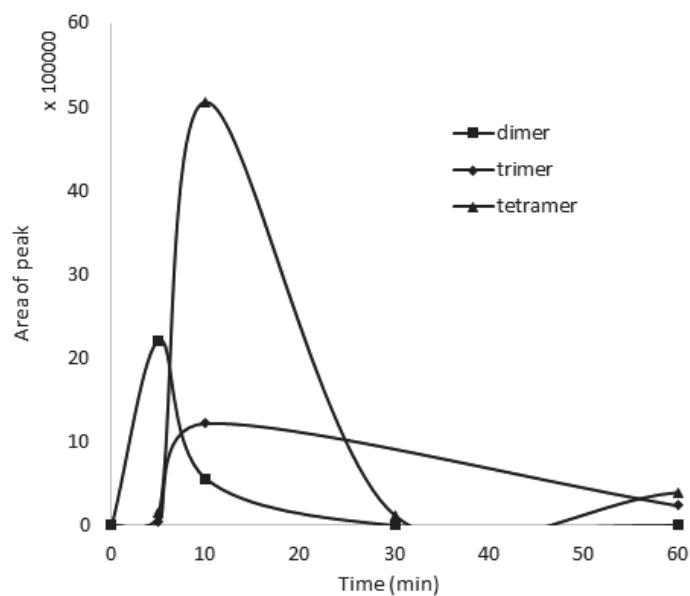


Fig. S8. The variation of peak areas of the detected TPs of phenol during the phenol degradation in CuO/PDS system.

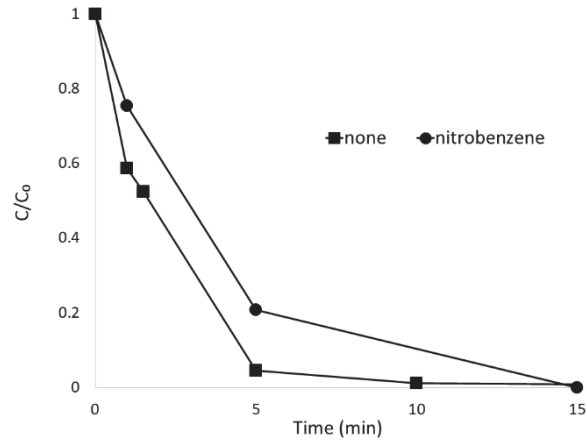


Fig. S9. Degradation kinetics of phenol in CuO/PDS system in presence of nitrobenzene at neutral pH using a Tris buffer. [CuO] = 10 g/L; [PDS] = 1 mM; [phenol] = 20 mg/L; [nitrobenzene] = 19.4 mM.

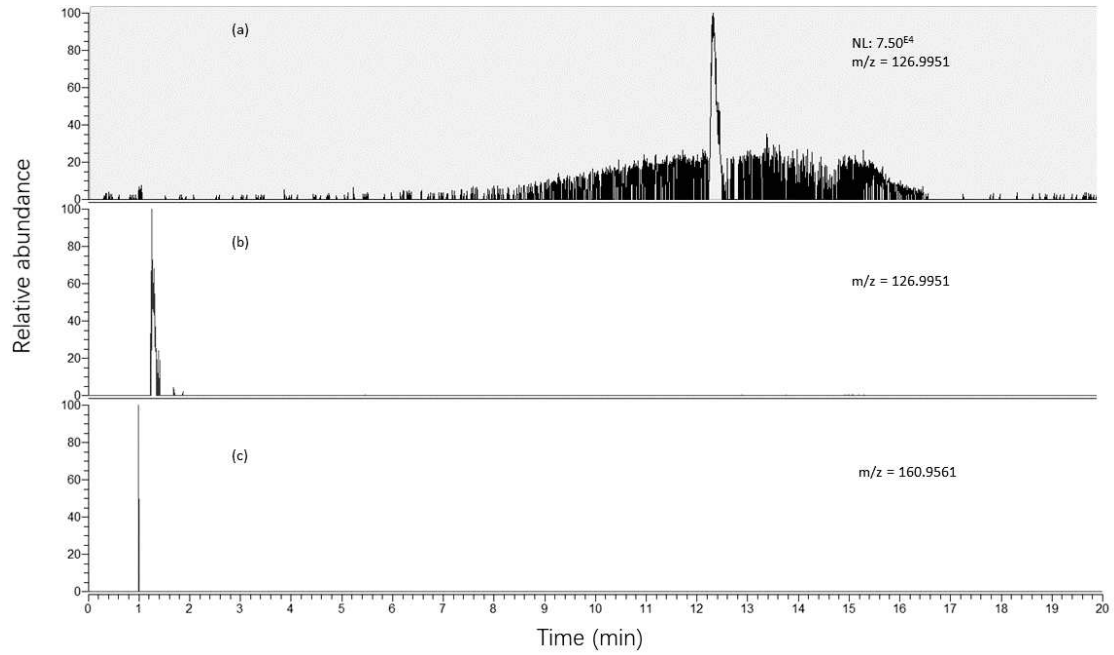


Fig. S10. Extracted Ion Chromatograms (EIC) of (a) 4-chlorophenol analytical standard (500 µg/L), (b) of $m/z = 126.9951$ corresponding to 2-chlorophenol and 4-chlorophenol and (c) of $m/z = 160.9561$ corresponding to 2,4-dichlorophenol).

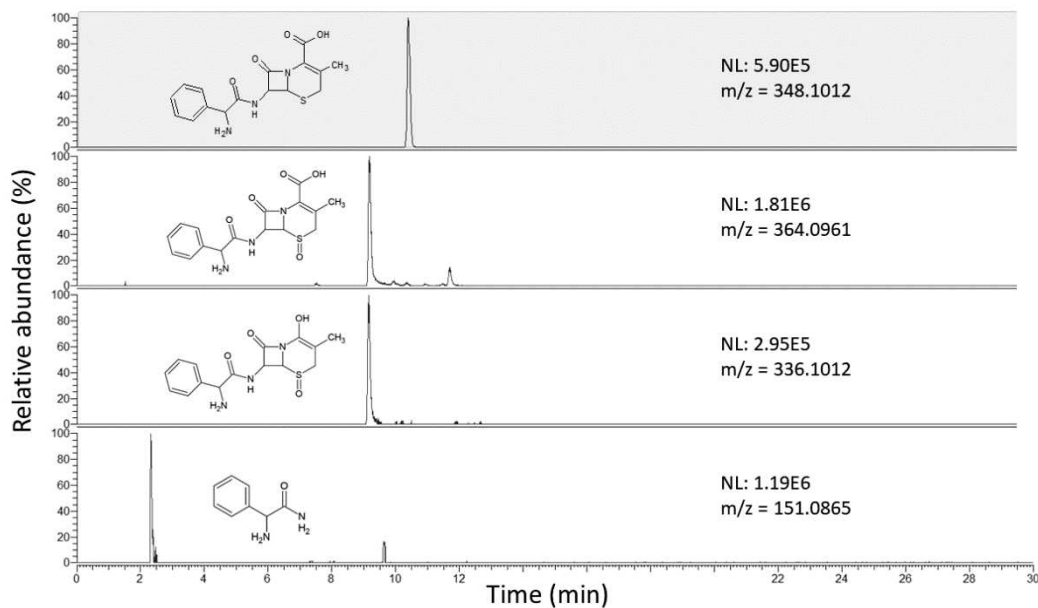


Fig. S11. Extracted Ion Chromatograms (EIC) of detected cephalixin (CFX) transformation products.

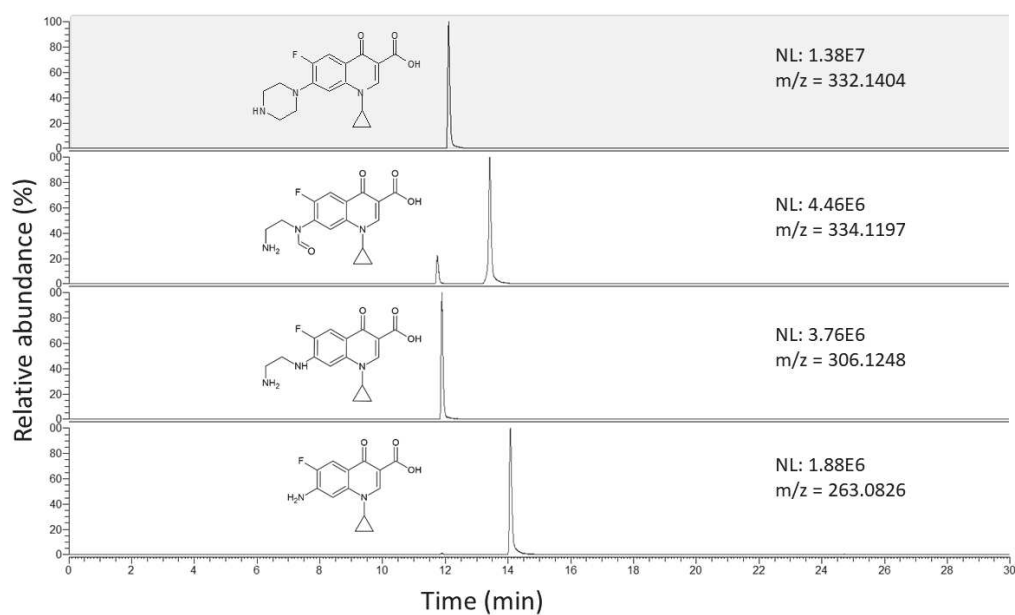


Fig. S12. Extracted Ion Chromatograms (EIC) of detected ciprofloxacin (CIP) transformation products.

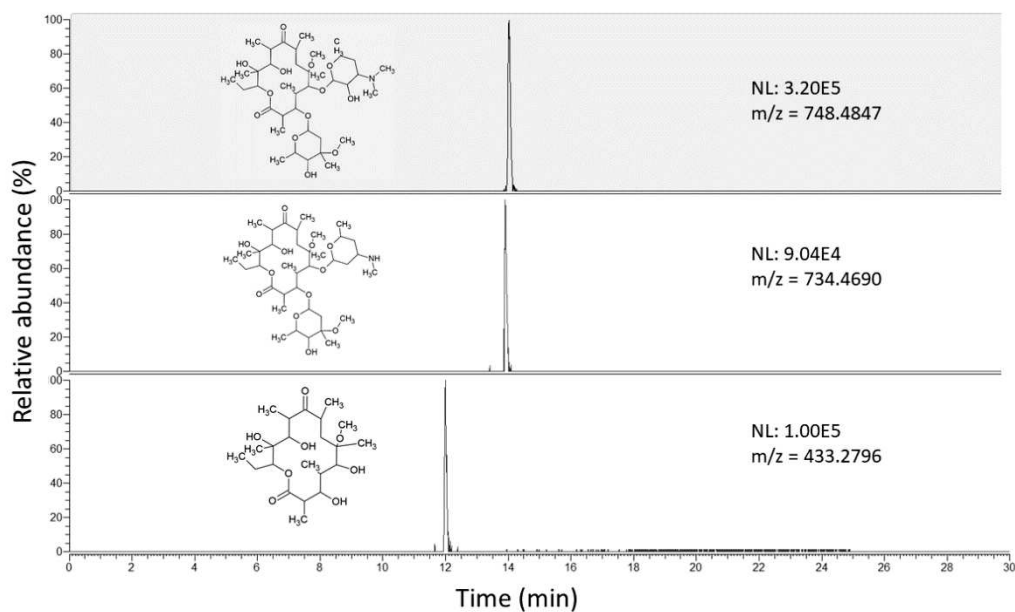


Fig. S13. Extracted Ion Chromatograms (EIC) of detected clarithromycin (CLA) transformation products.

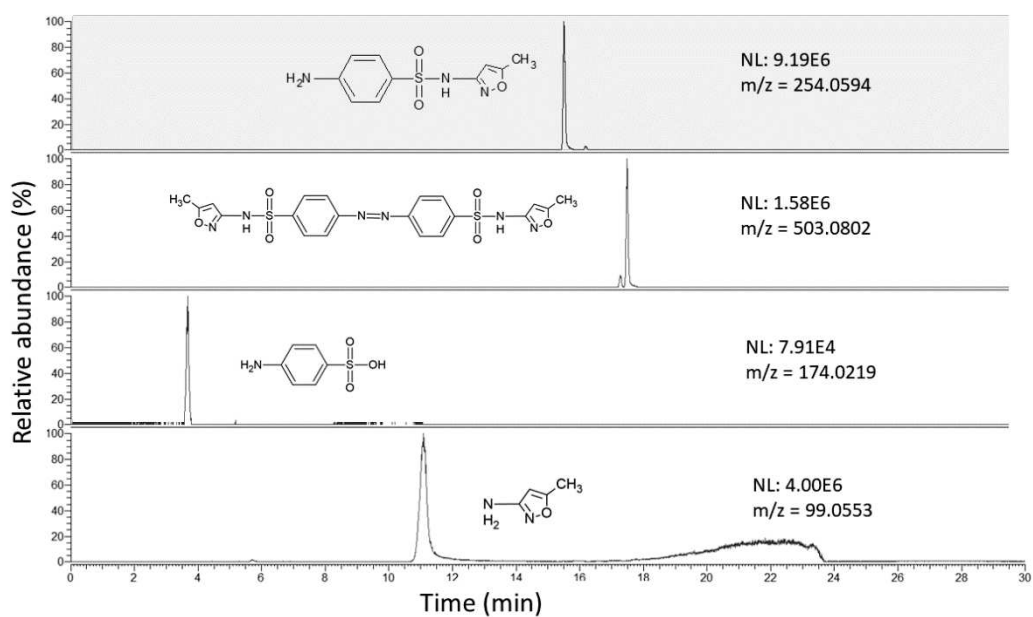


Fig. S14. Extracted Ion Chromatograms (EIC) of detected sulfamethoxazole (SMX) transformation products.

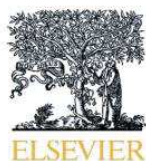
References

- [1] T. Olmez-hanci, I. Arslan-alaton, Comparison of sulfate and hydroxyl radical based advanced oxidation of phenol, *Chem. Eng. J.* 224 (2013) 10–16. <https://doi.org/10.1016/j.cej.2012.11.007>.
- [2] S. Wu, H. Liu, Y. Lin, C. Yang, W. Lou, J. Sun, C. Du, D. Zhang, L. Nie, K. Yin, Y. Zhong, Insights into mechanisms of UV/ferrate oxidation for degradation of phenolic pollutants: Role of superoxide radicals, *Chemosphere.* 244 (2020) 125490. <https://doi.org/10.1016/j.chemosphere.2019.125490>.
- [3] Y. Zhou, J. Jiang, Y. Gao, S.Y. Pang, Y. Yang, J. Ma, J. Gu, J. Li, Z. Wang, L.H. Wang, L.P. Yuan, Y. Yang, Activation of peroxymonosulfate by phenols: Important role of quinone intermediates and involvement of singlet oxygen, *Water Res.* 125 (2017) 209–218. <https://doi.org/10.1016/j.watres.2017.08.049>.
- [4] J. Chen, X. Zhou, P. Sun, Y. Zhang, C. Huang, Complexation Enhances Cu(II)-Activated Peroxydisulfate: A Novel Activation Mechanism and Cu(III) Contribution, (2019). <https://doi.org/10.1021/acs.est.9b03873>.
- [5] J. He, Y. Zhang, Y. Guo, G. Rhodes, J. Yeom, H. Li, W. Zhang, Photocatalytic degradation of cephalexin by ZnO nanowires under simulated sunlight: Kinetics, influencing factors, and mechanisms, *Environ. Int.* 132 (2019) 105105. <https://doi.org/10.1016/j.envint.2019.105105>.
- [6] N. Li, Y. Tian, J. Zhao, J. Zhang, W. Zuo, L. Kong, H. Cui, Z-scheme 2D/3D g-C₃N₄@ZnO with enhanced photocatalytic activity for cephalexin oxidation under solar light, *Chem. Eng. J.* 352 (2018) 412–422. <https://doi.org/10.1016/j.cej.2018.07.038>.
- [7] P. Bansal, A. Verma, Synergistic effect of dual process (photocatalysis and photo-Fenton) for the degradation of Cephalexin using TiO₂ immobilized novel clay beads with waste fly ash/foundry sand, *J. Photochem. Photobiol. A Chem.* 342 (2017) 131–142. <https://doi.org/10.1016/j.jphotochem.2017.04.010>.
- [8] P. Bansal, A. Verma, Pilot-scale single-step reactor combining photocatalysis and photo-Fenton aiming at faster removal of Cephalexin, *J. Clean. Prod.* 195 (2018) 540–551. <https://doi.org/10.1016/j.jclepro.2018.05.219>.
- [9] Y. Qian, G. Xue, J. Chen, J. Luo, X. Zhou, P. Gao, Q. Wang, Oxidation of cephalexin by

- thermally activated persulfate: Kinetics, products, and antibacterial activity change, *J. Hazard. Mater.* 354 (2018) 153–160. <https://doi.org/10.1016/j.jhazmat.2018.05.004>.
- [10] Y. Yan, Y. Pengmao, X. Xu, L. Zhang, G. Wang, Q. Jin, L. Chen, Migration of antibiotic ciprofloxacin during phytoremediation of contaminated water and identification of transformation products, *Aquat. Toxicol.* 219 (2020) 1–7. <https://doi.org/10.1016/j.aquatox.2019.105374>.
- [11] A. Salma, S. Thoröe-Boveleth, T.C. Schmidt, J. Tuerk, Dependence of transformation product formation on pH during photolytic and photocatalytic degradation of ciprofloxacin, *J. Hazard. Mater.* 313 (2016) 49–59. <https://doi.org/10.1016/j.jhazmat.2016.03.010>.
- [12] A. Kaur, W.A. Anderson, S. Tanvir, S.K. Kansal, Solar light active silver/iron oxide/zinc oxide heterostructure for photodegradation of ciprofloxacin, transformation products and antibacterial activity, *J. Colloid Interface Sci.* 557 (2019) 236–253. <https://doi.org/10.1016/j.jcis.2019.09.017>.
- [13] S. Li, J. Hu, Transformation products formation of ciprofloxacin in UVA/LED and UVA/LED/TiO₂ systems: Impact of natural organic matter characteristics, *Water Res.* 132 (2018) 320–330. <https://doi.org/10.1016/j.watres.2017.12.065>.
- [14] N.S. Shah, J. Ali Khan, M. Sayed, Z. Ul Haq Khan, H. Sajid Ali, B. Murtaza, H.M. Khan, M. Imran, N. Muhammad, Hydroxyl and sulfate radical mediated degradation of ciprofloxacin using nano zerovalent manganese catalyzed S₂O₈²⁻, *Chem. Eng. J.* 356 (2019) 199–209. <https://doi.org/10.1016/j.cej.2018.09.009>.
- [15] I. Michael-Kordatou, M. Iacovou, Z. Frontistis, E. Hapeshi, D.D. Dionysiou, D. Fatta-Kassinos, Erythromycin oxidation and ERY-resistant *Escherichia coli* inactivation in urban wastewater by sulfate radical-based oxidation process under UV-C irradiation, *Water Res.* 85 (2015) 346–358. <https://doi.org/10.1016/j.watres.2015.08.050>.
- [16] P. Calza, C. Medana, E. Padovano, V. Giancotti, C. Minero, Fate of selected pharmaceuticals in river waters, *Environ. Sci. Pollut. Res.* 20 (2013) 2262–2270. <https://doi.org/10.1007/s11356-012-1097-4>.
- [17] R. Tian, R. Zhang, M. Uddin, X. Qiao, J. Chen, G. Gu, Uptake and metabolism of clarithromycin and sulfadiazine in lettuce, *Environ. Pollut.* 247 (2019) 1134–1142.

- <https://doi.org/10.1016/j.envpol.2019.02.009>.
- [18] A. Buchicchio, G. Bianco, A. Sofo, S. Masi, D. Caniani, Biodegradation of carbamazepine and clarithromycin by *Trichoderma harzianum* and *Pleurotus ostreatus* investigated by liquid chromatography - high-resolution tandem mass spectrometry (FTICR MS-IRMPD), *Sci. Total Environ.* 557–558 (2016) 733–739. <https://doi.org/10.1016/j.scitotenv.2016.03.119>.
- [19] M. Gmurek, H. Horn, M. Majewsky, Phototransformation of sulfamethoxazole under simulated sunlight: Transformation products and their antibacterial activity toward *Vibrio fischeri*, *Sci. Total Environ.* 538 (2015) 58–63. <https://doi.org/10.1016/j.scitotenv.2015.08.014>.
- [20] T. Su, H. Deng, J.P. Benskin, M. Radke, Biodegradation of sulfamethoxazole photo-transformation products in a water/sediment test, *Chemosphere.* 148 (2016) 518–525. <https://doi.org/10.1016/j.chemosphere.2016.01.049>.
- [21] S. Poirier-Larabie, P.A. Segura, C. Gagnon, Degradation of the pharmaceuticals diclofenac and sulfamethoxazole and their transformation products under controlled environmental conditions, *Sci. Total Environ.* 557–558 (2016) 257–267. <https://doi.org/10.1016/j.scitotenv.2016.03.057>.
- [22] M. Majewsky, D. Wagner, M. Delay, S. Bräse, V. Yargeau, H. Horn, Antibacterial activity of sulfamethoxazole transformation products (TPs): General relevance for sulfonamide TPs modified at the para position, *Chem. Res. Toxicol.* 27 (2014) 1821–1828. <https://doi.org/10.1021/tx500267x>.
- [23] J. Yan, J. Li, J. Peng, H. Zhang, Y. Zhang, B. Lai, Efficient degradation of sulfamethoxazole by the CuO@Al₂O₃ (EPC) coupled PMS system: Optimization, degradation pathways and toxicity evaluation, *Chem. Eng. J.* 359 (2019) 1097–1110. <https://doi.org/10.1016/j.cej.2018.11.074>.

Chapter 3. Copper oxide / peroxydisulfate system for urban wastewater disinfection: Performances, reactive species, and antibiotic resistance genes removal



Copper oxide/peroxydisulfate system for urban wastewater disinfection: Performances, reactive species, and antibiotic resistance genes removal

Chan Li^a, Vincent Goetz^b, Serge Chiron^{a,*}

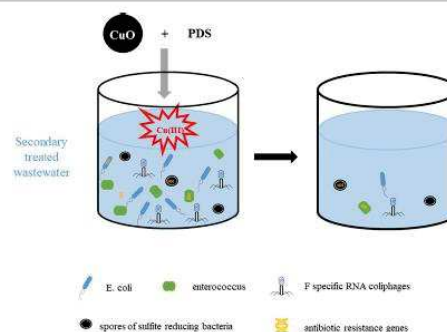
^a UMRS 151 HydroSciences Montpellier, University of Montpellier, IRD, 15 Ave Charles Flahault, 34093 Montpellier cedex 5, France

^b PROMES-CNRS UPR 8521, PROcess Material and Solar Energy, Rambla de la Thermodynamique, 66100 Perpignan, France

HIGHLIGHTS

- CuO/PDS system was firstly used for raw wastewater and secondary-treated wastewater disinfection.
- Excellent disinfection performances for bacteria (*E. coli*, *Enterococcus*) and viruses.
- Cupryl ion (Cu(III)) was the predominant reactive species for pathogens inactivation.
- Effective removal (73–99%) of selected ARGs and SMX-resistant bacteria was achieved.

GRAPHICAL ABSTRACT



ARTICLE INFO

Article history:

Received 17 July 2021

Received in revised form 29 September 2021

Accepted 30 September 2021

Available online xxx

Editor: Damia Barcelo

Keywords:

Urban wastewater

Disinfection

CuO

Antibiotic resistance genes

Cupryl ion

ABSTRACT

In this study, copper oxide (CuO) catalyzed peroxydisulfate (PDS) system was investigated for the inactivation of a broad range of pathogenic microorganisms from urban wastewater. Complete inactivation of *Escherichia coli*, *Enterococcus*, *F-specific RNA bacteriophages* from secondary treated wastewater was achieved after a short time (15–30 min) treatment with CuO (10 g/L)/PDS (1 mM) system, but *spores of sulfite-reducing bacteria* took 120 min. No bacterial regrowth occurred during storage after treatment. Significant reduction of the pathogens was explained by the generation of the highly selective Cu(III) oxidant, as the predominant reactive species, which could quickly oxidize guanine through a one-electron oxidation pathway. Additionally, the potential of the CuO (10 g/L)/PDS (1 mM) system to inactivate antibiotic-resistant bacteria and antibiotic resistance genes (ARB&Gs) was explored. Sulfamethoxazole-resistant *E. coli* was used as the model ARB and a 3.2 log of reduction was observed after 10 min of treatment. A considerable reduction (0.7–2.3 log) of selected ARGs including *bla*TEM, *qnrS*, *emrB*, *sul1*, and genes related to the dissemination of antibiotic resistance, including the Class 1 integron-integrase (*int1*), and the insertion sequence (*IS613*) was achieved after 60 min treatment. All these findings indicated the promising applicability of the CuO/PDS system as a disinfection technology for wastewater reuse in agriculture.

© 2021 Elsevier B.V. All rights reserved.

* Corresponding author.

E-mail address: serge.chiron@umontpellier.fr (S. Chiron).

savings for the environment, wastewater treatment, and farmers (Akhoundi and Nazif, 2018; Hong et al., 2013). WW after secondary or tertiary treatments is usually considered, but people in some poor and developing countries have to reuse untreated raw wastewater because of the lack of provisions by the authorities (Aslani et al., 2014). Whatever the resource, this latter contains various microbial contaminants, mainly including pathogenic bacteria, viruses, and protozoa. These biological contaminants have posed potential risks in spreading foodborne diseases and threaten public health when reclaimed WW has been used for irrigation (Hong et al., 2018; Hwangbo et al., 2019). In addition, WW also is seen as the reservoir and environmental supplier of antibiotics resistance, where antibiotic-resistance genes (ARGs), acquired by different bacteria species via genes transfer or extracellular uptake (Karkman et al., 2018; Pazda et al., 2019) intensively spread. Although antibiotic-resistant bacteria and antibiotic resistance genes (ARB&Gs) are not currently included in any international regulation, they have been recognized as one of the major challenges for human health by the World Health Organization (WHO, 2015). To meet the minimum quality requirements for the safe reuse of WW in agricultural irrigation, inactivating a broad range of pathogenic microorganisms and limiting the spread of antibiotics resistance (ARB&Gs) by effective disinfection technologies are highly recommended.

The most commonly used disinfection technologies are chlorination, UV-C treatment, and peracetic acid. Chlorine is still the most widely used disinfectant due to its low cost and high efficiency for the inactivation of microbes. However, it is not efficient for cryptosporidium removal together with the well-known problem of unhealthy disinfection by-products generation (Hashemi et al., 2013; Vasilyak, 2021). UV irradiation requires extensive secondary treatment and sand filtration to reach a recommended water transmittance value over 50% and is not adapted to open treatment systems (e.g., lagooning or constructed wetlands) where green colored microscopic algae can grow (Hashemi et al., 2013). Besides, potential bacterial regrowth problems during treated WW storage for UV doses below 40–60 mJ/cm² have been reported (Hashemi et al., 2013; Vasilyak, 2021). Peracetic acid has shown poor effectiveness in removing enteric viruses, and potential microbial regrowth (Gehr et al., 2003; Kitis, 2004).

Homogeneous advanced oxidation processes (AOPs) employing hydrogen peroxide (H₂O₂) and persulfate (PDS) and relying on hydroxyl and/or sulfate radical ($\cdot\text{OH}$ and $\text{SO}_4\cdot^-$) production have obtained increasing attention and have shown high disinfection capacity but can only be an interesting option when organic micropollutants have to be simultaneously removed due to the high operational and maintenance costs of those processes (Chen et al., 2021). To overcome the disadvantages of the traditional homogeneous Fenton reaction and AOPs such as the narrow pH range of implementation and the production of a large amount of iron-containing sludge (Chen et al., 2021), heterogeneous Fenton-like oxidation processes (HFOPs) make use of recyclable solid catalysts, such as iron oxides (de la Obra Jiménez et al., 2020; Xia et al., 2017), copper oxide (Cho et al., 2020; Zhang et al., 2014), metal-organic frameworks (MOFs, Lu et al., 2021), layered double hydroxides (LDHs, de Melo Costa-Serge et al., 2021), developed rapidly in recent years. It should be noted that disinfection processes are widely applied as the last barrier in the WW reclamation train after carbon and nutrients removals. However, in irrigation application, what is needed is a disinfection method that can work in presence of high contents of dissolved organic matter and nutrients because both are valuable agronomic parameters to be preserved (Jaramillo and Restrepo, 2017). Organic matter is a well-known hydroxyl and sulfate radical scavenger, limiting the efficiency of those processes (Chen et al., 2021). However, HFOPs still mostly rely on radical generation. This work contemplated the possibility to implement a HFOP relying on more selective reactive species than sulfate and hydroxyl radicals, which might work in organic-rich WW.

For this purpose, this work benefited from recent results of our research group, which have shown that the copper oxide (CuO)/

peroxydisulfate (PDS) system is a good generator of the highly selective cuprous (Cu(I)) and cupryl (Cu(III)) as well as singlet oxygen (¹O₂) species and could efficiently eliminate phenol and a mixture of antibiotics from WW (Li et al., 2021). As Cu(I), Cu(III), and ¹O₂ are well identified as excellent biocidal species in the literature (García-Fresnadillo, 2018; Kim et al., 2015), good disinfection performance of the CuO/PDS system was anticipated, but to our knowledge, the study of CuO/PDS on urban wastewater disinfection has not been reported yet. Consequently, the main objective of this work was to demonstrate the performances of this system in inactivating a broad range of pathogenic microorganisms. Specific objectives included i) a comparison of the disinfection capacity in raw and secondary-treated WW, ii) the identification of the predominant reactive species and iii) the evaluation of the abundance reduction of selected ARB&Gs.

2. Material and methods

2.1. Chemicals

Micrometer copper oxide particles (CuO, 44 μm particle size on average) were purchased from Alfa Aesar (Kandel, Germany). Guanine, thymine, adenosine, L-tyrosine, ranitidine, ranitidine N-oxide, ranitidine sulfoxide, sodium hydroxide (NaOH), sodium thiosulfate (Na₂S₂O₃), sulfamethoxazole (SMX), and EDTA were purchased from Sigma-Aldrich (Saint Quentin Fallavier, France). Potassium persulfate (K₂S₂O₈), sodium hypochlorite (NaOCl), formic acid, ammonium acetate, Chromocult coliforms agar, Slanetz Bartley agar, and tris(hydroxymethyl)aminomethane (Tris) were purchased from Merck KGaA (Germany). Acetonitrile (HPLC grade) and methanol (HPLC grade) were purchased from Carlo Erba reagents (France). All solutions were prepared with ultrapure water obtained from a Milli-Q Plus system (Millipore, Bedford, MA). Stock solutions of adenosine (100 mg/L), thymine (100 mg/L), ranitidine (100 mg/L), L-tyrosine (100 mg/L) and PDS (100 mM) were prepared in ultrapure water. Guanine stock solution (500 mg/L) was prepared in 10% NaOH solution due to its poor water solubility at neutral pH.

2.2. Pathogens inactivation

2.2.1. Wastewater disinfection

Influent and effluents were collected at the inlet and the outlet of a conventional activated sludge wastewater treatment plant (WWTP, 20,000 equivalent inhabitants). The major physico-chemical properties of collected influent and effluent samples are shown in Table 1. The main differences when switching from influent to effluent were the decrease of total suspended solids (TSS, 14 folds decrease) and chemical oxygen demand (COD, 20 folds decrease) values, and the simultaneous decrease of NH₄⁺ and increase of NO₃⁻ ions caused by nitrification. Before

Table 1
Major physico-chemical properties of the investigated urban wastewater.

Parameter	Influent	Effluent
EC (mS/cm)	2.1 ± 0.5	1.6 ± 0.4
pH	7.5 ± 0.1	7.7 ± 0.1
TSS (mg/L)	115 ± 32	8.2 ± 2.6
COD (mg/L)	657 ± 55	32.4 ± 5
HCO ₃ ⁻ (mg/L)	n.d	514.3
Cl ⁻ (mg/L)	n.d	195.3
NO ₃ ⁻ (mg/L)	< LOD	12.9 ± 1.5
NH ₄ ⁺ (mg/L)	26 ± 5	0.5
PO ₄ -P (mg/L)	6.8 ± 1.2	0.6 ± 0.2
SO ₄ ²⁻ (mg/L)	n.d	58.9
Cu (μg/L)	n.d	3.75

n.d: not determined.

being subjected to treatment, the wastewater samples were firstly filtered through a 200 μm sieve to remove the biggest suspended solid particles. This effluent was named pre-filtered effluent along the manuscript. The filtration had no significant influence on the number of microorganisms present in WW. In other words, the microbial load did not change before and after filtration.

To the tests devoted on the efficiency of the CuO/PDS system, chlorine considered as the reference for disinfection operation and thermal activation of persulfate as the $\text{SO}_4^{\bullet-}$ radical based process were also carried out. Before the use of CuO, this latter was rinsed around 10 times with tap water in a 1-liter bottle to remove the suspended particles until almost all CuO could settle down within 1 min. The washed CuO was dried in an oven (50 $^{\circ}\text{C}$) for further use. CuO (10 g/L), PDS (1 mM), CuO (10 g/L)/PDS (1 mM), and free chlorine (2.6 mg/L) were added to the pre-filtered effluent, separately. One liter WW bottles with or without PDS (1 mM) addition were immersed in a water bath (15 L) at 70 $^{\circ}\text{C}$ to ensure the full activation of PDS into sulfate radicals. CuO particles were easily removed by spontaneous decantation, and analyses were performed on the supernatant. Samples (500 mL) were collected in sterilized plastic bottles at defined time intervals of treatment. Excess EDTA (5 mM) and/or sodium thiosulfate (5 mM) were added immediately for released Cu^{2+} complexation and excess PDS removal, respectively. Samples were stored at 4 $^{\circ}\text{C}$ and pathogens analysis was conducted less than 24 h after sample collection. Potential bacterial regrowth was evaluated by analyzing treated effluent samples collected at various time intervals after 24 and 48 h of storage in the ambient environment. For influent, the procedures are the same as the effluent disinfection experiment using CuO (10 g/L) and PDS at different concentration levels (i.e., 1, 2.5, and 10 mM).

2.2.2. Enumeration of pathogens

The NF EN ISO 9308-3 and NF EN ISO 7899-1 standard protocols were used to enumerate *Escherichia coli* (*E. coli*) and *Enterococcus* respectively. These methods are based on the culture of the bacteria in a liquid medium and the determination of the most probable number (MPN) according to the level of dilution. The NF EN 26461-2 standard protocol was used to enumerate the colony-forming unit (CFU) of spores of sulfite-reducing bacteria after filtration and cultivation on a specific agar solid medium. *F-specific RNA bacteriophages* were measured according to the ISO 10705-1 method. This method allows for a count on the agar medium of plaque-forming unit (PFU), corresponding to the number of viruses. All results are presented as an average of two experiments.

2.2.3. Analysis of Cu

Cu was analyzed by inductively coupled plasma - optical emission spectrometry (ICP-OES) using an iCap Duo 7400 spectrometer (Thermo Fischer Scientific, Les Ulis, France) using the axial mode of detection at wavelength $\lambda = 324.754 \text{ nm}$.

2.2.4. Analysis of PDS

The analytical method for PDS is reported in Li et al. (2021).

2.2.5. Analysis of trihalomethanes (THMs)

Chloroform (CFL), dichloromonobromomethane (DCB), monochlorodibromomethane (MCB), and bromoform (BRF) were determined following the EPA 551A method.

2.3. Identification of reactive species

2.3.1. Experimental procedures

Batch experiments were conducted in 100 mL glass serum bottles under continuous shaking at 60 rpm using a roller mixer (STUART® SRT19D, UK) and 200 mM Tris buffer adjusted to pH 7 with HCl. Typically, target compounds (guanine, thymine, adenosine, ranitidine, L-tyrosine), CuO, and PDS were sequentially added into the bottles to

reach initial concentrations of 20 mg/L, 10 g/L, and 1 mM, respectively. Sample aliquots (5 mL) were taken at predetermined times and filtered through 0.45 μm cellulose membrane filters, and then stored in 6 mL glass tubes at 4 $^{\circ}\text{C}$ before analysis. Control experiments in presence of CuO or PDS alone were also performed under the same experimental conditions. 100 mM of methanol was added to the CuO/PDS system as a hydroxyl and sulfate radical scavenger.

2.3.2. Analytical methods

Degradation kinetics of selected compounds were followed by liquid chromatography (LC) with a diode-array detector (DAD) and using an Agilent ZORBAX Eclipse XDB C18 column (150 \times 3 mm i.d., 3.5 μm particle size). The separation and detection conditions are shown in Table S1. Transformation products (TPs) of guanine, L-tyrosine, and ranitidine were identified by LC-high resolution-mass spectrometry (LC-HRMS) composed of a Dionex Ultimate 3000 liquid chromatograph equipped with an electrospray source operated in the positive ionization mode and an Exactive Orbitrap mass spectrometer (ThermoFisher Scientific, Les Ulis, France) operated in full scan mode (mass range m/z 50–900) and using the reverse phase PFP (pentafluorophenylpropyl) analytical column (100 mm \times 2.1 mm; 3 μm particle size). LC gradient consisting of Milli-Q water with 1% ACN and 0.1% formic acid (solvent A) and ACN with 1% Milli-Q water and 0.1% formic acid (solvent B) was as follow: 0–1.5 min, 98% A; 11.25 min, 55% A; 12.75 min, 30% A; 13.0–20 min, 98% A. The flow rate was set at 0.3 mL/min. The energy collisional dissociation was set to 20 eV and a drying gas temperature of 300 $^{\circ}\text{C}$ was used. TPs of guanine, L-tyrosine, and ranitidine were identified following a suspect screening workflow in LC-HRMS. The databases were made up of a list of possible TPs with their molecular formula and exact mass (Table S3–S5) collected from the literature.

2.4. Antibiotic-resistant bacteria and antibiotic resistance genes (ARB&Gs)

2.4.1. Antibiotic-resistant bacteria

SMX-resistant *E. coli* and *Enterococcus* were quantified before and after treatment to examine the ARBs inactivation performances. Considering the observed minimum inhibitory concentration (MIC) (Iakovides et al., 2019; CLSI, 2020), 516 mg/L of SMX was added to the Chromocult coliform agar (*E. coli*) and Slanetz Bartley agar (*Enterococcus*), respectively. After membrane filtration and cultivation, the colony-forming unit (CFU) of SMX-resistant and total *E. coli* and *Enterococcus* on the agar was counted. The prevalence of SMX-resistant *E. coli* and SMX-resistant *Enterococcus* were calculated as the ratio between the CFU/100 mL observed on the antibiotic supplemented culture medium and the CFU/100 mL observed on the same medium without antibiotic ($\text{prevalence (\%)} = \frac{\text{CFU } 100 \text{ mL}^{-1} \text{ medium with SMX}}{\text{CFU } 100 \text{ mL}^{-1} \text{ medium without SMX}} \times 100$). All results are presented as an average of two experiments.

2.4.2. Antibiotic resistance genes

100 mL of pre-filtered effluents collected before and after treatment were filtered on 0.22 μm polyethersulfone filters (Millipore, France). DNA extraction was performed with the filters by following the specific protocols of the Qiagen DNeasy® PowerWater® Kit (Qiagen GmbH, Hilden, Germany). DNA purity and concentrations were estimated by spectrophotometry (Infinite NanoQuant M200, Tecan, Austria). The extracted DNA was stored at -20°C before analysis. Four ARGs and two genes linked to the dissemination of antibiotic resistance were quantified by droplet digital PCR (ddPCR) using EvaGreen chemistry: qnrS (reduced susceptibility to fluoroquinolone); sulI (resistance to sulfonamides); blaTEM (resistance to β -lactams), ermB (resistance to macrolide), int1 encoding the integrase of Class I integron-integrase used as a proxy for the potential capacity of the bacterial community to disseminate resistance (Iakovides et al., 2019), and IS613 selected as one representative of insertion sequences in DNA transposons (Babakhani and Oloomi, 2018). The 16S rRNA gene, as an indicator of

total bacteria, was quantified by quantitative PCR (qPCR) using EvaGreen chemistry. The amplification and quantification processes were conducted as the following protocol: 2 min at 95 °C for pre-incubation of the DNA template, followed by 40 cycles at 95 °C for 15 s for denaturation and 60 s for annealing (at specific annealing temperature) and amplification. Primers' information and annealing temperature are listed in Table S2. Specificity of amplification was validated both by melting curve analyses and by checking the size of the amplicons on 2100 Bioanalyzer (Agilent, Waldbronn, Germany). All results are presented as an average of three replicates.

3. Results and discussion

3.1. Inactivation performances of pathogens

3.1.1. Effluent

E. coli is commonly used as an organism indicator to indicate the fecal contamination level (Odonkor and Ampofo, 2013). However, the thin cell wall of Gram-negative *E. coli* makes it poorly resistant to many types of disinfectants. Thus, the Gram-positive *Enterococcus* with a relatively thick and dense layer composed cell wall was adopted as a more resistant and reliable indicator of fecal pollution (Núñez-Salas et al., 2021). Considering that bacterial indicators are unable to indicate the occurring level of viral pathogens (Dias et al., 2018), *F-specific RNA bacteriophages* was used as the appropriate pathogenic viral indicator. *Spores of sulfite-reducing bacteria* were selected as an indicator of protozoa. All these indicators are also included in the EU Regulation 2020/741 of the European Parliament and of the Council of 25 May 2020 on minimum requirements for water reuse" (EU, 2020) to evaluate performances of disinfection technologies.

The initial abundances in secondary-treated effluent samples before treatment were $4.6 \pm 0.1 \log_{10}$ MPN/100 mL of *E. coli*, $3.5 \pm 0.2 \log_{10}$

MPN/100 mL of *Enterococcus*, $2.7 \pm 0.2 \log_{10}$ PFU/100 mL of *F-specific RNA bacteriophages*, and $3.2 \pm 0.1 \log_{10}$ CFU/100 mL of *spores of sulfite-reducing bacteria* and are comparable to the values found in the literature (Haramoto et al., 2015; Mandilara et al., 2006). The inactivation performances on four pathogenic indicators by PDS alone, CuO alone, CuO/PDS, thermally activated PDS system (SO_4^-), and chlorination (Cl_2) are shown from Fig. 1(a) to Fig. 1(d). No effective inactivation performance of any indicator was observed by using PDS alone. As shown in Fig. 1(a)–(b), significant reduction of *E. coli* ($> 3.0 \log$) and *Enterococcus* ($> 1.7 \log$) was observed for the other three systems after a short treatment time (15–30 min) and no cultivable cells were detected after that. This result is comparable to UV-C irradiation, which can usually inactivate 2–4 log of *E. coli* (Collivignarelli et al., 2018). All the disinfection systems except PDS alone efficiently removed *F-specific RNA bacteriophages* (Fig. 1(c)). However, this result was not strong enough to fully demonstrate the effective inactivation activity of these systems for viral pathogens because the initial concentration of *F-specific RNA bacteriophages* ($2.7 \pm 0.2 \log_{10}$ PFU/100 mL) was too low and close to the detection limit ($2 \log_{10}$ PFU/100 mL). Significant reduction ($> 1.5 \log$) of *spores of sulfite-reducing bacteria* was only obtained with Cl_2 and CuO/PDS systems after 15 min and 120 min treatment time, respectively (Fig. 1(d)). As a whole, CuO/PDS system took a longer time than chlorination for the removal of targeted indicators. However, the CuO/PDS system did not imply the generation of unhealthy trihalomethanes (THMs) as shown in Table 2. The lack of THMs production held also true for the sulfate radical-based treatment.

Interestingly, CuO alone demonstrated good disinfection performances for all pathogenic indicators. The released cupric ion ($Cu(II)$) was suggested to be responsible for the antimicrobial activity of CuO (Dizaj et al., 2014; Suleiman et al., 2015), which is mainly due to the cytotoxicity of cellularly generated cuprous ion ($Cu(I)$) (Kim et al., 2015).

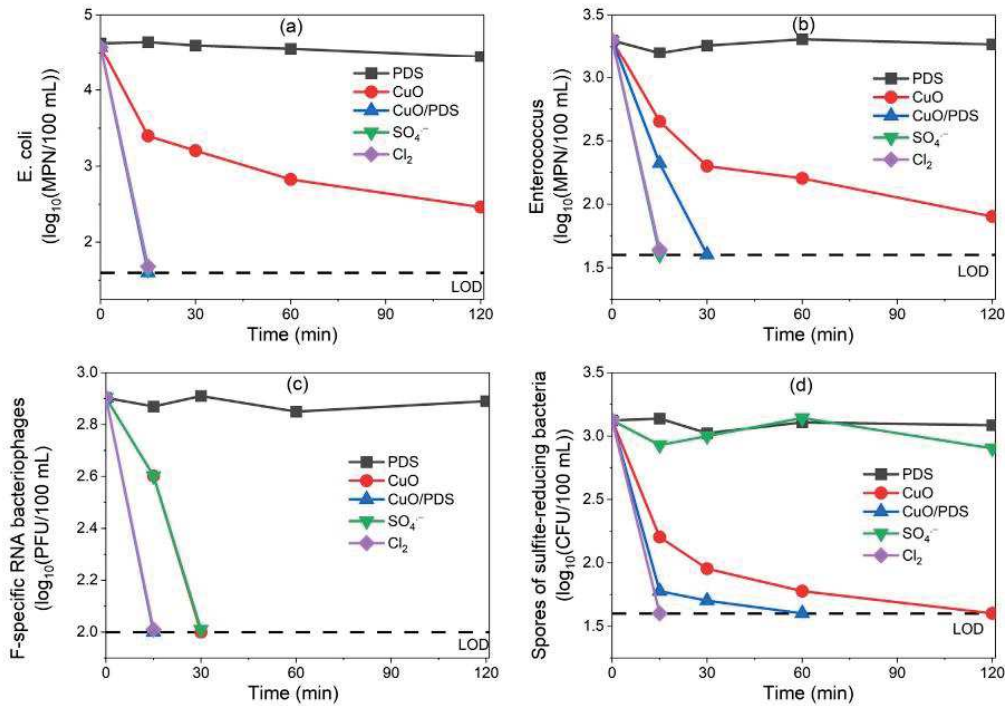


Fig. 1. Inactivation profiles of pathogens: (a) *E. Coli*, (b) *Enterococcus*, (c) *F-specific RNA bacteriophages* and (d) spore of sulfite-reducing bacteria by different disinfection systems: CuO, PDS, CuO/PDS, thermally activated persulfate (SO_4^-) and chlorination (Cl_2). [CuO] = 10 g/L, [PDS] = 1 mM, secondary treated wastewater. Note: the unshown rectangles from 15 min to 120 min represent that the concentrations of pathogens were lower than the limit of detection (LOD).

Table 2

Concentration ($\mu\text{g/L}$) of chloroform (CFL), dichloromonobromomethane (DCB), monochlorodibromomethane (MCB), bromoform (BRF) and total trihalomethanes (THMs) formed in different disinfection systems after 120 min of treatment.

DBPs ($\mu\text{g/L}$)	Cl_2	CuO	SO_4^{2-}	CuO/PDS
CFL	30	<0.5	<0.5	<0.5
DCB	10	<0.5	<0.5	<0.5
MCB	2.7	<0.5	<0.5	<0.5
BRF	<0.5	<0.5	<0.5	<0.5
THMs	42.7	<0.5	<0.5	<0.5

In this study, the Cu(II) released from CuO was up to $315 \pm 15 \mu\text{g/L}$, so that the antimicrobial level was reached. It is reported that Cu(II) can effectively inactivate bacteria, yeast cells and algae, but has minor effects on virus inactivation (Kim et al., 2015). However, in combination with PDS, the biocidal activity was significantly improved due to an acceleration in the generation of high-valent copper species such as the virucide Cu(III) ions as detailed in Section 3.2. For a better understanding of the role of dissolved Cu in disinfection processes, Cu was measured in the water phase together with the consumption of PDS at different times (Fig. 2). A positive correlation between Cu leaching and PDS consumption was observed. At the beginning of the reaction, the fast consumption of PDS was associated with a strong Cu release up to $848 \pm 42 \mu\text{g/L}$. After 60 min treatment, PDS consumption dramatically slowed down and Cu release decreased down to $392 \pm 20 \mu\text{g/L}$. The mechanisms of PDS activation by CuO might account for this specific behavior. At neutral pH, the CuO surface is positively charged as pH_{pzc} was 8–9 have been reported (Ghulam et al., 2013) and PDS is an anion calling for strong electrostatic interactions. The first step involves an electrostatic interaction of PDS on the CuO surface followed by PDS decomposition into superoxide radical anion (Li et al., 2021). As the reaction proceeds, active sites on CuO might become occupied by waterborne molecules or even by Cu^{2+} limiting PDS activation and Cu^{2+} leaching. As PDS was found not to be the limiting factor in disinfection, further studies using lower PDS doses are needed to reduce Cu(II) leaching.

For bacterial regrowth study, treated samples collected at various time intervals: 5, 10, and 30 min were stored under ambient conditions, and the occurrence and viability of *E. coli* and *Enterococcus* in treated WW after 24 h and 48 h of storage was evaluated. Complete inactivation of *E. coli* and *Enterococcus* was achieved after 30 min of treatment, no regrowth of bacteria in the treated WW was observed during the storage time while incomplete inactivation was observed after 5 and 10 min of treatment. CuO/PDS system achieved a reduction of 1.0 log and 2.3 log

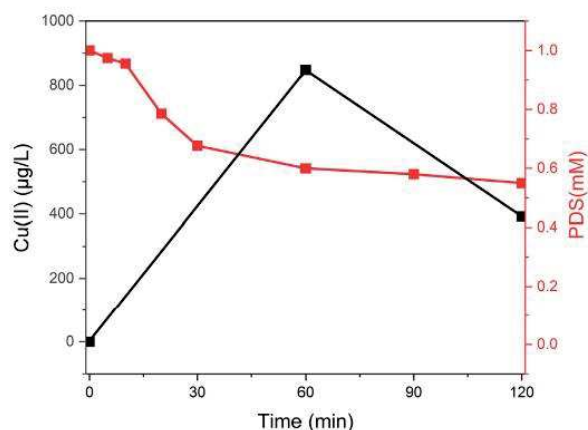


Fig. 2. Concentration of leached Cu(II) and PDS during CuO/PDS treatment of secondary treated wastewater. $[\text{CuO}] = 10 \text{ g/L}$, $[\text{PDS}] = 1 \text{ mM}$.

of *E. coli* and 0.3 log and 1.5 log of *Enterococcus*, respectively (Fig. 3). Still no regrowth of *E. coli* and *Enterococcus* in treated WW samples was observed after 24 h and 48 h of storage at ambient conditions, which might indicate that the possibility for damaged DNA repair was restricted in the CuO/PDS system.

3.1.2. Influent

The inefficiency of raw WW disinfection has often been attributed to chemical/radical disinfectant inhibition in presence of the high concentrations of inorganic and organic matters. Sánchez-Ruiz et al. (1995) used peracetic acid to inactivate total coliforms in raw WW but great variability in inactivation efficiency under different pH conditions and bacterial regrowth were observed. In contrast, Aslani et al. (2014) demonstrated effective raw WW disinfection by using $\text{Cu(II)/H}_2\text{O}_2$. In this work, the CuO/PDS system was applied to disinfect raw influent of an urban WWTP. As expected, the initial pathogens abundances were much higher than those in effluent: $7.3 \pm 0.3 \log_{10}$ MPN/100 mL for *E. coli*, $6.9 \pm 0.3 \log_{10}$ MPN/100 mL for *Enterococcus*, and $5.5 \pm 0.6 \log_{10}$ PFU/100 mL for *F-specific RNA bacteriophages*. In contrast, spores of sulfite-reducing bacteria were similar, with a value of $3.3 \pm 0.7 \log_{10}$ CFU/100 mL. The abundances of these indicators are consistent with those found in the literature (Haramoto et al., 2015; Jofre et al., 2021). Different PDS concentrations were applied to the system to evaluate the influence of this parameter on the disinfection efficiency and results are shown in Fig. 4(a)–(d). The CuO/PDS system was not able to eliminate spores of sulfite-reducing bacteria at any PDS concentration (Fig. 4(d)). The removal efficiency of *E. coli*, *Enterococcus*, and *F-specific RNA bacteriophages* highly increased when increasing PDS concentration from 1 mM to 2.5 mM, but no further significant enhancement was noticed with 10 mM PDS (Fig. 4(a)–(c)). Significant reductions of 3.5 log of *E. coli* and 4.1 log of *Enterococcus* were only reached after 120 min treatment while the CuO/PDS system exhibited much better efficiency in removing viruses, a 3.5 log reduction of *F-specific RNA bacteriophages* being obtained after 30 min treatment when using 2.5 mM PDS. This result might be related to the generation of highly selective reactive species in the CuO/PDS system (see Section 3.2) which have not been inhibited by the very high carbon content (COD of $657 \pm 55 \text{ mg/L}$ vs $32.4 \pm 5 \text{ mg/L}$ in effluent).

3.2. Identification of reactive species

From our previous work, it was known that singlet oxygen, Cu(I) and Cu(III) are generated in the CuO/PDS system (Li et al., 2021). The involvement of singlet oxygen is often questionable because this latter species is quickly quenched by water. Consequently, the main aim was to confirm that copper species were the main reactive species involved in disinfection processes. For this purpose, the reactivity of selected nucleobases (i.e., guanine, adenosine and thymine) and that of the tyrosine amino acid, a phenolic compound which was anticipated to react with Cu(II) have been investigated. Degradation of ranitidine was also studied to investigate the reactivity of the disulfide bridge, which is an important component of the secondary and tertiary structure of proteins. This work included kinetic studies as well as the identification of TPs by LC-HRMS. At neutral pH, no target compound was absorbed on CuO (Fig. S1). As shown in Fig. 5(a), only guanine, L-tyrosine, and ranitidine can be degraded in the CuO/PDS system. Degradation kinetics of guanine and L-tyrosine fitted well to the first-order kinetic model. However, guanine reacted much faster than L-tyrosine with apparent kinetics rate constants $k_{\text{obs}} = 0.12 \pm 0.01$, and $0.003 \pm 0.0002 \text{ min}^{-1}$, respectively. In contrast, the degradation kinetics of ranitidine was not a first-order kinetic since the degradation stopped after 15 min. This was due to the direct reaction of ranitidine with PDS (Fig. S1) resulting in a quick PDS exhaustion. Methanol (100 mM) was added as a radicals scavenger (e.g., $\cdot\text{OH}$ and $\text{SO}_4^{\cdot-}$). As shown in Fig. 5(b), methanol showed no inhibitory effect on the guanine and ranitidine degradation and minor inhibitory effect on L-tyrosine degradation ($k_{\text{obs}} = 0.002 \pm$

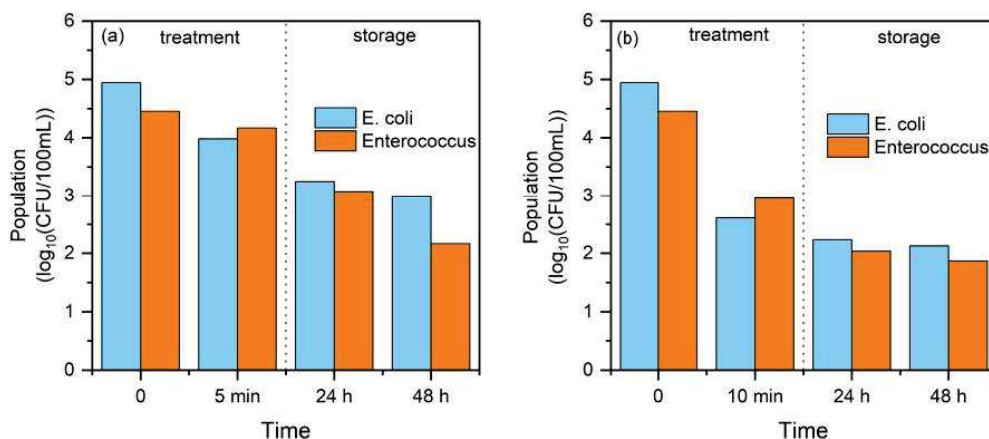


Fig. 3. Regrowth profiles of *E. Coli* and *Enterococcus* in secondary treated wastewater after (a) 5 min and (b) 10 min CuO/PDS treatment. [CuO] = 10 g/L, [PDS] = 1 mM.

0.0002 min^{-1}), indicating that radicals were not the predominant reactive species. This confirms the results of our previous study where singlet oxygen and Cu(III) were identified as the predominant oxidative species in the CuO/PDS system (Li et al., 2021), superoxide radical was produced from PDS decomposition, but mainly used to reduce Cu(II) to Cu(I) which contributes to the microbiocidal action of Cu(II).

To be able to discriminate between $^1\text{O}_2$ and Cu(III) contributions, TPs of guanine, L-tyrosine, and ranitidine were identified following a suspect screening workflow in LC-HRMS. For this purpose, a database

was made up of a list of possible TPs with their molecular formula, exact mass, and structure (Tables S3, S4, and S5). This list was established from a literature search of TPs. TPs with intensities lower than 1×10^4 cps, signal to noise ratios lower than 10, isotopic ratio higher than 10%, and mass accuracy errors higher than 5 ppm were discarded. The transformation pathways of guanine (GUA), L-tyrosine (TYR), and ranitidine (RAN) were also tentatively elucidated (Fig. 6). For guanine, two main TPs were detected (Fig. S2): GUA 1 ($m/z = 153.0407$) and GUA 2 ($m/z = 133.0243$). The first step of the reaction involved a deamination reaction more likely through a one-electron

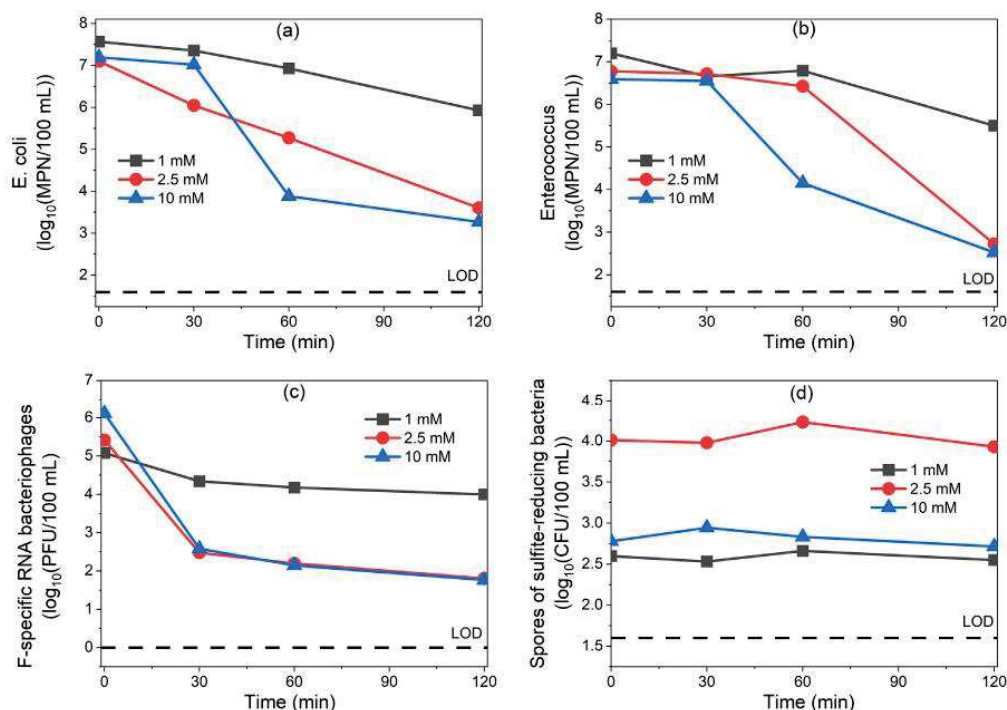


Fig. 4. Inactivation profiles of pathogens in raw wastewater using CuO/PDS system and different PDS concentrations: (a) *E. Coli*, (b) *Enterococcus*, (c) F-specific RNA bacteriophages and (d) spores of sulfite-reducing bacteria. [CuO] = 10 g/L, [PDS] = 1, 2.5, 10 mM Note: NM = not measured.

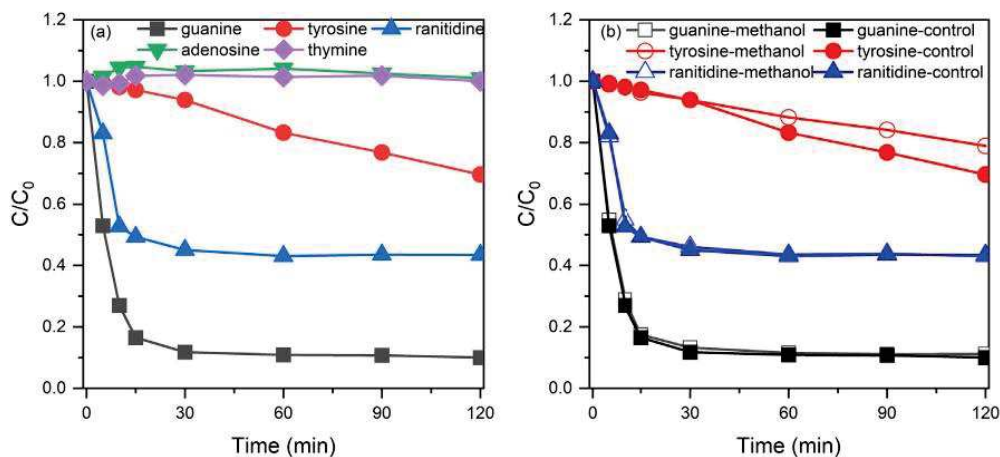


Fig. 5. Degradation kinetics of (a) targeted compounds, and (b) the effect of methanol in distilled water using the CuO/PDS system. [CuO] = 10 g/L, [PDS] = 1 mM, [adenosine] = [thymine] = [guanine] = [ranitidine] = [L-tyrosine] = 20 mg/L, [methanol] = 100 mM at pH = 7 (Tris buffer).

oxidation process and through nitrosation of its primary amine leading to the formation of xanthine (GUA 1) followed by pyrimidine and imidazole rings opening (GUA 2). Guanine susceptibly reacts with 1O_2 compared with other nucleobases (Di Mascio et al., 2019). However, 8-oxoguanine, a typical TP upon 1O_2 reactivity was not detected supporting the predominant implication of Cu(III). Guanine was the only targeted nucleobase which was degraded because guanine has

the lowest redox potential ($E^\circ = 0.81$ V) among nucleobases facilitating one-electron oxidation reactions (Wang et al., 2020a; Xie et al., 2007). Similar to phenol (Li et al., 2021), L-tyrosine could be selectively oxidized by Cu(III) to generate a phenoxy radical followed by tyrosine dimerization (TYR 1 ($m/z = 361.1394$)) and tyrosine trimerization (TYR 2 ($m/z = 540.1976$)) through a one-electron oxidation process (Fig. S3 and Fig. 6(b)). Compounds corresponding to a

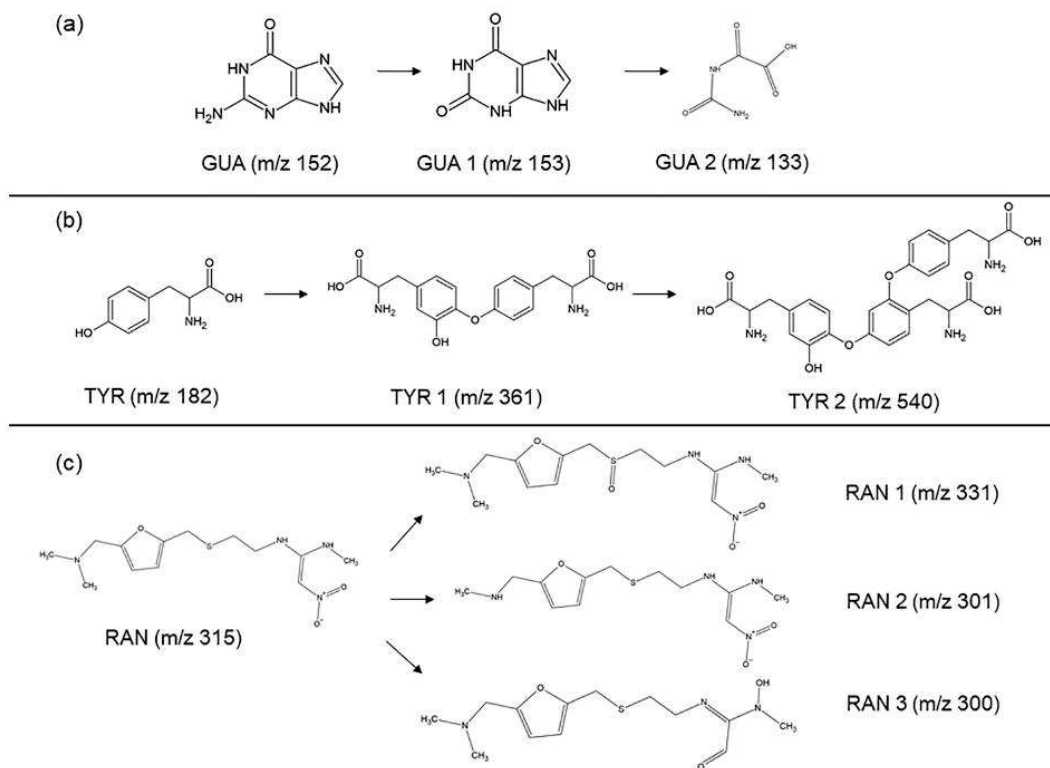


Fig. 6. Proposed transformation pathways of (a) guanine (GUA), (b) L-tyrosine (TYR), and (c) ranitidine (RAN) in CuO/PDS system.

higher degree of polymerization could not be detected more likely due to their precipitation in the reactive medium. As shown in Fig. S4 and Fig. 6(c), three main TPs of ranitidine were detected: RAN 1 ($m/z = 331.1434$), RAN 2 ($m/z = 301.1279$), and RAN 3 ($m/z = 300.1326$). RAN 1 resulted from the addition of one oxygen atom and was assigned the structure of ranitidine sulfoxide and not that of ranitidine N-oxide after injection of ranitidine N-oxide and ranitidine sulfoxide standards (Fig. S5). The formation of ranitidine sulfoxide could be ascribed to the reactivity of PDS (Fig. 6). However, the contribution of Cu(III) could not be fully discarded as its formation was previously reported in presence of diperiodatocuprate (III), a stable complex of Cu(III) known as a versatile one-electron oxidant for various organic compounds (Veeresh et al., 2008). Consequently, the oxidation of other sulfur-containing compounds, such as the methionine amino acid can be anticipated in the CuO/PDS system. Simultaneously to the S oxidation reaction ranitidine could undergo an N-dealkylation reaction (RAN 2) and further transformation at the nitro moiety leading to RAN 3 (tentative structure).

In summary, Cu(III) was found to be the predominant reactive species generated in the CuO/PDS system with extremely fast and selective reactivity with guanine which can lead to DNA damages. This result supports the higher efficiency of the CuO/PDS system in eliminating non-enveloped viruses (e.g., bacteriophages) in raw WW with respect to bacteria and the lack of bacterial regrowth. However, the CuO/PDS system can also selectively oxidize disulfide bridge and phenolic amino acids with a strong impact on proteins and enzyme integrity also facilitating pathogens inactivation.

3.3. Antibiotic-resistant bacteria and antibiotic resistance genes (ARBGs) removal

SMX (516 mg/L), as one of the first antibiotics for which bacterial resistance was observed (Pazda et al., 2019), was spiked to the culture medium to study the SMX-resistant bacteria. The initial concentration of SMX-resistant *E. coli* was $4.7 \log_{10}$ CFU/100 mL (Fig. 7(a)) and the prevalence was 15.8% (Fig. 7(b)). SMX-resistant *Enterococcus* was not detected, which suggests that no *Enterococcus* was cultivable under this SMX concentration level. A significant reduction of SMX-resistant *E. coli* ($3.2 \log$) was observed after 10 min of treatment (Fig. 7(a)). In addition, further abatement of SMX-resistant *E. coli* was also observed during storage time in untreated and treated WW samples (Fig. 7(a)), however, the prevalence of SMX-resistant *E. coli* in untreated WW samples was even increased up to 38.5% after 24 h storage (Fig. 7(b)), which indicated that the reduction of SMX-resistant *E. coli* was slower than that of total *E. coli*. Consequently, the CuO/PDS system presented an

excellent inactivation effect on SMX-resistant *E. coli* and could also effectively prevent from the enrichment of SMX-resistant bacteria.

The abundances reduction of ARGs was also evaluated. Antibiotic resistance spreads through getting resistance genes, which exist in their core genome or on mobile genetic elements, such as transposons, integrons, and plasmids (Babakhani and Oloomi, 2018). Therefore, the resistance genes (*bla*TEM, *qnr*S, *emr*B, and *sul*1) for the most commonly used groups of antibiotics (beta-lactams, quinolones, macrolides, and sulfonamides, respectively) were selected. Class 1 integron-integrase gene (*int*1), and the IS613 insertion sequence were also investigated. In addition to these, 16S rRNA gene was selected as a biomarker for bacteria, aiming at assessing the reduction in the load of total bacteria.

The mean values of initial abundances of examined genes were 3.1, 3.8, 4.3, 4.8, 4.9, 4.6, and 7.0 \log_{10} (N copies/mL) of *bla*TEM, *qnr*S, *emr*B, *sul*1, *int*1, IS613, and 16S rRNA, respectively (Fig. 8(a)), and these values are similar to those reported in urban WWTP effluents by Wang et al. (2020b) for instance. An average reduction of 1.0 \log *bla*TEM (90% abatement), 0.7 \log *qnr*S (81% abatement), 0.9 \log *emr*B (87% abatement), 1.0 \log *sul*1 (90% abatement), 2.3 \log *int*1 (99% abatement), 0.8 \log IS613 (83% abatement), and 0.6 \log 16S rRNA (90% abatement) was achieved after 60 min treatment (Fig. 8(a)), which is as effective as chlorination and UV irradiation, which caused 1.04–2.45 \log and 0.59–0.96 \log reduction of *bla*TEM and 2.98–3.14 \log and 2.48–2.74 \log reduction of *int*1 (Phattarapattamawong et al., 2021; Sharma et al., 2016). It is also noted that the reduction of pathogens and resistant *E. coli* by the system was much effective than the reduction of 16S rRNA gene. This was probably due to the Cu(III) reactivity that led to the induction of a 'Viable But Not Cultivable state' (VBNC) of bacteria and non-cultivable bacteria were detectable using the 16S rRNA measurement approach. In addition, chlorination, UV irradiation, and ozone treatments have been investigated to remove ARGs, but usually it is necessary to increase the disinfectant or UV doses and contact time to achieve a significant reduction in ARGs (Chen et al., 2020; Iakovides et al., 2019; Phattarapattamawong et al., 2021; Sharma et al., 2016; Yuan et al., 2015). The presence of the targeted genes within the total microbial community was estimated by using the relative abundances of ARGs, which were normalized to the 16S rRNA gene copy number. Results are expressed in the logarithmic scale and shown in Fig. 8(b), where values of -2 , -3 , and -4 indicate the presence of one resistance gene for every 100, 1000, and 10,000 copies of 16S rRNA gene, respectively. The initial relative abundances of targeted genes varied from $-3.85 \pm 0.1 \log$ of *bla*TEM to $-2.08 \pm 0.1 \log$ of *int*1 and the rank of abundances was determined as *int*1 > *sul*1 > IS613 > *erm*B > *qnr*S > *bla*TEM in WW, while the rank

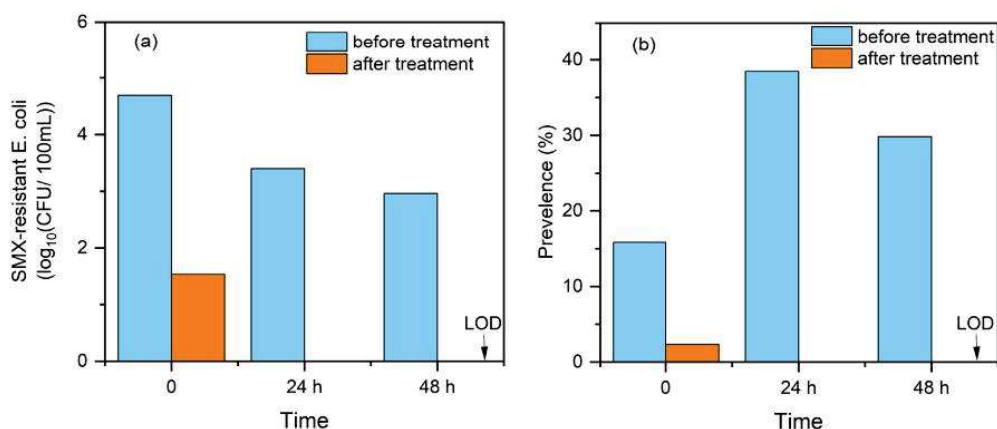


Fig. 7. Inactivation profiles of SMX-resistant *E. coli* after 10 min treatment by CuO/PDS systems in secondary treated wastewater. [CuO] = 10 g/L, [PDS] = 1 mM. Note: the unshown rectangles after treatment mean that the concentrations were lower than the limits of detection of methods.

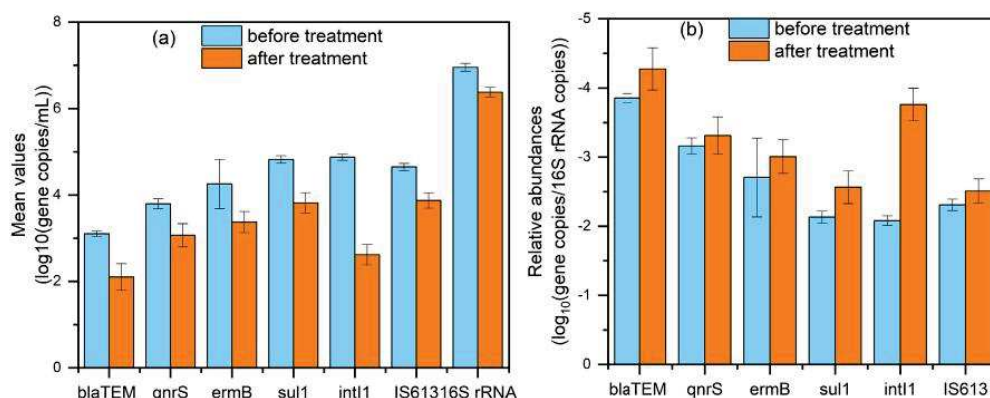


Fig. 8. Reduction profiles of selected ARGs after 60 min treatment by CuO/PDS system in secondary treated wastewater, expressed as (a) mean value and (b) relative abundances of ARGs normalized to 16S rRNA. [CuO] = 10 g/L, [PDS] = 1 mM.

of abundances in treated WW was determined as IS613 (-2.5 ± 0.2 log) > sul1 > ermB > qnrS > int1 > blaTEM (-4.3 ± 0.3 log). The relative abundances reduction was observed for all targeted genes, especially for int1, which indicated that the spread of ARGs was effectively limited by using the CuO/PDS system. Optimizing operational conditions such as longer contact time and/or the use of higher doses of CuO should improve the removal rates of targeted ARGs but this was outside the scope of this work.

4. Conclusions

Studies on the disinfection of raw and secondary treated WW demonstrated that CuO/PDS system was an effective disinfection technology in comparison to CuO alone, and sulfate radical-based system. Chlorination was probably more effective but the CuO/PDS had the advantage to avoid the production of halogenated DBPs in organic-rich WW. This work also revealed that Cu(III) instead of singlet oxygen might be the major reactive species responsible for pathogens inactivation. Due to the high selectivity of Cu(III), disinfection was still effective in raw WW as this latter oxidative species was not inhibited by the high content in organic matter. This was particularly true against viruses because of the very fast and selective reactivity of Cu(III) against guanine, possibly causing high DNA damages and avoiding bacterial regrowth after treatment. In addition, the effective reduction of selected ARB&Gs by CuO/PDS system was demonstrated by using SMX-resistant *E. coli* as a probe for ARBs, and blaTEM, qnrS, ermB, sul1, int1, and IS613 as selected ARGs. Collectively, all these findings led us to conclude that the CuO/PDS system might be a promising disinfection technology for WW treatment and reuse in irrigation mainly because it is effective in removing a large range of pathogens while preserving the carbon and nutrients content of WW and because it might be easily implemented at field-scale through filtration units. Nevertheless, this study was carried out in beakers, which is not a good option to achieve the recycling of CuO micro-particles. To overcome this shortcoming, a fixed-bed column packed with CuO has been set up by our research group for investigating wastewater disinfection, as well as wastewater decontamination. Also, economic analysis and risk assessment are needed to be made based on the fixed-bed column in terms of PDS consumption and CuO stability. These efforts will contribute to improving the feasibility of the CuO/PDS system in future water remediation applications.

CRedit authorship contribution statement

Chan Li: Analysis – writing – original draft, review & editing.
Vincent Goetz: Experimental data interpretation.
Serge Chiron: Conceptualization – writing, review & editing.

Declaration of competing interest

The authors declare that they have no known competing financial interests or personal relationships that could have appeared to influence the work reported in this paper.

Acknowledgements

This research was financially supported by the Water Joint Programming Initiative (JPI) through the research project IDOUM - Innovative Decentralized and low cost treatment systems for Optimal Urban wastewater Management and in part by the MITI CNRS/IRD program through the research project FREE - AC/CuO Filter Regenerated by solar Energy for water reuse. Chan Li thanks the Occitanie Region for her PhD grant.

Appendix A. Supplementary data

Supplementary data to this article can be found online at <https://doi.org/10.1016/j.scitotenv.2021.150768>.

References

- Akhoundi, A., Nazif, S., 2018. Sustainability assessment of wastewater reuse alternatives using the evidential reasoning approach. *J. Clean. Prod.* 195, 1350–1376. <https://doi.org/10.1016/j.jclepro.2018.05.220>.
- Aslani, H., Nabizadeh, R., Alimohammadi, M., Mesdaghinia, A., Nadafi, K., Nemati, R., Ghani, M., 2014. Disinfection of raw wastewater and activated sludge effluent using Fenton like reagent. *J. Environ. Health Sci. Eng.* 12, 1–7. <https://doi.org/10.1186/s40201-014-0149-8>.
- Babakhani, S., Oloomi, M., 2018. Transposons: the agents of antibiotic resistance in bacteria. *J. Basic Microbiol.* 58, 905–917. <https://doi.org/10.1002/jobm.201800204>.
- Chen, L., Zhou, Z., Shen, C., Xu, Y., 2020. Inactivation of antibiotic-resistant bacteria and antibiotic resistance genes by electrochemical oxidation/electroFenton process. *Water Sci. Technol.* 81, 2221–2231. <https://doi.org/10.2166/wst.2020.282>.
- Chen, Y., Di, Duan, X., Zhou, X., Wang, R., Wang, S., Ren, N., Qi, Ho, S.H., 2021. Advanced oxidation processes for water disinfection: features, mechanisms and prospects. *Chem. Eng. J.* 409, 128207. <https://doi.org/10.1016/j.cej.2020.128207>.
- Cho, Y.C., Lin, R.Y., Lin, Y.P., 2020. Degradation of 2,4-dichlorophenol by CuO-activated peroxydisulfate: importance of surface-bound radicals and reaction kinetics. *Sci. Total Environ.* 699, 134379. <https://doi.org/10.1016/j.scitotenv.2019.134379>.
- CLSI, 2020. CLSI M100: Performance Standards for Antimicrobial Susceptibility Testing, 29th edition. Clsi.
- Collivignarelli, M.C., Abbà, A., Benigna, I., Sorlini, S., Torretta, V., 2018. Overview of the main disinfection processes for wastewater and drinking water treatment plants. *Sustainability* 10, 1–21. <https://doi.org/10.3390/su10010086>.
- de la Odra Jiménez, I., Giannakis, S., Grandjean, D., Breider, F., Grunauer, G., Casas López, J.L., Sánchez Pérez, J.A., Pulgarin, C., 2020. Unfolding the action mode of light and homogeneous vs. heterogeneous photo-Fenton in bacteria disinfection and concurrent elimination of micropollutants in urban wastewater, mediated by iron oxides in raceway pond reactors. *Appl. Catal. B Environ.* 263, 118158. <https://doi.org/10.1016/j.apcatb.2019.118158>.

- de Melo Costa-Serge, N., Gonçalves, R., Rojas-Mantilla, H., Santilli, C., Hammer, P., Pupo Nogueira, R., 2021. Fenton-like degradation of sulfathiazole using copper-modified MgFe-CO₃ layered double hydroxide. *J. Hazard. Mater.* 413, 125388. <https://doi.org/10.1016/j.jhazmat.2021.125388>.
- Di Mascio, P., Martinez, G.R., Miyamoto, S., Ronsein, G.E., Medeiros, M.H.G., Cadet, J., 2019. Singlet molecular oxygen reactions with nucleic acids, lipids, and proteins. *Chem. Rev.* 119, 2043–2086. <https://doi.org/10.1021/acs.chemrev.8b00554>.
- Dias, E., Ebdon, J., Taylor, H., 2018. The application of bacteriophages as novel indicators of viral pathogens in wastewater treatment systems. *Water Res.* 129, 172–179. <https://doi.org/10.1016/j.watres.2017.11.022>.
- Dizaj, S.M., Lotfipou, F., Barzegar-jalali, M., Zarrintan Hossein, M., Adibkia, K., 2014. Antimicrobial activity of the metals and metal oxide nanoparticles. *Mater. Sci. Eng. C* 44, 278–284. <https://doi.org/10.1016/j.msec.2014.08.031>.
- European Union (EU) Regulation No. 2020/741, 2020. *Off. J. Eur. Union.* 63, L177/52.
- García-Fresnadillo, D., 2018. Singlet oxygen photosensitizing materials for point-of-use water disinfection with solar reactors. *ChemPhotoChem* 2 (7), 512–534. <https://doi.org/10.1002/cptc.201800062>.
- Gehr, R., Wagner, M., Veerasubramanian, P., Payment, P., 2003. Disinfection efficiency of peracetic acid, UV and ozone after enhanced primary treatment of municipal wastewater. *Water Res.* 37, 4573–4586. [https://doi.org/10.1016/S0043-1354\(03\)00394-4](https://doi.org/10.1016/S0043-1354(03)00394-4).
- Ghulam, M., Hajira, T., Muhammad, S., Nasir, A., 2013. Synthesis and characterization of cupric oxide (CuO) nanoparticles and their application for the removal of dyes. *Afr. J. Biotechnol.* 12, 6650–6660. <https://doi.org/10.5897/ajb2013.13058>.
- Haramoto, E., Fujino, S., Otogiri, M., 2015. Distinct behaviors of infectious F-specific RNA coliphage genogroups at a wastewater treatment plant. *Sci. Total Environ.* 520, 32–38. <https://doi.org/10.1016/j.scitotenv.2015.03.034>.
- Hashemi, H., Bovini, A., Hung, Y., Amin, M., 2013. A review on wastewater disinfection. *Int. J. Environ. Health Eng.* 2, 22. <https://doi.org/10.4103/2277-9183.113209>.
- Hong, P.Y., Al-Jassim, N., Ansari, M.I., Mackie, R.L., 2013. Environmental and public health implications of water reuse: antibiotics, antibiotic resistant bacteria, and antibiotic resistance genes. *Antibiotics* <https://doi.org/10.3390/antibiotics2030367>.
- Hong, P.Y., Julian, T.R., Pype, M.L., Jiang, S.C., Nelson, K.L., Graham, D., Pruden, A., Manaia, C.M., 2018. Reusing treated wastewater: consideration of the safety aspects associated with antibiotic-resistant bacteria and antibiotic resistance genes. *Water (Switzerland)* 10. <https://doi.org/10.3390/w10030244>.
- Hwangbo, M., Claycomb, E.C., Liu, Y., Alivio, T.E.G., Banerjee, S., Chu, K.H., 2019. Effectiveness of zinc oxide-assisted photocatalysis for concerned constituents in reclaimed wastewater: 1,4-dioxane, trihalomethanes, antibiotics, antibiotic resistant bacteria (ARB), and antibiotic resistance genes (ARGs). *Sci. Total Environ.* 649, 1189–1197. <https://doi.org/10.1016/j.scitotenv.2018.08.360>.
- Iakovides, I.C., Michael-Kordatou, I., Moreira, N.F.F., Ribeiro, A.R., Fernandes, T., Pereira, M.F.R., Nunes, O.C., Manaia, C.M., Silva, A.M.T., Fatta-Kassinos, D., 2019. Continuous ozonation of urban wastewater: removal of antibiotics, antibiotic-resistant *Escherichia coli* and antibiotic resistance genes and phytotoxicity. *Water Res.* 159, 333–347. <https://doi.org/10.1016/j.watres.2019.05.025>.
- Jaramillo, M.F., Restrepo, I., 2017. Wastewater reuse in agriculture: a review about its limitations and benefits. *Sustainability* <https://doi.org/10.3390/su9101734>.
- Jofre, J., Lucena, F., Blanch, A.R., 2021. Bacteriophages as a complementary tool to improve the management of urban wastewater treatments and minimize health risks in receiving waters. *Water (Switzerland)* 13. <https://doi.org/10.3390/w13081110>.
- Karkman, A., Do, T.T., Walsh, F., Virta, M.P.J., 2018. Antibiotic-resistance genes in waste water. *Trends Microbiol.* 26, 220–228. <https://doi.org/10.1016/j.tim.2017.09.005>.
- Kim, H.E., Nguyen, T.T.M.M., Lee, H., Lee, C., 2015. Enhanced inactivation of *Escherichia coli* and MS2 coliphage by cupric ion in the presence of hydroxylamine: dual microbicidal effects. *Environ. Sci. Technol.* 49, 14416–14423. <https://doi.org/10.1021/acs.est.5b04310>.
- Kitis, M., 2004. Disinfection of wastewater with peracetic acid: a review. *Environ. Int.* 30, 47–55. [https://doi.org/10.1016/S0160-4120\(03\)00147-8](https://doi.org/10.1016/S0160-4120(03)00147-8).
- Li, C., Goetz, V., Chiron, S., 2021. Peroxydisulfate activation process on copper oxide: Cu (III) as the predominant selective intermediate oxidant for phenol and waterborne antibiotics removal. *J. Environ. Chem. Eng.* 9, 105145. <https://doi.org/10.1016/j.jece.2021.105145>.
- Lu, S., Liu, L., Demissie, H., An, G., Wang, D., 2021. Design and application of metal-organic frameworks and derivatives as heterogeneous Fenton-like catalysts for organic wastewater treatment: a review. *Environ. Int.* 146, 106273. <https://doi.org/10.1016/j.envint.2020.106273>.
- Mandilara, G.D., Smeti, E.M., Mavridou, A.T., Lambiri, M.P., Vatopoulos, A.C., Rigas, F.P., 2006. Correlation between bacterial indicators and bacteriophages in sewage and sludge. *FEMS Microbiol. Lett.* 263, 119–126. <https://doi.org/10.1111/j.1574-6968.2006.00414.x>.
- Núñez-Salas, R.E., Rodríguez-Chueca, J., Hernández-Ramírez, A., Rodríguez, E., Maya-Treviño, M.D.L., 2021. Evaluation of B-ZnO on photocatalytic inactivation of *Escherichia coli* and *Enterococcus* sp. *J. Environ. Chem. Eng.* 9. <https://doi.org/10.1016/j.jece.2020.104940>.
- Odonkor, S.T., Ampofo, J.K., 2013. *Escherichia coli* as an indicator of bacteriological quality of water: an overview. *Microbiol. Res. (Pavia)* 4, 2. <https://doi.org/10.4081/mr.2013.e2>.
- Pazda, M., Kumirska, J., Stepnowski, P., Mulkiewicz, E., 2019. Antibiotic resistance genes identified in wastewater treatment plant systems – a review. *Sci. Total Environ.* 697, 134023. <https://doi.org/10.1016/j.scitotenv.2019.134023>.
- Phattarapattamawong, S., Chareewan, N., Polprasert, C., 2021. Comparative removal of two antibiotic resistant bacteria and genes by the simultaneous use of chlorine and UV irradiation (UV/chlorine): influence of free radicals on gene degradation. *Sci. Total Environ.* 755, 142696. <https://doi.org/10.1016/j.scitotenv.2020.142696>.
- Sánchez-Ruiz, C., Martínez-Royano, S., Tejero-Monzón, I., 1995. An evaluation of the efficiency and impact of raw wastewater disinfection with peracetic acid prior to ocean discharge. *Water Sci. Technol.* 32 (7), 159–166.
- Sharma, V.K., Johnson, N., Cizmas, L., McDonald, T.J., Kim, H., 2016. A review of the influence of treatment strategies on antibiotic resistant bacteria and antibiotic resistance genes. *Chemosphere* 150, 702–714. <https://doi.org/10.1016/j.chemosphere.2015.12.084>.
- Suleiman, M., Mousa, M., Hussein, A.J.A.A., 2015. Wastewater disinfection by synthesized copper oxide nanoparticles stabilized with surfactant. *J. Mater. Environ. Sci.* 6, 1924–1937.
- Vasilyak, L.M., 2021. Physical methods of disinfection (a review). *Plasma Phys. Rep.* 47, 318–327. <https://doi.org/10.1134/S1063780X21030107>.
- Veeresh, T.M., Patil, R.K., Nandibewoor, S.T., 2008. Thermodynamic quantities for the oxidation of ranitidine by diperiodatocuprate(III) in aqueous alkaline medium. *Transit. Met. Chem.* 33, 981–988. <https://doi.org/10.1007/s11243-008-9140-5>.
- W.H. Organization, 2015. Global Antimicrobial Resistance Surveillance System. http://apps.who.int/iris/bitstream/10665/188783/1/9789241549400_eng.pdf?ua=1.
- Wang, J., Yang, S., Zhang, Y., 2020a. One-electron oxidation and redox potential of nucleobases and deoxyribonucleosides computed by QM/MM simulations. *Chem. Phys. Lett.* 739, 136948. <https://doi.org/10.1016/j.cplett.2019.136948>.
- Wang, J., Chu, L., Wojnárovits, L., Takács, E., 2020b. Occurrence and fate of antibiotics, antibiotic resistant genes (ARGs) and antibiotic resistant bacteria (ARB) in municipal wastewater treatment plant: an overview. *Sci. Total Environ.* 744, 140997. <https://doi.org/10.1016/j.scitotenv.2020.140997>.
- Xia, D., Li, Y., Huang, G., Yin, R., An, T., Li, G., Zhao, H., Lu, A., Wong, P.K., 2017. Activation of persulfates by natural magnetic pyrrhotite for water disinfection: efficiency, mechanisms, and stability. *Water Res.* 112, 236–247. <https://doi.org/10.1016/j.watres.2017.01.052>.
- Xie, H., Yang, D., Heller, A., Gao, Z., 2007. Electrocatalytic oxidation of guanine, guanosine, and guanosine monophosphate. *Biophys. J.* 92, 70–72. <https://doi.org/10.1529/biophysj.106.102632>.
- Yuan, Q.Bin, Guo, M.T., Yang, J., 2015. Fate of antibiotic resistant bacteria and genes during wastewater chlorination: implication for antibiotic resistance control. *PLoS One* 10, 1–11. <https://doi.org/10.1371/journal.pone.0119403>.
- Zhang, T., Chen, Y., Wang, Y., Le Roux, J., Yang, Y., Croué, J.P., 2014. Efficient peroxydisulfate activation process not relying on sulfate radical generation for water pollutant degradation. *Environ. Sci. Technol.* 48, 5868–5875. <https://doi.org/10.1021/es501218f>.

Supporting Information

Copper oxide / peroxydisulfate system for urban wastewater disinfection: Performances, reactive species and antibiotic resistance genes removal

Chan Li¹, Vincent Goetz² and Serge Chiron^{1*}

¹UMR5151 HydroSciences Montpellier, University of Montpellier, IRD, 15 Ave Charles Flahault 34093 Montpellier cedex 5, France

²PROMES-CNRS UPR 8521, PROcess Material and Solar Energy, Rambla de la Thermodynamique, 66100 Perpignan, France

*Corresponding author: Tel: + 33 - 411759415; Fax: + 33 - 411759414; e-mail address: serge.chiron@umontpellier.fr

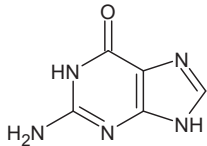
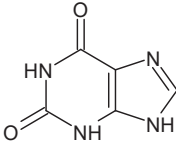
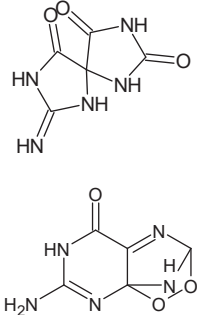
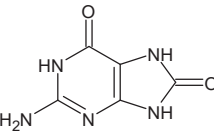
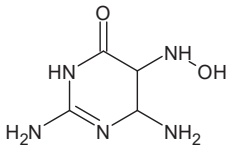
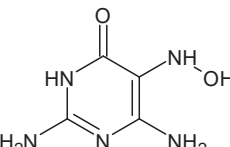
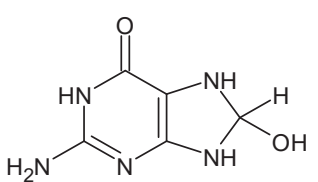
Table S1. HPLC-UV analytical methods for several nucleobases, tyrosine, and ranitidine.

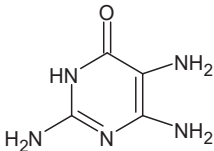
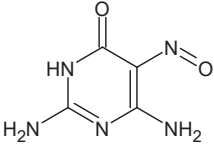
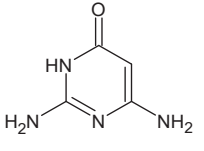
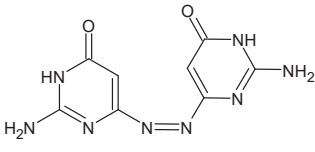
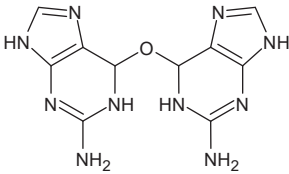
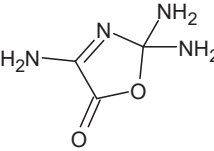
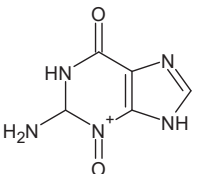
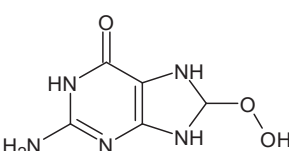
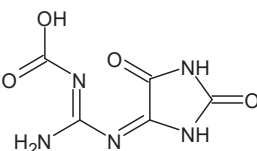
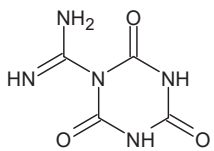
Compound	Eluent A	Eluent B	A/ B	Flow rate (mL/min)	RT (min)	λ (nm)
Guanine	MilliQ H ₂ O+0.1% formic acid	ACN	97/3	0.4	8	260
Thymine	25 mM ammonium acetate	ACN	0min, 97/3 10 min, 60/40	0.2	10	260
Adenine	25 mM ammonium acetate	ACN	90/10	0.2	8	260
L-tyrosine	MilliQ H ₂ O	ACN	100/0	0.4	8	280
Ranitidine	MilliQ H ₂ O+0.1% formic acid	ACN	80/20	0.1	15	320

Table S2. Information about qPCR primers and conditions used in quantification of target genes.

Gene	Primers	Sequence (5'–3')	Temperature of annealing	Concentration of primers	Reference
16S rRNA	Forward	ACGGTCCAGACTCCTACGGG	61°C	200 nM	Delbès et al., 2000
	Reverse	TTACCGCGGCTGCTGGCAC		200 nM	
<i>qnrS</i>	Forward	ATGCAAGTTTCCAACAATGC	62 °C	300 nM	Subirats et al., 2017
	Reverse	CTATCCAGCGATTTTCAAACA		300 nM	
<i>sulI</i>	Forward	CGCACCGGAAACATCGCTGCAC	60°C	250 nM	Cerqueira et al., 2018
	Reverse	TGAAGTTCCGCCGCAAGGCTCG		250 nM	
<i>bla_{TEM}</i>	Forward	TTCCTGTTTTTGCTCACCCAG	60°C	300 nM	Cerqueira et al., 2018
	Reverse	CTCAAGGATCTTACCGCTGTTG		300 nM	
<i>intI1</i>	Forward	GATCGGTCGAATGCGTGT	60°C	300 nM	Cerqueira et al., 2018
	Reverse	GCCTTGATGTTACCCGAGAG		300 nM	
<i>ermB</i>	Forward	AGCCATGCGTCTGACATCTA	60°C	200 nM	Shi et al., 2013
	Reverse	CTGTGGTATGGCGGGTAAGT		200 nM	
<i>IS613</i>	Forward	GTGGCGGTTATTGACGACTT	60°C	200 nM	Buelow et al., 2019
	Reverse	TTCAGCGTGCCTTCTGATG		200 nM	

Table S3. List of previously identified transformation products (TPs) of guanine generated with different reactive oxygen species (Joffe et al., 2003; Lu et al., 2018, 2016; Misiaszek et al., 2005; Ravanat and Cadet, 1995; Rokhlenko et al., 2012).

Compound	Formula	Structure	m/z [M+H] ⁺
Guanine	C ₅ H ₅ N ₅ O		152.0566
Xanthine	C ₅ H ₄ N ₄ O ₂		153.0407
	C ₅ H ₅ N ₅ O ₃		184.0465
8-Oxoguanine	C ₅ H ₅ N ₅ O ₂		168.0516
	C ₄ H ₈ N ₅ O ₂		159.0750
	C ₄ H ₇ N ₅ O ₂		158.0672
	C ₅ H ₇ N ₅ O ₂		170.0672

	$C_4H_7N_5O$		142.0723
	$C_4H_5N_5O_2$		156.0516
	$C_4H_6N_4O$		127.0614
	$C_8H_8N_8O_2$		249.0842
	$C_{10}H_{12}N_{10}O$		289.1268
	$C_3H_6N_4O_2$		131.0563
Guanine-N-oxide	$C_5H_7N_5O_2$		169.0594
	$C_5H_7N_5O_3$		186.0621
	$C_5H_5N_5O_4$		200.0414
	$C_5H_7N_5O_4$		202.0570

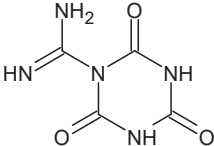
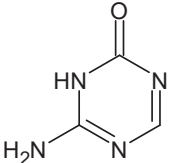
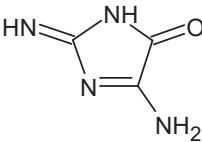
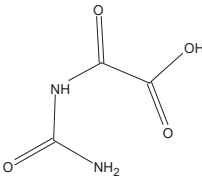
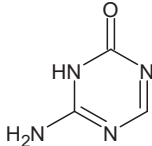
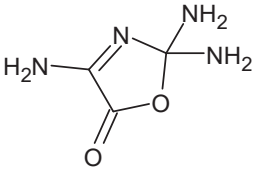
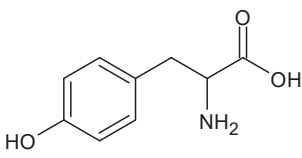
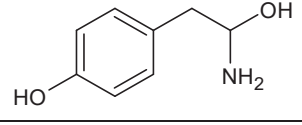
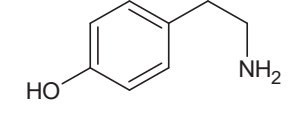
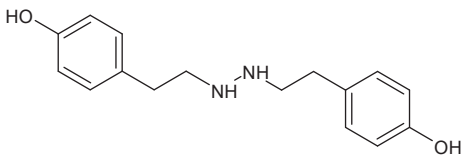
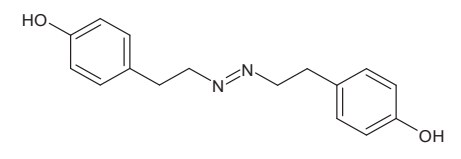
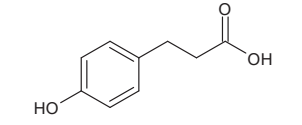
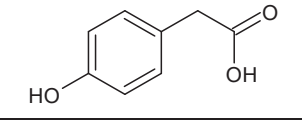
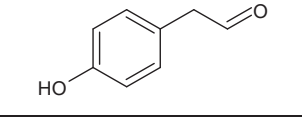
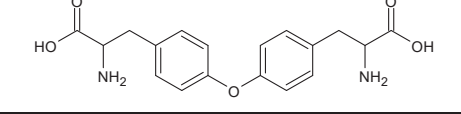
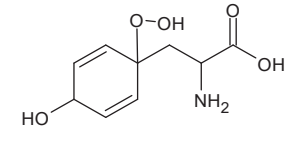
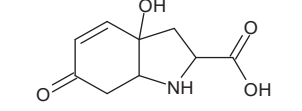
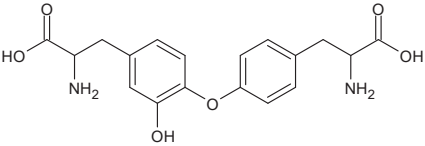
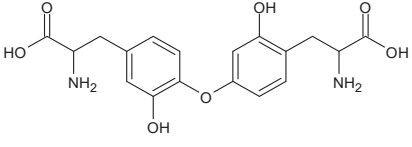
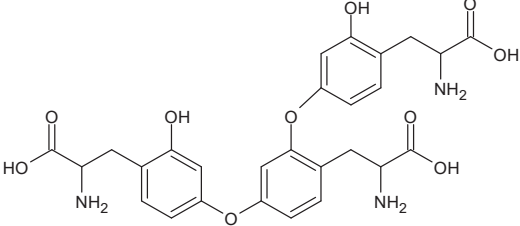
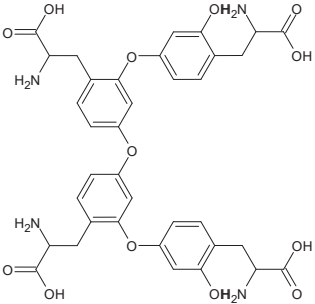
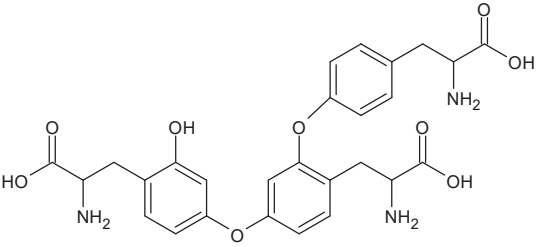
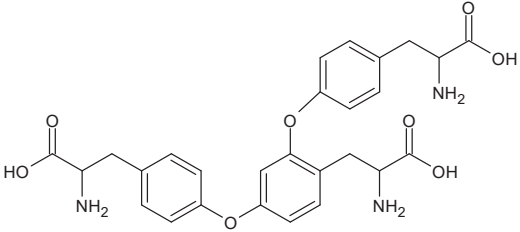
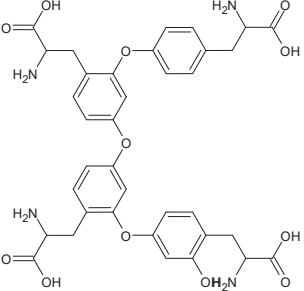
	$C_4H_5N_3O_3$		172.0465
	$C_3H_3N_3O_3$		130.0247
	$C_3H_2N_2O_3$		115.0138
	$C_3H_4N_2O_4$		133.0243
	$C_3H_4N_4O$		113.0457
	$C_3H_6N_4O_2$		131.0563

Table S4. List of previously identified TPs of L-tyrosine generated with different reactive oxygen species (Berto et al., 2016; Shetti et al., 2009; Zhoua et al., 2020).

Compound	Formula	Structure	m/z [M+H] ⁺
L-tyrosine	C ₉ H ₁₁ NO ₃		182.0811
	C ₈ H ₁₁ NO ₂		154.0862
	C ₈ H ₁₁ NO		138.0913
	C ₁₆ H ₁₈ N ₂ O ₂		273.1597
	C ₁₆ H ₂₀ N ₂ O ₂		271.1441
	C ₉ H ₁₀ O ₃		167.0702
	C ₈ H ₈ O ₃		153.0546
	C ₈ H ₈ O ₂		137.0597
	C ₁₈ H ₂₀ N ₂ O ₅		345.1444
	C ₉ H ₁₃ NO ₅		216.0866
	C ₉ H ₁₁ NO ₄		198.0760

	$C_{18}H_{20}N_2O_6$		361.1394
	$C_{18}H_{20}N_2O_7$		377.1343
	$C_{27}H_{29}N_3O_{10}$		556.1925
	$C_{36}H_{38}N_4O_{13}$		735.2508
	$C_{27}H_{29}N_3O_9$		540.1976
	$C_{27}H_{29}N_3O_8$		524.2027
	$C_{36}H_{38}N_4O_{12}$		719.2558

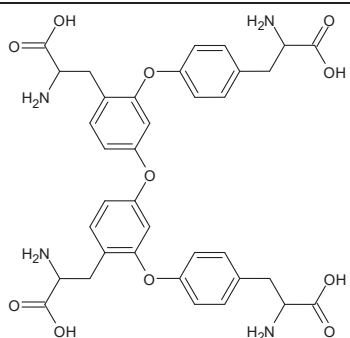
	$C_{36}H_{38}N_4O_{11}$	 <p>The chemical structure shows a dimeric molecule. It consists of two identical units linked together by two ether bridges. Each unit features a central benzene ring with two ether linkages to para-substituted phenyl rings. Each of these phenyl rings is further substituted with a 2-amino-3-carboxypropyl group.</p>	703.2609
--	-------------------------	---	----------

Table S5. List of previously identified TPs of ranitidine generated with different reactive oxygen species (Ashiru et al., 2007; Christophoridis et al., 2016; Naim and Ghauch, 2016; Veeresh et al., 2008).

Compound	Formula	m/z [M+H] ⁺
Ranitidine	C ₁₃ H ₂₂ N ₄ O ₃ S	315.1491
Ranitidine S oxide or N oxide	C ₁₃ H ₂₂ N ₄ O ₄ S	331.1440
Ranitidine sulfone	C ₁₃ H ₂₂ N ₄ O ₅ S	347.1389
Desmethyl ranitidine	C ₁₂ H ₂₀ N ₄ O ₃ S	301.1334
	C ₁₂ H ₂₀ N ₂ O ₅ S	305.1171
	C ₁₃ H ₂₁ N ₃ O ₄ S	316.1331
	C ₁₃ H ₂₁ N ₃ O ₅ S	332.1280
	C ₁₃ H ₂₁ N ₃ O ₃ S	300.1382
	C ₁₃ H ₂₃ N ₃ O ₅ S	334.1436
	C ₁₃ H ₂₁ N ₃ O ₂ S	284.1433
	C ₁₀ H ₁₈ N ₂ OS	215.1218
	C ₁₁ H ₁₅ N ₃ O ₃ S	270.0912
	C ₁₁ H ₁₅ N ₂ OS	224.0983
	C ₆ H ₄ OS	125.0061
	C ₅ H ₄ O	81.0340
	C ₁₂ H ₂₁ N ₃ O ₃ S	288.1382
	C ₁₀ H ₁₄ N ₂ O ₃ S	243.0803
	C ₈ H ₁₁ NO	138.0919
	C ₇ H ₁₁ N	110.0970
	C ₆ H ₅ O	94.0418
	C ₁₂ H ₂₁ N ₃ O ₂ S	272.1433
	C ₁₀ H ₁₄ N ₂ O ₂ S	227.0854
	C ₁₂ H ₂₁ N ₃ OS	256.1483
	C ₁₁ H ₁₄ N ₂ O ₃ S	255.0803
	C ₈ H ₁₁ NOS	170.0639
	C ₇ H ₉ NO	124.0762
	C ₁₁ H ₁₄ N ₂ O ₂ S	239.0854
	C ₆ H ₆ O	95.0497
	C ₈ H ₁₃ NO	140.1075
	C ₄ H ₉ N ₃ O ₂	132.0773
	C ₆ H ₈ O ₄ S	177.0221

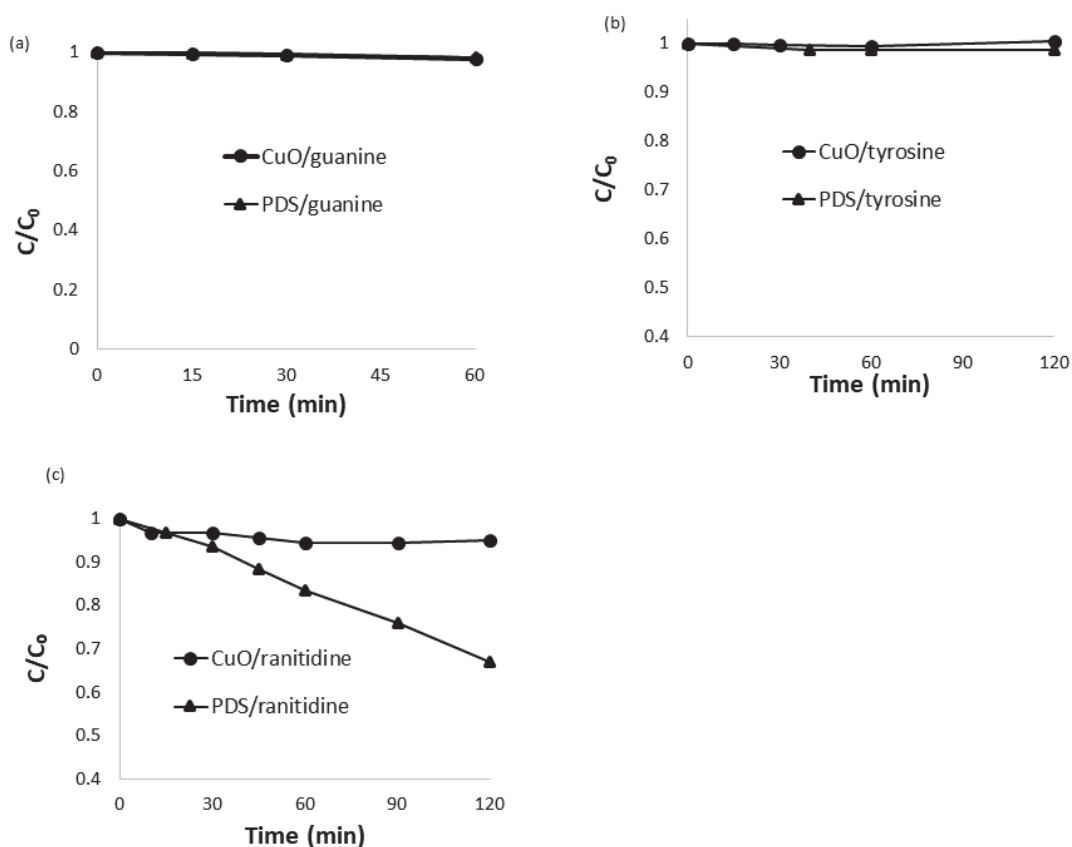


Fig. S1. Degradation kinetics of (a) guanine, (b) L-tyrosine, and (c) ranitidine in presence of CuO alone or PDS alone. [CuO] = 10 g/L, [PDS] = 1 mM, [guanine] = [L-tyrosine] = [ranitidine] = 20 mg/L, pH = 7.

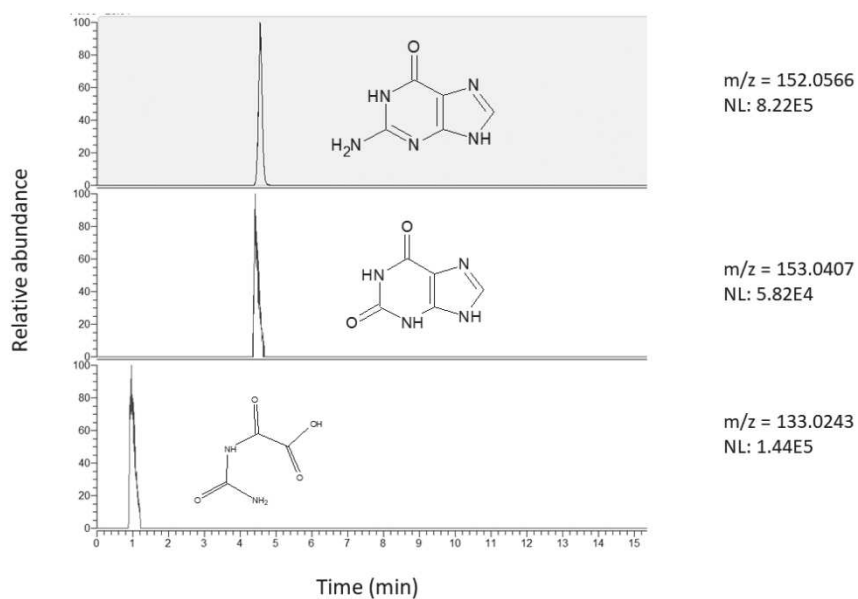


Fig. S2. Extracted Ion Chromatograms (EIC) of detected guanine TPs.

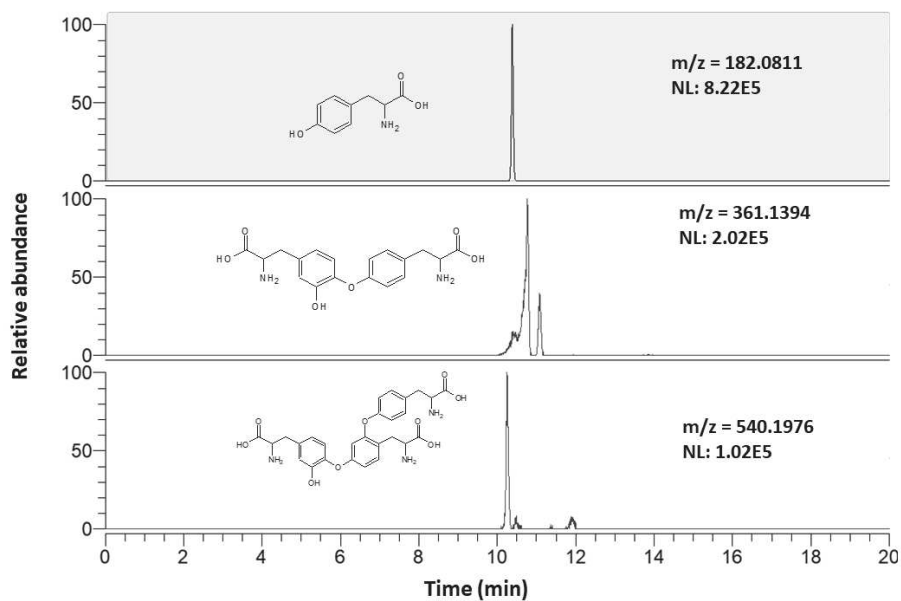


Fig. S3. Extracted Ion Chromatograms (EIC) of detected L-tyrosine TPs.

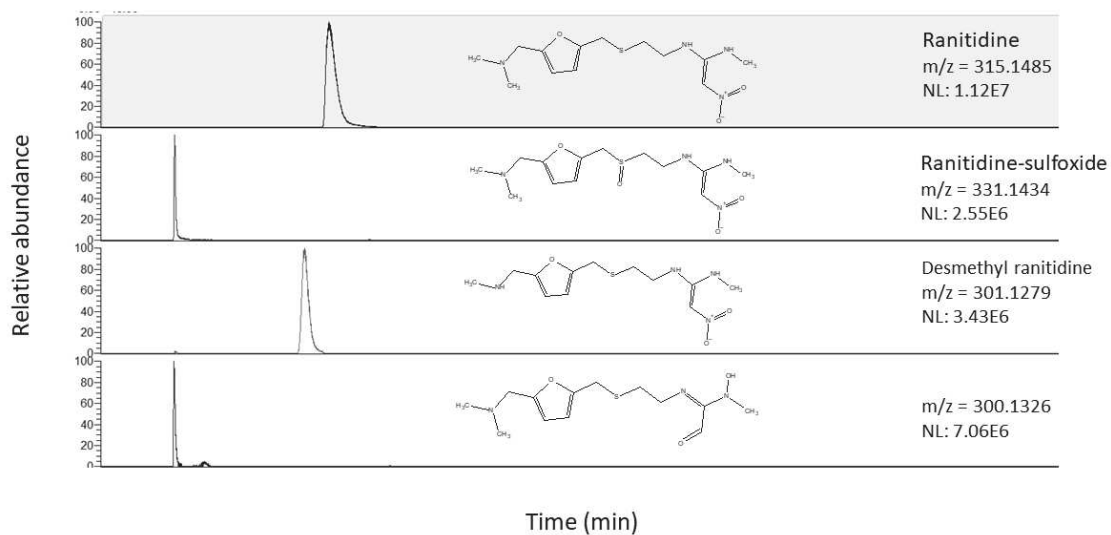


Fig. S4. Extracted Ion Chromatograms (EIC) of detected ranitidine TPs.

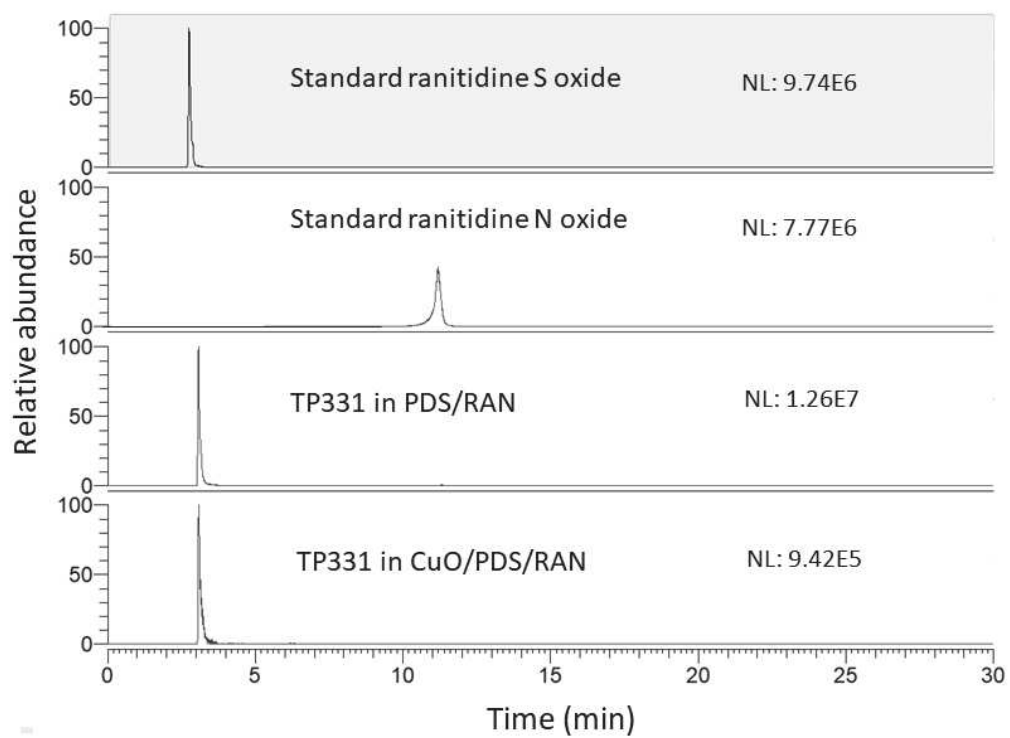


Fig. S5. Extracted Ion Chromatograms (EIC) of detected TPs at $m/z = 331.1440$.

References

- Ashiru, D.A.I., Patel, R., Basit, A.W., 2007. Simple and universal HPLC-UV method to determine cimetidine, ranitidine, famotidine and nizatidine in urine: Application to the analysis of ranitidine and its metabolites in human volunteers. *J. Chromatogr. B Anal. Technol. Biomed. Life Sci.* 860, 235–240. <https://doi.org/10.1016/j.jchromb.2007.10.029>
- Berto, S., De Laurentiis, E., Tota, T., Chiavazza, E., Daniele, P.G., Minella, M., Isaia, M., Brigante, M., Vione, D., 2016. Properties of the humic-like material arising from the photo-transformation of L-tyrosine. *Sci. Total Environ.* 545, 434–444. <https://doi.org/10.1016/j.scitotenv.2015.12.047>
- Buelow E., Rico A., Gaschet M., Lourenço J., Kennedy S., Wiest L., Ploy M-C., Dagot C., 2019. Classification of hospital and urban wastewater resistome and microbiota over time and their relationship to the eco-exposome. *bioRxiv*, 697433. <https://doi.org/10.1101/697433>
- Cerqueira F., Matamoros V., Bayona J., Piña B., 2019. Antibiotic resistance genes distribution in microbiomes from the soil-plant-fruit continuum in commercial *Lycopersicon esculentum* fields under different agricultural practices. *Sci. Total Environ.* 652, 660–670. <https://doi.org/10.1016/j.scitotenv.2018.10.268>
- Christophoridis, C., Nika, M.C., Aalizadeh, R., Thomaidis, N.S., 2016. Ozonation of ranitidine: Effect of experimental parameters and identification of transformation products. *Sci. Total Environ.* 557–558, 170–182. <https://doi.org/10.1016/j.scitotenv.2016.03.026>
- Delbès, C., Moletta, R., Godon, J. J., 2000. Monitoring of activity dynamics of an anaerobic digester bacterial community using 16S rRNA polymerase chain reaction–single-strand conformation polymorphism analysis. *Environ. Microbiol.*, 2(5), 506–515.
- Joffe, A., Geacintov, N.E., Shafirovich, V., 2003. DNA Lesions Derived from the Site Selective Oxidation of Guanine by Carbonate Radical Anions. *Chem. Res. Toxicol.* 16, 1528–1538. <https://doi.org/10.1021/tx034142t>
- Lu, W., Sun, Y., Zhou, W., Liu, J., 2018. pH-dependent singlet oxygen oxidation kinetics of guanine and 9-methylguanine: An online mass spectrometry and spectroscopy study combined with theoretical exploration. *J. Phys. Chem. B.* 122, 40–53. <https://doi.org/10.1021/acs.jpcc.7b09515>
- Lu, W., Teng, H., Liu, J., 2016. How protonation and deprotonation of 9-methylguanine alter its singlet oxygen addition path: About the initial stage of guanine nucleoside oxidation. *Phys. Chem. Chem. Phys.* 18, 15223–15234. <https://doi.org/10.1039/c6cp01350c>
- Misiaszek, R., Crean, C., Geacintov, N.E., Shafirovich, V., 2005. Combination of nitrogen dioxide radicals with 8-oxo-7,8-dihydroguanine and guanine radicals in DNA: Oxidation and nitration end-products. *J. Am. Chem. Soc.* 127, 2191–2200. <https://doi.org/10.1021/ja044390r>
- Naim, S., Ghauch, A., 2016. Ranitidine abatement in chemically activated persulfate systems: Assessment of industrial iron waste for sustainable applications. *Chem. Eng. J.* 288, 276–288. <https://doi.org/10.1016/j.cej.2015.11.101>
- Ravanat, J.L., Cadet, J., 1995. Reaction of singlet oxygen with 2'-deoxyguanosine and DNA.

- Isolation and characterization of the main oxidation products. *Chem. Res. Toxicol.* 8, 379–388. <https://doi.org/10.1021/tx00045a009>
- Rokhlenko, Y., Geacintov, N.E., Shafirovich, V., 2012. Lifetimes and reaction pathways of guanine radical cations and neutral guanine radicals in an oligonucleotide in aqueous solutions. *J. Am. Chem. Soc.* 134, 4955–4962. <https://doi.org/10.1021/ja212186w>
- Shetti, N.P., Hegde, R.N., Nandibewoor, S.T., 2009. Mechanistic aspects of oxidation on L-tyrosine by diperiodatocuprate(III) complex in alkali media: A kinetic model. *Cent. Eur. J. Chem.* 7, 929–937. <https://doi.org/10.2478/s11532-009-0085-0>
- Shi P, Jia S, Zhang XX, Zhang T, Cheng S, Li A., 2013. Metagenomic insights into chlorination effects on microbial antibiotic resistance in drinking water. *Water Res.* 47(1),111-20. <https://doi.org/10.1016/j.watres.2012.09.046>
- Subirats J., Triadó-Margarit X., Mandaric L., Acuña V., Balcázar J-L., Sabater S., Borrego C-M., 2017. Wastewater pollution differently affects the antibiotic resistance gene pool and biofilm bacterial communities across streambed compartments. *Mol. Ecol.* 26(20), 5567-5581.
- Veeresh, T.M., Patil, R.K., Nandibewoor, S.T., 2008. Thermodynamic quantities for the oxidation of ranitidine by diperiodatocuprate(III) in aqueous alkaline medium. *Transit. Met. Chem.* 33, 981–988. <https://doi.org/10.1007/s11243-008-9140-5>
- Zhoua, Q., Zhang, X., Zhou, C., 2020. Transformation of amino acid tyrosine in chromophoric organic matter solutions: Generation of peroxide and change of bioavailability. *Chemosphere* 245, 125662. <https://doi.org/10.1016/j.chemosphere.2019.125662>

Chapter 4. Peroxydisulfate activation by CuO pellet in a fixed-bed column for antibiotics degradation and urban wastewater disinfection

Abstract

A fixed-bed column packed with copper oxide pellet (FBC-CuO) combined with peroxydisulfate (PDS) as a primary oxidant was assessed as an option for simultaneously wastewater decontamination (antibiotics) and disinfection (bacteria, viruses, and protozoa). Preliminary to these experiments, phenol was used as the target molecule to investigate the working mode of FBC-CuO under various operating conditions, such as varying flow rates, initial persulfate and phenol concentrations. The removal of a mix of five representative antibiotics (i.e., amoxicillin (AMX), cefalexin (CFX), ofloxacin (OFL), sulfamethoxazole (SMX), and clarithromycin (CLA)) in distilled water and secondary treated urban wastewater (STWW) was evaluated. AMX, CFX, and OFL were effectively removed by simply flowing through the FBC-CuO at 1.5 mL/min, and the addition of PDS (500 μ M) systematically enhanced the degradation of all targeted antibiotics, which is also the necessary condition for the removal of SMX and CLA. Urban wastewater disinfection was evaluated by monitoring targeted pathogens presented originally in the STWW. A significant reduction of *E. coli*, *Enterococcus*, *F-specific RNA bacteriophages* was observed after the treatment by FBC-CuO with 500 μ M PDS and 1.5 mL/min. Phase analyses and morphology of CuO pellet before and after treatment were performed by X-ray diffraction measurement and scanning electron microscopy, indicated that the structure of the catalyst was preserved without any phase segregation. Cu(II) released from FBC-CuO in wastewater was low (0.4 mg/L). All the findings of this study underline the potential of the FBC-CuO combined with PDS at the field scale for the degradation of micropollutants and inactivation of pathogens in wastewater after a necessary consolidation of these first but very promising results.

Keywords: Fixed bed column; copper oxide pellet; operating parameters; antibiotics; disinfection; secondary treated wastewater

1. Introduction

Conventional urban wastewater treatment plants are poorly effective to comprehensively remove most organic micropollutants, pathogens, as well as antibiotic resistance.^{1,2} The occurrence and the large discharging amounts of these contaminants in municipal wastewater is a concern due to its potential ecotoxicological and hazardous effects on receiving nature waters or reclaimed wastewater reuse.³ Therefore, effective additional treatment steps for micropollutants degradation, pathogens inactivation, as well as antibiotic resistance reduction are required.

Advanced oxidant processes (AOPs) employing hydrogen peroxide (H_2O_2) and persulfate (PS) have been seen as a promising technology for water decontamination and disinfection simultaneously, which rely on reactive species produced by activating oxidants, such as hydroxyl and sulfate radicals ($\cdot\text{OH}$ and $\text{SO}_4^{\cdot-}$), singlet oxygen ($^1\text{O}_2$), and high valent metal ions.^{1,4-6} Oxidants activation can be achieved by an input of energy (UV, heat), electrolysis, transition metal ions, metal oxides, carbon materials, etc..^{6,7} However, the high cost of the required extra energy, the recycling difficulty of metal ions limit their application. To overcome these disadvantages, heterogeneous Fenton-like processes make use of recyclable solid catalysts, such as iron oxides,^{8,9} copper oxide,^{10,11} have recently obtained increasing attention and have shown high decontamination and disinfection capacity.

The recent study of our research group conducted in a batch operating mode,¹⁰ has shown that the system composed of micro-sized copper oxide (CuO) in suspension in the effluent in contact with peroxydisulfate (PDS) is a good generator of the highly selective cuprous (Cu(I)) and cupryl (Cu(III)) as well as $^1\text{O}_2$ species, which lead to effective removal of micropollutants. These species are also well identified as excellent biocidal species in disinfection processes.^{4,12,13} These previous studies make the system CuO/PDS a promising option for a simultaneously removal of micropollutants as well as pathogens (bacteria, viruses) in secondary treated urban wastewater (STWW).

However, direct application of CuO microparticles, as well as nanoparticles, may not be appropriated from an environmental perspective due to the possible release of CuO particles into the environment, which may lead to catalyst losses and adverse effects on aquatic life. Therefore, the mixed reactor composed of a suspension of CuO particles is probably not the optimal option in the perspective of dissemination of such a process at the outlet of a wastewater treatment plant.

Fixed bed column is very well known and commonly used in chemical engineering to provide efficient components separation by sorption, catalytic treatment as well as chemical reaction.^{14,15} Laboratory-scale fixed-bed reactors have been widely used when developing a new process to treat harmful and toxic substances and can provide a basis for further upscale.¹⁶ Thus, the use of CuO in the form of millimetric pellets packed in a fixed-bed column (FBC-CuO) is an option to be studied within this objective. In addition, the millimeter size makes it possible to respect the requirement of limiting the pressure drop inside the column¹⁷ and preventing potential clogging problems and make it possible to take advantage of the well-defined working mode of the fixed bed reactive system.^{14,15}

To our knowledge, laboratory-scale fixed bed column based on the use of CuO has only been reported by one study, which used CuO in form of nanoparticles and supported on alumina granules for virus removal evaluation.¹⁸ Therefore, the main objective of this work is to evaluate the wastewater decontamination and disinfection performance of the peroxydisulfate oxidation by a fixed-bed column filled with millimetric particles of CuO (FCB-CuO). Specific objectives included: i) a comprehensive experimental study in the case of the simplest solution to be treated that consisted of phenol in distilled water with Tris buffer (DW) to determine the effect of operational parameters, such as the inflow PDS concentration, flow rate, and to better understand the working mode of this new process, ii) the evaluation of the micropollutants removal performance by using a mixture of antibiotics (i.e. amoxicillin (AMX), cefalexin (CFX), ofloxacin (OFL), sulfamethoxazole (SMX), and clarithromycin (CLA)) in DW and STWW, iii)

the evaluation of STWW disinfection performance by using *Escherichia coli* (*E. coli*), *Enterococcus*, *F-specific RNA coliphages*, and *spores of sulfite-reducing bacteria* as pathogenic indicators, and iv) catalyst stability evaluation by analyzing the Cu(II) leaching and comparing the morphology and crystallinity of CuO pellet before and after treatment.

2. Experimental section

2.1 Chemicals

CuO pellet (> 99.9%) was purchased from Merck (Germany). Phenol, amoxicillin (AMX), cephalexin (CFX, > 99%), clarithromycin (CLA, > 99.9%), ofloxacin (OFL, > 99.9%), sulfamethoxazole (SMX, > 99.9%), potassium peroxydisulfate ($K_2S_2O_8$, > 99.9%), sodium thiosulfate (NaS_2O_3), and EDTA were purchased from Sigma-Aldrich (Saint Quentin Fallavier, France). Potassium iodide (KI), potassium periodate (KIO_4), and tris(hydroxymethyl)aminomethane (Tris) were purchased from Merck KGaA (Germany). Acetonitrile (HPLC grade), methanol (MeOH, HPLC grade), and sodium chloride (NaCl) were purchased from Carlo Erba reagents (France). All the reagents used were of analytical grade and were used as received. Milli-Q water from a Direct-Q® system (Millipore) was used for the stock solution preparation and the HPLC analyses.

2.2 Characterization of CuO pellet

The CuO pellet (0.71-2 mm) morphology was analyzed using JEOL 6490 scanning electron microscope (SEM). X-ray diffractometry (XRD) was performed using a Bruker D8 Advance in Bragg-Brentano geometry with a Cu source. Diffraction signal has been acquired through theta/2theta scans from 10 to 80° with 0.02° step, with an acquisition time of 1s/step.

2.3 Fixed-bed column set up

A cylinder stainless steel column reactor (18 mm internal diameter (I.D.) \times 200 mm height) was filled with 140 g CuO pellet, and two metal grids with a mesh smaller than the size of the CuO pellet were positioned at the inlet and the outlet of the column. FBC-CuO consists of a volume occupied by the solid CuO pellet (22 mL) and an empty bed volume (EBV, 29 mL). As shown in Figure 1, the FBC-CuO was vertically oriented and silicone tubes were connected at both ends. The inlet at the bottom of the column was driven by a peristaltic pump (lab 2015, Shenchen, China) to control flow rates, and the outlet was at the top of the column. Three micro-valves were evenly located on the column evenly 5 cm for local sampling and accessed the internal concentration profiles of the different components. All experiments were operated in upflow mode at a controlled flow rate.

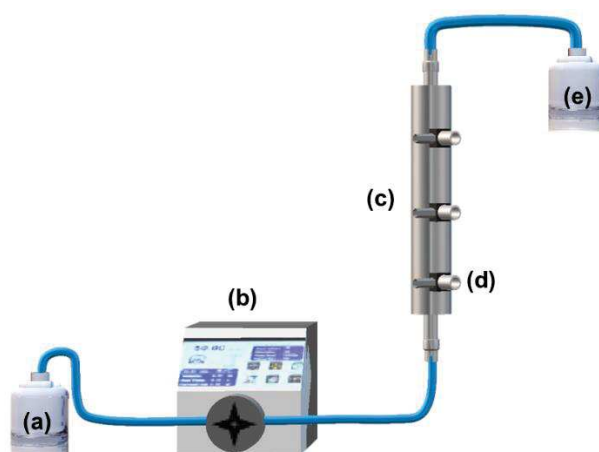


Figure 1. The schematic of the column. (a) inlet solution, (b) peristaltic pump, (c) column filled with CuO pellets, (d) column valve, and (e) outlet solution.

2.4 Experimental procedures

2.4.1 Phenol degradation with FCB-CuO process

To have a thorough understanding of the working mode, phenol was selected as the probe compound. Tris buffer (20 mM) was used as the water matrix to maintain the neutral pH of the solution for all the experiments with phenol. As no adsorption or degradation of phenol by CuO alone were observed,¹⁰ it was decided to start the experiment with a column filled with the phenol solution. Pure phenol solution (5 mg/L)

flowed into the column with a 3 mL/min flow rate until the outlet concentration equal the inlet concentration. Then, a uniform concentration of phenol inside the column represented the initial conditions of the degradation experiments. They were systematically triggered by the addition of PDS at a constant concentration to the inlet phenol solution and a flow into the column according to the selected flow rate. From this starting point, the inflow phenol and PDS concentration and flow rate kept unchanged. Aliquots of treated water samples were collected at the predetermined time from the outlet and three valves. Samples were stored at 4 °C before analysis. The working mode of the phenol removal was expected to happen in a first phase in dynamic regime and followed by a second phase in permanent regime.

2.4.2 Antibiotics degradation with FCB-CuO process

The most commonly used and frequently detected in the environment family of antibiotics in the world are the β -lactam antibiotics, including penicillins and cephalosporins. Amoxicillin (AMX) and cefalexin (CFX) are belongings to the aminopenicillin and cephalosporins family, which have been detected in raw sewage, effluents of sewage treatment plants, and even surface waters.^{19,20} In addition to β -lactam antibiotics, sulfonamide, macrolide, as well as fluoroquinolone antibiotics are the most prominent classes of antimicrobial agents, with widespread usage in both human and veterinary medicines, which occurs ubiquitously in aquatic systems that are influenced by anthropogenic activities.²¹⁻²⁴ To evaluate the degradation performance of antibiotic micropollutants on the FCB-CuO column, 250 μ g/L of AMX, CFX, OFX, SMX, and CLA, which have been commonly detected in urban wastewater, were spiked to DW and STWW from an activated sludge wastewater treatment plant, respectively. The physio-chemical properties of STWW are listed in Table S1. STWW was firstly filtered through a 200 μ m sieve to remove the big suspended solids and prevent the clogging problem.

Differently with phenol, the interaction between Cu(II) with some specific antibiotics was previously reported.^{25,26} Thus, the starting point of the antibiotic degradation

experiments was corresponding to the FCB-CuO filled with pure water. For the first stage, the antibiotics mixture first flowed through the column without PDS, then a constant inlet concentration of PDS was added in the second step. Aliquots of treated water samples were collected at the predetermined time from the column outlet, and stored at 4 °C before analysis.

2.4.3 Pathogens inactivation with FCB-CuO process

STWW was collected from the same activated sludge wastewater treatment plant and was also filtered through a 200 µm sieve before the disinfection experiment. To evaluate the disinfection performances of FBC-CuO/PDS and to comply with the EU Regulation 2020/741 of the European Parliament and of the Council of 25 May 2020 on minimum requirements for water reuse,²⁷ *E. coli*, *Enterococcus*, *F-specific RNA bacteriophages*, and *spores of sulfite-reducing bacteria* were selected as the indicator of Gram-negative, Gram-positive bacteria, virus, and protozoa, respectively. The pathogenic indicators originally presented in wastewater were targeted to monitor.

CuO alone, may interact and provide non-negligible disinfection effects,^{28,29} especially when implemented in the form of nanoparticles. For this reason, disinfection experiments were operated as in the case of the experiments dedicated to antibiotic degradation. A first step corresponding to the flowing of the effluent through the FCB-CuO system without PDS. A second step corresponding to the flowing of the effluent, at the same flow rate with a constant concentration of PDS at the inlet of the column.

The column was design to operate with flow rates of few mL/min to provide consistent residence times. Measurement of the four targeted pathogens needed to collect one liter of each sample. As a consequence, it was not possible to investigate the pathogens inactivation process in dynamic regime due to the long sampling period, and the sampling was carried out in the both cases (with and without PDS) when the permanent regime was reached after at least 2 hours of operating.

To ensure the stable viability of pathogens, the effluents in the sterile water tanks at the

inlet and outlet of the column were surrounded by ice pads. Samples were stored at 4 °C and pathogens analysis was conducted less than 24 h after sample collection.

2.5 Analytical methods

2.5.1 Quantification of phenol and PDS

Phenol concentrations were quantified by LC with a diode-array detector at $\lambda = 280$ nm using an Agilent ZORBAX Eclipse XDB C8 column (150 × 3 mm i.d., 3.5 μ m particle size). The separation was performed using an isocratic mode of elution with a mobile phase composed of 0.1% formic acid in Milli-Q water and acetonitrile at a volume ratio of 50/50. The flow rate was set at 0.5 mL/min.

PDS was determined by using a UV-Vis spectrophotometer (Shimadzu, Japan). Briefly, the method consisted in analyzing adsorption spectra of mixed solutions of 1 mL sample, 1 mL 60 mM NaHCO₃, and 1 mL 600 mM KI in a quartz cuvette at $\lambda = 352$ nm.

2.5.2 Quantification and transformation products analysis of antibiotics

Quantification of targeted antibiotics were analyzed by LC-HRMS composed of a Dionex Ultimate 3000 liquid chromatograph equipped with an electrospray source operated in the positive ionization mode and a Exactive Orbitrap mass spectrometer (Thermo Fisher Scientific, Les Ulis, France) operated in full scan MS (mass range m/z 50-900) and using an Agilent ZORBAX Eclipse XDB C18 plus column (150 × 2.1 mm i.d., 3.5 μ m particle size). LC gradient of Milli-Q water with 1% acetonitrile and 0.1% formic acid (solvent A) and acetonitrile with 1% Milli-Q water and 0.1% formic acid (solvent B) was as follow: 0-5 min, 95% A; 15-20 min, 5% A; 21-30 min, 95% A. The flow rate was 0.15 mL/min. The energy collisional dissociation was set to 20 eV and a drying gas temperature of 300 °C was used.

To gain insights into the targeted antibiotic degradation mechanisms of FBC-CuO alone, and FBC-CuO in presence of PDS, transformation products (TPs) of AMX, CFX, OFL, SMX, CLA were identified following a suspect screening workflow in LC-HRMS. The

databases were made up of a list of possible TPs with their molecular formula and exact mass collected from the literature. The list of possible TPs of CFX, SMX, CLA were reported in the supplementary information in our previous study.¹⁰ Possible TPs of AMX and OFL were listed in Table S2-S3.

2.5.3 Enumeration of pathogens

The NF EN ISO 9308-3 and NF EN ISO 7899-1 standard protocols were used to enumerate *E. Coli* and *Enterococcus* respectively. These methods are based on the culture of the bacteria in a liquid medium and the determination of the most probable number (MPN) according to the level of dilution. *F-specific RNA bacteriophages* were measured according to the ISO 10705-1 method. This method allows for a count on the agar medium of plaque-forming unit (PFU), corresponding to the number of viruses. The NF EN 26461-2 standard protocol was used to enumerate the colony-forming unit (CFU) of *spores of sulfite-reducing bacteria* after filtration and cultivation on a specific agar solid medium.

2.5.4 Cu(II) analysis

Cu(II) leached from CuO pellet was analyzed by inductively coupled plasma - optical emission spectrometry (ICP-OES) using an iCap Duo 7400 spectrometer (Thermo Fischer Scientific, Les Ulis, France) using the axial mode of detection at wavelength $\lambda = 324.754$ nm.

3 Results and discussion

3.1 Working mode of the CuO pellet fixed-bed column

As detailed in the section 2.4.1, before each degradation experiment, the column was charged with a phenol solution at a given concentration. Here are presented the breakthrough curve of the phenol at the outlet of the column (Figure 2a) in the case of a volume flow rate equal to 3 mL/min and an inlet concentration of phenol (C_{ph_i}) equal

to 5 mg/L. After the breakthrough, the outlet phenol concentration (C_{ph_o}) was very close to the inlet, indicating that there is no scalable interaction between this component and the CuO pellet surface without the assistance of a primary oxidant. The Reynolds number (Re) under flowing conditions was much smaller than 1, indicating a highly laminar flow regime in the column. The axial diffusion coefficient is estimated to be in the range of 3×10^{-7} and $2 \times 10^{-6} \text{ m}^2 \text{ s}^{-1}$ with the popular and simplified Chun and Wen empirical equation³⁰ when $Re < 1$. As expected, and in agreement with the low value of the Peclet number (around 0.2), the shape of the breakthrough curve was characteristic of a plug-flow with an important axial dispersion resulting in an "S-curve". Finally, the theoretical phenol quantity calculated based on the filling amount of the liquid phase, taking into account the EBC and the minor dead volumes at the inlet and the outlet of the column, was equal to the actual phenol quantity calculated from the breakthrough curve (around 0.14 mg), which further confirmed that there was no detectable adsorption of phenol at the surface of the CuO pellet.

Measurements of outlet concentrations of the two reactive species, phenol and PDS, combined with the internal profiles of these components when the permanent regime was reached (Figure 2) make it possible to have a clear understanding of the operating mode of the process during phenol removal. For the record, the initial time ($t = 0$) in Figure 2b corresponds to a column with a uniform inlet and outlet phenol concentration ($C_{ph_i} = C_{ph_o} = 5 \text{ mg/L}$) and without any trace of PDS but operating, from this moment with a volume flow of 3 mL/min, and inlet PDS (C_{PDS_i}) and phenol concentration equal to 500 μM and 5 mg/L respectively. As expected, the column operated in two different regimes. The first dynamic regime corresponded to the establishment of the PDS concentration profile in the fixed packed bed, which was the result of it flowing from the inlet to the outlet. During this phase, the concentrations of both species inside the column were the result of the coupling between the convective mass transport, mass diffusion of both species, kinetic of phenol removal, and kinetic of PDS consumption. The breakthrough time of the PDS (Figure 2b) is consistent with the one obtained in

the case of phenol during the preliminary charge, which gave the limit between the dynamic and the permanent regime. It took at least 40 to 50 min for a completed establishment of the permanent regime, and then the concentrations of both species remained constant at the outlet. Their absolute values depended on the operating parameters of the column i.e., the volume flow rate and the inlet concentrations of phenol and PDS. In this case, phenol was almost complete removed but PDS was not fully consumed. After 60 min, the local concentrations of phenol and PDS were very stable at any position inside the column during the entire measurement period of several hours (Figure 2c and 2d), which well confirmed the steady-state operation of the process. The profiles also clearly indicated that, for these particular operating conditions, the inlet concentration of the PDS was not fully optimized. PDS remained at the outlet of the column while only half of the column was necessary to provide complete removal of the inlet phenol flux.

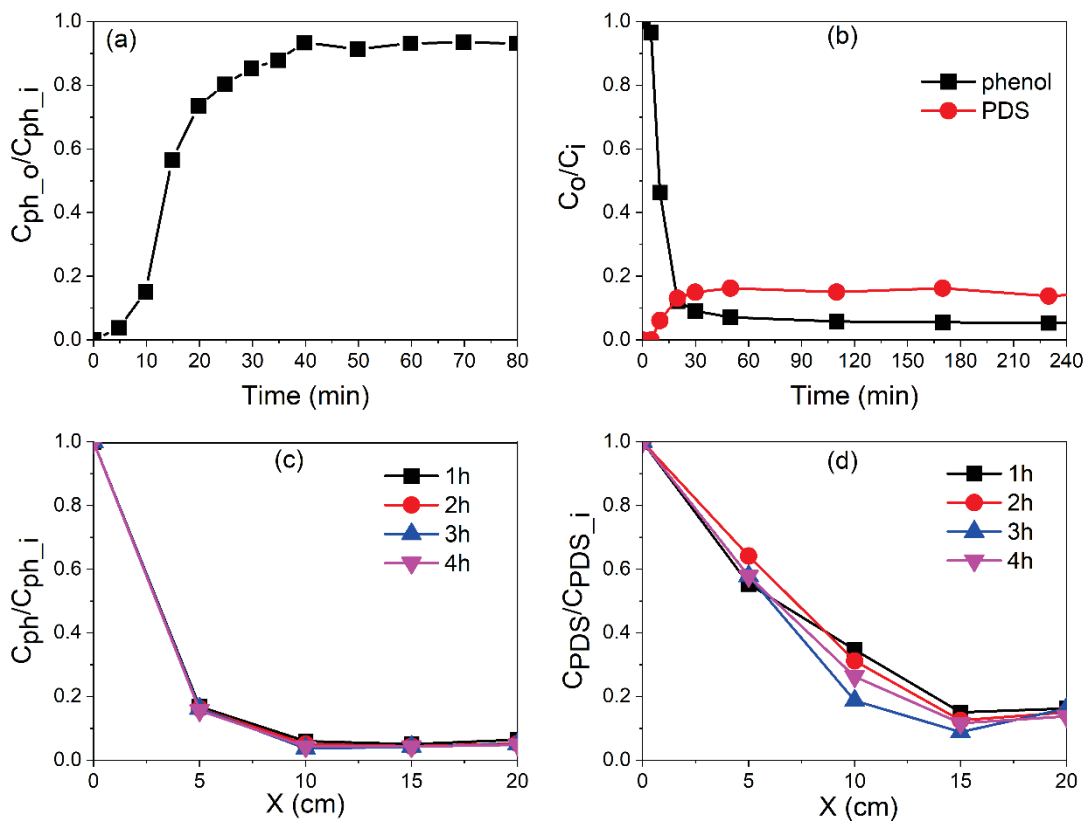


Figure 2. (a) Breakthrough curve of phenol in FBC-CuO; (b) phenol and PDS concentration profiles at the outlet of FBC-CuO; internal (c) phenol and (d) PDS

concentration profiles of FBC-CuO. $C_{ph_i} = 5$ mg/L, $C_{PDS_i} = 500$ μ M, flow rate = 3 mL/min.

The performance of the FBC-CuO with 5 mg/L influent phenol and 3 mL/min flow rate was tested at varying influent PDS concentrations. Whatever were the working conditions, the two regimes were checked with a period necessary for the establishment of the quasi-static regime almost independent of the PDS inlet concentration (Figure 3a and 3b). Obviously, PDS dosage is an important factor of the column performances on phenol degradation. Consistently with our previous batch study¹⁰, higher influent PDS concentration promoted the oxidative mechanisms and led to higher phenol removal efficiency and treatment capacity (Table 1). For example, a twofold increase in the treatment capacity was observed when PDS concentration varying from 125 μ M to 500 μ M. Besides, most of the phenol abatement occurred in the first 5 cm of the column (Figure 3b). Specifically, with 125 μ M at the inlet, there was no more PDS in the solution at a position between 5 and 10 mm (Figure 3d). From this position, the concentration of the phenol was kept constant (Figure 3b). This indicates that a too much lower inlet PDS concentration could be all consumed in the front part of the column, leading to an unused bed length and preventing any degradation of the pollutant. On the contrary, a too high inlet PDS concentration is inefficient and counterproductive. No improvement of the treatment capacity was detected when PDS inlet concentration was increased from 500 μ M to 1000 μ M (Table 1) while a useless release of PDS at the outlet happened (Figure 3c). As in the previous case but for a different reason, a too high dosage of PDS (1000 μ M) also led to an unused bed length. In the first part of the column, the high removal kinetic of phenol linked to the high level of PDS concentration led to complete removal of the phenol between 5 and 10 mm (Figure 3b). Therefore, for these particular conditions, a mass flow of 3 mL/min and an inlet concentration of phenol of 5 mg/L, an inlet concentration of PDS between 250 and 500 μ M would have probably been the optimal value to achieve no PDS release at the outlet with a total removal thanks to optimal use of the length of the column.

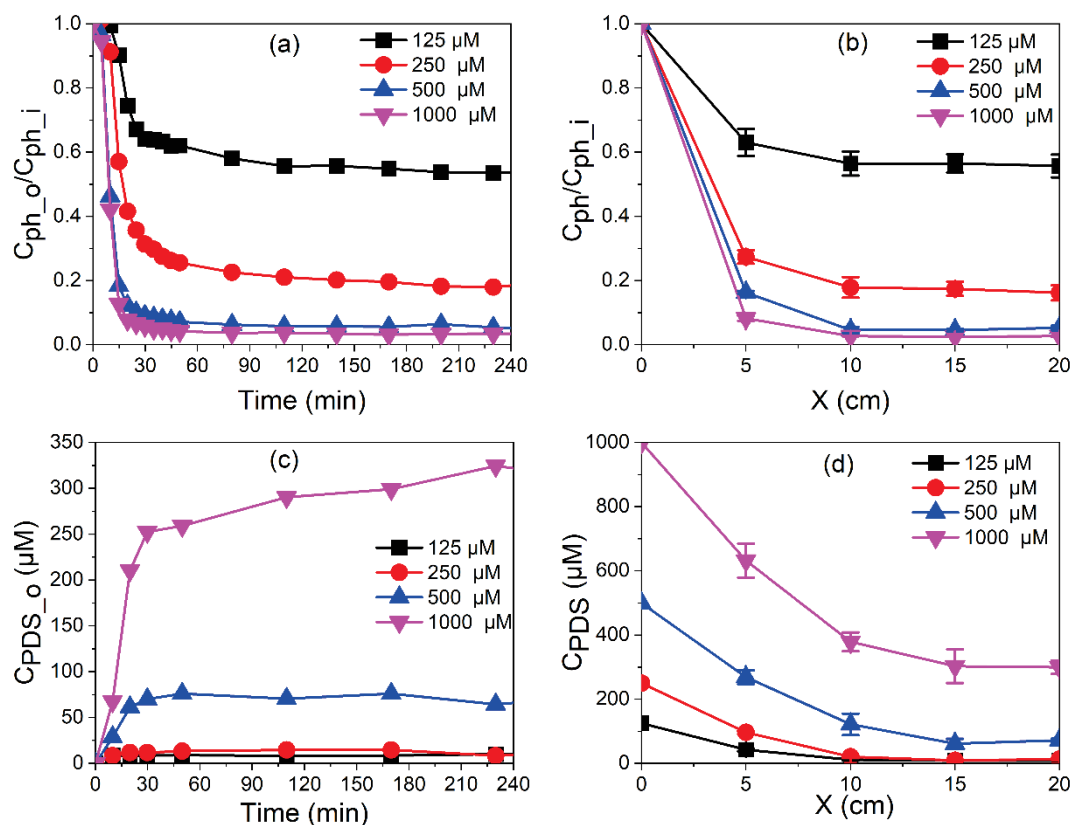


Figure 3. The effect of different inlet PDS concentration on phenol and PDS concentration profiles at outlet of FBC-CuO: (a) and (c); and at different column positions when permanent regimes were reached: (b) and (d). $C_{ph_i} = 5$ mg/L, $C_{PDS_i} = 125, 250, 500,$ and 1000 μM, flow rate = 3 mL/min.

Table 1. Removal efficiency and treatment capacity of phenol by FBC-CuO/PDS system with varying influent PDS concentration.

Flow rate (mL/min)	C_{ph_i} (mg/L)	C_{PDS_i} (μM)	Removal efficiency (%)	Treatment capacity of phenol (μg/min)
3	5	0	0	0
		125	46	7.41
		250	81	12.36
		500	95	14.14
		1000	97	14.55

Even if only specific operating conditions were provided for a particular column design, this qualitative report clearly demonstrated that the control of the FCB-CuO process can easily be achieved by controlling and regulating the inlet oxidant concentration as

a function of the operating conditions. This is further confirmed by the results conducted within the objective of studying the effects of the inlet concentration phenol, the volume flow, and presented as supplementary material (Figure S1-S2).

3.2 Degradation of antibiotics

As detailed in the section devoted to the experimental procedure, in a first step, a mixture of AMX (penicillin), CFX (cephalosporin), OFL (quinolone), SMX (sulfonamide), and CLA (macrolide) in DW flowed through FBC-CuO at a flow rate of 1.5 mL/min. Different trends were noticed (Figure 4a). In this case, corresponding to a more complex mixture with probably competitive phenomena between the surface of CuO and the some of the pharmaceutical compounds, the breakthrough times of each species were not uniform. However, only a few tens of minutes separated the breakthrough times of SMX and CLA, the two species with a fully breakthrough at the outlet of the column which happened around 1 h. This order of magnitude was in agreement with a breakthrough derived from the resident time (35 min in the working conditions) combined with significant diffusional transport phenomena. CFX and OFX corresponded to an intermediate behavior. Breakthrough happened but saturation of the column was never reached. The outlet concentrations of both species kept lower than the inlet concentrations, even after a very long operating period (18 h) and a permanent regime definitively established as clearly indicated by the concentration profiles of the species. Finally, whatever was the operating period, AMX was always undetectable at the outlet of FCB-CuO. AMX, CFX, and OFL were effectively removed by FBC-CuO alone (Table 2).

Hydrolysis of β -lactam antibiotic family can be a significant degradation pathway in the environment, but it usually takes 5.3-27 days at pH 7 and 25°C.³¹ It could not be the main degradation pathway in this study. Adsorption mechanism was excluded because of the very low specific surface area of CuO.¹⁰ Another possible mechanism may be the complexation of Cu(II) with β -lactam antibiotics (AMX and CFX) and

fluoroquinolones (OFL). AMX and CFX contain the carboxylic, amide, and amino groups, which resemble dipeptides in acid-base and ligand properties, and exist as anions at neutral pH, then subsequently interact with Cu(II).^{25,26,32} Transformation products of AMX, CFX, and OFL in FBC-CuO were identified following a suspect screening workflow in LC-HRMS. For this purpose, a database was made up of a list of possible TPs with their molecular formula, exact mass, and structure (see Table S1 and S2, and SI of previously work by our group¹⁰). This list was established from a literature search of TPs. TPs with intensities lower than 1×10^4 cps, signal to noise ratios lower than 10, isotopic ratio higher than 10%, and mass accuracy errors higher than 5 ppm were discarded. The identified TPs of CFX, AMX, and OFL were shown from Figure S3, S4, and S5, representatively. The transformation pathways of AMX, CFX, and OFL in FBC-CuO were tentatively elucidated (Figure S6). A deep discussion of the mechanism of TPs formation was outside the main objective of this work. However, the formation of TPs most likely through a one electron transfer from the antibiotic to the metal in the complex, demonstrated the degradation of AMX, CFX and OFL by FBC-CuO alone.

After 18 h of operation, the column was in permanent regime, 500 μ M PDS was added to the inlet water tank to initiate FBC-CuO/PDS system at a 1.5 mL/min flow rate for the second stage operation. As shown in Figure 4b, the addition of PDS systematically and significantly enhanced the degradation of the antibiotics. The residual outlet concentration of CFX and OFL were rapidly removed. The presence of PDS was also the necessary condition for a partial but significant, removal of SMX and CLA. CFX and OFL were completely degraded after 30 min. $51 \pm 2\%$ of SMX and $34 \pm 1\%$ of CLA were removed in the tested operating conditions when the quasi-permanent regime was reached.

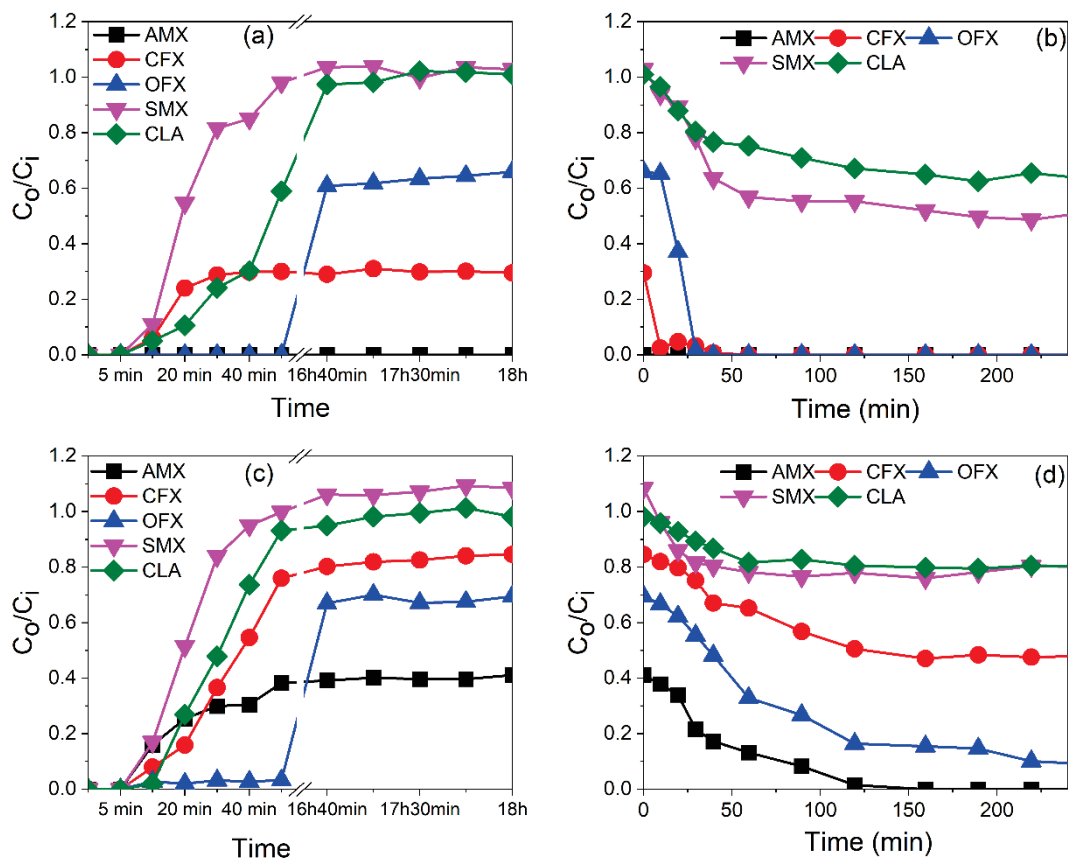


Figure 4. Degradation of target antibiotics in DW and STWW by FBC-CuO: (a), (c); and by FBC-CuO/PDS: (b), (d). $C_{AMX_i} = C_{CFX_i} = C_{OFL_i} = C_{SMX_i} = C_{CLA_i} = 250 \mu\text{g/L}$, $C_{PDS_i} = 500 \mu\text{M}$, flow rate = 1.5 mL/min.

In addition to DW, the removal efficiency of target antibiotics mixture in the actual wastewater operating under the same conditions was also evaluated, as shown in Figure 4c and 4d. The degradation tendency of target antibiotics in DW and STWW was the same, however, the removal efficiency of targeted antibiotics decreased under the influence of various competitive components in the STWW (Figure 4 and Table 2). For the first stage of FBC-CuO, the dissolved organic matter and anions (e.g. sulfate anions) in STWW could interact with Cu(II) or adsorbed on the CuO, resulting in less available activated sites on the CuO surface, and limited Cu(II) complexation with targeted antibiotics (Figure 4a and 4c). For the second stage of FBC-CuO/PDS, less PDS could interact with CuO, resulting in less PDS consumption (Figure S7), less reactive species production, and lower degradation efficiency for all targeted antibiotics (Figure 4b and

4d). The removal efficiency of antibiotics DW and STWW is shown in Table 2.

Table 2. Removal efficiency (RE) of selected antibiotics by FBC-CuO and FBC-CuO/PDS in DW and STWW.

RE	DW		STWW	
	FBC-CuO	FBC-CuO/PDS	FBC-CuO	FBC-CuO/PDS
AMX (%)	100	100	59 ± 3	100
CFX (%)	70 ± 2	100	25 ± 1	52 ± 2
OFX (%)	34 ± 1	100	31 ± 1	90 ± 2
SMX (%)	0	51 ± 2	0	20 ± 1
CLA (%)	0	34 ± 1	0	20 ± 1

3.3 Pathogens inactivation

In a first step, the STWW was flowed through the FCB-CuO at a flow rate equal to 3 mL/min. After 2 h of operation, the working mode of FBC-CuO was expected to reach the permanent regime. From this moment, the sampling at the outlet of the column started to collect the necessary 1 L effluent for pathogens analysis. Comparison between the inlet and the outlet pathogens concentrations is provided in Figure 5a. The abundances in secondary-treated effluent samples before treatment were $5.3 \pm 0.1 \log_{10}$ MPN/100 mL of *E. coli*, $4.6 \pm 0.1 \log_{10}$ MPN/100 mL of *Enterococcus*, $4.0 \pm 0.1 \log_{10}$ PFU/100 mL of *F-specific RNA bacteriophages*, and $3.5 \pm 0.2 \log_{10}$ CFU/100 mL of *spores of sulfite-reducing bacteria* and are comparable to the values found in the literature^{33,34}. When the effluent simply flowed through FBC-CuO without PDS, the reduction of bacteria and parasite was very limited for *E. coli* (0.2 log), *Enterococcus* (0.2 log), and *spores of sulfite-reducing bacteria* (0.3 log), but for virus, a considerable reduction of *F-specific RNA bacteriophages* (2.7 log) was observed. This was most likely a consequence of the presence at low concentration of Cu(II) due to leaching from the surface of CuO pellets. As detailed in the next section, this species, which presents well known biocidal characteristics, was identified by suitable methods in the

effluent at the column outlet.

In a similar way to the test carried out on antibiotics, the second step was initiated by the addition of 500 μM of PDS to the inlet water tank and sampling started when the permanent regime was reached. Prior to this experiment, it was checked that PDS alone at ambient temperature had no measurable effects on the abundances of pathogens. When the effluent flowed through FBC-CuO with PDS, the reduction of 3 out of the 4 pathogens indicators significantly increased. *E. coli* (3.6 log) and *F-specific RNA bacteriophages* (3.8 log) were respectively removed up to or just above the limit of detection. *Enterococcus* was also significantly inactivated (1.3 log). However, the reduction of *spores of sulfite-reducing bacteria* (0.2 log, 38% abatement), the indicator representative of the parasite, was still limited. Such pathogens are well identified in the literature as extremely difficult to inactivate and resistant to disinfection processes, such as chlorination³⁵ and UV³⁶, but can alternatively be removed by low cost slow sand filtration system.³⁷

Pathogens were ranked as *E. coli* and *F-specific RNA bacteriophages* > *Enterococcus* > *spores of sulfite-reducing bacteria* according to the treatment effectiveness criteria, and was fully confirmed by the tests carried out at different flow rates (Figure 5b). Spores were not inactivated by the FCB_CuO/PDS, whatever the operating conditions. At the opposite, the evolution of conversion rates for the other three treatment-sensitive pathogens attested of the influence of operating conditions, and more specifically the residence time. As expected, in such a process based on the coupling between kinetic of inactivation and mass transport, an increase of the residence time almost systematically resulted in an increase of the conversion rates. Finally, the triplicate performed with a flow rate equal for 1.5 mL/min brought to light the well-known uncertainty linked to the quantification of any pathogens populations, especially in the case of non-stabilized and non-controlled effluents such as STWW. This does not affect the major contribution of the experiments that have to be considered as mainly qualitative.

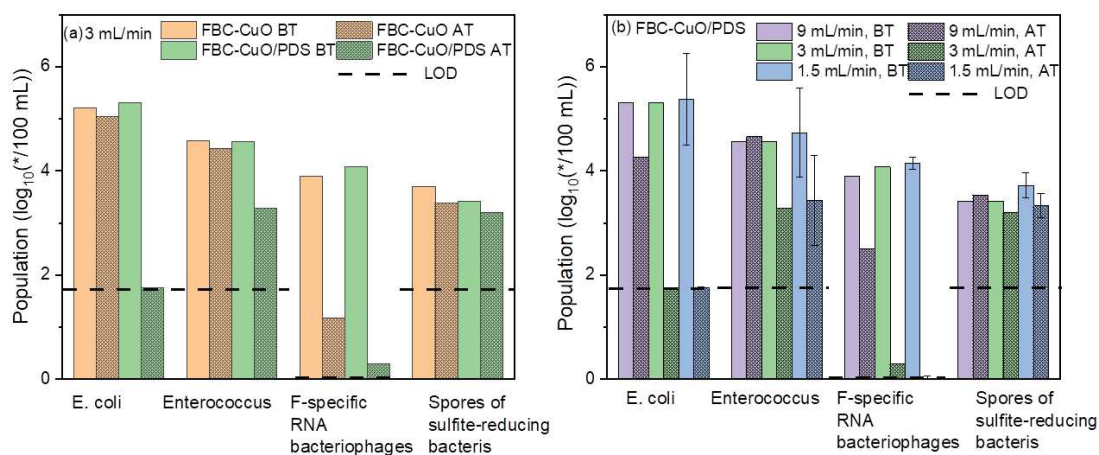


Figure 5. Inactivation profiles of pathogens in secondary treated wastewater by CuO pellet column (a) with and without PDS at one flow rate. Flow rate = 3 mL/min, (b) with PDS at different flow rates. Flow rates = 1.5, 3, and 9 mL/min. $C_{PDS_i} = 500 \mu\text{M}$. Note: * represents MPN for *E. coli* and *Enterococcus*, PFU for F-specific RNA bacteriophages, and CFU for spores of sulfite-reducing bacteria. BT: before treatment; AT: after treatment.

3.4 Stability of FBC-CuO

One of the essential characteristics for a catalyst to be a candidate for application in large-scale wastewater treatment is its stability and ability to maintain catalytic activity during long period of operation. Consequently, possible structural changes of the CuO pellet were evaluated by analyzing the catalyst recovered after all the measurement campaigns presented using SEM and X-ray diffractograms.

The SEM images of the surface of the millimetric CuO pellets were analyzed before and after the campaigns to know if there was any change in their morphology. The Figure 6a and 6b highlighted that the surface was made off aggregates. No significant difference was observed for the average diameter particle-size of CuO pellet aggregates before and after treatment, $623 \pm 74 \text{ nm}$ and $700 \pm 30 \text{ nm}$ being obtained, respectively.

The XRD diffractogram before and after treatment (Figure 6c) shows well-defined and intense diffraction peaks located at the positions $2\theta = 32.66, 35.63, 38.78, 46.37, 48.92, 53.61, 58.37, 61.70, 65.95, 66.39, 68.17$ and 72.51 . According to the literature, these

peaks correspond to the monoclinic structure of CuO.³⁶⁻³⁸ Lattice parameters were calculated and are $a = 4.70 \text{ \AA}$, $b = 3.42 \text{ \AA}$, $c = 5.10 \text{ \AA}$. The intensities, positions of the peaks and the lattice parameters are in good agreement with the reported values JCPDS file N°. 96-901-6058.

The stability of the catalyst was assessed against the leached concentration of Cu measured in solution by ICP-AES after a filtration step on 0.45 \mu m cellulose filters. The Cu leaching from CuO in presence of PDS was investigated in DW and STWW ($\text{pH} = 7.8$). The results are shown in Figure 6d. Surprisingly, the Cu leaching decreased when moving from DW (6.8 and 8.0 mg/L after 1 and 4 h reaction) to STWW (0.3 and 0.4 mg/L after 1 and 4 h reaction). The low Cu leaching in STWW might be ascribed to a lesser degree of PDS activation (Figure S7) due to sorption of dissolved organic matter to CuO. The Cu leaching value was far less than that of 2 mg/L which is required by environmental quality standards for surface water and by drinking water regulations.³⁹ Therefore, the results showed that the material presented phase purity and stability before and after treatment. The good stability and catalytic efficiency of CuO pellet at near neutral pH, make this system promising for application.

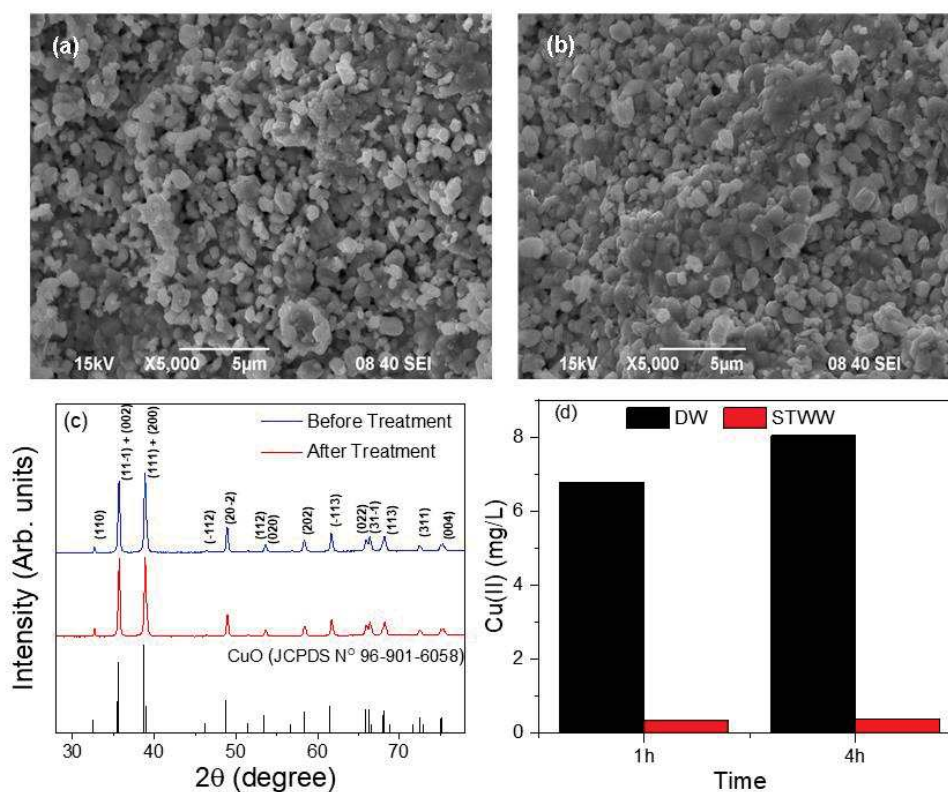


Figure 6. SEM images of CuO pellet (a) before and (b) after treatment; (c) X-ray diffractograms of CuO pellet before and after treatment; (d) copper leaching from FBC-CuO in presence of PDS in DW and STWW.

4 Conclusions

PDS activation by using CuO pellet as heterogeneous catalyst in a fixed-bed column was for the first time designed and applied for wastewater decontamination and disinfection. The first set of experiments performed with a simple solution of phenol in distilled water have demonstrated that this process, as any process based on the flowing of a reactive mixture through a fixed packed bed was sensitive to operating conditions, especially for flow rate and influent PDS concentration. FBC-CuO alone presented significant removal performance on β -lactam and fluoroquinolones antibiotics through Cu(II) complexation and degradation. But FBC-CuO alone demonstrated limited disinfection performance. The combination of PDS with FBC-CuO was the necessary condition for the degradation of SMX and CLA, not only improving the antibiotics degradation, but also greatly enhancing the pathogens inactivation performances,

excepted for *spores of sulfite-reducing bacteria*, the indicator selected as representative of the parasites. It is suggested that after FBC-CuO/PDS, post-treatment by low-cost slow sand filtration or ionized clay filtration, may overcome the main limitations of this process. The characterization comparison of CuO pellet before and after treatment and the measurement of Cu(II) leaching demonstrated the excellent stability and reusability FBC-CuO. Overall, it was shown that FBC-CuO/PDS constitutes an efficient and promising treatment option for the removal of micropollutants and microorganisms from urban wastewater effluents. In addition, this study provided the basis for further numerical modelling of FBC-CuO/PDS, which will be discussed in a coming article.

Associated content

Supporting Information

Phenol and PDS profiles under varying operational conditions (Figure S1 and S2); electron ion chromatograms (Figure S3, S4, and S5); transformation pathway of antibiotics in FBC-CuO (Figure S6); PDS consumption for antibiotics degradation in DW and STWW (Figure S7); physiochemical properties of wastewater (Table S1); list of previous identified TPs of AMX and OFL (Table S2 and S3).

Acknowledgements

This research was financially supported by the Water Joint Programming Initiative (JPI) through the research project IDOUM - Innovative Decentralized and low cost treatment systems for Optimal Urban wastewater Management and in part by the MITI CNRS/IRD program through the research project FREE (AC/CuO Filter Regenerated by solar Energy for water rEuse. Chan Li thanks the Occitanie Region for her PhD grant. Nayara de Melo Costa Serge thanks the São Paulo Research Foundation, Brazil, (FAPESP, grants #2019/24642-0 and #2018/17517-0) for financial support and doctoral scholarship.

References

- (1) Rizzo, L.; Gernjak, W.; Krzeminski, P.; Malato, S.; McArdell, C. S.; Perez, J. A. S.; Schaar, H.; Fatta-Kassinos, D. Best Available Technologies and Treatment Trains to Address Current Challenges in Urban Wastewater Reuse for Irrigation of Crops in EU Countries. *Sci. Total Environ.* **2020**, *710*, 136312. <https://doi.org/10.1016/j.scitotenv.2019.136312>.
- (2) Ternes, T. A.; Prasse, C.; Eversloh, C. L.; Knopp, G.; Cornel, P.; Schulte-Oehlmann, U.; Schwartz, T.; Alexander, J.; Seitz, W.; Coors, A.; Oehlmann, J. Integrated Evaluation Concept to Assess the Efficacy of Advanced Wastewater Treatment Processes for the Elimination of Micropollutants and Pathogens. *Environ. Sci. Technol.* **2017**, *51* (1), 308–319. <https://doi.org/10.1021/acs.est.6b04855>.
- (3) Wang, J.; Chu, L.; Wojnárovits, L.; Takács, E. Occurrence and Fate of Antibiotics, Antibiotic Resistant Genes (ARGs) and Antibiotic Resistant Bacteria (ARB) in Municipal Wastewater Treatment Plant: An Overview. *Sci. Total Environ.* **2020**, *744*, 140997. <https://doi.org/10.1016/j.scitotenv.2020.140997>.
- (4) Chen, Y. di; Duan, X.; Zhou, X.; Wang, R.; Wang, S.; Ren, N. qi; Ho, S. H. Advanced Oxidation Processes for Water Disinfection: Features, Mechanisms and Prospects. *Chem. Eng. J.* **2021**, *409* (August 2020), 128207. <https://doi.org/10.1016/j.cej.2020.128207>.
- (5) Waclawek, S.; Lutze, H. V.; Grübel, K.; Padil, V. V. T.; Černík, M.; Dionysiou, D. D. Chemistry of Persulfates in Water and Wastewater Treatment: A Review. *Chem. Eng. J.* **2017**, *330* (July), 44–62. <https://doi.org/10.1016/j.cej.2017.07.132>.
- (6) Lee, J.; Von Gunten, U.; Kim, J. H. Persulfate-Based Advanced Oxidation: Critical Assessment of Opportunities and Roadblocks. *Environ. Sci. Technol.* **2020**, *54* (6), 3064–3081. <https://doi.org/10.1021/acs.est.9b07082>.
- (7) Wang, J.; Wang, S. Activation of Persulfate (PS) and Peroxymonosulfate (PMS) and Application for the Degradation of Emerging Contaminants. *Chem. Eng. J.* **2018**, *334* (July 2017), 1502–1517. <https://doi.org/10.1016/j.cej.2017.11.059>.
- (8) de la Obra Jiménez, I.; Giannakis, S.; Grandjean, D.; Breider, F.; Grunauer, G.; Casas López, J. L.; Sánchez Pérez, J. A.; Pulgarin, C. Unfolding the Action Mode of Light and Homogeneous vs. Heterogeneous Photo-Fenton in Bacteria Disinfection and Concurrent Elimination of Micropollutants in Urban Wastewater, Mediated by Iron Oxides in Raceway Pond Reactors. *Appl. Catal. B Environ.* **2020**, *263* (October 2019), 118158. <https://doi.org/10.1016/j.apcatb.2019.118158>.
- (9) Yan, J.; Lei, M.; Zhu, L.; Anjum, M. N.; Zou, J.; Tang, H. Degradation of Sulfamonomethoxine with Fe₃O₄ Magnetic Nanoparticles as Heterogeneous Activator of Persulfate. *J. Hazard. Mater.* **2011**, *186* (2–3), 1398–1404. <https://doi.org/10.1016/j.jhazmat.2010.12.017>.
- (10) Li, C.; Goetz, V.; Chiron, S. Peroxydisulfate Activation Process on Copper Oxide:

- Cu(III) as the Predominant Selective Intermediate Oxidant for Phenol and Waterborne Antibiotics Removal. *J. Environ. Chem. Eng.* **2021**, 9 (2), 105145. <https://doi.org/10.1016/j.jece.2021.105145>.
- (11) Du, X.; Zhang, Y.; Hussain, I.; Huang, S.; Huang, W. Insight into Reactive Oxygen Species in Persulfate Activation with Copper Oxide: Activated Persulfate and Trace Radicals. *Chem. Eng. J.* **2017**, 313, 1023–1032. <https://doi.org/10.1016/j.cej.2016.10.138>.
 - (12) Kim, H. E.; Nguyen, T. T. M. M.; Lee, H.; Lee, C. Enhanced Inactivation of Escherichia Coli and MS2 Coliphage by Cupric Ion in the Presence of Hydroxylamine: Dual Microbicidal Effects. *Environ. Sci. Technol.* **2015**, 49 (24), 14416–14423. <https://doi.org/10.1021/acs.est.5b04310>.
 - (13) García-Fresnadillo, D. Singlet Oxygen Photosensitizing Materials for Point-of-Use Water Disinfection with Solar Reactors. *ChemPhotoChem* **2018**, 2 (7), 512–534. <https://doi.org/10.1002/cptc.201800062>.
 - (14) Levenspiel, O. *Chemical Reaction Engineering*; 1999. <https://doi.org/10.1201/9781420087567-13>.
 - (15) John C. Crittenden, R. Rhodes Trussell, David W. Hand, K. J. H. and G. T. *MHW's Water Treatment Principles and Design*; 2012.
 - (16) Andrigo, P.; Bagatin, R.; Pagani, G. *Fixed Bed Reactors*; 1999; Vol. 52. [https://doi.org/10.1016/S0920-5861\(99\)00076-0](https://doi.org/10.1016/S0920-5861(99)00076-0).
 - (17) Mehta, D.; Hawley, M. C. Wall Effect in Packed Columns. *Ind. Eng. Chem. Process Des. Dev.* **1969**, 8 (2), 280–282. <https://doi.org/10.1021/i260030a021>.
 - (18) Mazurkow, J. M.; Yüzbasi, N. S.; Domagala, K. W.; Pfeiffer, S.; Kata, D.; Graule, T. Nano-Sized Copper (Oxide) on Alumina Granules for Water Filtration: Effect of Copper Oxidation State on Virus Removal Performance. *Environ. Sci. Technol.* **2020**, 54 (2), 1214–1222. <https://doi.org/10.1021/acs.est.9b05211>.
 - (19) Hirte, K.; Seiwert, B.; Schüürmann, G.; Reemtsma, T. New Hydrolysis Products of the Beta-Lactam Antibiotic Amoxicillin, Their pH-Dependent Formation and Search in Municipal Wastewater. *Water Res.* **2016**, 88, 880–888. <https://doi.org/10.1016/j.watres.2015.11.028>.
 - (20) Qian, Y.; Xue, G.; Chen, J.; Luo, J.; Zhou, X.; Gao, P.; Wang, Q. Oxidation of Cefalexin by Thermally Activated Persulfate: Kinetics, Products, and Antibacterial Activity Change. *J. Hazard. Mater.* **2018**, 354 (May), 153–160. <https://doi.org/10.1016/j.jhazmat.2018.05.004>.
 - (21) Poirier-Larabie, S.; Segura, P. A.; Gagnon, C. Degradation of the Pharmaceuticals Diclofenac and Sulfamethoxazole and Their Transformation Products under Controlled Environmental Conditions. *Sci. Total Environ.* **2016**, 557–558, 257–267. <https://doi.org/10.1016/j.scitotenv.2016.03.057>.
 - (22) Gmurek, M.; Horn, H.; Majewsky, M. Phototransformation of Sulfamethoxazole under Simulated Sunlight: Transformation Products and Their Antibacterial Activity toward Vibrio Fischeri. *Sci. Total Environ.* **2015**, 538, 58–63. <https://doi.org/10.1016/j.scitotenv.2015.08.014>.

- (23) Schönfeld, W.; Knöller, J.; Bremm, K. D.; Dahlhoff, A.; Weber, B.; König, W. Determination of Ciprofloxacin, Norfloxacin, and Ofloxacin by High Performance Liquid Chromatography. *Zentralblatt für Bakteriologie, Mikrobiologie und Hygiene - Abteilung I Originalien* **1986**, *261* (3), 338–344. [https://doi.org/10.1016/S0176-6724\(86\)80051-7](https://doi.org/10.1016/S0176-6724(86)80051-7).
- (24) Senta, I.; Krizman-Matasic, I.; Terzic, S.; Ahel, M. Comprehensive Determination of Macrolide Antibiotics, Their Synthesis Intermediates and Transformation Products in Wastewater Effluents and Ambient Waters by Liquid Chromatography–Tandem Mass Spectrometry. *J. Chromatogr. A* **2017**, *1509*, 60–68. <https://doi.org/10.1016/j.chroma.2017.06.005>.
- (25) Lapshin, S. V.; Alekseev, V. G. Copper(II) Complexation with Ampicillin, Amoxicillin, and Cephalexin. *Russ. J. Inorg. Chem.* **2009**, *54* (7), 1066–1069. <https://doi.org/10.1134/S0036023609070122>.
- (26) Chen, J.; Zhou, X.; Sun, P.; Zhang, Y.; Huang, C. H. Complexation Enhances Cu(II)-Activated Peroxydisulfate: A Novel Activation Mechanism and Cu(III) Contribution. *Environ. Sci. Technol.* **2019**, *53* (20), 11774–11782. <https://doi.org/10.1021/acs.est.9b03873>.
- (27) EU. Official Journal of the European Union. *Official Journal of the European Union*. 2020.
- (28) Ren, G.; Hu, D.; Cheng, E. W. C.; Vargas-Reus, M. A.; Reip, P.; Allaker, R. P. Characterisation of Copper Oxide Nanoparticles for Antimicrobial Applications. *Int. J. Antimicrob. Agents* **2009**, *33* (6), 587–590. <https://doi.org/10.1016/j.ijantimicag.2008.12.004>.
- (29) Suleiman, M.; Mousa, M.; Hussein, A. I. A. A. Wastewater Disinfection by Synthesized Copper Oxide Nanoparticles Stabilized with Surfactant. *J. Mater. Environ. Sci.* **2015**, *6* (7), 1924–1937.
- (30) Chung, S. F.; Wen, C. Y. Longitudinal Dispersion of Liquid Flowing through Fixed and Fluidized Beds. *AIChE J.* **1968**, *14* (6), 857–866. <https://doi.org/10.1002/aic.690140608>.
- (31) Mitchell, S. M.; Ullman, J. L.; Teel, A. L.; Watts, R. J. pH and Temperature Effects on the Hydrolysis of Three β -Lactam Antibiotics: Ampicillin, Cefalotin and Cefoxitin. *Sci. Total Environ.* **2014**, *466–467*, 547–555. <https://doi.org/10.1016/j.scitotenv.2013.06.027>.
- (32) Lipunova, G. N.; Nosova, E. V.; Charushin, V. N. Metallocomplexes of Fluoroquinolonecarboxylic Acids. *Russ. J. Gen. Chem.* **2009**, *79* (12), 2753–2766. <https://doi.org/10.1134/S1070363209120342>.
- (33) Haramoto, E.; Fujino, S.; Otagiri, M. Distinct Behaviors of Infectious F-Specific RNA Coliphage Genogroups at a Wastewater Treatment Plant. *Sci. Total Environ.* **2015**, *520*, 32–38. <https://doi.org/10.1016/j.scitotenv.2015.03.034>.
- (34) Mandilara, G. D.; Smeti, E. M.; Mavridou, A. T.; Lambiri, M. P.; Vatopoulos, A. C.; Rigas, F. P. Correlation between Bacterial Indicators and Bacteriophages in Sewage and Sludge. *FEMS Microbiol. Lett.* **2006**, *263* (1), 119–126.

- <https://doi.org/10.1111/j.1574-6968.2006.00414.x>.
- (35) Shields, J. M.; Hill, V. R.; Arrowood, M. J.; Beach, M. J. Inactivation of *Cryptosporidium Parvum* under Chlorinated Recreational Water Conditions. *J. Water Health* **2008**, *6* (4), 513–520. <https://doi.org/10.2166/wh.2008.068>.
- (36) Hijnen, W. A. M.; Beerendonk, E. F.; Medema, G. J. Inactivation Credit of UV Radiation for Viruses, Bacteria and Protozoan (Oo)Cysts in Water: A Review. *Water Res.* **2006**, *40* (1), 3–22. <https://doi.org/10.1016/j.watres.2005.10.030>.
- (37) Timms, S.; Slade, J. S.; Fricker, C. R. Removal of *Cryptosporidium* by Slow Sand Filtration. *Water Sci. Technol.* **1995**, *31* (5–6), 81–84. [https://doi.org/10.1016/0273-1223\(95\)00245-I](https://doi.org/10.1016/0273-1223(95)00245-I).
- (36) Lanje, A.S.; Sharma, S.J.; Pode, R.B. Synthesis and Characterization of Copper Oxide Nanoparticles, *Int. J. Adv. Eng. Res. Dev.* **2017**, *04*. <https://doi.org/10.21090/ijaerd.ncn01>.
- (37) Angi, A.; Sanli, D.; Erkey, C.; Birer, Ö. Catalytic activity of copper (II) oxide prepared via ultrasound assisted Fenton-like reaction, *Ultrason. Sonochem.* **2014**, *25*, 854–859. <https://doi.org/10.1016/j.ultsonch.2013.09.006>.
- (38) Asbrink, S.; Waskowska, A. CuO: X-ray single-crystal structure determination at 196 K and room temperature, *J. Phys. Condens. Matter.* **1991**, *3*, 8173–8180. <https://doi.org/10.1088/0953-8984/3/42/012>.
- (39) Copper in drinking water, Background document for development of WHO guidelines for drinking-water quality. **2004**. https://www.who.int/water_sanitation_health/dwq/chemicals/copper.pdf.

Supplementary Information

Peroxydisulfate activation by CuO pellet in a fixed-bed column for antibiotics degradation and urban wastewater disinfection

Chan Li¹, Nayara de Melo Costa Serge², Raquel Fernandes Pupo Nogueira², Serge Chiron¹, and Vincent Goetz^{3*}

¹UMR5151 HydroSciences Montpellier, University of Montpellier, IRD, 15 Ave Charles Flahault 34093 Montpellier cedex 5, France

²São Paulo State University (UNESP), Institute of Chemistry, Araraquara, 14800-900, Araraquara (SP), Brazil

³PROMES-CNRS UPR 8521, PROcess Material and Solar Energy, Rambla de la Thermodynamique, 66100 Perpignan, France

*Corresponding author: Tel: + 33 - 468682236; Fax: + 33 - 468682213; e-mail address: vincent.goetz@promes.cnrs.fr

Table S1. Major physico-chemical properties of the investigated secondary treated urban wastewater.

Parameter	Effluent
EC (mS/cm)	1.6 ± 0.4
pH	7.7 ± 0.1
TSS (mg/L)	8.2 ± 2.6
COD (mg/L)	32.4 ± 5
HCO ₃ ⁻ (mg/L)	514.3
Cl ⁻ (mg/L)	195.3
NO ₃ ⁻ (mg/L)	12.9 ± 1.5
NH ₄ ⁺ (mg/L)	0.5
PO ₄ -P (mg/L)	0.6 ± 0.2
SO ₄ ²⁻ (mg/L)	58.9
Cu (µg/L)	3.75

Table S2. List of previously identified transformation products (TPs) of amoxicillin (AMX) via hydrolysis, photocatalysis, and different advanced oxidation processes¹⁻³.

Compound	Formula	m/z [M+H] ⁺
AMX	C ₁₆ H ₁₉ N ₃ O ₅ S	366.1123
AMX desaminated	C ₁₆ H ₁₇ N ₂ O ₅ S	350.0936
Amoxicillin penilloic acid	C ₁₅ H ₂₂ N ₃ O ₄ S	341.1409
Diketopiperazine amoxicillin	C ₁₆ H ₂₀ N ₃ O ₅ S	367.1202
Amoxicillin penicilloic acid	C ₁₆ H ₂₂ N ₃ O ₆ S	385.1307
Amoxicilloic acid methyl ester	C ₁₇ H ₂₃ N ₃ O ₆ S	398.1386
4-Hydroxyphenylglycyl amoxicillin	C ₂₄ H ₂₇ N ₄ O ₇ S	516.1678
AMX-S-oxide	C ₁₆ H ₂₀ N ₃ O ₆ S	383.1151
Thiazolidinecarboxylic acid	C ₆ H ₁₀ NO ₂ S	161.0510
4-Hydroxyphenylglycine	C ₈ H ₉ NO ₃	168.0660
6-Aminopenicillanic acid	C ₈ H ₁₂ N ₂ O ₃ S	217.0647
N-pivaloyl-4- hydroxyphenylglycine	C ₁₃ H ₁₇ NO ₄	252.1236
PP-2-OH-3-(4-OH) phenylpyrazine	C ₁₀ H ₈ N ₂ O ₂	189.0664
Penicillamine disulfide	C ₁₀ H ₂₁ N ₂ O ₄ S ₂	298.1021
L-5,5-dimethylthiazolidin-4 carbonic acid	C ₆ H ₁₂ NO ₂ S	163.0667
Dehydrocarboxylated AMX penilloic acid	C ₁₆ H ₁₈ N ₃ O ₅ S	365.1045
	C ₈ H ₁₅ N ₂ O ₄ S	236.0831
Amoxicillin penicilloaldehyde	C ₁₄ H ₁₉ N ₃ NaO ₂ S	317.1174
	C ₂₀ H ₂₁ N ₄ O ₄	382.1641
Amoxicillin penicilloaldehyde	C ₁₀ H ₁₂ N ₂ O ₃	209.0926
	C ₁₁ H ₁₂ N ₂ O ₅ S	285.0545
Amoxicillin penaldic acid	C ₁₁ H ₁₂ N ₂ O ₅	253.0824
	C ₁₅ H ₂₀ N ₃ O ₅ S	355.1202
	C ₁₆ H ₂₂ N ₃ O ₇ S	401.1256
	C ₁₆ H ₁₉ N ₂ O ₇ S	384.0991
	C ₁₄ H ₂₀ N ₃ O ₃ S	311.1303
	C ₈ H ₁₁ N ₂ O ₄ S	232.0518
	C ₁₆ H ₁₈ N ₃ O ₉ S	429.0842
	C ₆ H ₁₀ NO ₃ S	177.0459
	C ₁₄ H ₂₀ N ₃ O ₂ S	295.1354
	C ₁₆ H ₁₈ N ₃ O ₈ S	413.0893

$C_8H_8NO_2$	151.0633
$C_9H_{10}N_2NaO_3$	218.0667
$C_{10}H_{11}N_2O_3$	208.0848
$C_7H_9N_2O$	138.0793
$C_{16}H_{20}N_3O_5S$	367.1202
$C_{11}H_{21}N_2O_5S_2$	326.0970
$C_{12}H_{11}N_2O_4$	248.0797
$C_{10}H_9N_2O_3$	206.0691
$C_{11}H_{11}N_2O_2$	204.0899
$C_{13}H_{17}N_2O_3$	250.1317
$C_7H_{12}NO_4S$	207.0565
$C_{13}H_{17}N_2O_3$	250.1317
$C_9H_{16}NO_2S_2$	235.0700
$C_{10}H_{10}NO_3$	193.0739
$C_{13}H_{13}N_2O_3$	246.1004
$C_{10}H_{10}N_2NaO_4$	246.0616
$C_{32}H_{39}N_6O_{10}S_2$	732.2247
$C_{32}H_{41}N_6O_{11}S_2$	750.2353
$C_{20}H_{21}N_4O_5$	398.1590
$C_{19}H_{17}N_4O_5$	382.1277
$C_{20}H_{23}N_4O_6$	416.1696
$C_{17}H_{20}N_3O_5S$	379.1202
$C_9H_{11}NNaO_3$	205.0715

Table S3. List of previously identified transformation products (TPs) of ofloxacin under advanced oxidation processes ⁴⁻⁷.

Compound	Formula	[M+H] ⁺
Ofloxacin	C ₁₈ H ₂₀ FN ₃ O ₄	362.1510
TP334	C ₁₇ H ₂₀ FN ₃ O ₃	334.1561
TP318	C ₁₇ H ₂₀ FN ₃ O ₂	318.1612
TP316	C ₁₇ H ₁₈ FN ₃ O ₃	316.1456
TP275	C ₁₅ H ₁₅ FN ₂ O ₂	275.1190
TP261	C ₁₄ H ₁₃ FN ₂ O ₂	261.1034
TP233	C ₁₂ H ₉ FN ₂ O ₂	233.0721
TP221	C ₁₁ H ₉ FN ₂ O ₂	221.0721
TP219	C ₁₁ H ₇ FN ₂ O ₂	219.0564
TP348	C ₁₇ H ₁₈ FN ₃ O ₄	348.1354
TP378	C ₁₈ H ₂₀ FN ₃ O ₅	378.1460
TP394	C ₁₈ H ₂₀ FN ₃ O ₆	394.1409
TP376	C ₁₈ H ₁₈ FN ₃ O ₅	376.1303
TP336	C ₁₆ H ₁₈ FN ₃ O ₄	336.1354
TP279	C ₁₃ H ₁₁ FN ₂ O ₄	279.0775
TP338	C ₁₆ H ₂₀ FN ₃ O ₄	338.1511
TP354	C ₁₆ H ₂₀ FN ₃ O ₅	354.1460
TP326	C ₁₅ H ₂₀ FN ₃ O ₄	326.1511
TP312	C ₁₄ H ₁₈ FN ₃ O ₄	312.1354
TP360	C ₁₈ H ₁₈ FN ₃ O ₄	360.1354
TP358	C ₁₈ H ₁₆ FN ₃ O ₄	358.1197
TP304	C ₁₆ H ₁₈ FN ₃ O ₂	304.1455
TP391	C ₁₈ H ₁₇ FN ₃ O ₆	391.1174
TP278	C ₁₃ H ₁₀ FN ₂ O ₄	278.0697
TP260	C ₁₃ H ₁₁ N ₂ O ₄	260.0791
TP169	C ₇ H ₆ NO ₄	169.0369
TP153	C ₇ H ₆ NO ₃	153.0420
TP329	C ₁₇ H ₁₈ N ₃ O ₄	329.1370
TP327	C ₁₇ H ₁₆ N ₃ O ₄	327.1213
TP277	C ₁₃ H ₁₂ N ₂ O ₅	277.0818
TP251	C ₁₂ H ₁₁ FN ₂ O ₃	251.0826
TP207	C ₁₁ H ₁₁ FN ₂ O	207.0928
TP205	C ₁₁ H ₉ FN ₂ O	205.0772
TP395	C ₁₈ H ₂₂ FN ₃ O ₆	396.1565
TP414	C ₁₈ H ₂₃ FN ₃ O ₇	413.1593
TP344	C ₁₈ H ₂₁ N ₃ O ₄	344.1605
TP372	C ₁₈ H ₁₈ N ₃ O ₆	373.1268
TP311	C ₁₅ H ₂₁ FN ₃ O ₃	311.1640
TP301	C ₁₅ H ₁₄ N ₃ O ₄	301.1057

TP229	$C_{12}H_8N_2O_3$	229.0608
TP175	$C_{10}H_9NO_2$	176.0706
TP149	$C_8H_7NO_2$	150.054955
TP579	$C_{28}H_{23}F_2N_5O_7$	580.1638

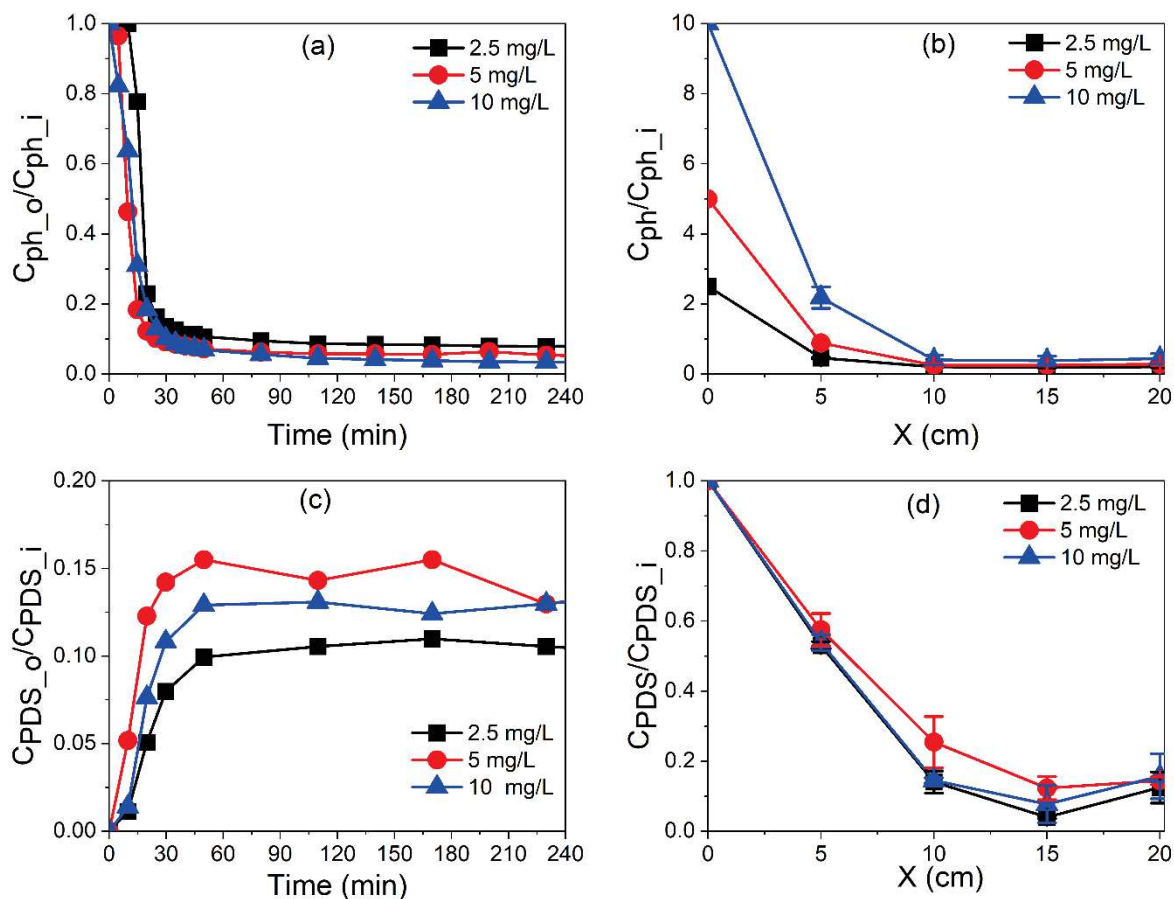


Figure S1. The effect of different inlet phenol concentration on outlet phenol concentration profile at different time (a) and at different column positions (b) and the outlet PDS concentration profile at different time (c) and at different column positions (d). $C_{PDS_i} = 500 \mu\text{M}$, $C_{ph_i} = 0, 2.5, 5, 10 \text{ mg/L}$, flow rate = 3 mL/min.

Figure S1: Performance of the FBC-CuO with 500 μM influent PDS at 3 mL/min was tested at varying influent phenol concentration. As shown in Figure S1 (a) and (b), for inlet phenol concentration varying from 2.5 to 10 mg/L, the column presented excellent phenol degradation efficiency. Even in the case of the higher inlet phenol concentration no release at the outlet. This indicated that the limit of the treatment capacity under this condition (500 μM influent PDS at 3 mL/min) is not reached. PDS consumption was only slightly affected by varying influent phenol concentration (Figure S1 (c) and (d)).

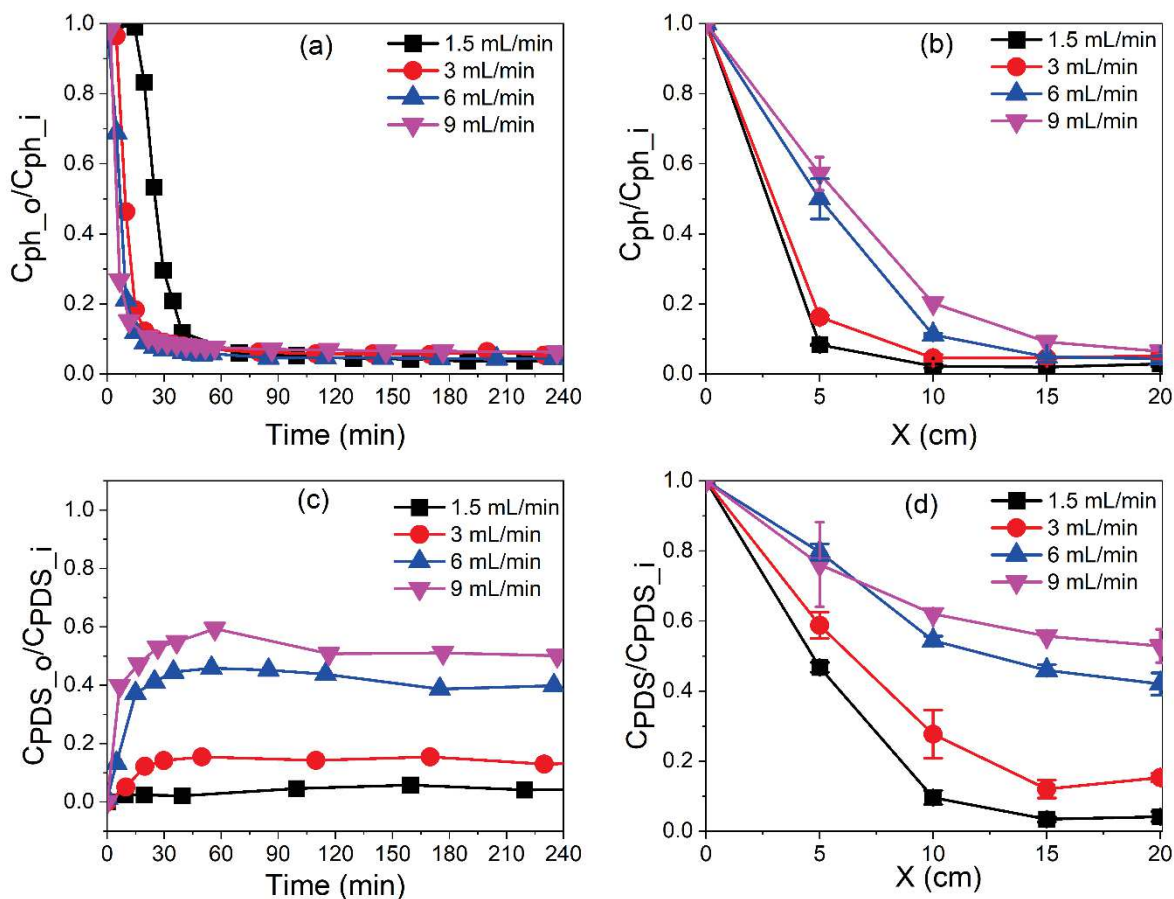


Figure S2. The effect of different flow rate on outlet phenol concentration profile at different time (a) and at different column positions (b) and the outlet PDS concentration profile at different time (c) and at different column positions (d). $C_{PDS_i} = 500 \mu\text{M}$, $C_{ph_i} = 5 \text{ mg/L}$, flow rate = 1.5, 3, 6, 9 mL/min.

Figure S2: Performance of the FBC with 5 mg/L influent phenol and 500 μM PDS was tested at varying flow rates. As shown in Figure S2 (a), phenol removal efficiency is independent of flow rate in the studied range. But consistently with the natural coupling between mass transport and reaction kinetic, the rate of removal of phenol as well as the rate of consumption of PDS tended to decrease at a given length of the bed. The unused bed length decreased at higher flow rate (Fig. S2 (b)). 9 mL/min was probably the limit before a breakthrough of the phenol at the outlet of the column in permanent regime.

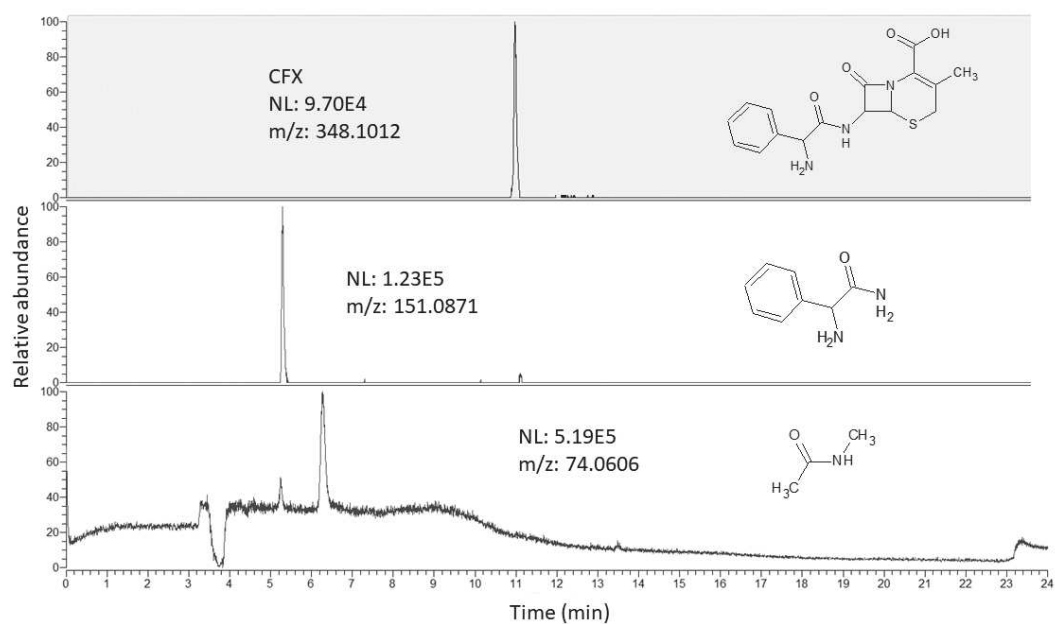


Figure S3. Extracted Ion Chromatograms (EIC) of detected cefalexin (CFX) TPs in FBC-CuO.

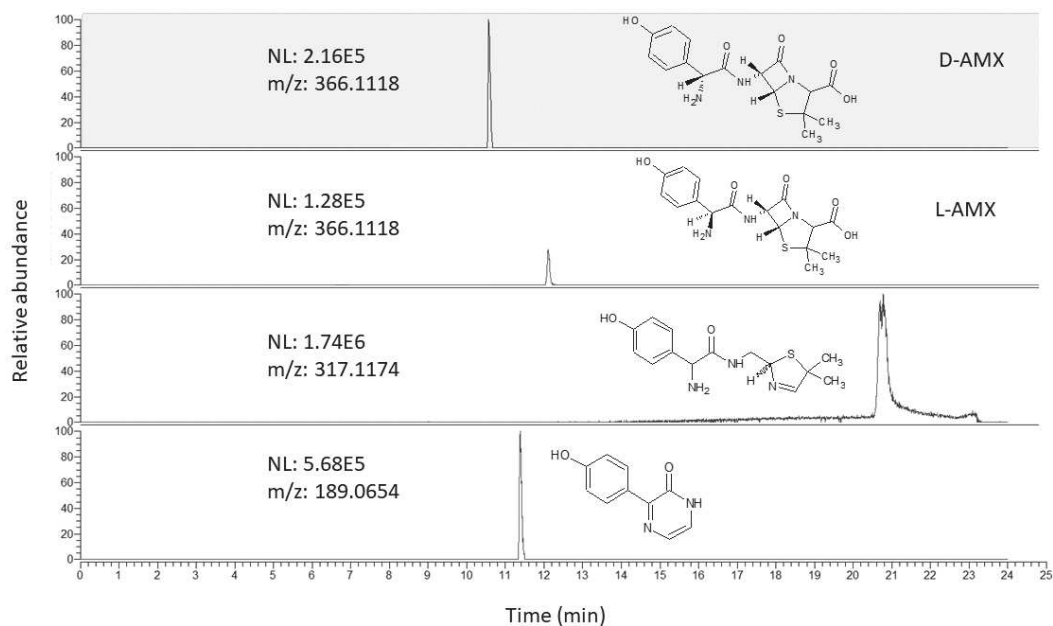


Figure S4. Extracted Ion Chromatograms (EIC) of detected amoxicillin (AMX) TPs in FBC-CuO.

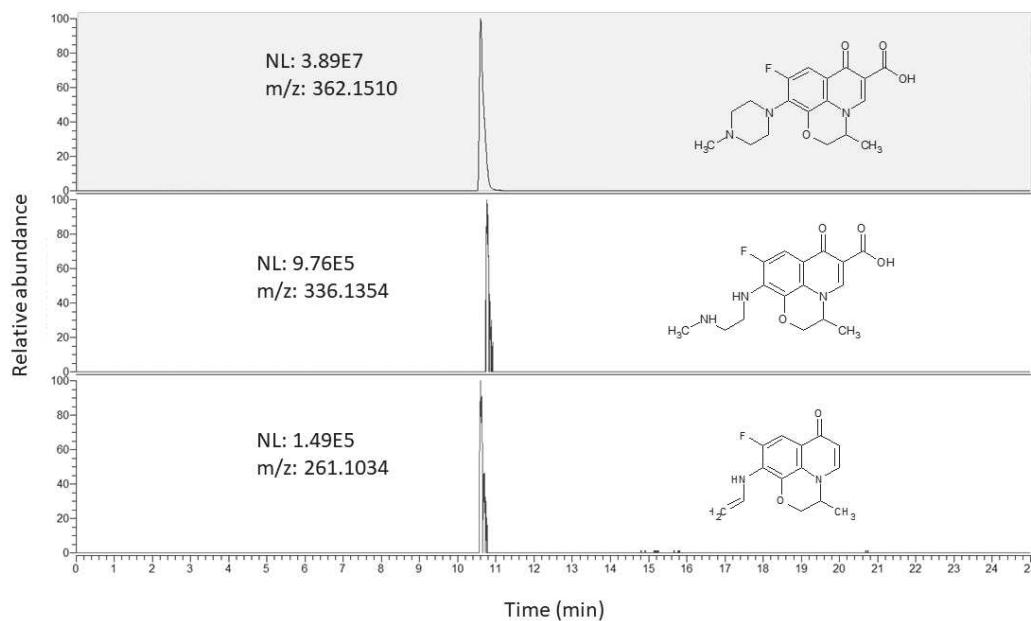


Figure S5. Extracted Ion Chromatograms (EIC) of detected ofloxacin TPs in FBC-CuO.

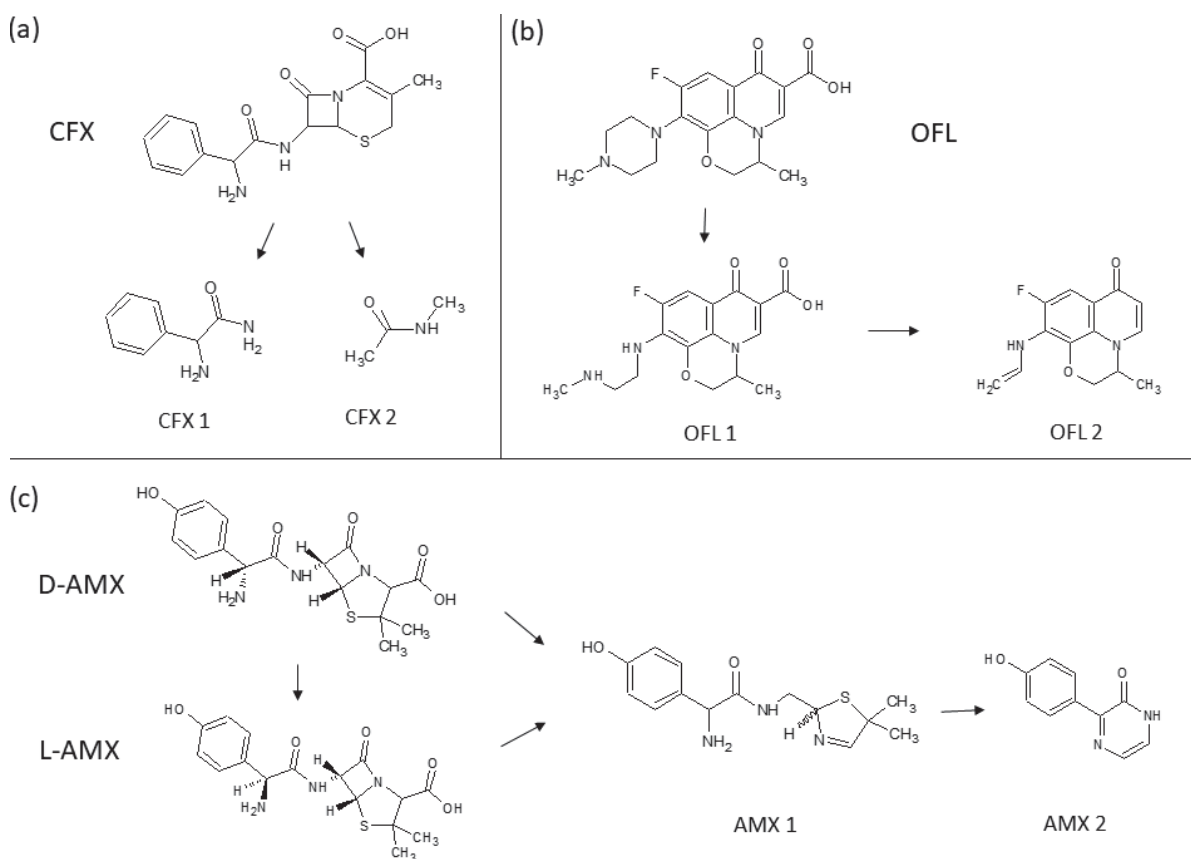


Figure S6. Proposed transformation pathways of (a) CFX, (b) OFL, and (c) AMX in CuO column.

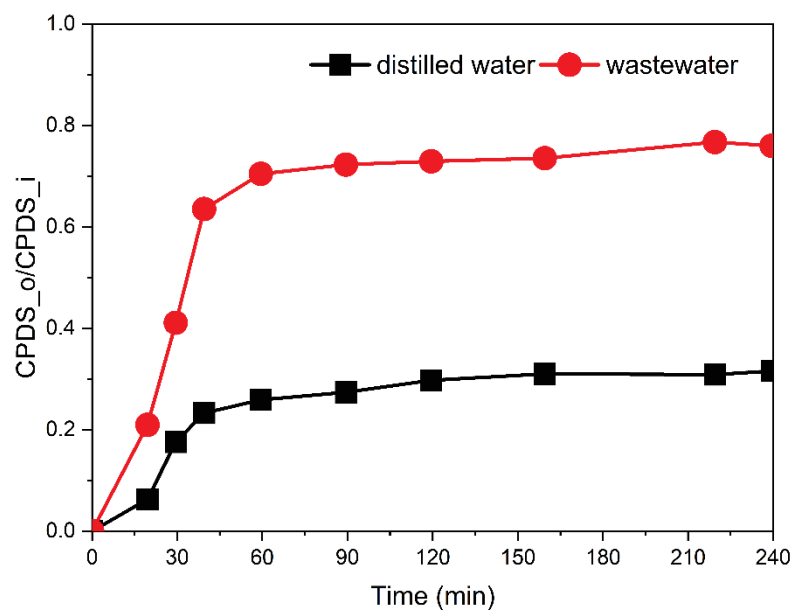


Figure S7. PDS consumption in distilled water (DW) and secondary treated wastewater (WW) for ATBs degradation. $C_{PDS_i} = 500 \mu\text{M}$, $C_{antibiotics_i} = 250 \mu\text{g/L}$, 1.5 mL/min.

References

- (1) Hirte, K.; Seiwert, B.; Schüürmann, G.; Reemtsma, T. New Hydrolysis Products of the Beta-Lactam Antibiotic Amoxicillin, Their PH-Dependent Formation and Search in Municipal Wastewater. *Water Res.* **2016**, *88*, 880–888. <https://doi.org/10.1016/j.watres.2015.11.028>.
- (2) Jung, Y. J.; Kim, W. G.; Yoon, Y.; Kang, J. W.; Hong, Y. M.; Kim, H. W. Removal of Amoxicillin by UV and UV/H₂O₂ Processes. *Sci. Total Environ.* **2012**, *420*, 160–167. <https://doi.org/10.1016/j.scitotenv.2011.12.011>.
- (3) Arsand, J. B.; Hoff, R. B.; Jank, L.; Meirelles, L. N.; Silvia Díaz-Cruz, M.; Pizzolato, T. M.; Barceló, D. Transformation Products of Amoxicillin and Ampicillin after Photolysis in Aqueous Matrices: Identification and Kinetics. *Sci. Total Environ.* **2018**, *642* (November), 954–967. <https://doi.org/10.1016/j.scitotenv.2018.06.122>.
- (4) Hapeshi, E.; Fotiou, I.; Fatta-Kassinos, D. Sonophotocatalytic Treatment of Ofloxacin in Secondary Treated Effluent and Elucidation of Its Transformation Products. *Chem. Eng. J.* **2013**, *224* (1), 96–105. <https://doi.org/10.1016/j.cej.2012.11.048>.
- (5) Vasquez, M. I.; Hapeshi, E.; Fatta-Kassinos, D.; Kümmerer, K. Biodegradation Potential of Ofloxacin and Its Resulting Transformation Products during Photolytic and Photocatalytic Treatment. *Environ. Sci. Pollut. Res.* **2013**, *20* (3), 1302–1309. <https://doi.org/10.1007/s11356-012-1096-5>.
- (6) Pi, Y.; Feng, J.; Song, M.; Sun, J. Degradation Potential of Ofloxacin and Its Resulting Transformation Products during Fenton Oxidation Process. *Chinese Sci. Bull.* **2014**, *59* (21), 2618–2624. <https://doi.org/10.1007/s11434-014-0293-7>.
- (7) Carbajo, J. B.; Petre, A. L.; Rosal, R.; Herrera, S.; Letón, P.; García-Calvo, E.; Fernández-Alba, A. R.; Perdigón-Melón, J. A. Continuous Ozonation Treatment of Ofloxacin: Transformation Products, Water Matrix Effect and Aquatic Toxicity. *J. Hazard. Mater.* **2015**, *292*, 34–43. <https://doi.org/10.1016/j.jhazmat.2015.02.075>.
- (8) Li, C.; Goetz, V.; Chiron, S. Peroxydisulfate Activation Process on Copper Oxide: Cu(III) as the Predominant Selective Intermediate Oxidant for Phenol and Waterborne Antibiotics Removal. *J. Environ. Chem. Eng.* **2021**, *9* (2), 105145. <https://doi.org/10.1016/j.jece.2021.105145>.

Chapter 5. Conclusions and perspectives

To safely reuse wastewater in agricultural irrigation, an advanced treatment process is still required after the conventional UWTs, which can remove a broad range of organic contaminants and pathogenic microorganisms, limit the formation of DBPs and the spread of antibiotic resistance while preserving the maximum amount of carbon and nutrients in wastewater. For this purpose, the copper oxide catalyzed peroxydisulfate system was investigated.

A micrometer CuO activated PDS system was initially studied in batch mode to explore the mechanisms since inconsistent and controversial oxidative reaction pathways of the CuO catalyzed PDS process have been reported in the literature from hydroxyl and sulfate radical pathway, surface activated persulfate mediated electron transfer, singlet oxygenation to Cu(III)-induced oxidation pathways. Phenol was selected as the probe compound because of its well-known reactions with common radical and non-radical species. The generated reactive species were investigated by using a series of radical scavengers and different spectroscopic techniques including high-resolution mass spectrometry for phenol transformation products identification, which demonstrated that phenol degradation was not a radical-based process. Based on all the evidence and the clues from the data exploitations and for the first time Cu(III) was suggested to be the predominant reactive species and a polymerization reaction accounted for the phenol transformation pathway in the CuO / PDS oxidation system. The mechanism mainly involved the generation of $\cdot\text{O}_2^-$ resulting from an outer-sphere surface PDS complexation which prompted the reduction of Cu(II) in Cu(I). Cu(I) was oxidized to Cu(III) by PDS, then Cu(III) was reduced to Cu(II) by one-electron oxidation of phenol so that the catalytic effect involved alternate oxidation and reduction of the copper. $^1\text{O}_2$ was also heavily produced from $\cdot\text{O}_2^-$ decomposition but was found to be slightly involved in the degradation since it was rapidly quenched by water. These non-radical oxidants presented great advantages for wastewater treatment because of the poor reactivity with DOM and high resistance to background organic matters and anions. This system showed a preference to react with electron-rich compounds and could work

in presence of high contents of dissolved organic matter and nutrients and preserve the valuable content for agronomy.

The ability of the system to treat a large number of emerging pollutants has been evaluated by a first measurement campaign carried out on working with pharmaceutical compounds. CFX, CIP, CLA, and SMX were selected as the representatives of β -lactam, fluoroquinolone, macrolide, and sulfonamide antibiotics, respectively, because of their intensive use and potential environmental concern. The CuO (10 g/L)/PDS (1 mM) system demonstrated effective degradation on waterborne antibiotics and specific TPs resulted from Cu(III) oxidant were identified, such as CFX sulfoxide and SMX dimer, further confirmed the predominant role of Cu(III) in this CuO/PDS system. Moreover, Cu(III) oxidant appeared to restrict the number of generated TPs of toxicological concern in case of SMX.

The reactive species (i.e., Cu(III), $^1\text{O}_2$, and Cu(I)) generated in the CuO/PDS system are known to be efficient biocides and effective inactivation performance of pathogenic microorganisms was anticipated. *E. coli*, *Enterococcus*, *F-specific RNA*, and *spores of sulfite-reducing bacteria* were selected as the indicator to comply with the EU regulation 2020/741 for secondary treated urban wastewater reuse in irrigation. Complete inactivation of *E. coli*, *Enterococcus*, *F-specific RNA bacteriophages* from secondary treated wastewater was achieved after a short time (15-30 min) treatment by CuO/PDS system under the same conditions as for antibiotics degradation, but *spores of sulfite-reducing bacteria* took 120 min. A significant reduction of *E. coli* (3.5 log), *Enterococcus* (4.1 log), and *F-specific RNA bacteriophages* (3.5 log) from raw wastewater were also observed by CuO/PDS system with a longer reaction time (120 min) and a higher dose of PDS (2.5 mM), which opens the possibility to use this system for disinfection in some poor countries without well-established WWTPs. Importantly, trihalomethanes were not detected and no bacterial regrowth occurred during storage after treatment.

In addition to the microbial risk caused by pathogens, concerns about antibiotic-resistant bacteria and antibiotic resistance genes in wastewater are growing due to the potential ecological environmental and human health risks. The inactivation performance of the CuO/PDS system was further explored with ARB&Gs. SMX-resistant *E. coli* and SMX-resistant *Enterococcus* were used as the model ARBs. SMX-resistant *Enterococcus* was not detected in the collected wastewater. A significant reduction of SMX-resistant *E. coli* (3.2 log) was achieved after only 10 min of treatment. Four ARGs including qnrS (reduced susceptibility to fluoroquinolone); sul1 (resistance to sulfonamides); blaTEM (resistance to β -lactams), ermB (resistance to macrolides) were selected as ARGs because of their high occurrence in urban wastewater. Two genes linked to the dissemination of antibiotic resistance including intI1, which encoding the integrase of Class I integron-integrase, and IS613 as the insertion sequences in DNA transposons were selected as the proxy for the potential capacity of the bacterial community to disseminate resistance. 16S rRNA gene as the indicator of total bacteria was also selected. A considerable reduction (0.7-2.3 log) of selected genes was achieved after 60 min treatment by CuO/PDS.

All these findings in the batch mode indicated the promising applicability of the CuO/PDS system as an advanced technology for wastewater reuse in irrigation. If suspension of perfectly mixed nano and micro-sized CuO particles carried in closed reactors is well adapted to laboratory studied to test reactivity or carry out kinetic study, this is no more the case for practical on-site application. Such a perspective needs to implement the solid particles in a way consistent with an open continuous flow reactor. Within this objective, the packed fixed bed operating in plug flow is one of the most widespread design to provide the necessary contact between a liquid to be treated and a reactive solid. Such a design, which avoid any catalyst release in the environment and the related adverse effect on aquatic life, necessitate millimeter size particles to respect the requirement of limiting the pressure drop inside the column and to prevent potential clogging problems. Thus, persulfate oxidation by using CuO in the form of millimetric

pellets as a heterogeneous catalyst in a packed fixed-bed column, FBC-CuO, was for the first time designed and applied for wastewater decontamination and disinfection.

The working mode of FBC-CuO was first studied by using a simple solution of phenol in distilled water. These tests have shown a high stability of the column once it was put into operation, demonstrating that the process is working, for constant inlet, according to a very well-established permanent regime. FBC-CuO is sensitive to operating conditions, especially for influent PDS concentration, an excellent parameter to control the removal rate of phenol. FBC-CuO alone could effectively remove AMX, CFX and OFL antibiotics through Cu(II) complexation promoted structure decomposition transformation pathways. However, as expected, FBC-CuO alone failed to disinfect the STWW, which is consistent with the results obtained in batch mode using CuO microparticles. The combination of PDS with FBC-CuO is the necessary condition for the degradation of sulfonamides (e.g., SMX) and macrolide (e.g., CLA), not only improved the removal efficiency of antibiotics, but also greatly enhanced the disinfection performance, excepted for *spores of sulfite-reducing bacteria*. Phase analyses and morphology of CuO pellet before and after treatment were performed by SEM and XRD and Cu²⁺ leaching study demonstrated the excellent stability and reusability of FBC-CuO. Overall, it was shown that FBC-CuO/PDS constitutes an efficient and promising treatment option for the removal of micropollutants and microorganisms from wastewater effluents.

To consolidate and confirm these promising results, we mention few perspectives and the following items should be completed or addressed.

1. Additional work should be dedicated to the investigation of mechanisms in heterogeneous Fenton-like oxidation processes because these systems demonstrated great potential for urban wastewater treatment, but there is a great deal of uncertainty concerning the controversial and inconsistent mechanisms. Only one

system has been studied in a comprehensive way, which is far from reaching the position of predicting the working reactive species in another HFOP system without conducting experiments.

2. On micropollutants degradation capacity of this system, additional batch experiment using no-doped urban wastewater with a much larger panel of micropollutants are need to evaluate the completeness of this system in real working condition. Studies were focused on selected antibiotics, the removal efficiency regarding other CECs remains unknown.
3. On the FCB-CuO tests, need to develop a model able to simulate the operation of the column in the simplest case, with phenol in DW, this work started during this PhDs. After validation, such a model could be the starting point for future work devoted to the establishment of a simulating tools in the case much more complicate of a complex mixture of pollutants in complex matrix, such as urban wastewater.
4. On FCB-CuO tests, needs to operate directly on site on a small scale FCB-CuO to be able to characterize the management of the system for non-constant operating conditions such as level of concentration of emergent pollutants as well as pathogens. In any cases, there is a need of additional data acquisition to consolidate, especially for disinfection results.
5. Cu^{2+} leaching from FBC-CuO in operating condition corresponding to appropriate rate of removal of pollutant as well as pathogens leads to a level of concentration at the outlet in the range of 0.4 mg/L, two times higher than the requirement for irrigation (0.2 mg/L). This experimental statement, is a drastic constraint to the dissemination of this process to be overcome. One possible solution is to incorporate CuO nanoparticles or microparticles on supports, such as metal oxides, layered double hydroxides, carbonaceous materials (e.g., biochar) or ceramic. However, these studies have only been carried out in laboratory-scale, and to apply for wastewater treatment, the preparation of novel materials should be simple and cost-effective. Another option to be explored to solve this major problem is the

implementation of a low-cost post-treatment filter after the CuO unit, such as ionized clay filtration, slow sand filtration, and metal oxide coated sand filter. Such filters can also make up for another shortcoming of this system, which can effectively remove parasites that were resistant to the CuO/PDS system.

Therefore, the CuO/PDS system might be a promising technology because it met the requirement for safely reuse wastewater in irrigation, specifically, it effectively removed organic pollutants, pathogens, ARB&Gs simultaneously as well as preserving the carbon and nutrients content of wastewater. Equally importantly, it might be easily implemented at field-scale through filtration units.

Appendix

List of publications

C. Li, V. Goetz, S. Chiron, Peroxydisulfate activation process on copper oxide: Cu(III) as the predominant selective intermediate oxidant for phenol and waterborne antibiotics removal, J. Environ. Chem. Eng. 9 (2021) 105145. <https://doi.org/10.1016/j.jece.2021.105145>.

C. Li, V. Goetz, S. Chiron, Copper oxide / peroxydisulfate system for urban wastewater disinfection: Performances, reactive species, and antibiotic resistance genes removal, Sci. Total Environ. (2021) 150768. <https://doi.org/10.1016/j.scitotenv.2021.150768>.

C. Li, N. De Melo Costa-Serge, R.F.P. Nogueira, S. Chiron, V. Goetz, Peroxydisulfate activation by CuO pellet in a fixed-bed column for antibiotics degradation and urban wastewater disinfection, Ind. Eng. Chem. Res. Submitted.

N. De Melo Costa-Serge, C. Li, R.F.P. Nogueira, S. Chiron, Disinfection of wastewater and pharmaceuticals degradation by heterogeneous Fenton-like processes using CuMgFe-BO₃ layered double hydroxide. In preparation.

N. De Melo Costa-Serge, R.G.L. Gonçalves, M.A.R. Ubillus, C. Li, C.V. Santilli, P. Hammer, S. Chiron, R.F.P. Nogueira, Fenton-like degradation of anticancer 5-Fluorouracil on CuMgFe-LDH: Effect of interlamellar anion, solar radiation, and degradation products. In preparation.